

University of Windsor

Scholarship at UWindor

Electronic Theses and Dissertations

Theses, Dissertations, and Major Papers

2008

Electrical surface properties of HTV silicone rubber used for high voltage insulation

Mansab Ali
University of Windsor

Follow this and additional works at: <https://scholar.uwindsor.ca/etd>

Recommended Citation

Ali, Mansab, "Electrical surface properties of HTV silicone rubber used for high voltage insulation" (2008). *Electronic Theses and Dissertations*. 8095.
<https://scholar.uwindsor.ca/etd/8095>

This online database contains the full-text of PhD dissertations and Masters' theses of University of Windsor students from 1954 forward. These documents are made available for personal study and research purposes only, in accordance with the Canadian Copyright Act and the Creative Commons license—CC BY-NC-ND (Attribution, Non-Commercial, No Derivative Works). Under this license, works must always be attributed to the copyright holder (original author), cannot be used for any commercial purposes, and may not be altered. Any other use would require the permission of the copyright holder. Students may inquire about withdrawing their dissertation and/or thesis from this database. For additional inquiries, please contact the repository administrator via email (scholarship@uwindsor.ca) or by telephone at 519-253-3000ext. 3208.

NOTE TO USERS

This reproduction is the best copy available.

UMI[®]

**Electrical Surface Properties of HTV Silicone Rubber
Used for High Voltage Insulation**

by

Mansab Ali

A Thesis

Submitted to the Faculty of Graduate Studies through the
Department of Electrical and Computer Engineering in Partial Fulfillment
of the Requirements for the Degree of Master of Applied Science at the
University of Windsor

Windsor, Ontario, Canada

2008

© 2008 Mansab Ali



Library and Archives
Canada

Published Heritage
Branch

395 Wellington Street
Ottawa ON K1A 0N4
Canada

Bibliothèque et
Archives Canada

Direction du
Patrimoine de l'édition

395, rue Wellington
Ottawa ON K1A 0N4
Canada

Your file *Votre référence*
ISBN: 978-0-494-57607-6
Our file *Notre référence*
ISBN: 978-0-494-57607-6

NOTICE:

The author has granted a non-exclusive license allowing Library and Archives Canada to reproduce, publish, archive, preserve, conserve, communicate to the public by telecommunication or on the Internet, loan, distribute and sell theses worldwide, for commercial or non-commercial purposes, in microform, paper, electronic and/or any other formats.

The author retains copyright ownership and moral rights in this thesis. Neither the thesis nor substantial extracts from it may be printed or otherwise reproduced without the author's permission.

AVIS:

L'auteur a accordé une licence non exclusive permettant à la Bibliothèque et Archives Canada de reproduire, publier, archiver, sauvegarder, conserver, transmettre au public par télécommunication ou par l'Internet, prêter, distribuer et vendre des thèses partout dans le monde, à des fins commerciales ou autres, sur support microforme, papier, électronique et/ou autres formats.

L'auteur conserve la propriété du droit d'auteur et des droits moraux qui protègent cette thèse. Ni la thèse ni des extraits substantiels de celle-ci ne doivent être imprimés ou autrement reproduits sans son autorisation.

In compliance with the Canadian Privacy Act some supporting forms may have been removed from this thesis.

While these forms may be included in the document page count, their removal does not represent any loss of content from the thesis.

Conformément à la loi canadienne sur la protection de la vie privée, quelques formulaires secondaires ont été enlevés de cette thèse.

Bien que ces formulaires aient inclus dans la pagination, il n'y aura aucun contenu manquant.

■ ■ ■
Canada

Author's Declaration of Originality

I hereby certify that I am the sole author of this thesis and that no part of this thesis has been published or submitted for publication.

I certify that, to the best of my knowledge, my thesis does not infringe upon anyone's copyright nor violate any proprietary rights and that any ideas, techniques, quotations, or any other material from the work of other people included in my thesis, published or otherwise, are fully acknowledged in accordance with the standard referencing practices. Furthermore, to the extent that I have included copyrighted material that surpasses the bounds of fair dealing within the meaning of the Canada Copyright Act, I certify that I have obtained a written permission from the copyright owner(s) to include such material(s) in my thesis and have included copies of such copyright clearances to my appendix.

I declare that this is a true copy of my thesis, including any final revisions, as approved by my thesis committee and the Graduate Studies office, and that this thesis has not been submitted for a higher degree to any other University or Institution.

Abstract

This thesis presents a laboratory study on the aging mechanisms responsible for loss and recovery of hydrophobicity of high temperature vulcanized silicone rubber used as a high voltage insulator. The effects of different stresses of heat and water salinity on the hydrophobicity were determined as a function of time, by measuring intermittently the static contact angle, the weight and average surface roughness during aging as well as recovery.

The SEM, EDS and ATR-FTIR spectroscopy were utilized to study the physical and chemical changes on the surface. In addition, the surface free energies γ_s , γ_{sl} and W_{sl} of the specimens were calculated from the measured data of the contact angles of θ_w and θ_{MI} .

The loss and recovery of hydrophobicity of the specimens due to migration of the low molecular weight (LMW) fluid from bulk to the surface under different stress conditions was investigated. The contents of the extracted LMW fluid were characterized by mass spectrometry, IR and NMR spectroscopy.

*To my beloved parents, wife and children
for their inspiration, understanding and never-ending support*

Acknowledgements

I would like to express my sincere gratitude to my supervisor, Dr. R. Hackam for his invaluable guidance, encouragement and tremendous support throughout the course of this work. It has indeed been a great privilege to work with him.

I wish to thank my departmental reader, Professor P. H. Alexander and the external reader, Dr. Murty K. S. Madugula, for their cooperation, comments and useful suggestions.

I would like to thank the Natural Sciences and Engineering Research Council of Canada for providing the funds for this Research Work and Assistantship. Thanks also to ENWIN Utilities Ltd., for supplying the HTV silicone rubber insulators for this study.

I would like to thank Dr. R. Aroca, Mr. G. Moula and Mr. M. Iqbal of the Chemistry department for their time and technical assistance for ATR-FTIR spectroscopy of HTV SIR specimens. I would also like to thank Dr. J. Green, Dr. A. Bari and Mr. R. A. Taj for their technical assistance in performing MS, NMR and IR spectroscopy of the extracted LMW fluid. It would not be possible to complete this work without their valuable assistance.

I am grateful to Mr. J. Robinson of the Department of Mechanical, Automotive and Materials engineering for carrying out SEM-EDS analysis of HTV SIR. Also, great appreciation is expressed to Mr. Frank Cicchello, the Technical Assistant and Ms. Andria Turner, the Graduate Secretary of the Electrical and Computer Engineering Department for their kind help and support.

Contents

Author's Declaration of Originality	iii
Abstract	iv
Dedication	v
Acknowledgements	vi
List of Figures	ix
List of Tables	xx
Nomenclature	xxii
1 Introduction	1
1.1 General	1
1.2 Properties of Silicone Rubber	3
1.3 Fillers in Silicone Rubber	4
1.4 Performance of HTV SIR (Literature Review)	5
1.5 The Scope of Research	10
2 Experimental Method	11
2.1 Preparation of specimens	11
2.2 Conductivity and Temperature of Saline Solution	11
2.3 Measurement of Surface Roughness	12
2.4 Contact Angle	13
2.5 Measurement of the Contact Angle	13
2.6 Drop-Bubble Methods	16
2.6.1 Direct Observation-Tangent Method	16
2.6.2 Reflected Light Method	17
2.6.3 Interference Microscopy Method	17
2.6.4 Drop Dimensions Method	17
2.6.5 Formation of Drops	18
2.7 Accuracy of the Measurements	18
3 Surface Properties of HTV SIR Insulator during Short Term Aging	20
3.1 Introduction	20
3.2 Effect of Temperature and Saline Water on Weight	21
3.3 Effect of Temperature and Salinity on Contact Angle	30
3.4 Effect of Temperature and Salinity on Surface Roughness	38
3.5 Change in Weight during Recovery	45
3.6 Change in Contact Angle during Recovery	52
3.7 ASR during Recovery	60
3.8 SEM and EDS Results	68
3.8.1 Experimental Procedure	68
3.8.2 Results	69
3.9 ATR-FTIR Spectroscopy Results	80
3.9.1 Experimental Procedure	80
3.9.2 Results	80
4 Surface Properties of HTV SIR Insulator during Long Term Aging	87
4.1 Introduction	87
4.2 Effect of Temperature and Saline Water on Weight	87
4.3 Effect of Temperature and Salinity on Contact Angle	96

4.4	Effect of Temperature and Salinity on Surface Roughness.....	104
4.5	Change in Weight during Recovery.....	111
4.6	Change in Contact Angle during Recovery	119
4.7	ASR during Recovery.....	129
4.8	SEM and EDS Results	138
4.9	ATR-FTIR Spectroscopy Results	149
5	Surface Free Energies of HTV SIR	156
5.1	Introduction	156
5.2	Definition of Surface Energy.....	157
5.3	Contact Angle and Surface Free Energies	158
5.4	Calculating Surface Free Energies.....	160
5.4.1	Harmonic Mean Method.....	160
5.5	Results	162
6	LMW Fluid Contents in HTV SIR Insulator	176
6.1	Introduction	176
6.2	Extracting the LMW Fluid	177
6.2.1	Immersion in Hexane	177
6.2.2	Results and Comparisons.....	178
6.3	Characterization of LMW Fluid	184
6.3.1	NMR Spectroscopy	184
6.3.2	Infrared Spectroscopy	185
6.3.3	Mass Spectrometry	185
6.4	Effect of Heat on Regeneration of LMW Fluid.....	194
6.4.1	Hexane-Heat-Hexane Test Sequence for Virgin Samples	194
6.4.2	Hexane-Heat-Hexane Test Sequence for Aged Samples	197
7	Conclusions and Suggestions for Future Work	201
7.1	Conclusions.....	201
7.1.1	Short Term Aging Results	201
7.1.2	Long Term Aging Results.....	204
7.1.3	Summary of the Results.....	207
7.2	Suggestions for Future Research.....	209
	Appendix A: Some Statistical Concepts.....	221
A.1	Population and Sample	221
A.2	Parameter and statistic	221
A.3	Measures of Central Tendency	221
A.4	Arithmetic Mean, Mode and Median	221
A.5	Measures of dispersion	222
A.6	Variance and Standard Deviation	222
A.7	Interval Estimation	223
A.8	Confidence Interval Estimation of a Population Mean.....	223
	Appendix B. MATLAB Code for Calculations of Surface Energies.....	225
	Vita Auctoris	227

List of Figures

Figure 2.1. Variation in the contact angle of water as a function of time after placing the droplet on the surface of HTV SIR specimen. Conductivity of water is 0.005 mS/cm and the volume of droplet 4-5 μ l.....	15
Figure 2.2. Data sample of 33 readings of the contact angle of a droplet of distilled water on the surface of a virgin HTV SIR specimen.	18
Figure 3.1. Time variation of percentage change in weight of HTV SIR specimens immersed in solutions of different conductivities at 0 °C during aging for 576 h.	24
Figure 3.2. Time variation of percentage change in weight of HTV SIR specimens immersed in solutions of different conductivities at 22 °C during aging for 576 h.	25
Figure 3.3. Time variation of percentage change in weight of HTV SIR specimens immersed in solutions of different conductivities at 50 °C during aging for 576 h.	26
Figure 3.4. Time variation of percentage change in weight of HTV SIR specimens immersed in solutions of different conductivities at 75 °C during aging for 576 h.	27
Figure 3.5. Time variation of percentage change in weight of HTV SIR specimens immersed in solutions of different conductivities at 98 °C during aging for 576 h.	28
Figure 3.6. Percentage change in weight of HTV SIR specimens as a function of time during aging in stationary air at different temperatures for 576 h.	29
Figure 3.7. Time variation of contact angle of distilled water on the surface of HTV SIR specimens during aging in water solutions of different conductivities at 0 °C for 576 h.	32
Figure 3.8. Time variation of contact angle of distilled water on the surface of HTV SIR specimens during aging in water solutions of different conductivities at 22 °C for 576 h.	33
Figure 3.9. Time variation of contact angle of distilled water on the surface of HTV SIR specimens during aging in water solutions of different conductivities at 50 °C for 576 h.	34
Figure 3.10. Time variation of contact angle of distilled water on the surface of HTV SIR specimens during aging in water solutions of different conductivities at 75 °C for 576 h:.....	35

Figure 3.11. Time variation of contact angle of distilled water on the surface of HTV SIR specimens during aging in water solutions of different conductivities at 98 °C for 576 h.....	36
Figure 3.12. Time variation of contact angle of distilled water on the surface of HTV SIR specimens during aging in stationary air at different temperatures for 576 h.....	37
Figure 3.13. Time variation of average surface roughness of HTV SIR specimens during aging in different salinities at 0 °C for 576 h.....	39
Figure 3.14. Time variation of average surface roughness of HTV SIR specimens during aging in different salinities at 22 °C for 576 h.....	40
Figure 3.15. Time variation of average surface roughness of HTV SIR specimens during aging in different salinities at 50 °C for 576 h.....	41
Figure 3.16. Time variation of average surface roughness of HTV SIR specimens during aging in different salinities at 75 °C for 576 h.....	42
Figure 3.17. Time variation of average surface roughness of HTV SIR specimens during aging in different salinities at 98 °C for 576 h.....	43
Figure 3.18. Time variation of average surface roughness of HTV SIR specimens during aging in stationary air at different temperatures for 576 h...	44
Figure 3.19. Percentage change in the weight of HTV SIR specimens as a function of time during recovery in stationary air at room temperature for 2700 h. The specimens had been aged in solutions of different conductivities at 0 °C for 576 h.....	47
Figure 3.20. Percentage change in the weight of HTV SIR specimens as a function of time during recovery in stationary air at room temperature for 2700 h. The specimens had been aged in solutions of different conductivities at 25 °C for 576 h.....	48
Figure 3.21. Percentage change in the weight of HTV SIR specimens as a function of time during recovery in stationary air at room temperature for 2700 h. The specimens had been aged in solutions of different conductivities at 50 °C for 576 h.....	49
Figure 3.22. Percentage change in the weight of HTV SIR specimens as a function of time during recovery in stationary air at room temperature for 2700 h. The specimens had been aged in solutions of different conductivities at 75 °C for 576 h.....	50
Figure 3.23. Percentage change in the weight of HTV SIR specimens as a function of time during recovery in stationary air at room temperature for 2700 h. The specimens had been aged in solutions of different conductivities at 98 °C for 576 h.....	51
Figure 3.24. Time variation of the contact angle of distilled water on the surface of HTV SIR specimens during recovery in stationary air at room	

	temperature for 2700 h. The specimens had been aged in solutions of different conductivities at 0 °C for 576 h.	55
Figure 3.25.	Time variation of the contact angle of distilled water on the surface of HTV SIR specimens during recovery in stationary air at room temperature for 2700 h. The specimens had been aged in solutions of different conductivities at 25 °C for 576 h.	56
Figure 3.26.	Time variation of the contact angle of distilled water on the surface of HTV SIR specimens during recovery in stationary air at room temperature for 2700 h. The specimens had been aged in solutions of different conductivities at 50 °C for 576 h.	57
Figure 3.27.	Time variation of the contact angle of distilled water on the surface of HTV SIR specimens during recovery in stationary air at room temperature for 2700 h. The specimens had been aged in solutions of different conductivities at 75 °C for 576 h.	58
Figure 3.28.	Time variation of the contact angle of distilled water on the surface of HTV SIR specimens during recovery in stationary air at room temperature for 2700 h. The specimens had been aged in solutions of different conductivities at 98 °C for 576 h.	59
Figure 3.29.	Time variation of the surface roughness of HTV SIR specimens during recovery in stationary air at room temperature for 2700 h. The specimens had been aged in solutions of different conductivities at 0 °C for 576 h.	63
Figure 3.30.	Time variation of the surface roughness of HTV SIR specimens during recovery in stationary air at room temperature for 2700 h. The specimens had been aged in solutions of different conductivities at 22 °C for 576 h.	64
Figure 3.31.	Time variation of the surface roughness of HTV SIR specimens during recovery in stationary air at room temperature for 2700 h. The specimens had been aged in solutions of different conductivities at 50 °C for 576 h.	65
Figure 3.32.	Time variation of the surface roughness of HTV SIR specimens during recovery in stationary air at room temperature for 2700 h. The specimens had been aged in solutions of different conductivities at 75 °C for 576 h.	66
Figure 3.33.	Time variation of the surface roughness of HTV SIR specimens during recovery in stationary air at room temperature for 2700 h. The specimens had been aged in solutions of different conductivities at 98 °C for 576 h.	67
Figure 3.34.	SEM image of the surface of a virgin HTV SIR specimen with magnification: x100 and width: 132 μm.	72
Figure 3.35.	Same as top figure except the magnification: x1000.	72

Figure 3.36. SEM image of the surface of the HTV SIR specimen aged in distilled water at 50 °C for 576 h and dried in stationary air at room temperature for 2700 h prior to the imagery; magnification: x100 and width: 132 µm.....	73
Figure 3.37. Same as the top figure, except the magnification: x1000	73
Figure 3.38. SEM image of the surface of the HTV SIR specimen aged in distilled water at 75 °C for 576 h and dried in stationary air at room temperature for 2700 h prior to the imagery; magnification: x100 and width: 132 µm.....	74
Figure 3.39. Same as the top figure, except the magnification: x1000.	74
Figure 3.40. SEM image of the surface of the HTV SIR specimen aged in distilled water at 98 °C for 576 h and dried in stationary air at room temperature for 2700 h prior to the imagery; magnification: x100 and width: 132 µm.....	75
Figure 3.41. Same as the top figure, except the magnification: x1000.	75
Figure 3.42. Energy dispersive X-ray spectrum of a virgin HTV SIR specimen ..	76
Figure 3.43. Energy dispersive X-ray spectrum of HTV SIR specimen aged in distilled water (0.005 mS/cm) at 50 °C for 576 h and allowed to recover at room temperature for 2700 h prior to spectroscopy.	77
Figure 3.44. Energy dispersive X-ray spectrum of HTV SIR specimen aged in distilled water (0.005 mS/cm) at 75 °C for 576 h and allowed to recover at room temperature for 2700 h prior to spectroscopy.	78
Figure 3.45. Energy dispersive X-ray spectrum of HTV SIR specimen aged in distilled water (0.005 mS/cm) at 98 °C for 576 h and allowed to recover at room temperature for 2700 h prior to spectroscopy.	79
Figure 3.46. Comparison between the ATR FTIR spectra of a virgin HTV SIR specimen and the aged-I, the specimen aged in saline water of 1 mS/cm conductivity at 0 °C for 576 h. The aged specimen had been allowed to recover in stationary air at room temperature for 2700 h before the spectra.	83
Figure 3.47. Comparison between the ATR FTIR spectra of a virgin HTV SIR specimen and the aged-II, the specimen aged in saline water of 100 mS/cm conductivity at 0 °C for 576 h. The aged specimen had been allowed to recover in stationary air at room temperature for 2700 h before the spectra.....	84
Figure 3.48. Comparison between the ATR FTIR spectra of a virgin HTV SIR specimen and the aged-III, the specimen aged in saline water of 1 mS/cm conductivity at 98 °C for 576 h. The aged specimen had been allowed to recover in stationary air at room temperature for 2700 h before the spectra.....	85

mS/cm conductivity at 98 °C for 576 h. The aged specimen had been allowed to recover in stationary air at room temperature for 2700 h before the spectra.....	85
Figure 3.49. Comparison between the ATR FTIR spectra of a virgin HTV SIR specimen and the aged-IV, the specimen aged in saline water of 100 mS/cm conductivity at 98 °C for 576 h. The aged specimen had been allowed to recover in stationary air at room temperature for 2700 h before the spectra.....	86
Figure 4.1. Percentage change in weight of HTV SIR specimens as a function of time during immersion in saline solutions of different conductivities at 0 °C for 3000 h.....	90
Figure 4.2. Percentage change in weight of HTV SIR specimens as a function of time during immersion in saline solutions of different conductivities at 22 °C for 3000 h.....	91
Figure 4.3. Percentage change in weight of HTV SIR specimens as a function of time during immersion in saline solutions of different conductivities at 50 °C for 3000 h.....	92
Figure 4.4. Percentage change in weight of HTV SIR specimens as a function of time during immersion in saline solutions of different conductivities at 75 °C for 3000 h.....	93
Figure 4.5. Percentage change in weight of HTV SIR specimens as a function of time during immersion in saline solutions of different conductivities at 98 °C for 3000 h.....	94
Figure 4.6. Percentage change in weight of HTV SIR specimens as a function of time during aging in stationary air at different temperatures for 3000 h.....	95
Figure 4.7. Time variation of contact angle of distilled water on the surface of HTV SIR specimens during aging in water solutions of different conductivities at 0 °C for 3000 h.....	98
Figure 4.8. Time variation of contact angle of distilled water on the surface of HTV SIR specimens during aging in water solutions of different conductivities at 22 °C for 3000 h.....	99
Figure 4.9. Time variation of contact angle of distilled water on the surface of HTV SIR specimens during aging in water solutions of different conductivities at 50 °C for 3000 h.....	100
Figure 4.10. Time variation of contact angle of distilled water on the surface of HTV SIR specimens during aging in water solutions of different conductivities at 75 °C for 3000 h.....	101
Figure 4.11. Time variation of contact angle of distilled water on the surface of HTV SIR specimens during aging in water solutions of different conductivities at 98 °C for 3000 h.....	102

Figure 4.12. Time variation of contact angle of distilled water on the surface of HTV SIR specimens during aging in stationary air at different temperatures for 3000 h.....	103
Figure 4.13. Time variation of average surface roughness of HTV SIR specimens during aging in different salinities at 0 °C for 3000 h.....	105
Figure 4.14. Time variation of average surface roughness of HTV SIR specimens during aging in different salinities at 25 °C for 3000 h.	106
Figure 4.15. Time variation of average surface roughness of HTV SIR specimens during aging in different salinities at 50 °C for 3000 h.	107
Figure 4.16. Time variation of average surface roughness of HTV SIR specimens during aging in different salinities at 75 °C for 3000 h.	108
Figure 4.17. Time variation of average surface roughness of HTV SIR specimens during aging in different salinities at 98 °C for 3000 h.	109
Figure 4.18. Time variation of average surface roughness of HTV SIR specimens during aging in stationary air at different temperatures for 3000 h.	110
Figure 4.19. Percentage change in weight of HTV SIR specimens as a function of time during recovery in stationary air at room temperature for 3000 h. The specimens had been aged in solutions of different conductivities at 0 °C for 3000 h.	113
Figure 4.20. Percentage change in weight of HTV SIR specimens as a function of time during recovery in stationary air at room temperature for 3000 h. The specimens had been aged in solutions of different conductivities at 25 °C for 3000 h.	114
Figure 4.21. Percentage change in weight of HTV SIR specimens as a function of time during recovery in stationary air at room temperature for 3000 h. The specimens had been aged in solutions of different conductivities at 50 °C for 3000 h.	115
Figure 4.22. Percentage change in weight of HTV SIR specimens as a function of time during recovery in stationary air at room temperature for 3000 h. The specimens had been aged in solutions of different conductivities at 75 °C for 3000 h.	116
Figure 4.23. Percentage change in weight of HTV SIR specimens as a function of time during recovery in stationary air at room temperature for 3000 h. The specimens had been aged in solutions of different conductivities at 98 °C for 3000 h.	117
Figure 4.24. Percentage change in weight of HTV SIR specimens as a function of time during recovery in air at room temperature for 3000 h. The specimens had been aged in stationary air at different temperatures for 3000 h.	118

Figure 4.25. Time variation of the contact angle of distilled water on the surface of HTV SIR specimens during recovery in stationary air at room temperature for 3000 h. The specimens had been aged in solutions of different conductivities at 0 °C for 3000 h.	123
Figure 4.26. Time variation of the contact angle of distilled water on the surface of HTV SIR specimens during recovery in stationary air at room temperature for 3000 h. The specimens had been aged in solutions of different conductivities at 25 °C for 3000 h.	124
Figure 4.27. Time variation of the contact angle of distilled water on the surface of HTV SIR specimens during recovery in stationary air at room temperature for 3000 h. The specimens had been aged in solutions of different conductivities at 50 °C for 3000 h.	125
Figure 4.28. Time variation of the contact angle of distilled water on the surface of HTV SIR specimens during recovery in stationary air at room temperature for 3000 h. The specimens had been aged in solutions of different conductivities at 75 °C for 3000 h.	126
Figure 4.29. Time variation of the contact angle of distilled water on the surface of HTV SIR specimens during recovery in stationary air at room temperature for 3000 h. The specimens had been aged in solutions of different conductivities at 98 °C for 3000 h.	127
Figure 4.30. Time variation of the contact angle of distilled water on the surface of HTV SIR specimens during recovery in stationary air at room temperature for 3000 h. The specimens had been aged in air at different temperatures for 3000 h.	128
Figure 4.31. Time variation of the surface roughness of HTV SIR specimens during recovery in stationary air at room temperature for 3000 h. The specimens had been aged in solutions of different conductivities at 0 °C for 3000 h.	132
Figure 4.32. Time variation of the surface roughness of HTV SIR specimens during recovery in stationary air at room temperature for 3000 h. The specimens had been aged in solutions of different conductivities at 22 °C for 3000 h.	133
Figure 4.33. Time variation of the surface roughness of HTV SIR specimens during recovery in stationary air at room temperature for 3000 h. The specimens had been aged in solutions of different conductivities at 50 °C for 3000 h.	134
Figure 4.34. Time variation of the surface roughness of HTV SIR specimens during recovery in stationary air at room temperature for 3000 h. The specimens had been aged in solutions of different conductivities at 75 °C for 3000 h.	135
Figure 4.35. Time variation of the surface roughness of HTV SIR specimens during recovery in stationary air at room temperature for 3000 h.	

	The specimens had been aged in solutions of different conductivities at 98 °C for 3000 h.....	136
Figure 4.36.	Time variation of the surface roughness of HTV SIR specimens during recovery in air at room temperature for 3000 h. The specimens had been aged in stationary air at different temperatures for 3000 h.	137
Figure 4.37.	SEM image of the surface of the HTV SIR specimen aged in distilled water at 22 °C for 3000 h and dried in stationary air at room temperature for 3000 h prior to the imagery; magnification: x100 and width: 132 µm.....	141
Figure 4.38.	Same as top figure, except the magnification: x1000.....	141
Figure 4.39.	SEM image of the surface of the HTV SIR specimen aged in distilled water at 50 °C for 3000 h and dried in stationary air at room temperature for 3000 h prior to the imagery; magnification: x100 and width: 132 µm.....	142
Figure 4.40.	Same as the top figure, except the magnification: x1000	142
Figure 4.41.	SEM image of the surface of the HTV SIR specimen aged in distilled water at 75 °C for 3000 h and dried in stationary air at room temperature for 3000 h prior to the imagery; magnification: x100 and width: 132 µm.....	143
Figure 4.42.	Same as the top figure, except the magnification: x1000	143
Figure 4.43.	SEM image of the surface of the HTV SIR specimen aged in distilled water at 98 °C for 3000 h and dried in stationary air at room temperature for 3000 h prior to the imagery; magnification: x100 and width: 132 µm.....	144
Figure 4.44.	Same as the top figure, except the magnification: x1000	144
Figure 4.45.	Energy dispersive x-ray spectrum of HTV SIR specimen aged in distilled water at 22 °C for 3000 h and allowed to recover at room temperature for 3000 h prior to the spectroscopy.....	145
Figure 4.46.	Energy dispersive x-ray spectrum of HTV SIR specimen aged in distilled water at 50 °C for 3000 h and allowed to recover at room temperature for 3000 h prior to the spectroscopy.....	146
Figure 4.47.	Energy dispersive x-ray spectrum of HTV SIR specimen aged in distilled water at 75 °C for 3000 h and allowed to recover at room temperature for 3000 h prior to the spectroscopy.....	147
Figure 4.48.	Energy dispersive x-ray spectrum of HTV SIR specimen aged in distilled water at 98 °C for 3000 h and allowed to recover at room temperature for 3000 h prior to the spectroscopy.....	148
Figure 4.49.	Comparison between the ATR FTIR spectra of a virgin HTV SIR specimen and the aged-V, the specimen aged in saline water of 1	

	mS/cm conductivity at 22 °C for 3000 h. The aged specimen had been allowed to recover in stationary air at room temperature for 3000 h before the spectra.....	151
Figure 4.50.	Comparison between the ATR FTIR spectra of a virgin HTV SIR specimen and the aged-VI, the specimen aged in saline water of 1 mS/cm conductivity at 50 °C for 3000 h. The aged specimen had been allowed to recover in stationary air at room temperature for 3000 h before the spectra.....	152
Figure 4.51.	Comparison between the ATR FTIR spectra of a virgin HTV SIR specimen and the aged-VII, the specimen aged in saline water of 1 mS/cm conductivity at 75 °C for 3000 h. The aged specimen had been allowed to recover in stationary air at room temperature for 3000 h before the spectra.....	153
Figure 4.52.	Comparison between the ATR FTIR spectra of a virgin HTV SIR specimen and the aged-VIII, the specimen aged in saline water of 1 mS/cm conductivity at 98 °C for 3000 h. The aged specimen had been allowed to recover in stationary air at room temperature for 3000 h before the spectra.....	154
Figure 4.53.	Comparison between the ATR FTIR spectra of a virgin HTV SIR specimen and the aged-IX, the specimen aged in saline water of 100 mS/cm conductivity at 98 °C for 3000 h. The aged specimen had been allowed to recover in stationary air at room temperature for 3000 h before the spectra.....	155
Figure 5.1.	Time variation of the measured contact angle of distilled water and methylene iodide on the surface of HTV SIR specimen during aging in 1 mS/cm solution at 0 °C for 3000 h and also the calculated surface free energy along with its components.....	166
Figure 5.2.	Time variation of the measured contact angle of distilled water and methylene iodide on the surface of HTV SIR specimen during aging in 1 mS/cm solution at 22 °C for 3000 h and also the calculated surface free energy along with its components.....	167
Figure 5.3.	Time variation of the measured contact angle of distilled water and methylene iodide on the surface of HTV SIR specimen during aging in 1 mS/cm solution at 50 °C for 3000 h and also the calculated surface free energy along with its components.....	168
Figure 5.4.	Time variation of the measured contact angle of distilled water and methylene iodide on the surface of HTV SIR specimen during aging in 1 mS/cm solution at 75 °C for 3000 h and also the calculated surface free energy along with its components.....	169
Figure 5.5.	Time variation of the measured contact angle of distilled water and methylene iodide on the surface of HTV SIR specimen during aging in 1 mS/cm solution at 98 °C for 3000 h and also the calculated surface free energy along with its components.....	170

Figure 5.6. Time variation of the measured contact angle of distilled water and methylene iodide on the surface of HTV SIR specimen during aging in 0.005 mS/cm solution at 98 °C for 3000 h and also the calculated surface free energy, interfacial energy and energy of adhesion. ...	171
Figure 5.7. Time variation of the measured contact angle of distilled water and methylene iodide on the surface of HTV SIR specimen during aging in 1 mS/cm solution at 98 °C for 3000 h and also the calculated surface free energy, interfacial energy and energy of adhesion. ...	172
Figure 5.8. Time variation of the measured contact angle of distilled water and methylene iodide on the surface of HTV SIR specimen during aging in 10 mS/cm solution at 98 °C for 3000 h and also the calculated surface free energy, interfacial energy and energy of adhesion.....	173
Figure 5.9. Time variation of the measured contact angle of distilled water and methylene iodide on the surface of HTV SIR specimen during aging in 100 mS/cm solution at 98 °C for 3000 h and also the calculated surface free energy, interfacial energy and energy of adhesion.....	174
Figure 5.10. Restatement of the experimental data of θ_{MI} , collected from different stress conditions during aging of HTV SIR specimens in the solutions of conductivities, 0.005, 1, 10 and 100 mS/cm as well as stationary air at 98 °C for 3000 h, as given in Figures 5.6-5.9 and also the corresponding calculated γ_{sd} , γ_{sh} , γ_s , γ_{sl} and W_{sl} as a function of time.	175
Figure 6.1. Percentage of weight gain of HTV SIR specimens during short-term immersion in hexane at 22 °C.	180
Figure 6.2. Percentage of weight loss of HTV SIR specimens during short-term evaporation in air at 22 °C.....	181
Figure 6.3. Percentage of weight gain of HTV SIR specimens during long-term immersion in hexane at 22 °C.	182
Figure 6.4. Percentage of weight loss of HTV SIR specimens during long-term evaporation in air at 22 °C.....	183
Figure 6.5. NMR spectra for analytical hexane	187
Figure 6.6. NMR spectra for silicone fluid (1000 centipoise viscosity)	188
Figure 6.7. NMR spectra of the mixture of hexane and LMW fluid extracted from the HTV SIR specimens	189
Figure 6.8. IR spectrum of the fluid extracted from HTV SIR specimens in hexane	190
Figure 6.9. IR spectrum of PDMS.....	191
Figure 6.10. Mass spectrometry (MS) of the fluid extracted from the HTV SIR insulator specimens heated in distilled water at 98 °C for 576 h..	192

Figure 6.11. Percentage of total weight loss of the HTV SIR specimens at different steps of the hexane-heat-hexane sequential treatment for five different heating durations: 2, 4, 8, 16 and 32 h.	196
Figure 6.12. Percentage of total weight loss of the virgin as well as the aged HTV SIR specimens at different steps of the hexane-heat-hexane sequential treatment	200

List of Tables

Table 1.1. General Properties of HTV SIR, EPDM and PTFE (Teflon)	6
Table 2.1. Statistical measures and calculated confidence interval of different data samples of contact angle by distilled water on the surface of a virgin HTV SIR insulator specimen	19
Table 3.1. Percentage weight gain (+) or loss (-) of the HTV SIR specimens after aging in different stress conditions at the end of 576 hours.	23
Table 3.2 Percentage of net weight gain (+) or loss (-) of the HTV SIR specimens at the end of recovery period of 2700 h after aging in different stress conditions for 576 hours.....	46
Table 3.3. Comparison between the contact angles of HTV SIR specimens at different stages: (a) contact angle of the virgin specimens, (b) contact angle after aging of 576 h, (c) contact angle after recovery of 2700 h.	53
Table 3.4. Comparison between the surface roughness of HTV SIR specimens in μm at different stages: (a) virgin specimens, (b) after aging of 576 h, (c) after recovery of 2700 h.	62
Table 3.5. Chemical component changes with temperature in HTV SIR aged in distilled water (0.005 mS/cm) for 576 h and allowed to recover at room temperature for 2700 h prior to spectroscopy.....	70
Table 3.6. Characteristic IR Absorption Bands in Silicones [10]	81
Table 4.1. Percentage weight gain (+) or loss (-) of the HTV SIR specimens after aging in different stress conditions at the end of 576 hours.....	89
Table 4.2 Percentage of net weight gain (+) or loss (-) of the HTV SIR specimens at the end of recovery period of 3000 h after aging in different stress conditions for 3000 h.	112
Table 4.3. Comparison between the contact angles of HTV SIR specimens at different stages: (a) contact angle of the virgin specimens, (b) contact angle after aging of 3000 h, (c) contact angle after recovery of 3000 h.....	122
Table 4.4 Comparison of the surface roughness of HTV SIR specimens in μm at different stages: (a) virgin specimens, (b) after aging of 3000 h and (c) after recovery of 3000 h.	131
Table 4.5. Chemical component changes with temperature in HTV SIR aged in distilled water (0.005 mS/cm) for 3000 h and allowed to recover at room temperature for 3000 h prior to spectroscopy.....	140

Table 5.1. Literature values of γ_{ld} , γ_{lh} and γ_l for water and methylene iodide [4]	161
Table 5.2. Mathematical upper limit for θ_w for selected values of θ_{MI} in order to have non-negative surface energies when using the harmonic mean approximation [73]	162
Table 5.3. Effect of temperature on the surface energy of HTV SIR specimens after immersion in saline solution of 1 mS/cm for 3000 hours.....	163
Table 5.4. Effect of water salinity on the surface energies of HTV SIR after immersion in different saline solutions for 3000 hours at 98°C.	164
Table 6.1. Chemical structures along with the corresponding molecular weights of $n^+=2, 3, 4, 5$ and 6 units of siloxane identified from the mass spectrum of the fluid extracted from the HTV SIR specimens heated in distilled water at 98 °C.....	193
Table 6.2. Percentage of weight loss of HTV SIR specimens at different steps of hexane-heat-hexane sequential treatment.....	195
Table 6.3. The HTV SIR specimens selected from different aging conditions for Hexane-Heat-Hexane test sequence. The specimens had been allowed to recover for 3000 h prior to the test sequence.	197
Table 6.4. Percentage weight loss of different aged HTV SIR specimens of Table 6.3 compared with the virgin one through sequential hexane-heat-hexane treatment.....	198

Nomenclature

ASR	average surface roughness
ATH	aluminum trihydrate
ATR FTIR	attenuated total reflectance Fourier transform infrared
EDS	energy dispersive spectroscopy
EPDM	ethylene propylene diene monomer
GC	gas chromatography
HDPE	high density polyethylene
HTV SIR	high temperature vulcanized silicone rubber
IR	infrared
LMW	low molecular weight
MI	methylene iodide
MS	mass spectrometry
NMR	nuclear magnetic resonance
PDMS	polydimethylesiloxane

PP	polypropylene
PTFE	polytetrafluoroethylene
RF	radio frequency
RTV	room temperature vulcanized
SEM	scanning electron microscope
XLPE	crosslinked polyethylene
θ_w	contact angle of droplet of distilled water on the solid surface ($^\circ$)
θ_{MI}	contact angle of droplet of MI on the solid surface ($^\circ$)
γ	surface free energy per unit area (J/m^2)
γ_{ld}	dispersive component of surface free energy of liquid (J/m^2)
γ_{lh}	polar component of surface free energy of liquid (J/m^2)
γ_l	surface free energy of liquid (J/m^2)
γ_{sd}	dispersive component of surface free energy of solid (J/m^2)
γ_{sh}	polar component of surface free energy of solid (J/m^2)
γ_s	surface free energy of solid (J/m^2)
γ_{sl}	interfacial energy of liquid and solid (J/m^2)
W_{sl}	energy of adhesion of liquid on the surface of solid (J/m^2)

CHAPTER 1

1 Introduction

1.1 General

There has been a need for electrical insulation ever since the discovery of electricity. Therefore, high voltage insulators are essential elements of any power generation, transmission and distribution system. Also, their long term performance is a major concern of the electric power industry. Insulators are used to support and insulate current carrying conductors at various voltage levels in electrical equipment for indoor and outdoor applications. There are two main characteristics of an insulating material which are taken into consideration by the designer. The first is its mechanical strength and the second is its electrical property to withstand the high voltage electrical stress. Both the mechanical and electrical roles of outdoor insulators are performed in varying environmental conditions, which include temperature variation, moisture, contamination and ultra-violet radiation from sunlight. The study of the behaviour of the external surface of the insulator is very important because it is directly exposed to these environmental as well as electrical stresses.

Porcelain and glass have been most widely used insulating materials for high voltages. These are inert, stable materials and can take a substantial amount of arcing without serious surface degradation because of their capacity to withstand the heat of dry band arcing. However, these materials are highly wettable when exposed to fog, dew, or rain because of their high surface energy [1]. On these materials, water readily forms a continuous film due to their hydrophilic surface [2]. In the presence of contamination, leakage current develops which may result in a flashover of the insulator and may be followed by a power system outage. The penalties due to power interruption may range from the loss of millions of

dollars (direct lost revenue, production costs) to possible loss of human lives and property due to a blackout in metropolitan areas.

Composite polymeric insulators are increasingly being used by the traditionally cautious electric utilities worldwide, to overcome this problem. They currently represent about 70% of the installed new high voltage insulators in North America [3]. One major advantage is their low surface energy [4-5]. Moreover, they possess superior service properties in the presence of heavy pollution and wet condition, resistance to vandalism, good electrical parameters (low dielectric permittivity, high breakdown voltage, high surface and volume resistance) and lower weight in comparison to the porcelain and glass insulators [6-8]. This light weight results in more economic design of the towers and also reduces installation as well as maintenance costs. However as polymeric insulating materials are relatively new, so their expected life time is not yet known and is of critical interest to the users.

On the choice of a polymeric material suitable for outdoor insulation, silicone rubber has shown superior performance when compared to other materials for external housings of surge arresters, insulators and bushings. There are two types of silicone rubber which are being used in the field of high voltage insulation. RTV (room temperature vulcanized) silicone rubber in which the cross-linking of polymer chains takes place at room temperature in atmospheric air and is used as coatings as well as weathersheds of high voltage insulators.

The second is high temperature vulcanized silicon rubber (HTV SIR) and is prepared from dichlorosilane which is cross linked or vulcanized, by the action of heat in the presence of a vulcanizing agent (peroxide). HTV SIR shows good electrical performance as compared to other polymeric materials like ethylene propylene diene monomer (EPDM), polypropylene (PP), polytetrafluoroethylene (PTFE), cross-linked polyethylene (XLPE) and high density poly ethylene (HDPE). Its physical properties are enhanced by compounding with fillers like

silica and alumina trihydrate. Fibreglass reinforced rod insulators with HTV SIR weather sheds are accepted as standard overhead line insulators with a good experience of voltage rating up to 765 kV_{ac} and ±500 kV_{dc} [9].

1.2 Properties of Silicone Rubber

Silicone rubber contains low molecular weight (LMW) fluid in its bulk which consists of the chemical structure of the poly dimethyl siloxane (PDMS) molecule. Figure 1.1 shows the chemical structure of the PDMS molecule. This molecule is composed of methyl groups (CH₃), silicon (Si) and oxygen (O). The methylsiloxane chain has been shown to be extremely flexible. This flexibility results from the large Si-O-Si bond angle (and consequent large spacing between methyl groups) as well as the highly ionic (about 50%) character of the siloxane bond. It means that each silicone atom is free to rotate with its attached groups, 360° about the Si-O bond [10]. The methyl groups are hydrophobic and are responsible for the water repellency.

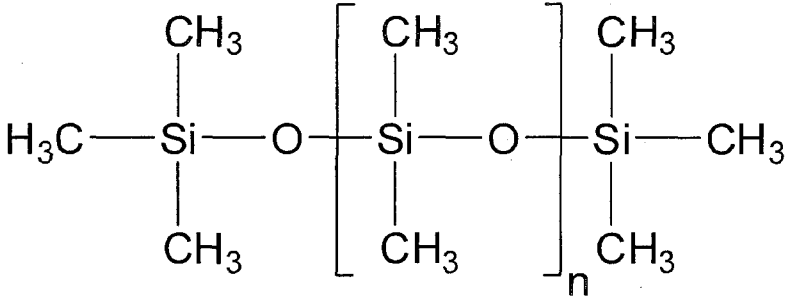


Figure 1.1 Chemical structure of polydimethylsiloxane (PDMS)

Many researchers have concluded that diffusion of LMW fluid from the bulk on to the surface regains the hydrophobicity lost by corona discharges, dust, pollution

or contamination and dry band arcing [11-20]. In addition, recovery of lost hydrophobicity during a resting period plays a significant role in determining the insulating performance in wet conditions [21-25].

1.3 Fillers in Silicone Rubber

Tracking is the production of a conductive path by arcing on the polymer surface, usually because of deposition of carbon and is conductive even under dry condition. Erosion is an irreversible and non-conducting deterioration of the surface that occurs from the loss of surface material which arises either from electrical discharges or from electrochemical reactions. Tracking and erosion increase with increasing density of leakage current and the severity of both can be limited by reducing the surface electric stress. Also, there is no such thing as a 'non-track' polymer but tracking can be minimized by two ways. One way is by avoiding known carbon generators like benzene rings and the second by arranging for liberated carbon to be scavenged by chemical means. Therefore, the filler, like hydrated alumina in conjunction with other catalysts, is used to oxidize the carbon into carbon monoxide and water vapour [26].

Like other polymers, pure silicone rubber also shows little tracking and erosion resistance; therefore, fillers like alumina tri-hydrate (ATH) and silica are added to the silicone rubber formulation. ATH and silica are the two fillers that are mostly being used by manufacturers of outdoor insulators. These fillers not only improve the tracking and erosion resistance [27-32] but also lower the cost of the materials. In general, it has been reported that the type of filler, the amount of filler and particle size have influence on the tracking and erosion resistances [33-35]. Depending on the specific formulation, fillers and additives can comprise on the order of 20% to 80% by weight of the formulation [36]. Moreover, it has been observed during a salt fog aging test that erosion and deterioration depend on the specimen configuration of the silicone rubber insulator [37].

1.4 Performance of HTV SIR (Literature Review)

The comparison of general properties of HTV SIR with EPDM and PTFE is given in Table 1. Youn and Huh [39] in their experiments exposed compounds of HTV SIR and EPDM to ultraviolet light (UV) for 5000 h and studied its effect on the surface degradation. It was observed that EPDM suffers more loss of hydrophobicity and surface resistivity than HTV SIR under ultra violet (UV) conditions. Also, HTV SIR appears to undergo mainly cross-linking reactions whereas the damage on EPDM primarily occurs through chain scission reactions followed by the generation of free radicals and oxygen-containing groups. Moreover, surface morphology showed no significant differences between unaged and aged HTV SIR samples and only a slightly larger number of loose filler particles were exposed out on the surface of aged samples. For EPDM, on the other hand, severe surface chalking and cracking were observed and significant amounts of loose filler were exposed on the sample surface

Silicone and ethylene propylene diene monomer (EPDM) rubbers were subjected to corona discharge for a specific period of time to destroy their surface hydrophobicity and later allowed to recover at various temperatures [40]. The hydrophobic recovery was monitored using the contact angle technique. It has been explained that corona discharge may generate oxide groups on the surface of the specimen. These oxide groups would have a given polarity which would give them an attraction to water. Thus the hydrophobicity and the measured contact angle would decrease. However, these oxide groups would have a higher surface free energy than the surrounding methyl groups. This surface would not be in equilibrium. The equilibrium state would be a surface with all methyl groups. Therefore, after the removal of the corona, the polar oxide groups would rotate or move into the bulk. Thus the surface would regain its hydrophobicity and the measured contact angle would increase over time. The rate of this rotation of polar groups into the bulk would be temperature dependent.

Table 1.1. General Properties of HTV SIR, EPDM and PTFE (Teflon) [9, 26, 38]

Material	HTV SIR	EPDM	PTFE (Teflon)
Specific Gravity	1.15-1.55	0.85	2.1-2.3
Density (gm/cm ³)	1.35-1.55	1.5	2.15
Minimum Service Temperature (°C)	-55	-54	-55
Maximum Service Temperature (°C)	200	177	300
Flame Resistance	Poor	Poor	Good
Tensile Strength (MPa)	11	17-24	25
Elongation, %	200	200	100-800
Dielectric Constant, ϵ_r	3.0-3.6	2.5-3.5	2.0-2.2
Volume Resistivity (Ω -cm)	10^{13}	10^{14}	10^{15} - 10^{17}
Dielectric Strength (kV/mm)	20	19.7-31.5	45
Water Resistance	Good	Excellent	Becomes wetable
Erosion Resistance	Good	Good	Good
Tracking Resistance	Excellent	Good	Excellent

Kumagai, Wang and Yoshimura [41] in Japan carried out laboratory experiments by soaking samples of ethylene-vinyl acetate (EVA), epoxy resins (EX) and silicone rubber (SIR) in boiling distilled water. According to the results, it was found that the contact angle θ decreased with the water absorbing time for all the samples. But as compared to EVA and EX, the contact angle θ of SIR does not become saturated easily and can keep its surface hydrophobicity high for longer time than other polymers. This can be attributed to the diffusion of silicone fluid of low molecular weight (LMW) chains from bulk to the surface. In other words, the water diffusion and storage on the surface are prevented by the silicone fluid motion. Also, it was suggested that the dried weight of SR decreased after it was subjected to boiling water for a long time which confirmed the migration of silicone fluid into ambient boiling water.

Zhu, Otsubo and Honda [42] in their study exposed unfilled high-temperature vulcanized SR (HTV-SR) and ATH-filled EVA specimens to corona discharges generated by a needle-plate electrode system. The test specimens used were plate-shaped of the size 60 mm×50 mm×2 mm, and the gap length between the two electrodes was kept 20 mm. The results were summarized as follows: Obvious cracks and mechanical damages caused by the corona discharge were visible on the surfaces of both the SR and EVA aged specimens. However, the surface degradation of EVA caused by the impingement of emitted photons was more severe because of the weaker linkage of its C–C backbones compared to that of siloxane bonds on silicone rubber. It has also been proved by FTIR technique that the byproducts of aging produced hydrophilic OH groups instead of hydrophobic C–H bonds on the surface of SR and EVA specimens aged by corona discharges, allowing the reduction of the hydrophobicity of polymeric materials.

Tracking tests were conducted for four polymeric materials viz ethylene propylene diene monomer (EPDM), silicone rubber (SR), high density polyethylene (HDPE) and polypropylene (PP) under both AC and DC voltage

level of 5 KV, with different concentrations of NH_4Cl in distilled water and a constant flow rate of 0.6 ml/min [31]. It was concluded that silicone rubber shows good performance compared to other three materials with AC, DC test voltages. Even though EPDM is worst in regard to tracking time, it does not show any fire hazards as that of polypropylene and HDPE. The tracking resistance of all the materials used except silicone rubber was found to be poor under DC environments. However, addition of some filler with these materials can improve their performance.

The change in weight and hydrophobicity characteristics of four HTV silicone rubber samples with different percentages (0~60%) of filler alumina trihydrate were studied [43]. The samples were put in water of conductivity 2.0 $\mu\text{S}/\text{cm}$ at different temperatures (20 °C~80 °C). It has been reported that the sample with 60% $\text{Al}(\text{OH})_3$, dissolved more into the water compared to that with 0%. The explanation for this has been given as; the surface of the silicone rubber without filler has fewer lattice holes making it difficult for silicone oil to diffuse into the water. The higher the ratio of the filler, the greater the change in weight has been observed. Also, the higher the water temperature compared with the initial condition, the greater the change in weight for the same sample. Moreover, with greater change in weight, lower hydrophobicity characteristics have been reported.

Tokoro and Hackam [7] in their experiments immersed HTV SIR specimens in a saline water at different temperatures in the range 0 to 98 °C up to 576 hours. It was concluded that the contact angle of a droplet of water on HTV SIR remained unchanged despite heating the specimens in air for 576 h in the range 0 to 98 °C. The hydrophobicity decreased after immersion in a saline solution and the decrease was larger with increasing time of immersion and increased salinity. The loss of hydrophobicity of the surface in the presence of water was due to the increased surface energy and it was largely due to the increased energy from the non-dispersive hydrogen bonding forces. Also, the increase in surface roughness

was reported with increasing Immersion time and temperature. After removal from the saline solution, the contact angle recovered in air but higher values of contact angle were obtained with increasing temperature.

Surface modification of HTV SIR resulting from corona discharges has been studied [44]. It was reported that obvious cracks and mechanical damages caused by the corona discharge appear on the aged SIR surface. Also, as ageing byproducts, hydrophilic OH groups are formed instead of hydrophobic CH₃ groups (the side chain of the original SIR) on the surface of corona-aged SIR, causing the reduction in the hydrophobicity of the polymeric materials. However, the generated hydroxyl groups physically adsorb moisture near the surface in the surroundings and this is a disadvantage of SIR when it is used as an insulating material in wet conditions.

Kim and Kim [14] measured the contact angles of silicone and EPDM rubber compounds at room temperature using water before and after the corona treatment to evaluate the change of the hydrophobicity. After the corona aging treatment, the contact angles of the test samples were measured multiple times during the recovery period from 0 (right after corona treatment) to 166 h to monitor the hydrophobicity recovery. The improvement of hydrophobicity was believed to be due to the reorientation of flexible polymer chains to the initial state during recovery. However, the hydrophobicity recovery was observed more with silicone rubber material as compared to EPDM material. This improved performance of silicone rubber as compared to EPDM rubber on account of hydrophobicity recovery is directly attributed to the diffusion or migration of LMW fluid from the bulk to the surface of the silicone rubber material which occurs more readily than that of EPDM.

1.5 The Scope of Research

The scope of this research work was guided by the following objective:

1. To determine the loss of hydrophobicity of HTV SIR after applying combined stresses of heat, wetting and salinity using saline solutions of 0.005, 1, 10 and 100 mS/cm and stationary air at 0, 25, 50, 75 and 98°C.
2. To study the changes in weight, the contact angle and the surface roughness of HTV SIR specimens during their immersion in saline solutions as a function of time, for 576 h and 3000 h.
3. To determine the surface free energies of the HTV SIR specimens as a function of time during the aging process.
4. To determine the recovery of hydrophobicity of the HTV SIR specimens as a function of time after removal of the stresses and the experimental results are to be supported by appropriate surface studies like attenuated total reflection Fourier transform infrared (ATR-FTIR), scanning electron microscope (SEM) and energy dispersive x-ray (EDS) spectroscopy in order to establish the mechanisms of loss and recovery of hydrophobicity.
5. To determine the amount of LMW fluid in HTV SIR samples by immersion in hexane after removal of the stresses and to compare it with the extracted LMW fluid from the virgin sample.
6. Characterization of the LMW fluid contents extracted from the HTV SIR insulator by the techniques like mass spectrometry (MS), nuclear magnetic resonance (NMR) and Infrared (IR) spectroscopy and to find its effect on maintaining the hydrophobicity at different temperatures.

CHAPTER 2

2 Experimental Method

2.1 Preparation of specimens

The HTV SIR specimens of size $1 \times 1 \times 0.5 \text{ cm}^3$ were cut from the weathersheds of a 46 KV outdoor insulator which had been in service for two years. The specimens had been formulated with 150 parts of alumina trihydrate $\text{Al}(\text{OH})_3$ with filler in parts per hundred (pph) by weight of HTV SIR. The filler was used to enhance the resistance to erosion and tracking from dry band discharges. The insulators did not fail while in service and were removed during upgrading of the system. The insulators were exposed to environmental stresses like rain, snow, humidity, ambient temperatures ranging from -30 to $35 \text{ }^\circ\text{C}$ as well as electrical stresses during the service. The surface of the specimens was cleaned using mild acetic acid (5 %) with distilled water in the ratio of 1:10 in an ultrasonic cleaner for five minutes. Afterwards, any remainder particles were removed using a soft brush and distilled water. The weight of the specimens was measured at different time intervals using a high precision (10^{-4} g) balance (Sartorius AG Gottingen Model BP110S).

2.2 Conductivity and Temperature of Saline Solution

In order to proceed with the experiments, solutions of four conductivity levels 0.005, 1, 10 and 100 mS/cm were used. The distilled water had a typical conductivity of $5 \text{ } \mu\text{S/cm}$ and table salt (NaCl) was added to the distilled water in order to increase the conductivity level. The conductivity of the solutions was measured by using a liquid conductivity meter (HORIBA ES-12). The specimens were subjected to combined thermal, water and salt stresses in glass containers containing saline solutions of four different conductivity levels. Five different temperatures of the solutions were 0, 25, 50, 75 and 98°C .

Three VWR_brand 1350GM microprocessor controlled gravity convection ovens were used in order to keep constant temperatures of 50, 75 and 98 °C over a long period whereas a refrigerator was utilized for 0 °C. The specimens were also aged in air at these temperatures. The weight, contact angle and surface roughness of each specimen were measured before immersion.

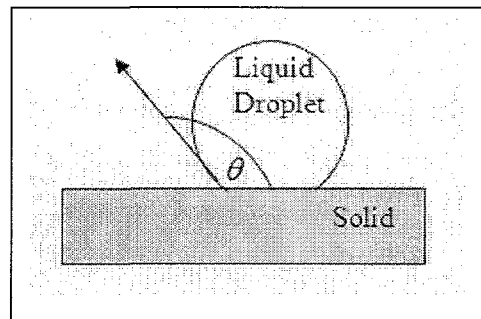
2.3 Measurement of Surface Roughness

The surface roughness of organic high voltage insulators has a direct influence on the development of leakage current and the initiation of dry band discharges. Therefore, it should be measured in order to study the degradation level of the surface of insulators due to the effect of salinity, wetness and heat during the aging process. The surface roughness can be determined by two methods: by a roughness detector or by a scanning electron microscope (SEM). In this study, both techniques have been used to explain the changes on the surface of HTV SIR specimens during aging and recovery process. The surface behaviour of the organic insulators using these techniques has previously been reported [7, 38].

The average surface roughness of the specimens was measured by using a roughness detector of type Mitutoyo SurfTest-212 having a high resolution of $\pm 0.05 \mu\text{m}$. The average surface roughness (ASR) is defined as the arithmetic average of the absolute surface roughness profile values throughout the evaluation length. The evaluation length was fixed at five times the cutoff length (0.8 mm). Therefore, for each reading, the detector completes a traversing length (1 mm + 0.8 x 5 mm) of 5 mm including 1 mm of start up length. On the other hand, the maximum surface roughness (MSR) is given as the maximum peak to valley height of the five adjacent sampling lengths. As hydrophobicity of a solid surface depends on the average surface roughness and not on maximum surface roughness, therefore, ASR has been measured throughout this research work in order to observe the changes on the surface of the HTV SIR specimens.

2.4 Contact Angle

The contact angle θ of a liquid droplet is defined as the angle between the surface of the solid and the tangent to the surface of the droplet at the point of contact to the horizontal surface. The higher the value of the contact angle, the solid surface is said to be more hydrophobic and vice versa. This contact angle depends on the surface tension (surface free energy) of the liquid as well as that of the solid surface on which the contact angle is measured. If the system is at rest, the measured contact angle is called the static contact angle whereas the measured contact angle is called the dynamic contact angle when the system is dynamic.



2.5 Measurement of the Contact Angle

The contact angle was measured by placing the specimen on a stable horizontal surface of the goniometer. This set up comprises two stands, one holds a horizontal platform and the other holds a vertical syringe. The one ml syringe was used to control the size of the water droplet within 4-5 μl in order to maintain the uniformity of the measurements throughout the course of experiments. A table lamp was used to illuminate the droplet clearly through the eyepiece of the goniometer. This technique of measuring the contact angle using a goniometer is very reliable as well as simple and known as "direct observation or tangent method" which is one of the several "sessile drop methods". The contact angle was measured within 30 s after placing the droplet of liquid on the specimen in order to minimize the effect of evaporation or absorption of liquid by the surface. Each contact angle reading used in this study is actually an average of five readings taken at different locations on the same specimen.

In order to ensure the reproducibility of the results, three specimens were used for each salinity-temperature condition. The contact angle of each washed virgin specimen was measured before the aging process and it was observed to be $100\pm 5^\circ$. The measured contact angle on the cleaned surface was found to be in reasonable agreement with the previously reported values in SIR of $95\pm 3^\circ$ [21], $96\pm 4^\circ$ [45], $97.3\pm 2.7^\circ$ [46], $98.8\pm 2.3^\circ$ [7], 100° [47, 13], 101° [48] and 105° [49].

Contact angle of a liquid droplet on the solid surface either decreases or increases with temperature, depending on the relative magnitudes of the surface entropies of the phases. This change in contact angle is quite small, about 0.05 degree/ $^\circ\text{C}$ at ordinary temperatures. However, when the temperature reaches the boiling point, the liquid surface tension decreases rapidly and ultimately, the contact angle approaches zero accordingly [4]. All the measurements of the contact angles in the present work were taken at $22\pm 3^\circ\text{C}$ and therefore, the overall change in the contact angle due to change in the ambient temperature within the range of $22\pm 3^\circ\text{C}$ is negligible.

Distilled water of conductivity $\sim 5\ \mu\text{S}/\text{cm}$ was used throughout the course of this study. The contact angle of a liquid droplet also depends on the time lapse between placing the sessile droplet on the solid surface and taking its measurement. The variation of the contact angle with time after placing a droplet of distilled water of $4\sim 5\ \mu\text{l}$ on the surface of the HTV SIR specimen is shown in Figure 2.1. The contact angle of the droplet decreased gradually from 105° to 75° after a lapse of 20 minutes.

Generally, the accuracy of the measurement of contact angle is not limited by the experimental technique, but by the reproducibility of the surfaces investigated. Instruments that measure to an accuracy of 1° are usually more than adequate. Usually, there is a good agreement among the results obtained by various methods if appropriate precautions are taken. There are several methods to measure the contact angles for liquids on solids in air. Most of these can also be

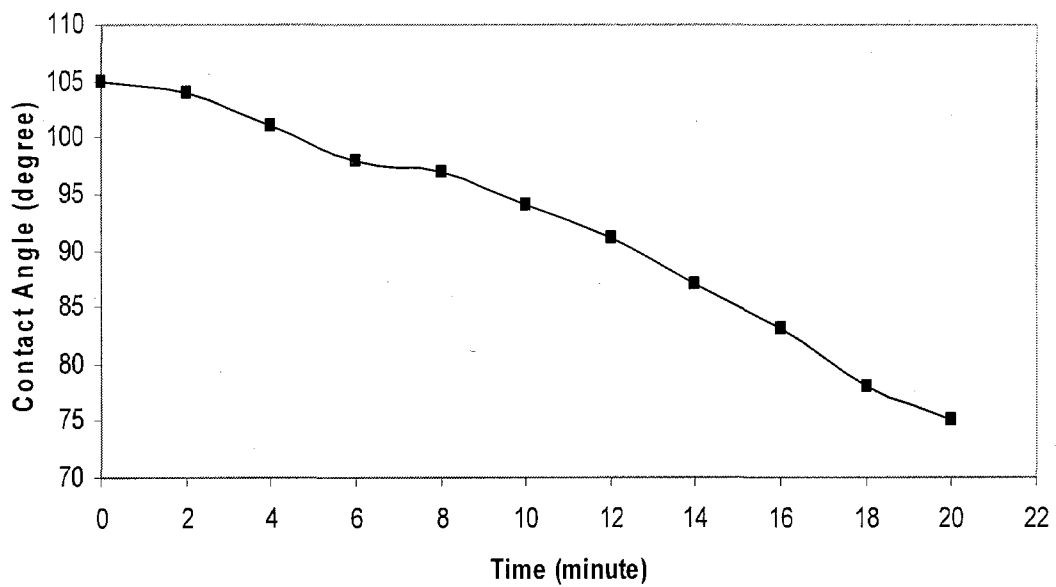


Figure 2.1. Variation in the contact angle of water as a function of time after placing the droplet on the surface of HTV SIR specimen. Conductivity of water is 0.005 mS/cm and the volume of droplet 4-5 μ l

used, with slight modifications, for liquids on solids immersed in other liquids. These are Drop-Bubble Methods, Tensiometric Method, Level-Surface Method and Capillary Rise Method [50]. Here, we will discuss only the Drop-Bubble Methods.

2.6 Drop-Bubble Methods

These methods use either liquid drops or air bubbles resting on plane solid surfaces. They are also known as “sessile drop methods” when liquid drops are used and “captive drop methods” when air bubbles are used. Direct Observation-Tangent Method, Reflected Light Method, Interference Microscopy Method, Determination from Drop Dimensions and Formation of Drops are different types of Drop-Bubble Methods [50].

2.6.1 Direct Observation-Tangent Method

This method has been used in this research and is the most commonly used method for measuring the contact angle involving direct observation of the profile of a liquid drop or an air bubble being placed on a plane solid surface. The contact angle θ is obtained by measuring the angle between the tangent to the droplet at the point of contact with the solid surface. This measurement method can be used in three different ways, first on a projected image, second by photograph of the drop profile and third directly measured using a telescope fitted with a goniometer eyepiece. Accuracy of the contact angle measured using this method is ± 1 or 2° . The range of the contact angles measured in this method is $10-160^\circ$ and uncertainty below and above this range is due to difficulty in locating the point of contact for inserting a tangent. Although, this method is simple and cheap, even then it is a very reliable and commonly used technique for measuring the contact angle in the above range [38, 50-51]

2.6.2 Reflected Light Method

In this method a light beam emitted from a microscope at right angles to the droplet surface is reflected back into the microscope. This reflected light beam is used to measure the contact angle and the limitation of this method is that the contact angle should be less than 90° . Moreover, all unwanted reflections must be eliminated from the drop surface in order to take the reading [38, 50-51].

2.6.3 Interference Microscopy Method

This method conquers the discrepancies of the tangent method as well as the reflected light method and is used to measure the contact angles less than 10° to an accuracy of $\pm 0.1^\circ$. In this method, a monochromatic light (5461-Å green mercury line) is reflected with a beam splitter onto the reflecting substrate to form interference bands parallel to the drop edge. Then, the contact angle is calculated from the spacing of the interference bands, the refractive index of the liquid and the wavelength of the light [38, 50-51].

2.6.4 Drop Dimensions Method

In this method, the contact angles are determined by measuring the dimensions of a liquid drop. The distorting effect of gravity is negligible for very small drops of the order of 10^{-4} ml and the drop takes the shape of a spherical segment, whereas for larger drops, the drop shapes are distorted by gravity and the drop profiles are described by some trigonometric equations. So, the contact angle θ can be calculated by the trigonometric relationship of the drop geometry [50].

2.6.5 Formation of Drops

Microsyringe is commonly used to place the liquid drops on solid surface suitable for contact angle measurement. Advancing and receding contact angles can be obtained by increasing or decreasing the drop volume until the three-phase boundary moves over the solid surface. There should be no vibration and distortion of the drop during the volume change in order to obtain reproducible results [50].

2.7 Accuracy of the Measurements

Contact angle of a droplet of distilled water of $\sim 5 \mu\text{l}$ on the surface of a washed virgin HTV SIR specimen has been measured 33 times at different locations and is shown in the shape of a graph in Figure 2.2. A statistical measure, confidence interval has been used to ensure/confirm the accuracy of the direct observation method for measuring the contact angle using a goniometer.

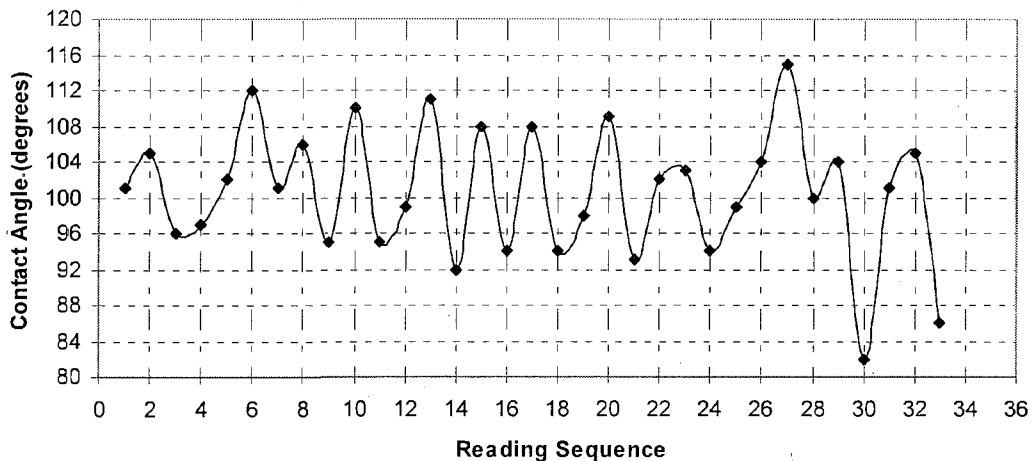


Figure 2.2. Data sample of 33 readings of the contact angle of a droplet of distilled water on the surface of a virgin HTV SIR specimen.

Basic statistical measures as well as the calculated 95% confidence interval for the specimen consisting of all 33 readings and the first five readings of the sampling are shown in Table 2.1. The definitions of some statistical concepts including confidence interval and a brief explanation of their calculation can be found in Appendix A. By rearranging the contact angle data, Minimum = 82°, Maximum = 115°, the median is found to be 101° which is 17th value in this case. Mean is 101 which is the average value of all the 33 readings and the Standard Deviation = 7.3. The unknown mean μ of the contact angle can be calculated, with 100(1- α) or 95% confidence limit, by the following procedure:

Here, in the case of five readings, the probability of next readings to fall between $100 \pm 4.6^\circ$ is more than 95 % which is good enough for the purpose of this study. However, it is worth mentioning here that the confidence interval does not tell us anything about the distribution of the actual collected data.

Table 2.1. Statistical measures and calculated confidence interval of different data samples of contact angle by distilled water on the surface of a virgin HTV SIR insulator specimen

n	Min	Max	Mean	Mode	Median	Standard Deviation	95% Confidence Interval
33	82	115	101	94, 101	101	7.28	(98.5, 103.5)
5	96	105	100	no mode	101	3.71	(95.4, 104.6)

CHAPTER 3

3 Surface Properties of HTV SIR Insulator during Short Term Aging

3.1 Introduction

Electrical utilities demand long life, high reliability and stability of high voltage insulators against degradation during service caused by salinity and oxidation in the presence of moisture and electric stress. HTV silicone rubber has outstanding electrical and mechanical properties which make it suitable for use as a high voltage insulator. In this chapter, the loss of hydrophobicity of HTV SIR in the presence of saline solutions of different conductivities and at different temperatures is reported. For this purpose, the HTV SIR specimens of size 1 x 1 x 0.5 cm³ were cut from the weather-sheds of a 46 kV outdoor insulator which had been in service for two years. The specimens were formulated with 150 parts of alumina trihydrate Al(OH)₃ filler in parts per hundred (pph) of weight of HTV SIR. The details regarding the preparation of the samples are given in chapter 2.

Hydrophobicity is the ability of solid materials to resist the formation of a continuous film of water, whereas the degradation of the insulators during service in wet and polluted conditions in the presence of high electric stress causes loss of hydrophobicity of the material. Therefore, the percentage changes in weight of the specimens during immersion in saline solution and afterwards their recovery as a function of time were measured using a high precision balance. The changes in surface roughness and hydrophobicity and their correlation with the weight of the specimens are also reported.

In this study, the samples of HTV SIR were immersed in glass jars containing different saline solutions that were kept at different temperatures for 576 hours.

Similar studies have previously been conducted on different high voltage organic insulating materials in order to observe their surface behavior during aging at different temperatures and the recovery of all the samples at room temperature. In the literature, different time durations utilized for aging were 576 h for HTV SIR [7] as well as for EPDM [55-56] and 336 h for Nylon [57-59].

3.2 Effect of Temperature and Saline Water on Weight

The weight of the HTV SIR specimens was measured at different time intervals during aging as well as during the recovery process using a Sartorius AG Gottingen Model BP110S balance having high precision and a resolution of 10^{-4} g. For each reading of weight, contact angle and surface roughness during the aging period, specimens were taken out of the jars, washed by a spray of distilled water and dried at room temperature for less than five minutes. Figures 3.1 to 3.5 show the percentage change in weight during immersion as a function of time due to absorption of water having four different conductivity levels of 0.005, 1, 10 and 100 mS/cm. At the same time, these saline solutions were kept at four different temperatures 0 ± 1 , 22 ± 3 , 50, 75 and 98 °C.

The absorption is the uptake of liquids or vapors by a material and sorption is usually a synonym for absorption, but may be used in reference to equilibrium uptake. As the HTV SIR specimens are immersed in saline solution, water penetrates into the polymer samples. It interacts strongly with polar groups of the polymer and forms clusters which are confined by the polymer chains. Water absorption causes degradation of the polymer by inducing some physical changes like swelling, alteration of tensile strength, hardness and dielectric constant [60].

Figure 3.1 shows the increase in weight after 576 h of immersion at 0 °C which is 0.59, 0.44, 0.38 and 0.1 % for solutions having conductivities of 0.005, 1, 10 and 100 mS/cm, respectively. Figure 3.2 shows the increase in weight at 22 °C and is

1.03, 0.89, 0.75 and 0.17 % for solutions having conductivities of 0.005, 1, 10 and 100 mS/cm respectively. Similarly, the increase in weight at 50 °C is 1.64, 1.21, 0.83 and 0.19 % for solutions having conductivities of 0.005, 1, 10 and 100 mS/cm respectively. As shown in Figures 3.1-3.3, there is a trend of increasing weight even after 576 hours of immersion at 0-50 °C for all conductivities except for 100 mS/cm at 50 °C which has almost reached the saturation point.

As shown in Figure 3.4, the maximum weight increase of 1.65 % reached after 300 hours of immersion in the solution of 0.005 ms/cm at 75 °C and then, it started decreasing. Also, a maximum weight increase of 1.22 and 0.92 % observed after 192-300 hours of immersion in the solutions of 1 and 10 ms/cm, respectively. However, the weight reached a saturation point of 0.19 % only after 50-96 hours of immersion in 100 mS/cm solution.

Figure 3.5 shows a greater change in weight over a short period of time at 98 °C as compared to the temperature range 0-75 °C. There was an increase in weight up to saturation and then it decreased with a greater weight-decrease gradient for all salinity levels. This may be due to the fact that the heat dissolved the silicone oil in the polymer material allowing it to escape. As the binding energy of Si-C (4.5 eV) is lower than that of Si-O (8.3 eV), so the Si-C bonding is broken down more easily and dissolved into the water [43].

The main cause of weight increase during immersion is due to the filler alumina trihydrate which has high water absorption characteristics. However, temperature also affects the amount of water that is absorbed and in order to understand this effect, one must understand the principle of glass transition temperature, T_g . This is a characteristic temperature above which the polymer chains are relaxed, mobile and rubbery and water diffusion above T_g is normally faster. Some of the absorbed water molecules undergo varying degrees of H-bonding to polar sites along the polymer chains and others are found in the pores formed by spaces

between the polymer chains [61]. During the experiments, it has been observed for all the conductivity levels that there is a greater change in weight as a function of time with the increase of temperature. This is consistent with the previous studies on HDPE [62], XLPE [63] and silicon rubber [7, 43, 64].

Figure 3.6 shows the changes in weight of the specimens kept in air at the five different temperatures described above. At 0 °C, there was a minor increase in weight of 0.07 % initially and afterwards there was no change. At 25 °C (room temperature), the minor change in weight is only due to variation in humidity. At 50 and 75 °C, there was a decrease in weight of 0.13 and 0.25 % respectively and afterwards, it became constant. This decrease in weight at a faster rate in the first few hours might be due to the instantaneous evaporation of water contents of the specimens at temperatures higher than room temperature. However, at 98 °C, a continuous decrease in weight has been observed over the entire period of 576 hours. Table 3.1 shows a summary of the changes in weight of the HTV SIR specimens during the aging process as explained above.

Table 3.1. Percentage weight gain (+) or loss (-) of the HTV SIR specimens after aging in different stress conditions at the end of 576 hours.

Aging Temperature (°C)	Aging in Air	Aging in Saline Water (mS/cm)			
		0.005	1	10	100
0	0.07	0.59	0.44	0.38	0.10
25	-0.02	1.03	0.89	0.75	0.17
50	-0.13	1.64	1.21	0.83	0.19
75	-0.25	1.44	1.01	0.80	-0.03
98	-0.64	-0.66	-0.85	-1.53	-1.71

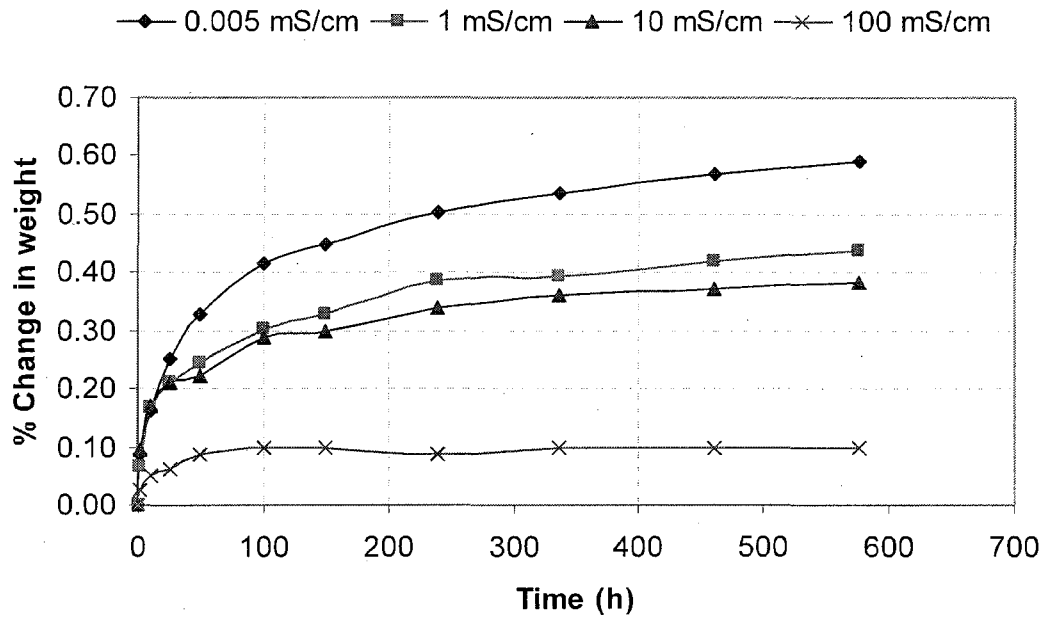


Figure 3.1. Time variation of percentage change in weight of HTV SIR specimens immersed in solutions of different conductivities at 0 °C during aging for 576 h.

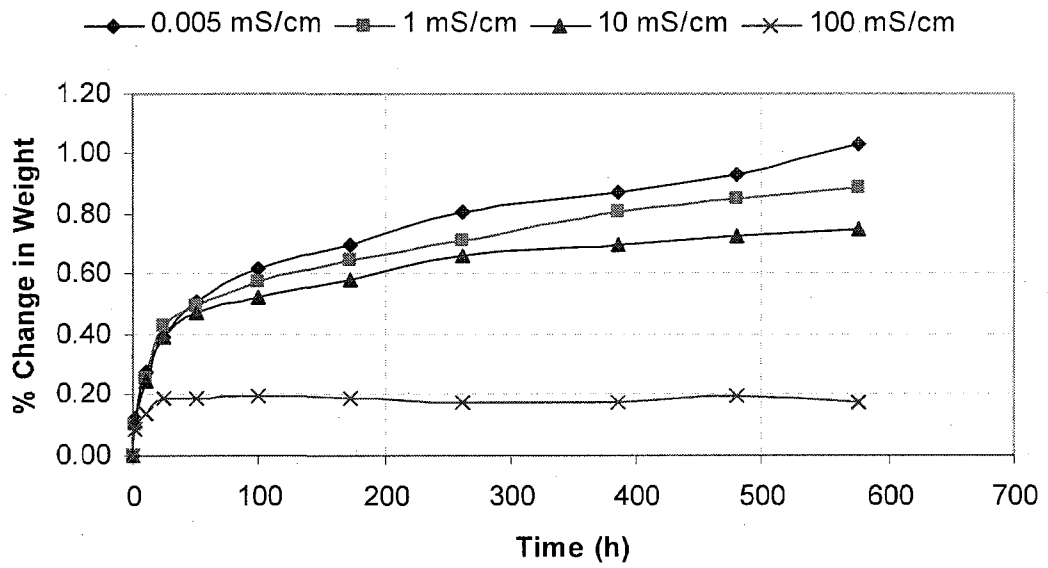


Figure 3.2. Time variation of percentage change in weight of HTV SIR specimens immersed in solutions of different conductivities at 22 °C during aging for 576 h.

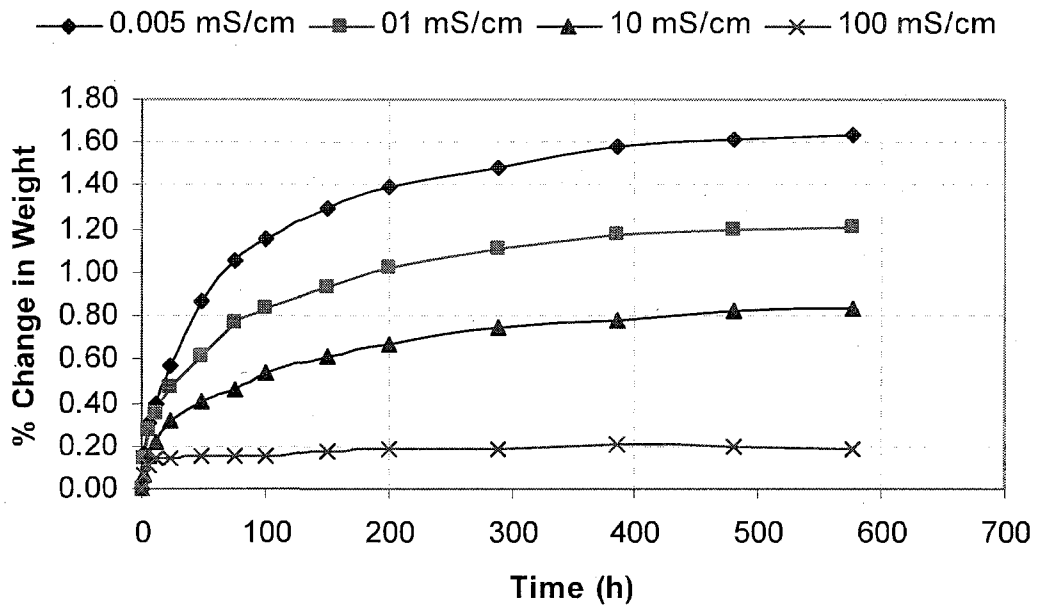


Figure 3.3. Time variation of percentage change in weight of HTV SIR specimens immersed in solutions of different conductivities at 50 °C during aging for 576 h.

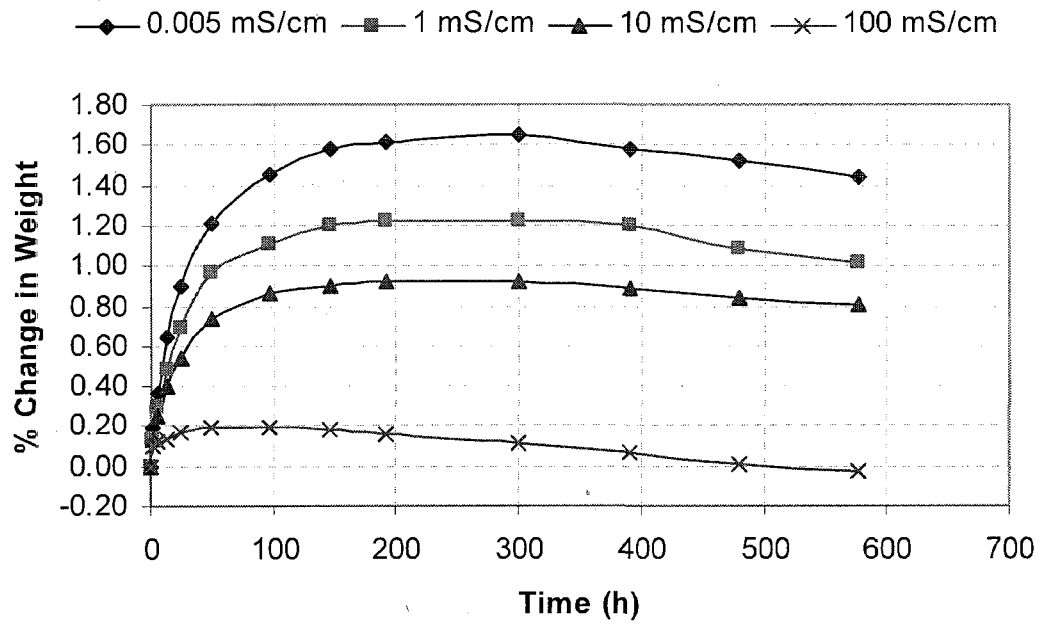


Figure 3.4. Time variation of percentage change in weight of HTV SIR specimens immersed in solutions of different conductivities at 75 °C during aging for 576 h.

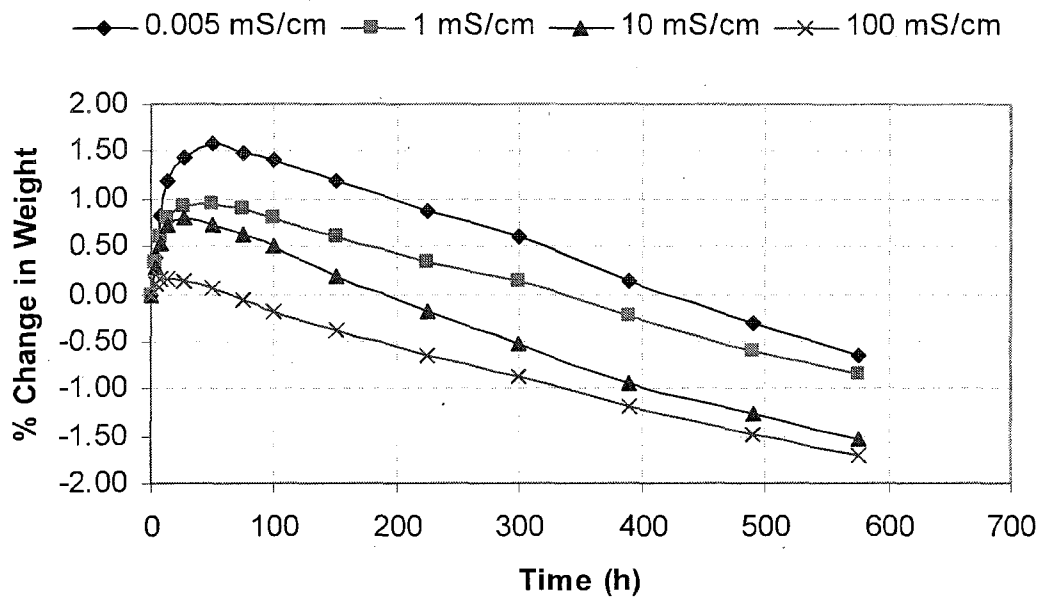


Figure 3.5. Time variation of percentage change in weight of HTV SIR specimens immersed in solutions of different conductivities at 98 °C during aging for 576 h.

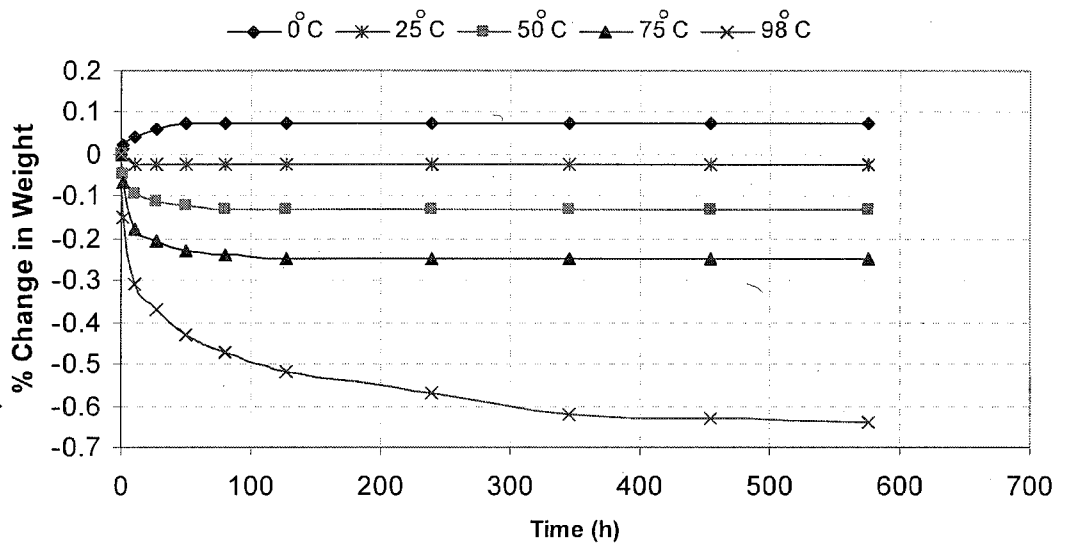


Figure 3.6. Percentage change in weight of HTV SIR specimens as a function of time during aging in stationary air at different temperatures for 576 h.

3.3 Effect of Temperature and Salinity on Contact Angle

The contact angle and its measurement techniques have already been explained in detail in chapter 2. Each reading of contact angle is actually, an average of at least five readings at different locations on the same specimen. Figures 3.7 to 3.11 show the variation of contact angle on the surface of the HTV SIR specimens as a function of time at temperatures of 0, 22, 50, 75 and 98 °C, respectively. There is an appreciable decrease in the contact angle within the first two hours of immersion and afterwards, this decrease is slow. For each temperature, four solutions of different conductivities of 0.005, 1, 10 and 100 mS/cm were used. The contact angle of the virgin specimen was measured to be $100 \pm 5^\circ$.

Figure 3.7-3.11 show that in the beginning, the contact angle and therefore the hydrophobicity decreased appreciably when the samples were immersed at 0-98 °C regardless of the conductivity of the solution. The greater decrease in the contact angle was observed at low salinity level and with increasing time of immersion. It is worth mentioning here that every time salt particles were removed from the surface by a spray of distilled water before measurement of the contact angle. A decrease in the contact angle of distilled water on the surface of HTV SIR specimens with the increase of salinity during aging has previously been reported [7] which is inconsistent to these observations. This decrease in the contact angle at high salinity might be related to the presence of salt particles on the surface of the specimens.

The greater loss of hydrophobicity for the specimens immersed in distilled water (0.005 mS/cm) may be linked to the greater change in weight due to absorption of water as is seen from Figures 3.7-3.11. This is consistent with the previous report in which it has been explained that the greater the change in weight, the lower the hydrophobicity characteristics. Also, moisture in the samples causes a reduction of the contact angle on the surface of the polymer, which is an indication of reduced hydrophobicity characteristics. This is a result of cohesive

forces present between the base polymer and filler particles, which are due to the difference between their coefficients of thermal expansion [43].

Figure 3.12 shows the change in contact angle of HTV SIR specimens kept in air at different temperatures from 0 to 98 °C. There was a slight decrease in contact angle at 0°C whereas effectively no change was observed at 22 °C. However, there was an increase in contact angle with the increase of temperature from 50 to 98°. This increase is consistent with the previous report [65] in which the increase in contact angle in the range from 105° to 115° has been observed at a temperature of 102 °C.

The change of wettability must be caused by structural changes in the polar groups of silicone rubber during immersion and this re-orientation of the polar groups can occur during only two minutes of immersion [66]. At the end of 576 h, there was a net decrease of 21, 16, 13 and 17° in the contact angles for 0.005, 1, 10 and 100 mS/cm saline solutions, respectively at 0°C. The reduction in the contact angle and therefore the loss of hydrophobicity was largely due to the absorption of water in the surface of the specimens. The higher decrease of the contact angle at low salinity levels is related to higher rate of absorption of water into the polymer during aging.

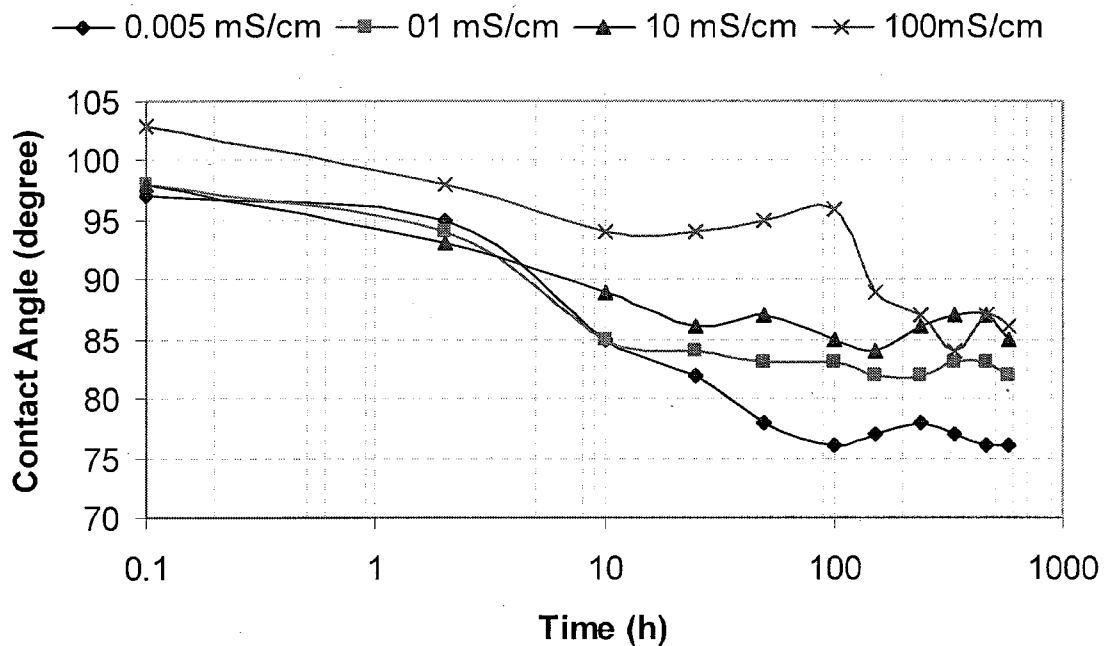


Figure 3.7. Time variation of contact angle of distilled water on the surface of HTV SIR specimens during aging in water solutions of different conductivities at 0 °C for 576 h.

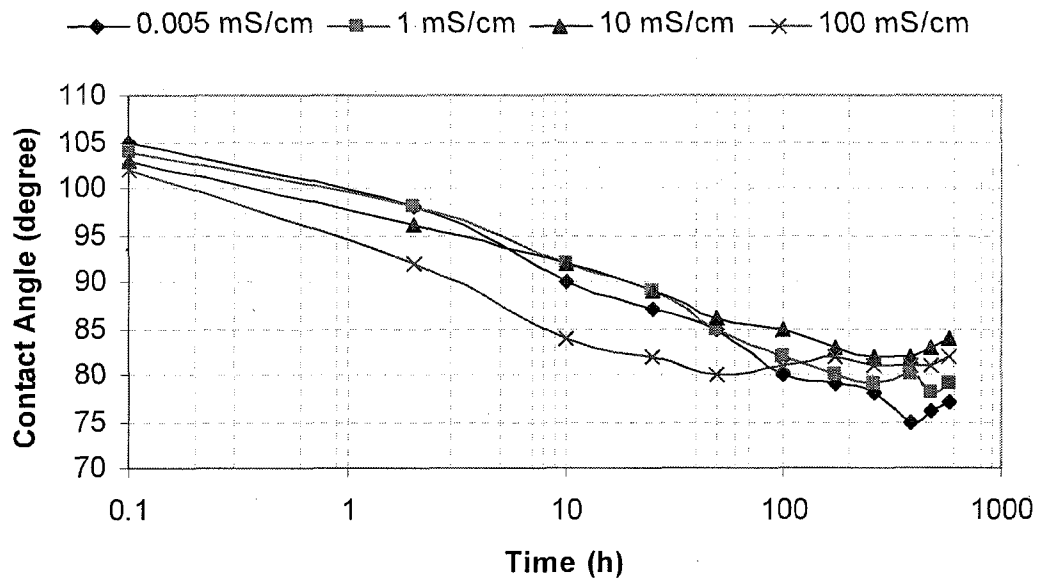


Figure 3.8. Time variation of contact angle of distilled water on the surface of HTV SIR specimens during aging in water solutions of different conductivities at 22 °C for 576 h.

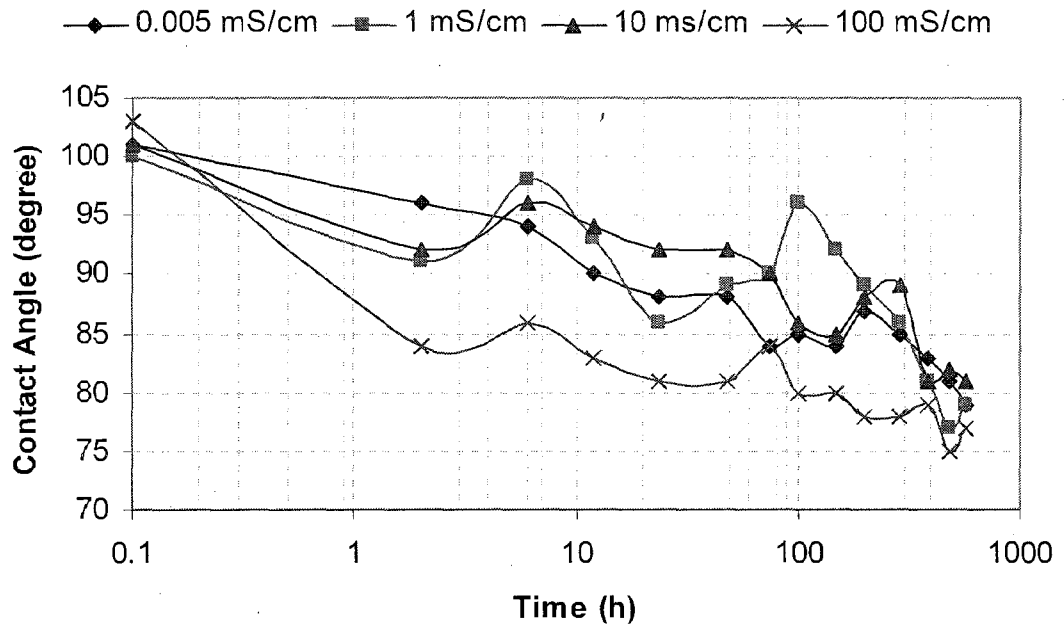


Figure 3.9. Time variation of contact angle of distilled water on the surface of HTV SIR specimens during aging in water solutions of different conductivities at 50 °C for 576 h.

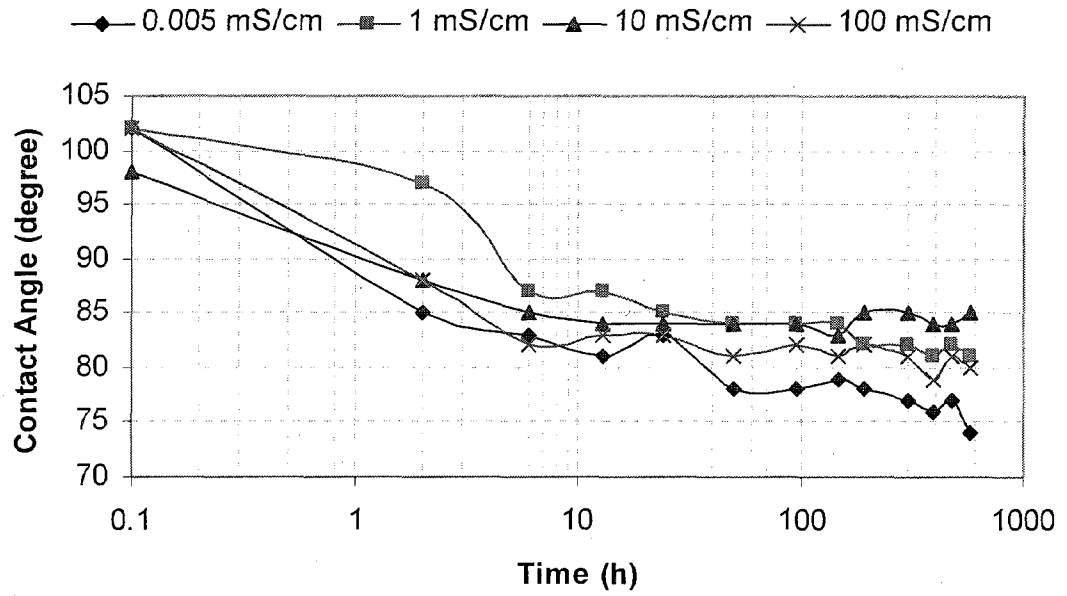


Figure 3.10. Time variation of contact angle of distilled water on the surface of HTV SIR specimens during aging in water solutions of different conductivities at 75 °C for 576 h.

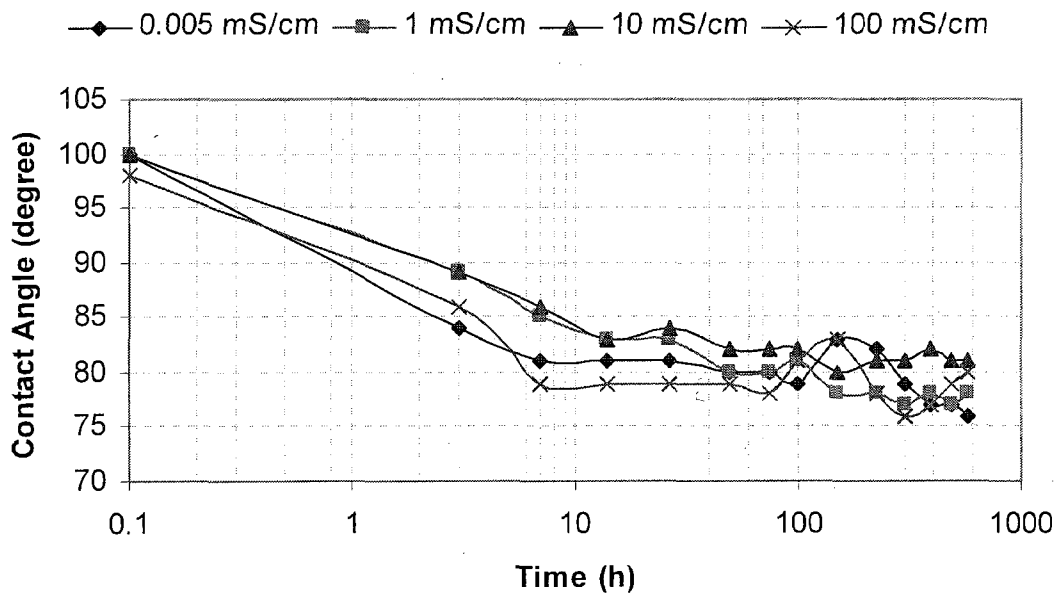


Figure 3.11. Time variation of contact angle of distilled water on the surface of HTV SIR specimens during aging in water solutions of different conductivities at 98 °C for 576 h.

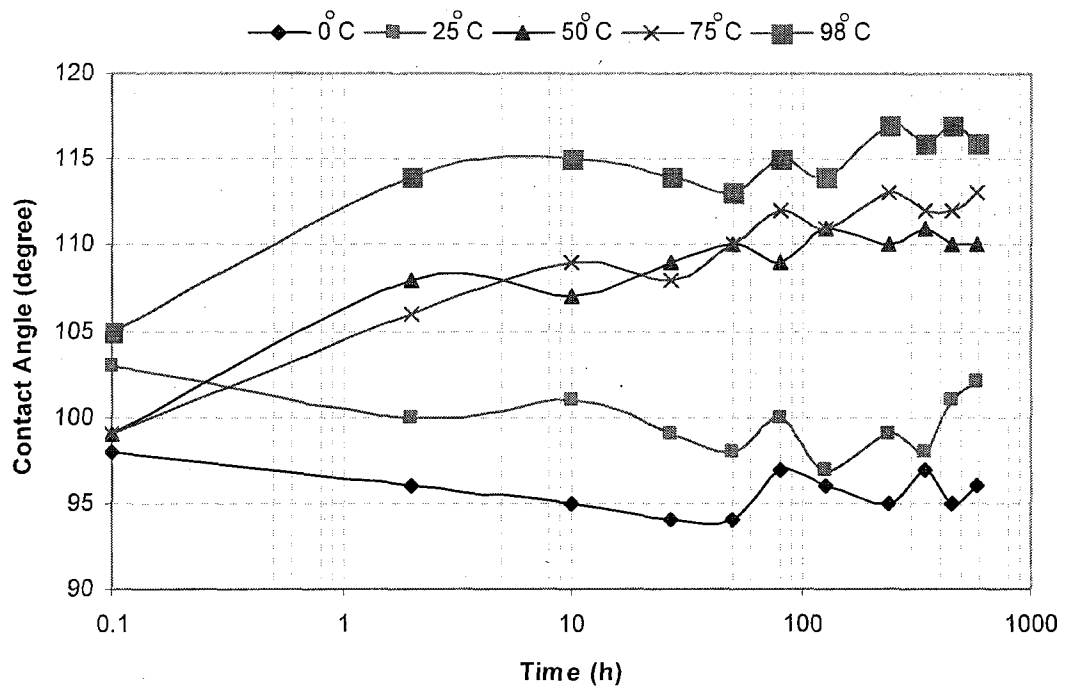


Figure 3.12. Time variation of contact angle of distilled water on the surface of HTV SIR specimens during aging in stationary air at different temperatures for 576 h.

3.4 Effect of Temperature and Salinity on Surface Roughness

It has been reported that the degree of hydrophobicity of insulating materials depends on the surface roughness and only samples of equal surface roughness can be reasonably compared to each other. Moreover, the hydrophobicity transfer into the pollution layer is slowed down with increasing roughness of the insulating material [67]. Therefore, the average surface roughness (ASR) was measured before and after the immersion of the specimens in the saline solution. The ASR of the virgin specimens was found varying between 0.40-0.80 μm and was determined using the roughness detector Mitutoyo SurfTest-212 having high resolution $\pm 0.01 \mu\text{m}$.

The variation in ASR of HTV SIR specimens as a function of time during immersion in saline solutions of different conductivities for 576 hours at 0, 25, 50, 75 and 98 $^{\circ}\text{C}$ is shown in figures 3.13-3.17, respectively. The maximum increase in ASR of up to 0.16 μm has been observed for the specimens immersed in distilled water (0.005 mS/cm) which might be related to the greater rate of water absorption in low conductivity solutions.

There is not any appreciable difference in the ASR of HTV SIR specimens during immersion in solution of 100 mS/cm up to a temperature of 75 $^{\circ}\text{C}$. This could be related to a very low rate of water absorption of the specimens in high conductivity solutions. However, a minor increase in ASR was observed at 98 $^{\circ}\text{C}$ in a solution of 100 mS/cm. This increase in ASR might be the result of decrease in weight as a function of time. It has been observed that a variation in weight caused a variation in ASR accordingly. Figure 3.18 shows a change in ASR as a function of time in air at different temperatures which is not appreciable at any temperature.

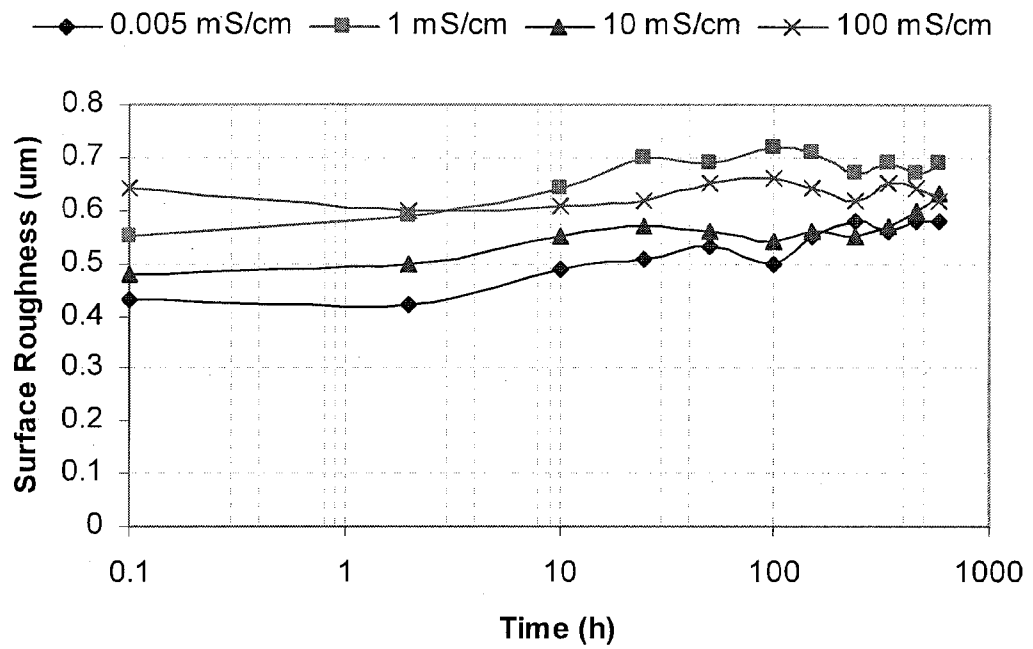


Figure 3.13. Time variation of average surface roughness of HTV SIR specimens during aging in different salinities at 0 °C for 576 h.

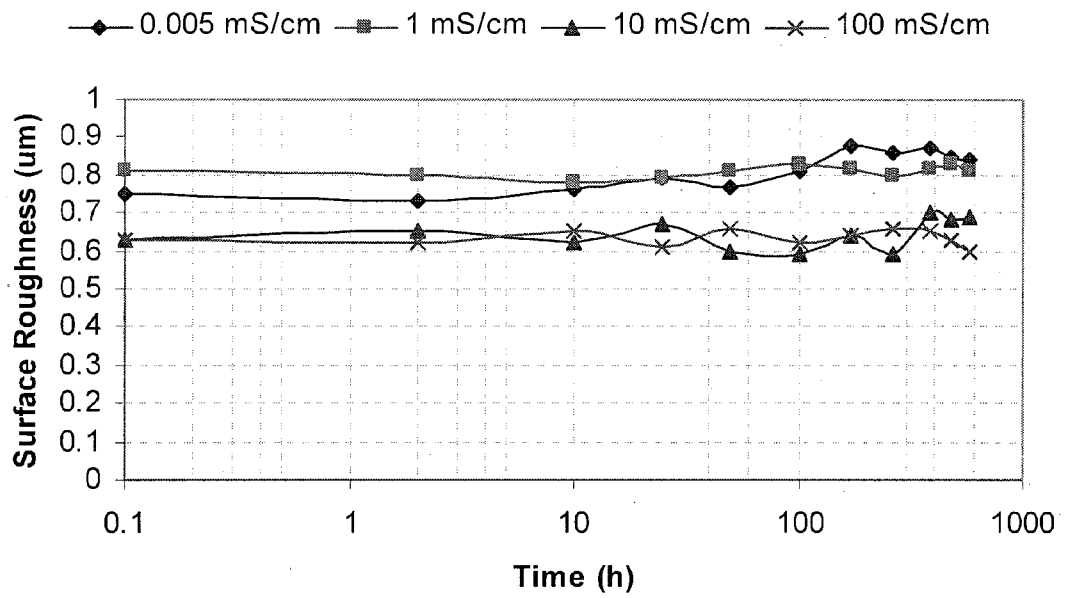


Figure 3.14. Time variation of average surface roughness of HTV SIR specimens during aging in different salinities at 22 °C for 576 h.

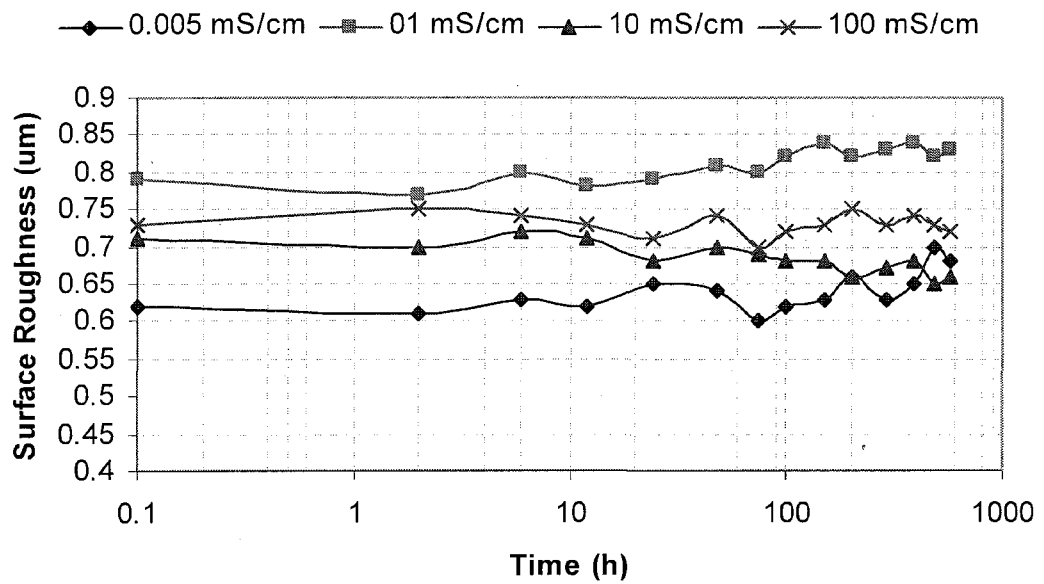


Figure 3.15. Time variation of average surface roughness of HTV SIR specimens during aging in different salinities at 50 °C for 576 h.

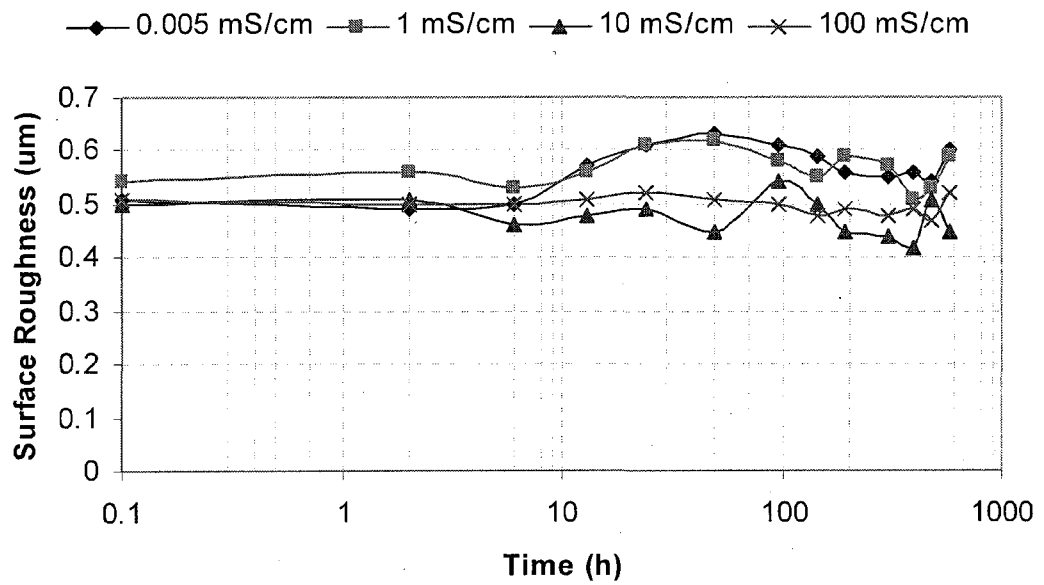


Figure 3.16. Time variation of average surface roughness of HTV SIR specimens during aging in different salinities at 75 °C for 576 h.

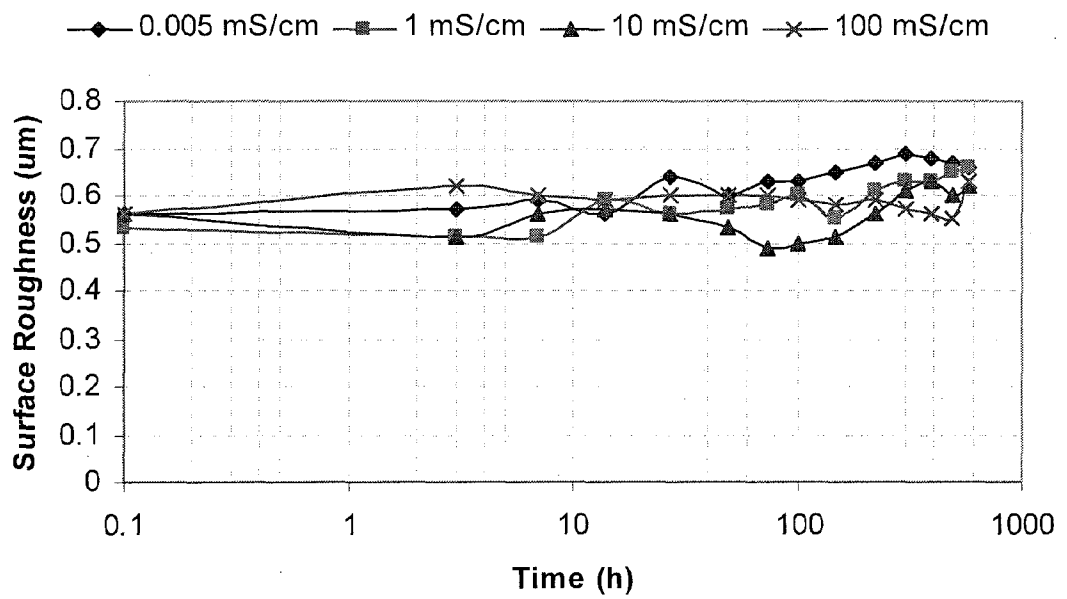


Figure 3.17. Time variation of average surface roughness of HTV SIR specimens during aging in different salinities at 98 °C for 576 h.

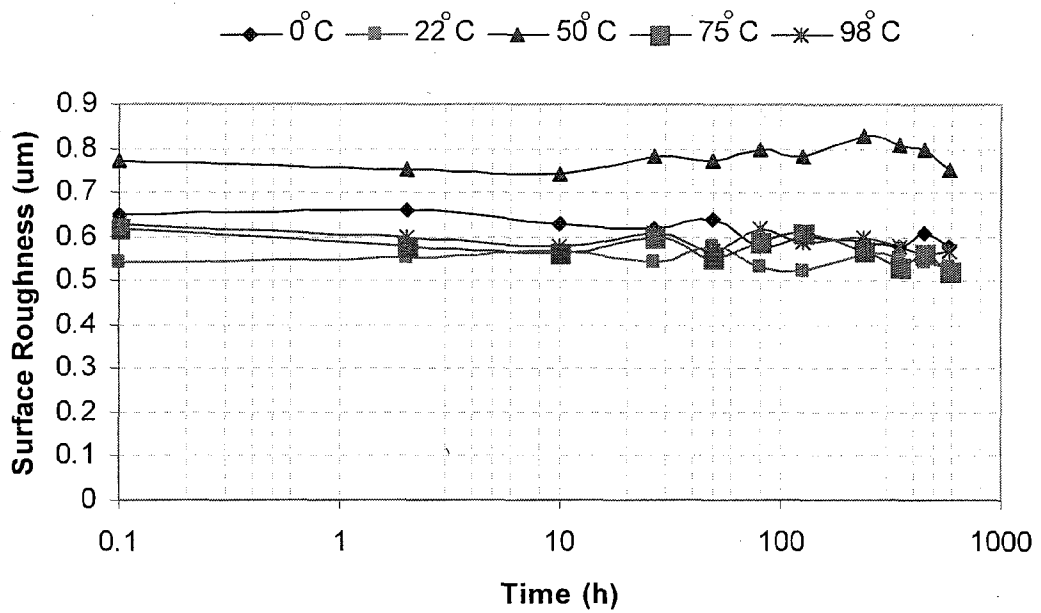


Figure 3.18. Time variation of average surface roughness of HTV SIR specimens during aging in stationary air at different temperatures for 576 h.

3.5 Change in Weight during Recovery

After removal of the specimens from the saline solutions they were left in air at 22 ± 3 °C and 55 ± 15 % humidity for up to 2700 h. The percentage reduction in weight due to drying of the specimens, recovery of the contact angle and the change in the ASR were determined. The changes in the weight and surface roughness of the specimens were correlated to the contact angle and hence to the recovery of the hydrophobicity of HTV SIR.

Figures 3.19 to 3.23 show the variation of weight as a function of time during the recovery process. All the specimens that were aged in saline solutions at different temperatures lost weight during recovery at room temperature. However, the loss of weight was faster in the beginning of the recovery period and then gradually saturated at the end. The time period for the weight to reach a saturation point during the recovery process, ranged from 24 h for the specimens aged in distilled water at 0 °C to more than 2700 h at 98 °C. Also, the weight loss ranged from 0.7 % for the specimens aged in distilled water at 0 °C to 2.5 % at 98 °C after 2700 h of recovery period. In other words, the higher the aging temperature, the greater was the percentage weight loss of the HTV SIR specimens during recovery in air.

It has been observed from the figures that at all temperatures, the percentage reduction in weight increased with decreasing salinity. This is because at a fixed temperature of the saline solution, the intake of water was observed to be higher in low salinity water. Therefore, the loss of water during the recovery in air was also expected to be higher. On the contrary, the higher the aging salinity level, the lower was the percentage of weight loss of the specimens during the recovery period which was the result of less absorption of water during aging at high salinity level. Table 3.2 shows a summery of the changes in weight of the HTV SIR specimens during the aging process.

Table 3.2 Percentage of net weight gain (+) or loss (-) of the HTV SIR specimens at the end of recovery period of 2700 h after aging in different stress conditions for 576 hours.

Aging Temperature (°C)	Aging in Air	Aging in Saline Water (mS/cm)			
		0.005	1	10	100
0	0	0	0	-0.06	-0.04
25	0	-0.08	0	0	0
50	0	-0.16	-0.07	-0.12	-0.06
75	-0.08	-0.67	-0.54	-0.44	-0.37
98	-0.24	-3.59	-2.42	-2.62	-2.24

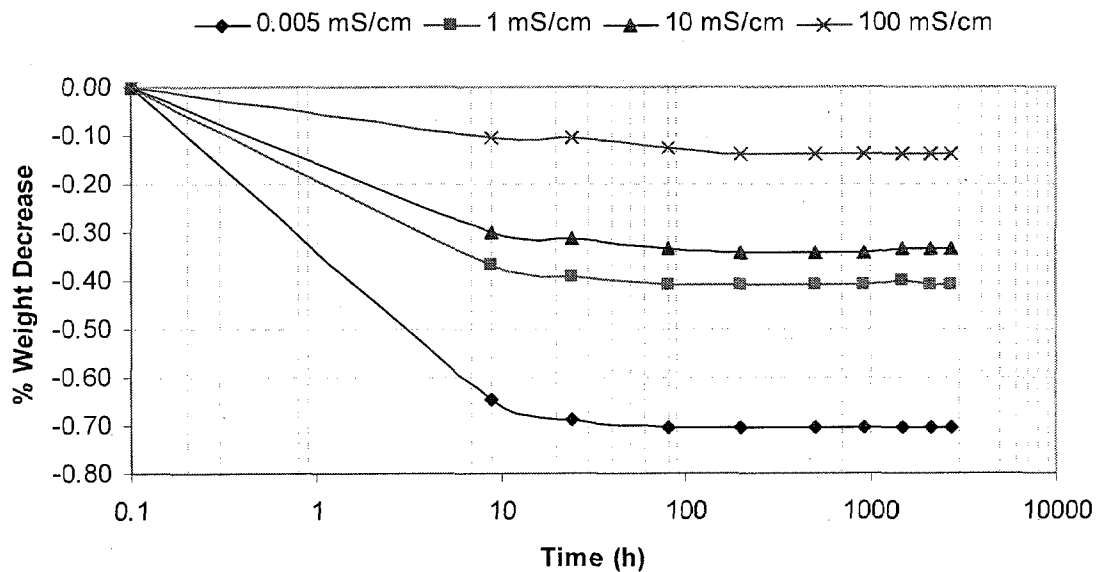


Figure 3.19. Percentage change in the weight of HTV SIR specimens as a function of time during recovery in stationary air at room temperature for 2700 h. The specimens had been aged in solutions of different conductivities at 0 °C for 576 h.

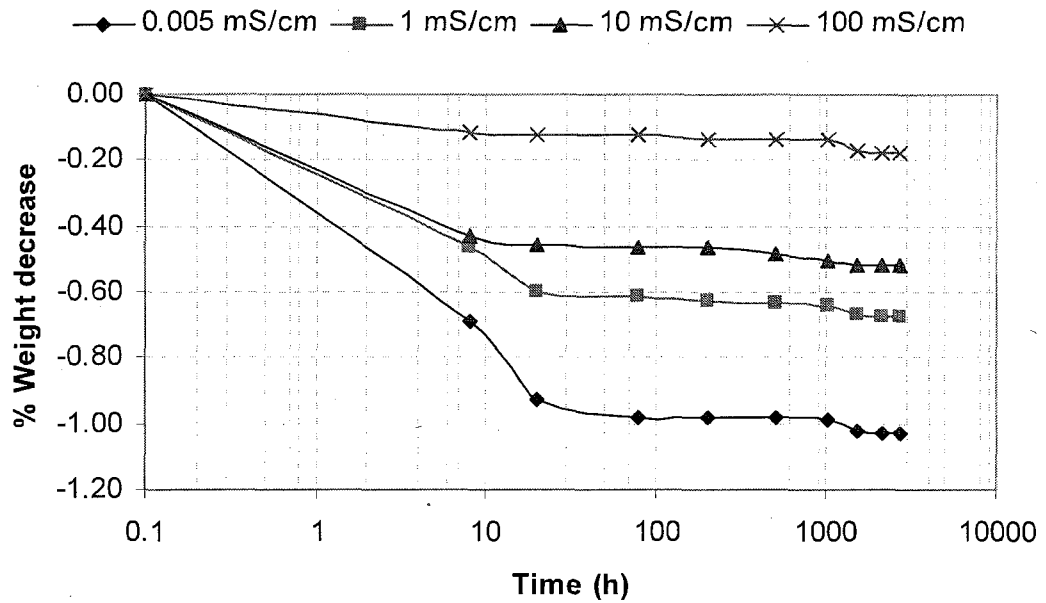


Figure 3.20. Percentage change in the weight of HTV SIR specimens as a function of time during recovery in stationary air at room temperature for 2700 h. The specimens had been aged in solutions of different conductivities at 25 °C for 576 h.

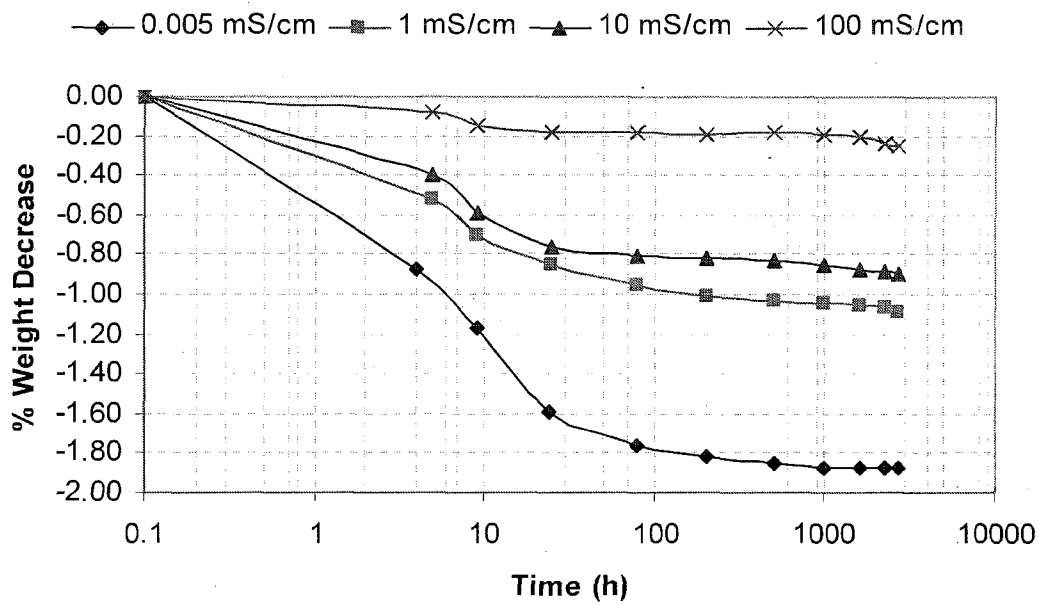


Figure 3.21. Percentage change in the weight of HTV SIR specimens as a function of time during recovery in stationary air at room temperature for 2700 h. The specimens had been aged in solutions of different conductivities at 50 °C for 576 h.

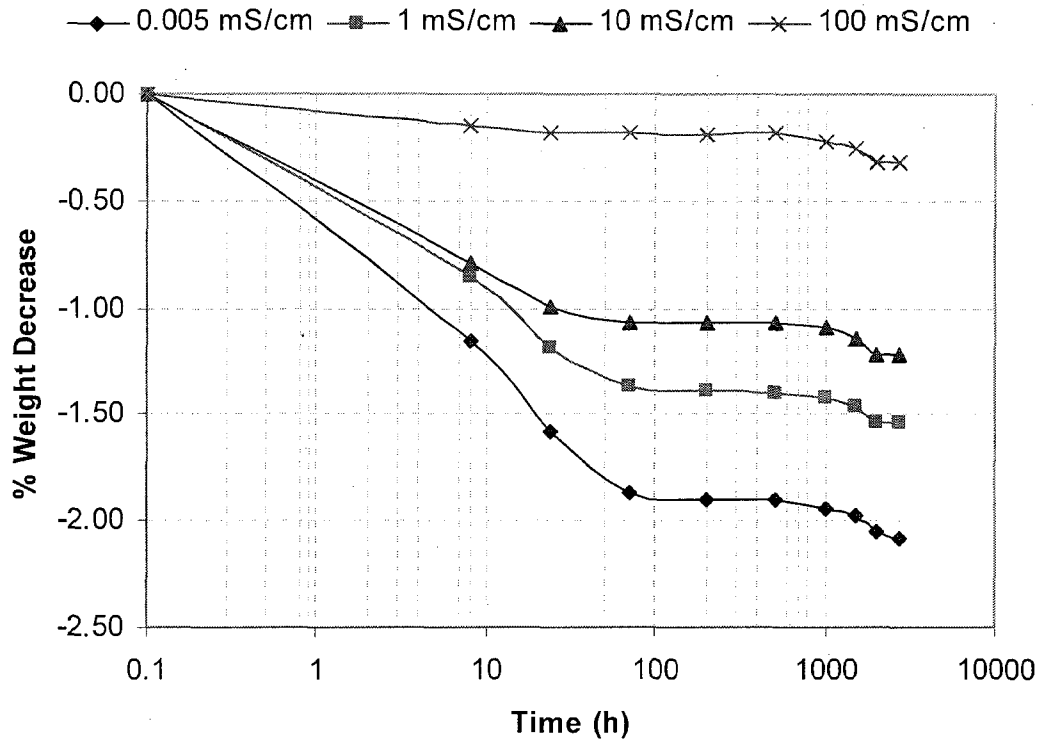


Figure 3.22. Percentage change in the weight of HTV SIR specimens as a function of time during recovery in stationary air at room temperature for 2700 h. The specimens had been aged in solutions of different conductivities at 75 °C for 576 h.

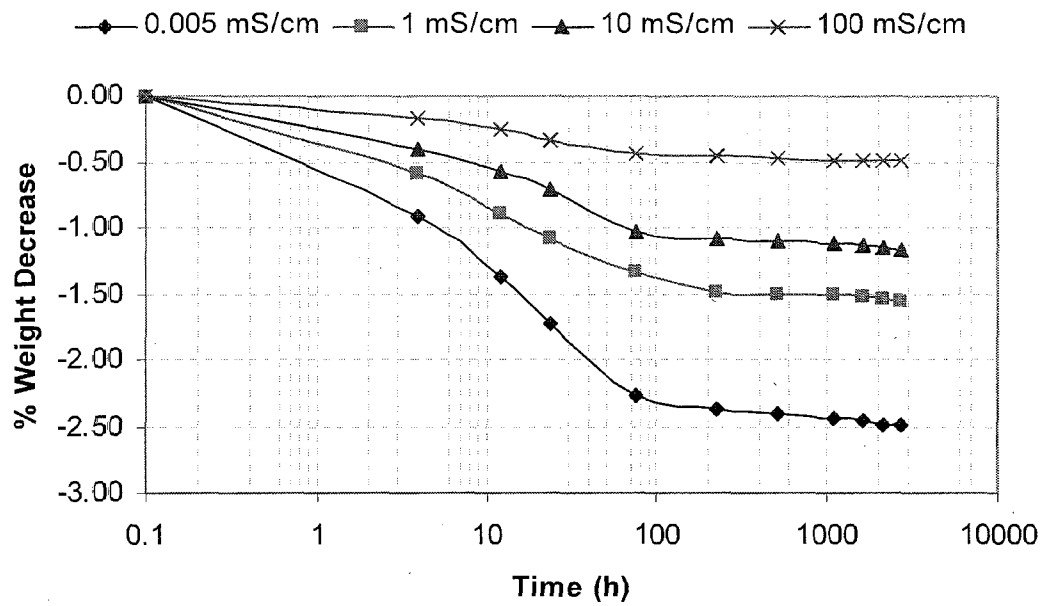


Figure 3.23. Percentage change in the weight of HTV SIR specimens as a function of time during recovery in stationary air at room temperature for 2700 h. The specimens had been aged in solutions of different conductivities at 98 °C for 576 h.

3.6 Change in Contact Angle during Recovery

Figures 3.24-3.28 show the time variation of the contact angle of distilled water on the surface of HTV SIR specimens during recovery in stationary air at room temperature. These specimens had previously been aged in saline solutions of four different conductivity levels of 0.005, 1, 10 and 100 mS/cm at 0, 23, 50, 75 and 98 °C for 576 hours. The initial values shown in the recovery graphs are actually the final values of contact angle at the end of the 576 h of immersion period. The recovery as a function of time of all the specimens in this chapter was monitored up to 2700 h.

The contact angle decreased from the original value of 100 ± 5 after immersion in the saline solutions. It has been observed that higher absorption of water caused the HTV SIR surface to be more hydrophilic. The recovery of the contact angle has two stages. Initially, it recovers quickly during the evaporation of the absorbed water. After this quick recovery the increase is slow that corresponds to the diffusion of LMW fluid from the interior to the surface of the SIR [58].

Moreover, higher values of the contact angle have been observed during recovery for the specimens that had previously been immersed in high salinity solutions in the temperature range (0-75 °C). This may be explained as due to the low absorption of water at high salinity. However, the details regarding higher hydrophobicity during the recovery period with the increase of salinity needs to be investigated further. Table 3.3 shows the comparison of the contact angles of distilled water on the surface of the specimens at three stages of aging and recovery process:

- Contact angle of the virgin specimens prior to aging
- Contact angle at the end of the aging that is also called the beginning of the recovery period
- Contact angle at the end of the recovery period

Table 3.3. Comparison between the contact angles of HTV SIR specimens at different stages: (a) contact angle of the virgin specimens, (b) contact angle after aging of 576 h, (c) contact angle after recovery of 2700 h.

Aging stress	Measurement condition	0 °C	25 °C	50 °C	75 °C	98 °C
0.005 (mS/cm)	Virgin	97	105	101	102	100
	After aging	76	77	79	74	76
	After recovery	100	91	91	83	103
1 (mS/cm)	Virgin	98	104	100	102	100
	After aging	82	79	79	81	78
	After recovery	105	93	92	90	112
10 (mS/cm)	Virgin	98	103	101	98	100
	After aging	85	84	81	85	81
	After recovery	108	97	103	96	114
100 (mS/cm)	Virgin	103	105	103	102	98
	After aging	86	82	79	80	78
	After recovery	114	103	111	102	104
Air	Virgin	98	103	99	99	105
	After aging	96	102	110	113	116
	After recovery	100	100	110	109	110

According to Table 3.3 specimens can be divided into the following categories based on the changes in their contact angles during aging and recovery processes:

- a) The contact angle regained its original value after recovery that is the contact angle of the virgin specimen, $100\pm 5^\circ$. These include the specimens aged in 0.005 mS/cm at 0 °C and 98 °C; 1 mS/cm at 0 °C; 10 mS/cm at 25, 50 and 75 °C; 100 mS/cm at 25, 75 and 98 °C; and in air at 0 and 25 °C.
- b) The contact angle of the samples reached higher than original values after recovery. These include samples aged in 1 mS/cm at 98 °C; 10 mS/cm at 0 and 98 °C; 100 mS/cm at 0 and 50 °C; and in air at 50, 75 and 98 °C.
- c) The contact angle did not regain its original value after recovery that is the contact angle of the virgin one $100\pm 5^\circ$. These include the specimens aged in 0.005 mS/cm and 1 mS/cm at 25, 50 and 75 °C.

From the above part a), it is clear that eleven of the specimens aged in different conditions recovered their original contact angle at room temperature. However, all of the six specimens mentioned in part c) above did not recover their virgin value when they previously had been aged in solutions of low conductivity of 0.005 mS/cm and 1 mS/cm.

On the other hand, three out of seven specimens recovered to a higher values of the contact angles than the virgin level when they were aged in saline solutions at 50, 75 and 98 °C. Two of them were aged in saline solutions of 1 mS/cm and 10 mS/cm at 98 °C. This recovery to the higher contact angles is linked to the diffusion of LMW fluid from the interior to the surface at high temperature. Moreover, aging in higher salinity at low temperatures also caused the contact angle to recover to a higher value than that of the virgin specimens.

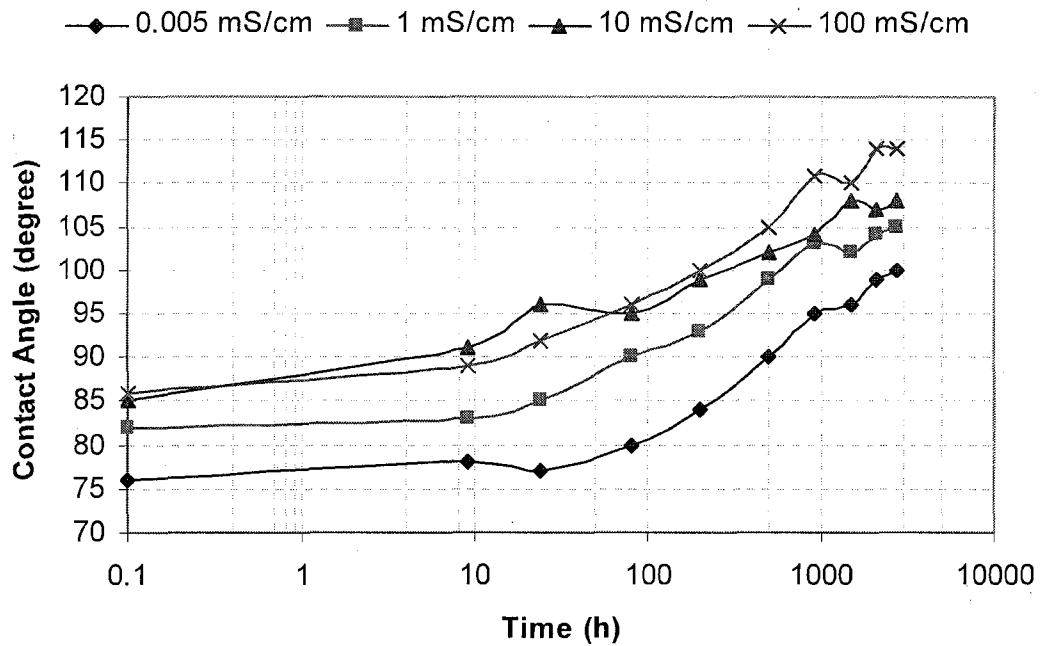


Figure 3.24. Time variation of the contact angle of distilled water on the surface of HTV SIR specimens during recovery in stationary air at room temperature for 2700 h. The specimens had been aged in solutions of different conductivities at 0 °C for 576 h.

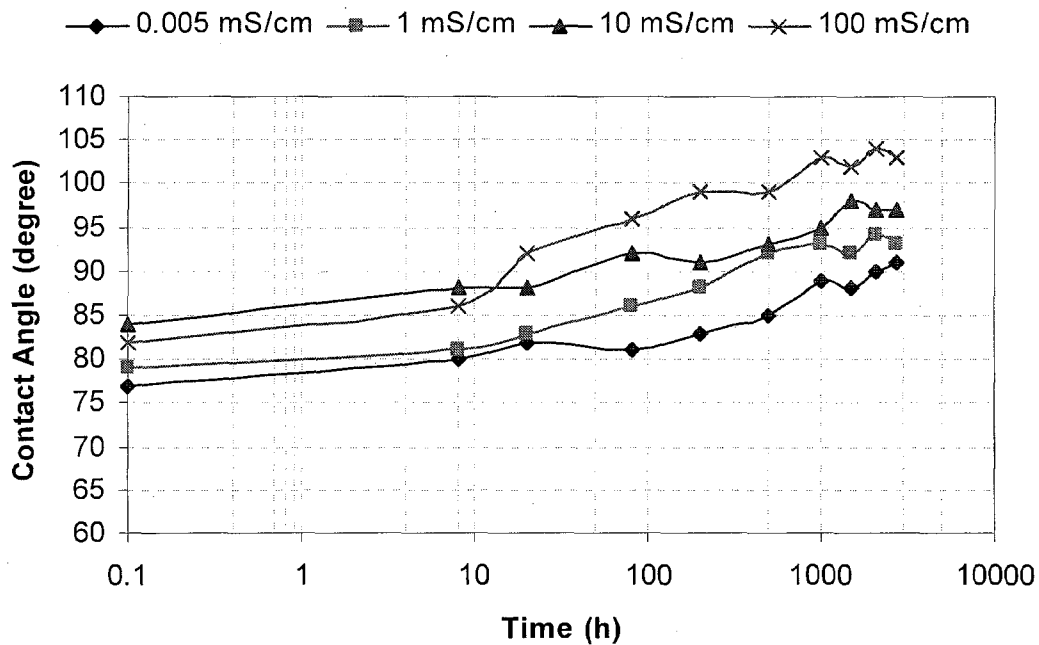


Figure 3.25. Time variation of the contact angle of distilled water on the surface of HTV SIR specimens during recovery in stationary air at room temperature for 2700 h. The specimens had been aged in solutions of different conductivities at 25 °C for 576 h.

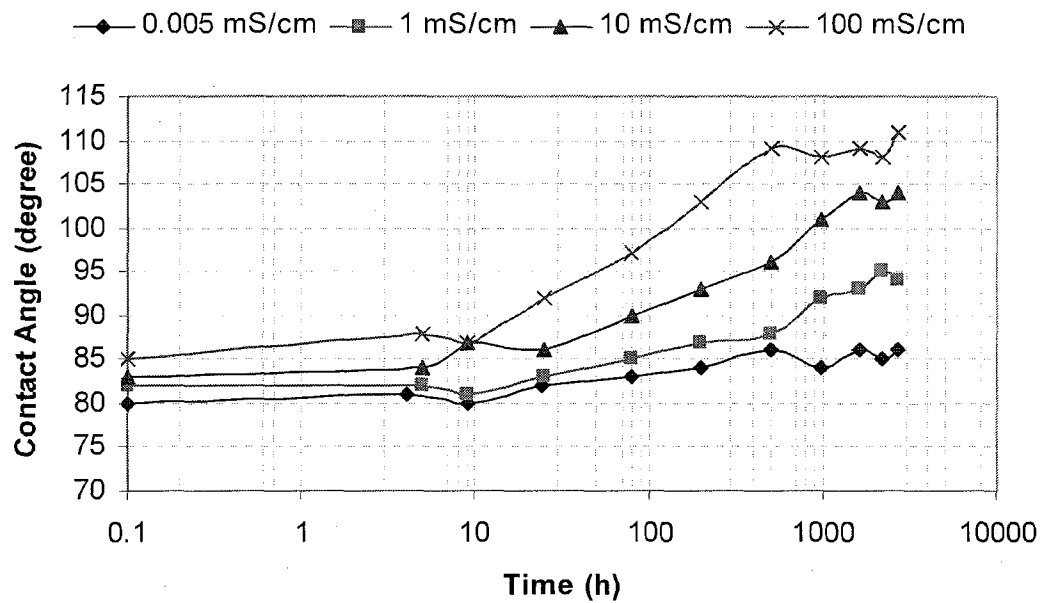


Figure 3.26. Time variation of the contact angle of distilled water on the surface of HTV SIR specimens during recovery in stationary air at room temperature for 2700 h. The specimens had been aged in solutions of different conductivities at 50 °C for 576 h.

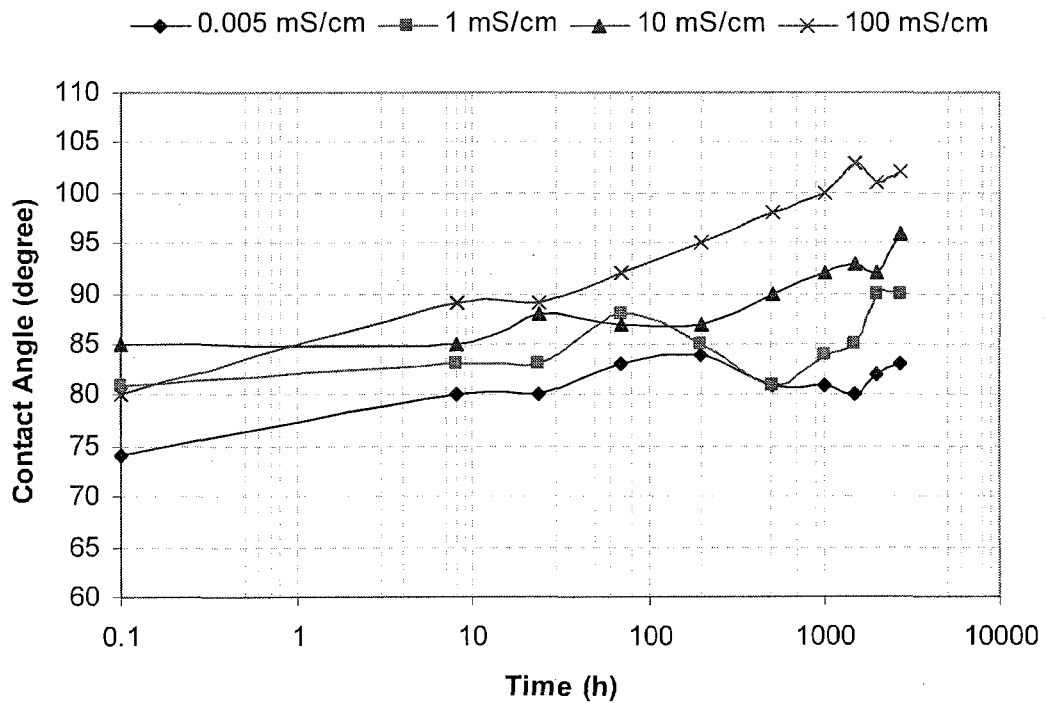


Figure 3.27. Time variation of the contact angle of distilled water on the surface of HTV SIR specimens during recovery in stationary air at room temperature for 2700 h. The specimens had been aged in solutions of different conductivities at 75 °C for 576 h.

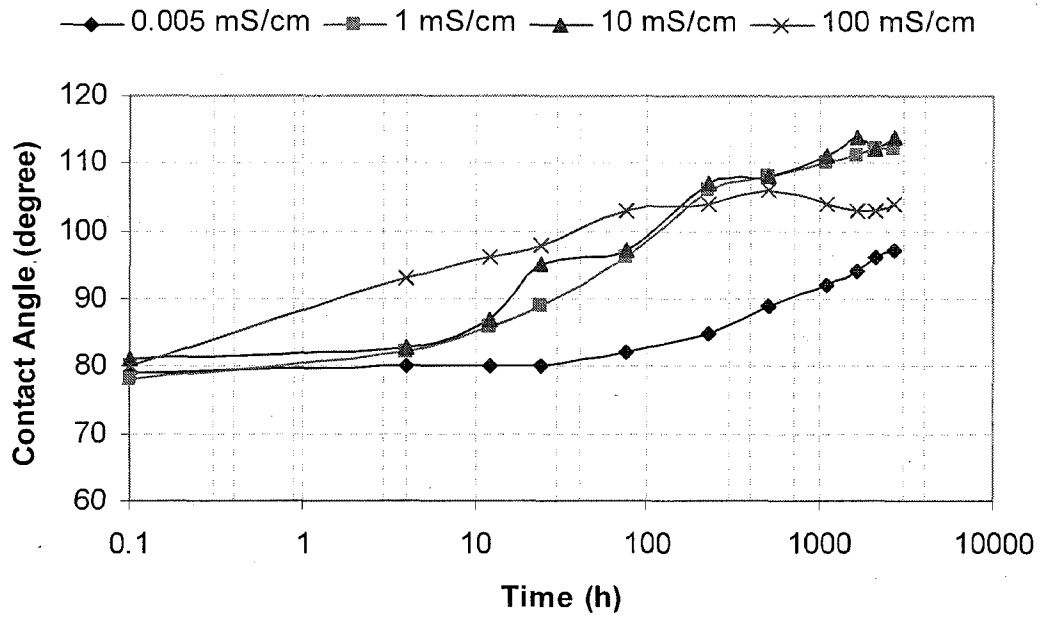


Figure 3.28. Time variation of the contact angle of distilled water on the surface of HTV SIR specimens during recovery in stationary air at room temperature for 2700 h. The specimens had been aged in solutions of different conductivities at 98 °C for 576 h.

3.7 ASR during Recovery

The change in ASR of HTV SIR specimens as a function of time at room temperature during 2700 h of recovery period is shown in Figures 3.29-3.33. In most of the cases, there is a decrease in surface roughness during the recovery process and this decrease may be related to the decrease in weight due to evaporation of water. This result is consistent with the previous observation in which the decrease in average surface roughness of PTFE specimens during drying in air has been reported [38].

Table 3.4 shows the comparison of surface roughness of HTV SIR specimens in μm at three different stages of aging and recovery process:

- Surface roughness of the virgin specimens prior to aging.
- Surface roughness at the end of aging for 576 h that is also called the beginning of the recovery period.
- Surface roughness at the end of the recovery period for 2700 h.

According to Table 3.3 specimens can be divided into the following two categories based on the changes in their ASR during aging and recovery processes:

- a) The HTV SIR specimens retained a higher ASR than its original value after recovery with an increase of 0.16, 0.16, 0.05 and 0.14 μm after aging at 98 °C in the solutions of 0.005, 1, 10 and 100 mS/cm, respectively.
- b) The specimens aged in different saline solutions at 0, 25, 50 and 75 °C regained their ASR either to the original value or dropped from their virgin value during the recovery process. Similar results have been observed after recovery of the specimens, previously aged in stationary air at different temperatures (0-98 °C) for 3000 h.

The increase in ASR during immersion in saline solutions of different conductivities up to a temperature of 75 °C was temporary which could be related to the absorption of water. However, the increase in ASR was permanent at 98 °C which might be associated with the weight loss of the specimens. The weight loss of 3.59 % has been observed for the specimens aged in distilled water (0.005 mS/cm) at 98 °C for 576 h and likewise the increase in the surface roughness was 0.16 µm. From these results, it is apparent that the variation in the ASR might be associated with the change in weight.

Table 3.4. Comparison between the average surface roughness of HTV SIR specimens in μm at different stages: (a) virgin specimens, (b) after aging of 576 h, (c) after recovery of 2700 h.

Aging stress	Measurement condition	0 °C	25 °C	50 °C	75 °C	98 °C
0.005 (mS/cm)	Virgin	0.43	0.75	0.62	0.51	0.56
	After aging	0.58	0.84	0.68	0.67	0.66
	After recovery	0.49	0.72	0.62	0.49	0.68
1 (mS/cm)	Virgin	0.55	0.78	0.79	0.54	0.53
	After aging	0.69	0.81	0.83	0.59	0.66
	After recovery	0.57	0.72	0.78	0.48	0.63
10 (mS/cm)	Virgin	0.48	0.63	0.71	0.50	0.56
	After aging	0.57	0.69	0.66	0.45	0.62
	After recovery	0.50	0.60	0.60	0.46	0.60
100 (mS/cm)	Virgin	0.64	0.67	0.73	0.51	0.56
	After aging	0.62	0.60	0.72	0.52	0.63
	After recovery	0.64	0.58	0.67	0.44	0.68
Air	Virgin	0.65	0.54	0.77	0.65	0.63
	After aging	0.58	0.53	0.75	0.52	0.57
	After recovery	0.58	0.50	0.64	0.60	0.52

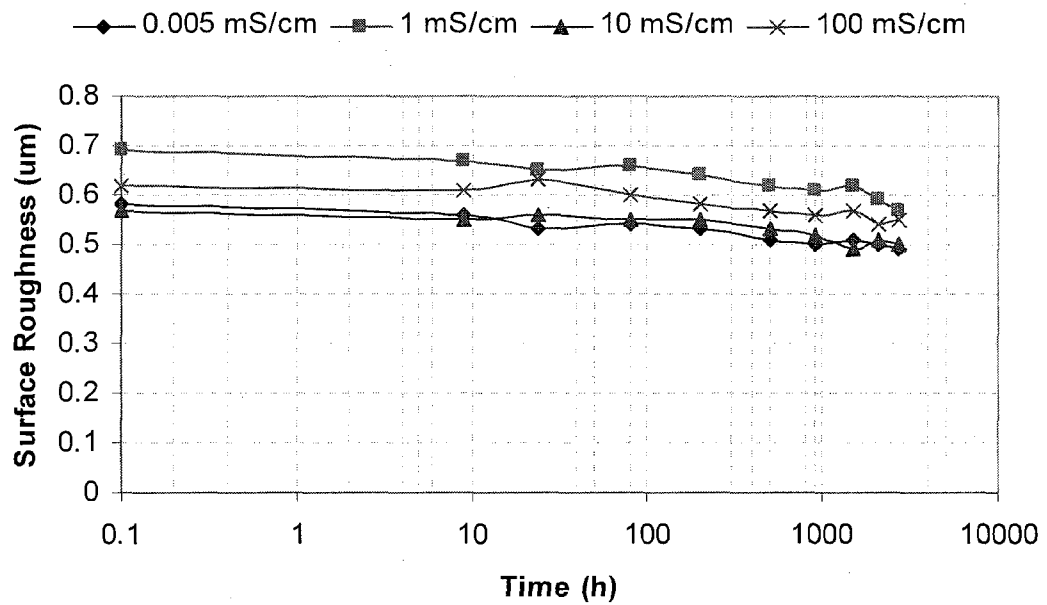


Figure 3.29. Time variation of the surface roughness of HTV SIR specimens during recovery in stationary air at room temperature for 2700 h. The specimens had been aged in solutions of different conductivities at 0 °C for 576 h.

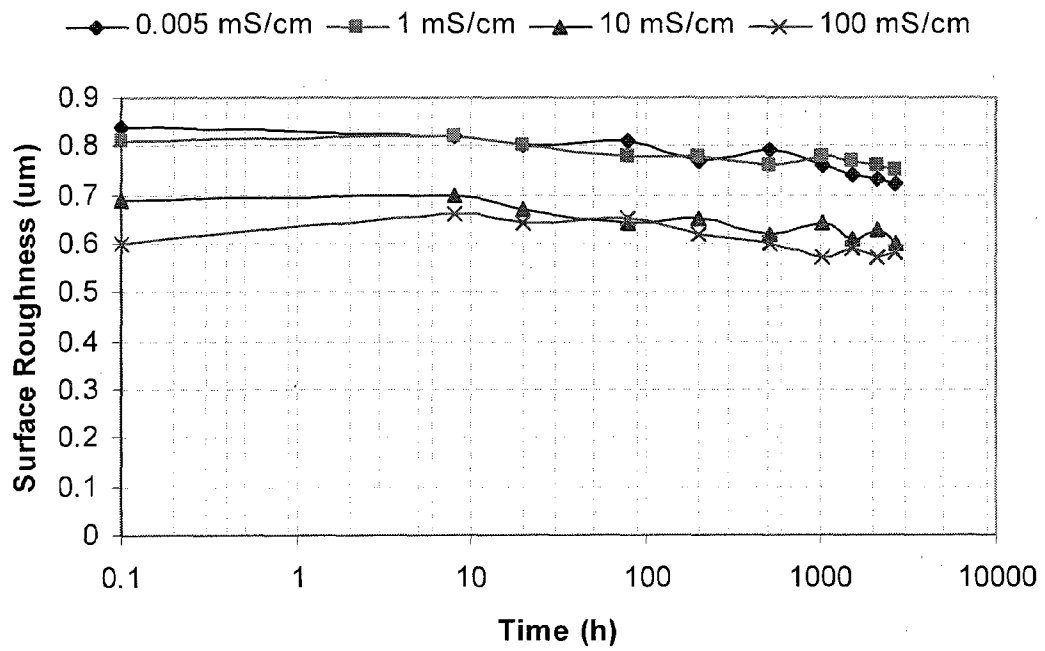


Figure 3.30. Time variation of the surface roughness of HTV SIR specimens during recovery in stationary air at room temperature for 2700 h. The specimens had been aged in solutions of different conductivities at 22 °C for 576 h.

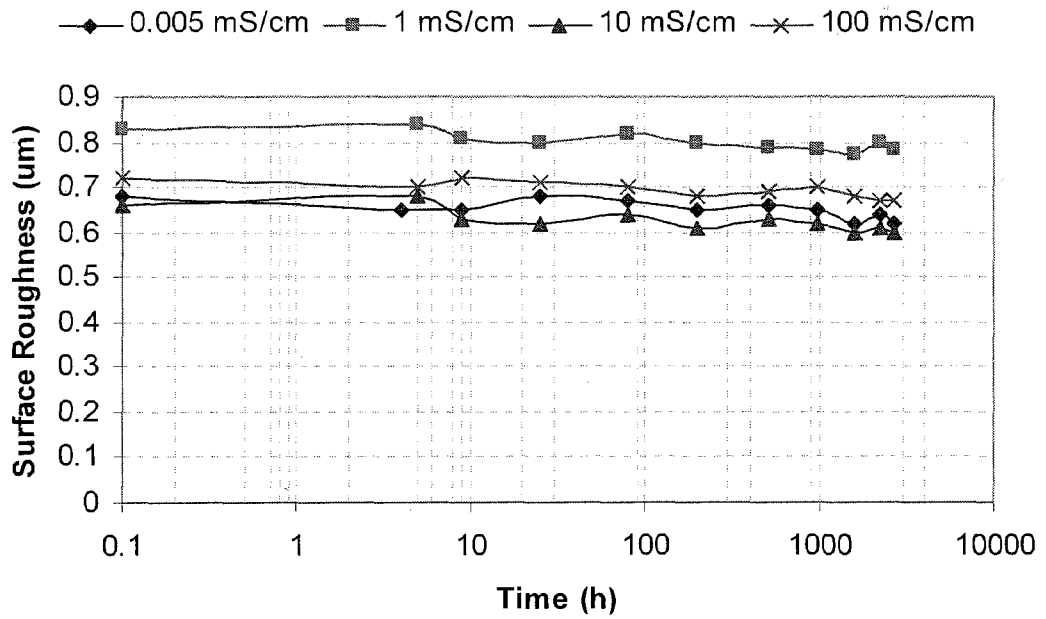


Figure 3.31. Time variation of the surface roughness of HTV SIR specimens during recovery in stationary air at room temperature for 2700 h. The specimens had been aged in solutions of different conductivities at 50 °C for 576 h.

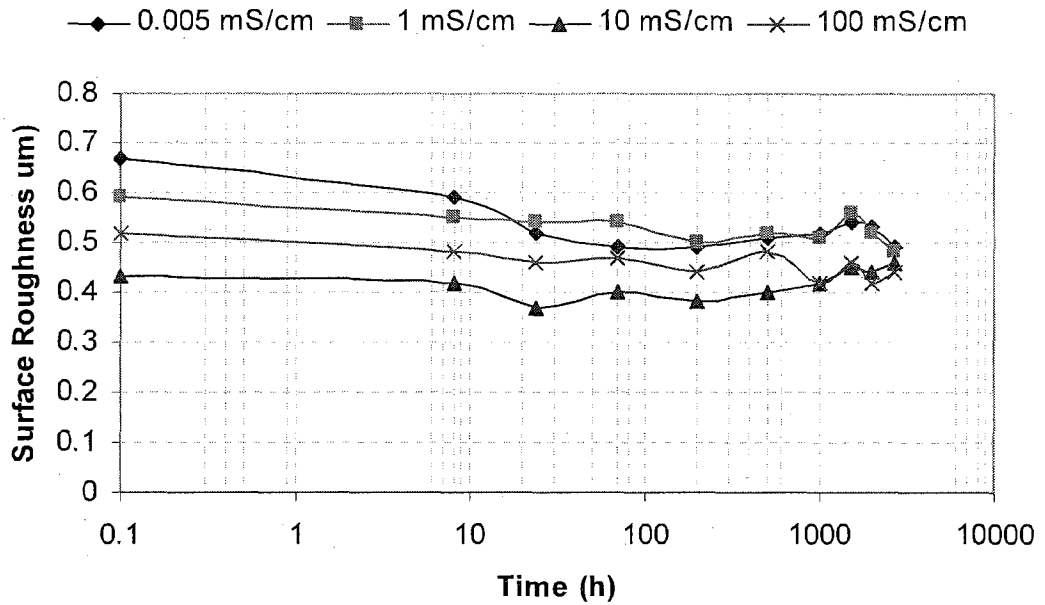


Figure 3.32. Time variation of the surface roughness of HTV SIR specimens during recovery in stationary air at room temperature for 2700 h. The specimens had been aged in solutions of different conductivities at 75 °C for 576 h.

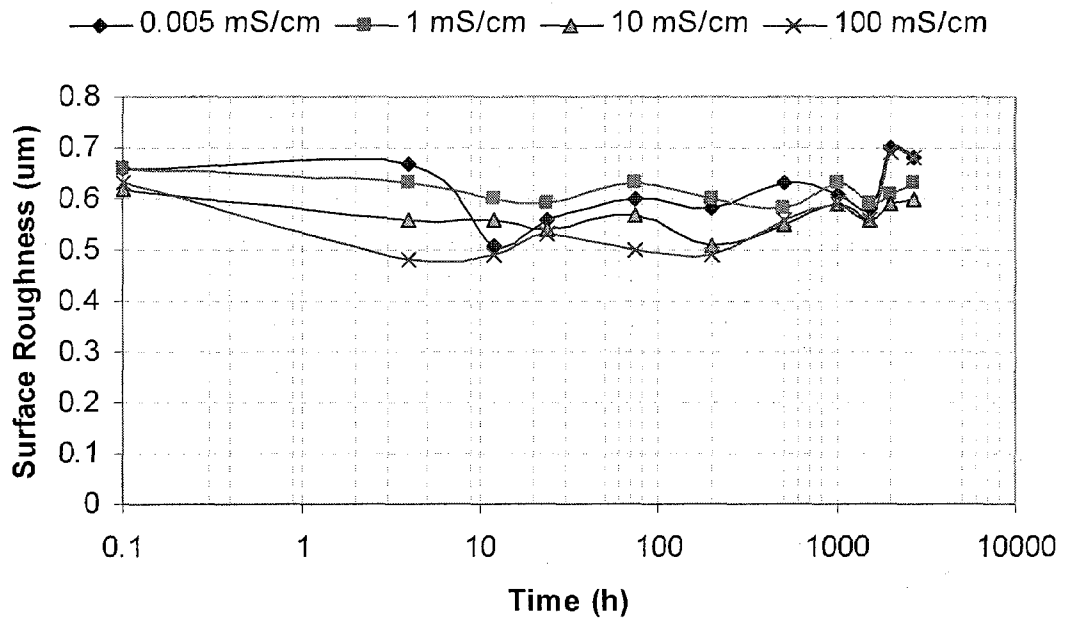


Figure 3.33. Time variation of the surface roughness of HTV SIR specimens during recovery in stationary air at room temperature for 2700 h. The specimens had been aged in solutions of different conductivities at 98 °C for 576 h.

3.8 SEM and EDS Results

3.8.1 Experimental Procedure

Scanning electron microscope (SEM) and energy dispersive x-ray spectroscopy (EDS) have been used to investigate the surface morphology and topography, surface erosion, inhomogeneities and cracks. Additionally, they have been used to detect the compositional changes in C, O and Si contents constituting polydimethylsiloxane in HTV SIR specimens caused by aging in various environmental stresses. Utilization of such techniques for surface analysis of organic insulators has previously been reported [14, 16, 30, 44, 68-71]

In order to find the chemical structure at the aged layer, a deep analyzing depth is necessary. Therefore, EDS is employed for analyzing the chemical changes which occurred due to the environmental stresses and aging. For this purpose, three of the aged HTV SIR specimens were utilized for SEM/EDS analysis and compared to a virgin specimen. These specimens were previously aged in 0.005 mS/cm conductivity solution at 50, 75 and 98 °C for 576 h and allowed to recover for a further 2700 h. All the four samples including a virgin specimen were then mounted, coated with a thin layer of gold and introduced to the vacuum chamber of the microscope.

The SEM studies have been conducted using a JEOL JSM-5800 LV scanning electron microscope to examine the aging effects on the surface of the specimens, with accelerating voltage of 5 kV under conventional vacuum. The SEM uses the secondary electrons produced by the scanning beam to give an image of the surface of the specimen being scanned. Simultaneously, an EDAX X-ray detector operating at an accelerating voltage of 15 kV was used to determine the composition of the HTV SIR insulator specimens with an analyzing depth of a few microns. This allowed studying the compositional variation of different elements near the surface of the specimens as a function of aging time.

3.8.2 Results

Figures 3.34-3.41 show the SEM photographs of some aged and un-aged HTV SIR specimens taken at 100 and 1000 times magnifications. The SEM images of the virgin sample in Figures 3.34-3.35 show that ATH filled silicone rubber does not have a higher packing density; therefore, a greater number of voids are present and this is consistent with the previous report [30]. However, the virgin surface is more homogeneous and smooth as compared to the surfaces of the aged specimens.

The loss and recovery of hydrophobicity depends on the physical and chemical changes of the surface of the insulating materials. The aged specimens exhibit rougher surfaces and phase difference due to compositional changes in the filler and rubber on the surface during aging. The specimen aged at 50 °C does not appear to be significantly different from the virgin specimen in surface morphology owing to a lower aging temperature as shown in Figures 3.36-3.37. However, Figures 3.38-3.41 of specimens aged at 75 °C and 98 °C in distilled water for 576 h showed a significant change in surface morphology and roughness due to adequate and uniform filler dispersion as compared to the virgin sample. The surface of these specimens also became hard along with an apparent change in their color as seen by the naked eye.

Figures 3.42-3.45 are the energy dispersive x-ray spectra of the same specimens described above for the SEM images. Al, Si, O and C are the significant elements which have been detected on the surface of all the HTV SIR specimens. The Au peaks found in all the spectra, actually come from the gold coating which is used to make the samples conducting for SEM analysis.

The Si and O detected in the X-ray count originate from (Si-O-Si) backbone of the silicone polymer chain, whereas the Al, was detected due to the presence of alumina trihydrate (ATH) filler which is added to the base polymer during the manufacturing process to improve its mechanical performance and to reduce the

flammability. Alumina trihydrate also lowers the cost and enhances the tracking and erosion resistance of the insulator material [27-32, 72].

The beam current in each spectrum may not be the same which results in a different number of counts per second in different spectra. Therefore, the number of counts per second may differ in different spectra and is not important. However, the ratio of the intensity of the peaks in the same spectrum depicts the ratio of concentration of the elements on the surface of the sample. Table 3.5 gives the concentration ratios of Al/Si, Al/O, Al/C and O/Si in each spectrum of the specimens aged in distilled water at 50, 75 and 98 °C along with the virgin one according to the EDS spectra of Figures 3.42-3.45. The analysis of Table 3.5 depicts a higher intensity of Al and lower intensity of Si as well as C with the increase of temperature which is consistent with the previous report [70].

Table 3.5. Chemical component changes with temperature in HTV SIR aged in distilled water (0.005 mS/cm) for 576 h and allowed to recover at room temperature for 2700 h prior to spectroscopy.

Aging Temperature	Al/Si	Al/O	Al/C	O/Si
Virgin	0.84	0.84	5.21	1.00
50 °C	0.82	0.91	5.04	0.89
75 °C	0.89	0.78	4.70	1.13
98 °C	2.83	0.96	9.70	2.94

The EDS spectrum of the surface of the HTV SIR specimens aged at 50 °C and 75 °C did not much differ from the virgin sample. However, the surface of the specimen aged at 98 °C differed appreciably in composition from the virgin one. There is 86% increase in the ratio Al/C on the surface of the specimen aged at 98 °C as compared to the virgin ratio. So, it is apparent that the ATH dissolved

into water as well as diffused to the surface at high temperature and ultimately, increased its intensity on the surface of the aged insulator specimens.

The increase in the ratio of O/Si on the surface of the HTV SIR specimens had been observed with the increase of aging temperature as given in Table 3.5. This increased level of O on the surface is responsible for developing hydrogen forces between the HTV SIR and the water. However, there is not any appreciable change in the ratio of Al/O due to aging at different temperatures which indicates that intensity of both of these elements increased at the same time on the surface with aging temperature.

Another explanation for the high Al/C, Al/Si and O/Si ratios can be that ATH decomposes on heating, thus releasing O on the surface. This O can combine with Al and Si to form alumina (Al_2O) and silicone dioxide (SiO_2), respectively on the surface of the specimens as a result of aging.

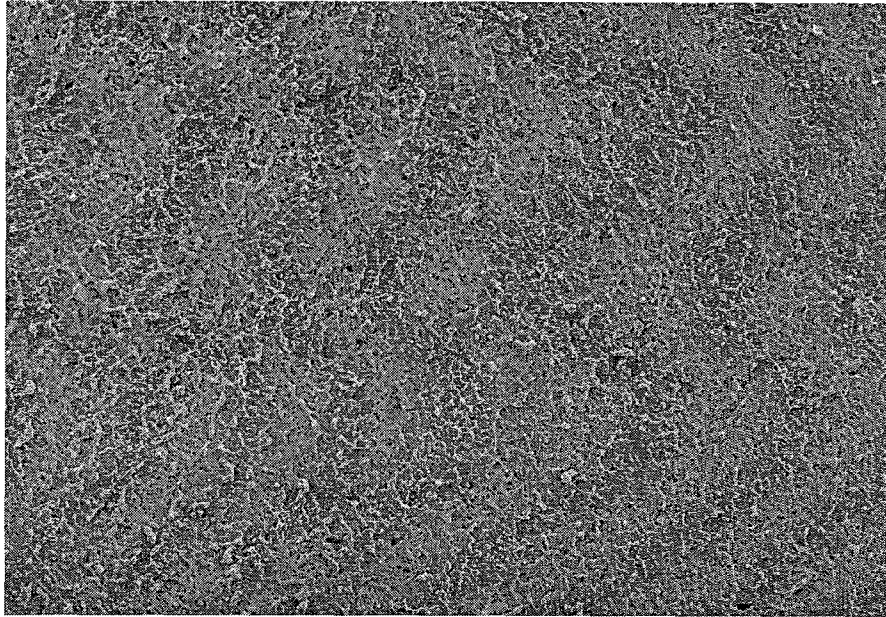


Figure 3.34. SEM image of the surface of a virgin HTV SIR specimen with magnification: x100 and width: 132 μm .

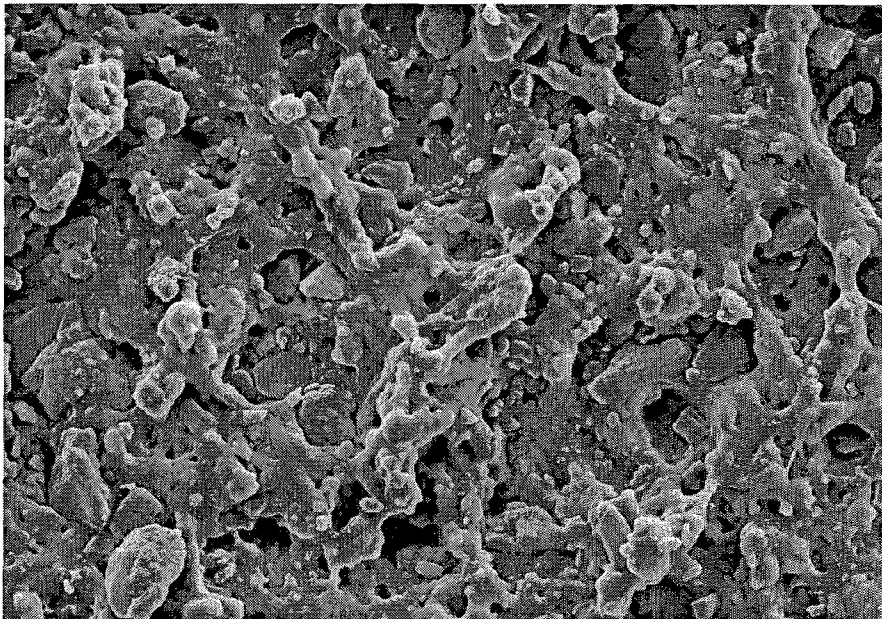


Figure 3.35. Same as top figure except the magnification: x1000.

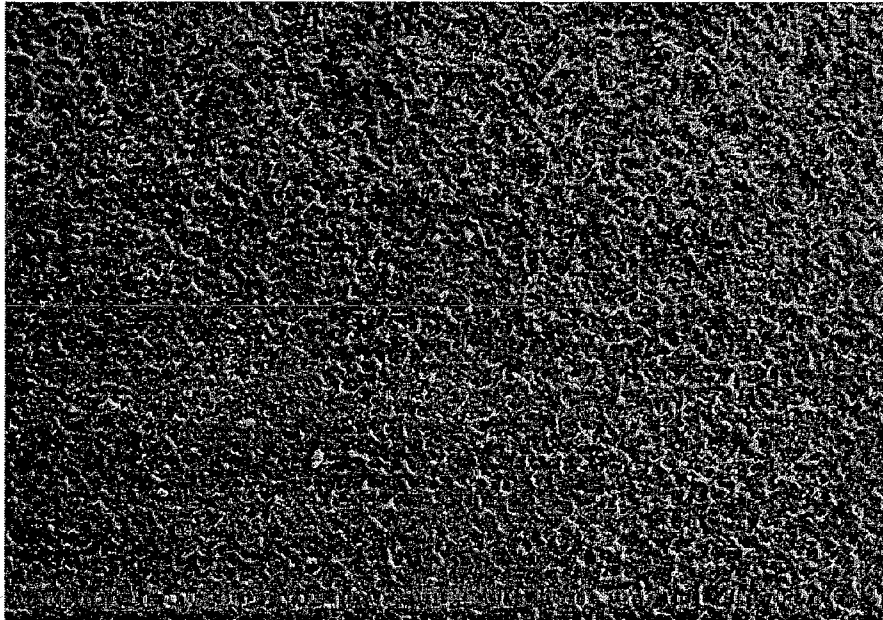


Figure 3.36. SEM image of the surface of the HTV SIR specimen aged in distilled water at 50 °C for 576 h and dried in stationary air at room temperature for 2700 h prior to the imagery; magnification: x100 and width: 132 μm .

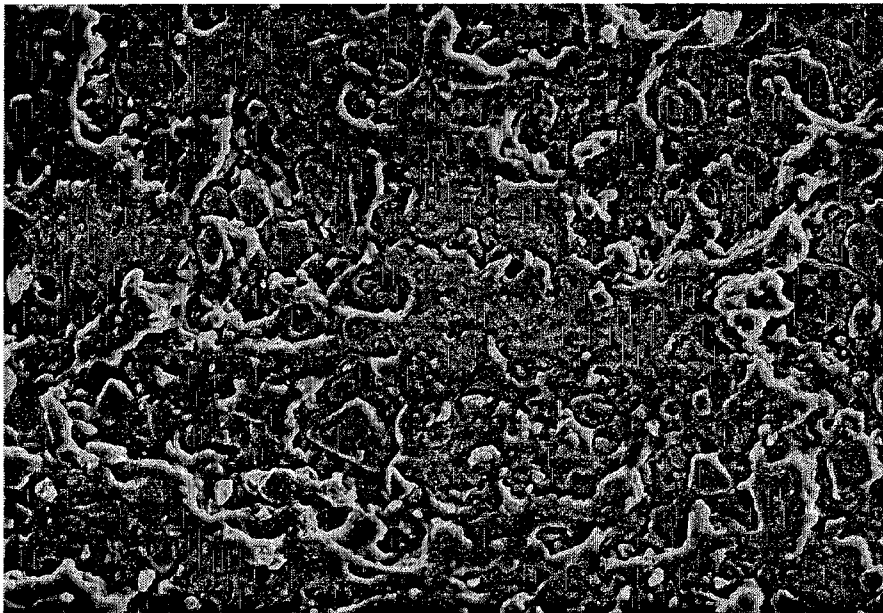


Figure 3.37. Same as the top figure, except the magnification: x1000

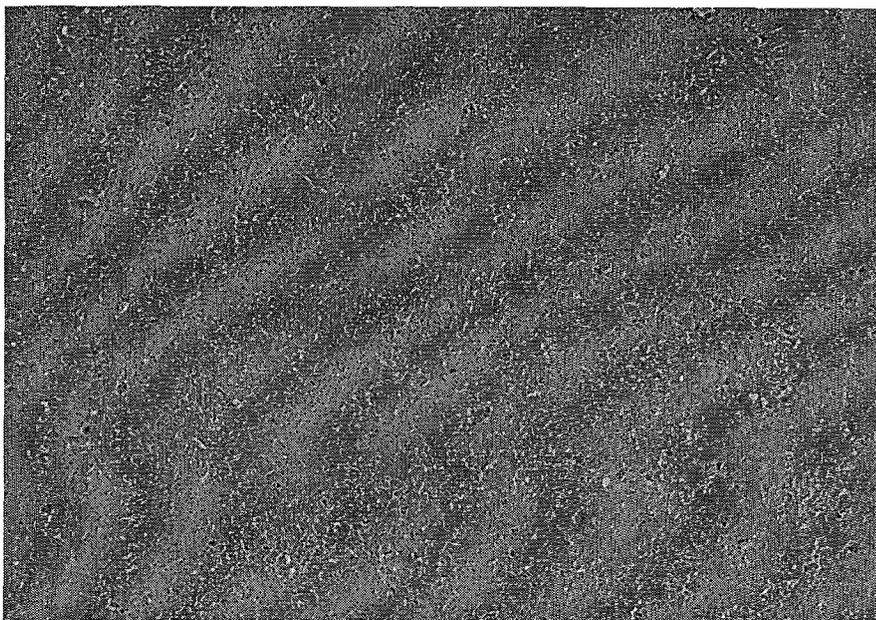


Figure 3.38. SEM image of the surface of the HTV SIR specimen aged in distilled water at 75 °C for 576 h and dried in stationary air at room temperature for 2700 h prior to the imagery; magnification: x100 and width: 132 μm .

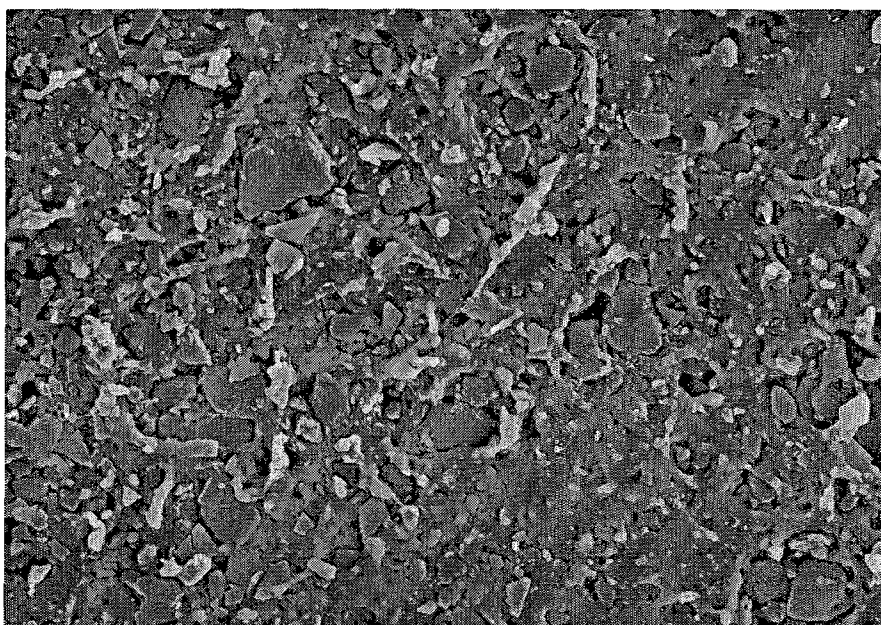


Figure 3.39. Same as the top figure, except the magnification: x1000.

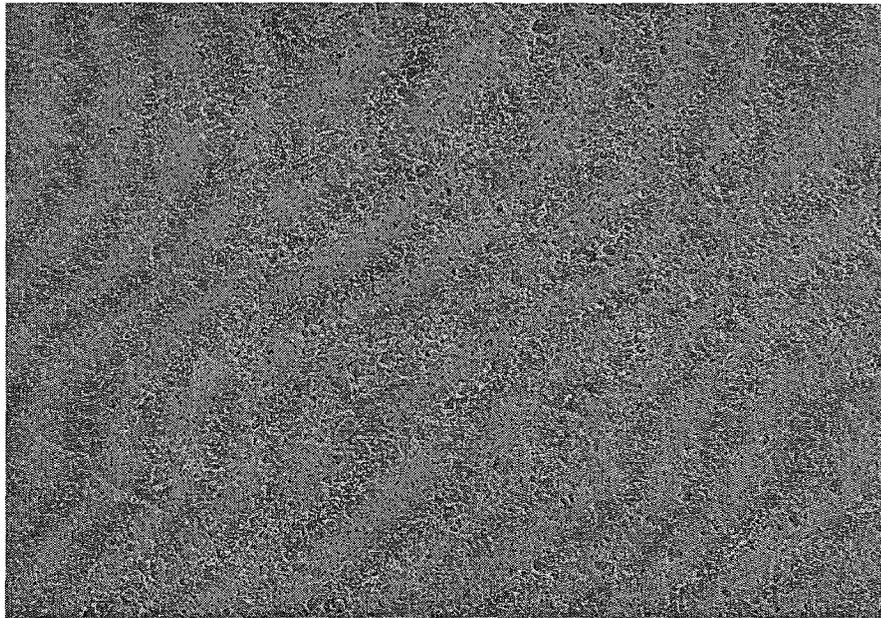


Figure 3.40. SEM image of the surface of the HTV SIR specimen aged in distilled water at 98 °C for 576 h and dried in stationary air at room temperature for 2700 h prior to the imagery; magnification: x100 and width: 132 μm .

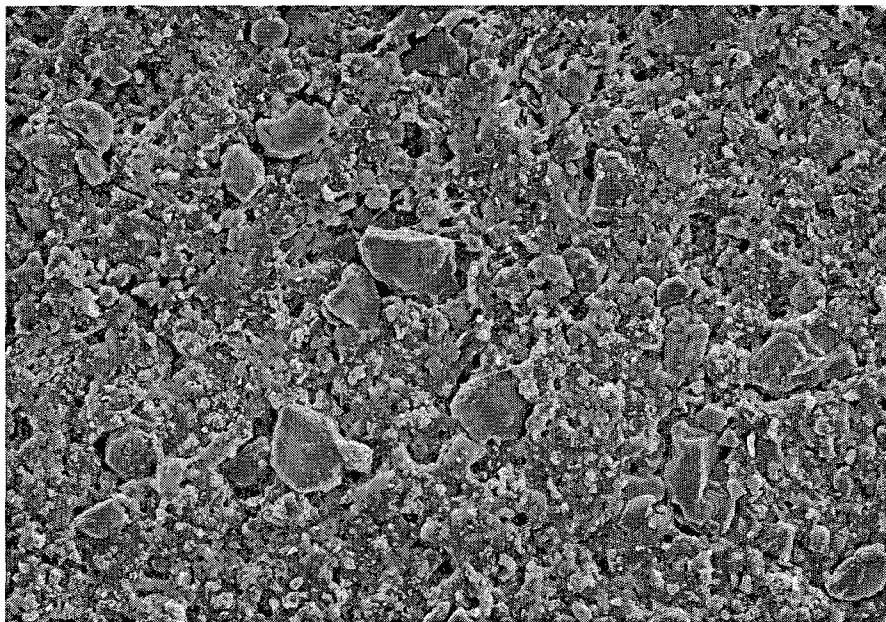


Figure 3.41. Same as the top figure, except the magnification: x1000.

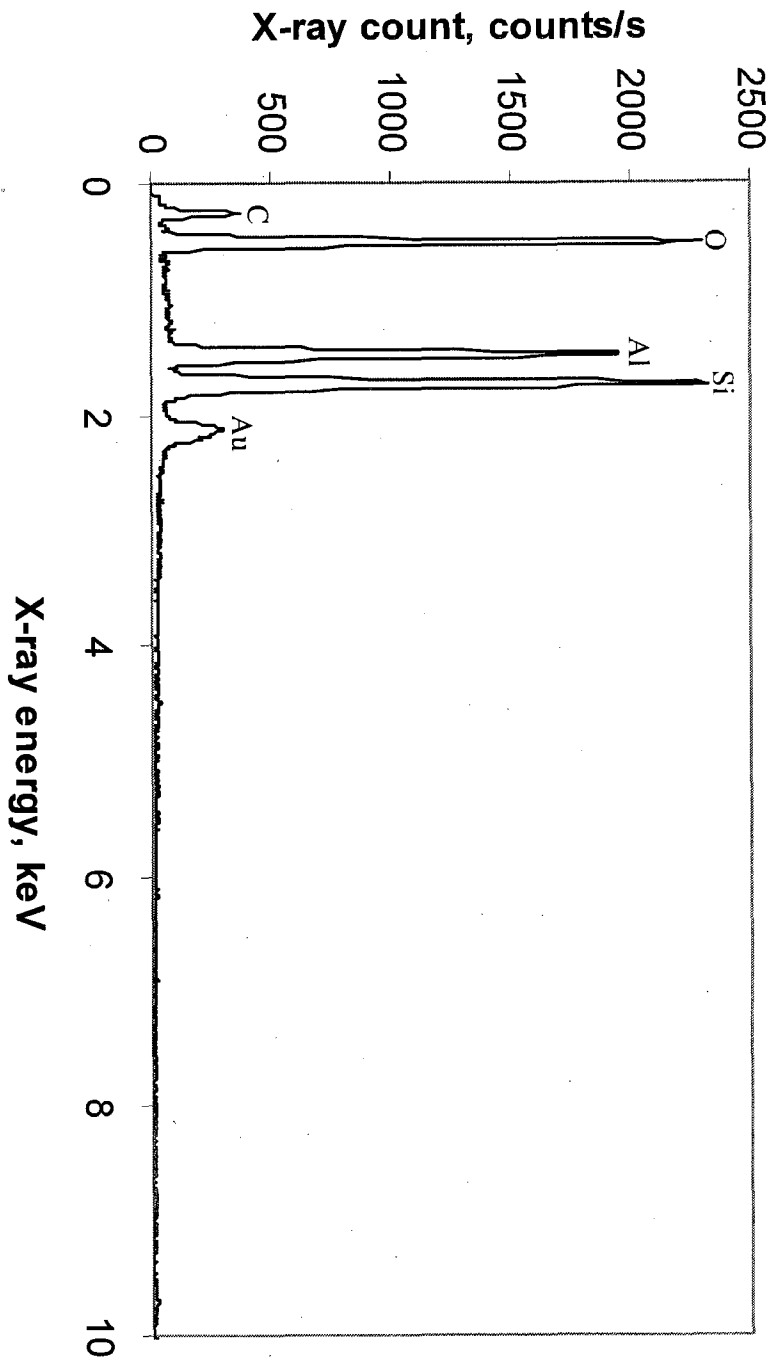


Figure 3.42. Energy dispersive X-ray spectrum of a virgin HTV SIR specimen

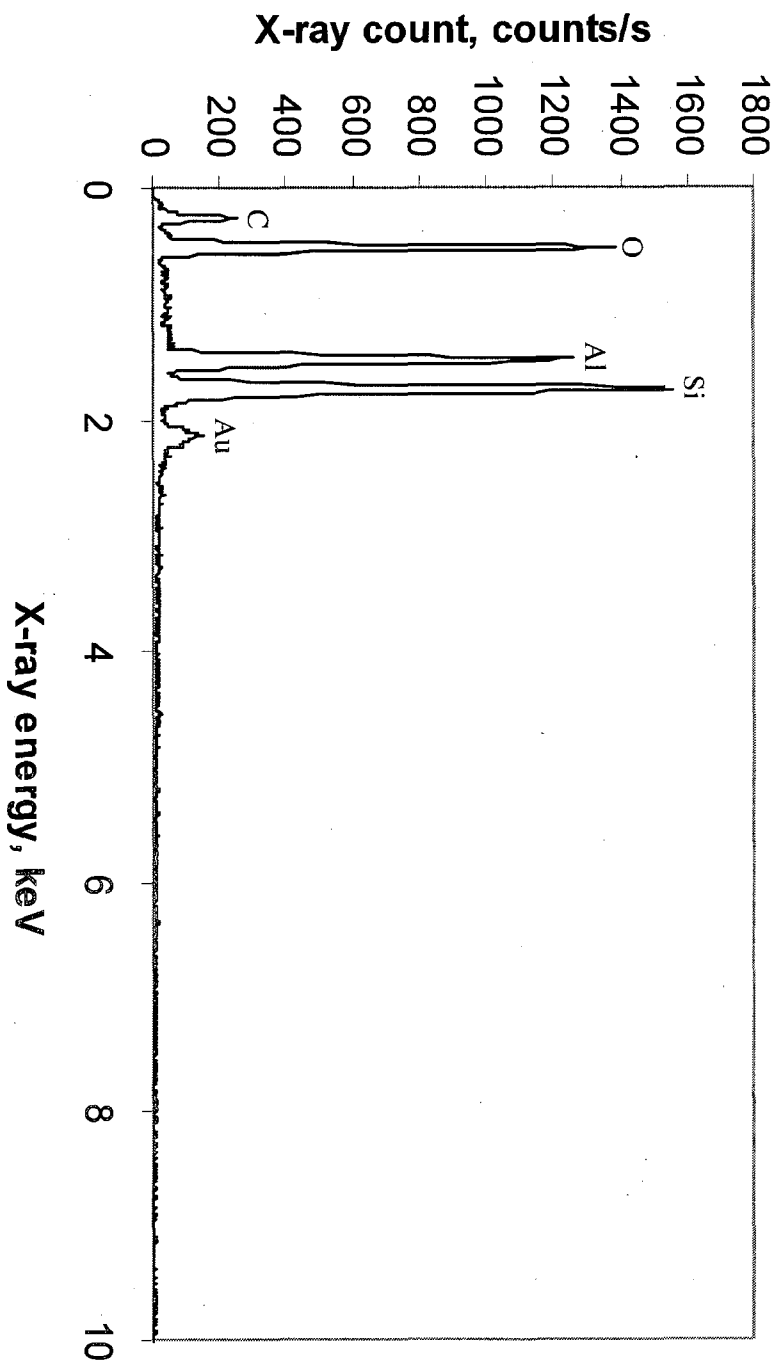


Figure 3.43. Energy dispersive X-ray spectrum of HTV SIR specimen aged in distilled water (0.005 mS/cm) at 50 °C for 576 h and allowed to recover at room temperature for 2700 h prior to spectroscopy.

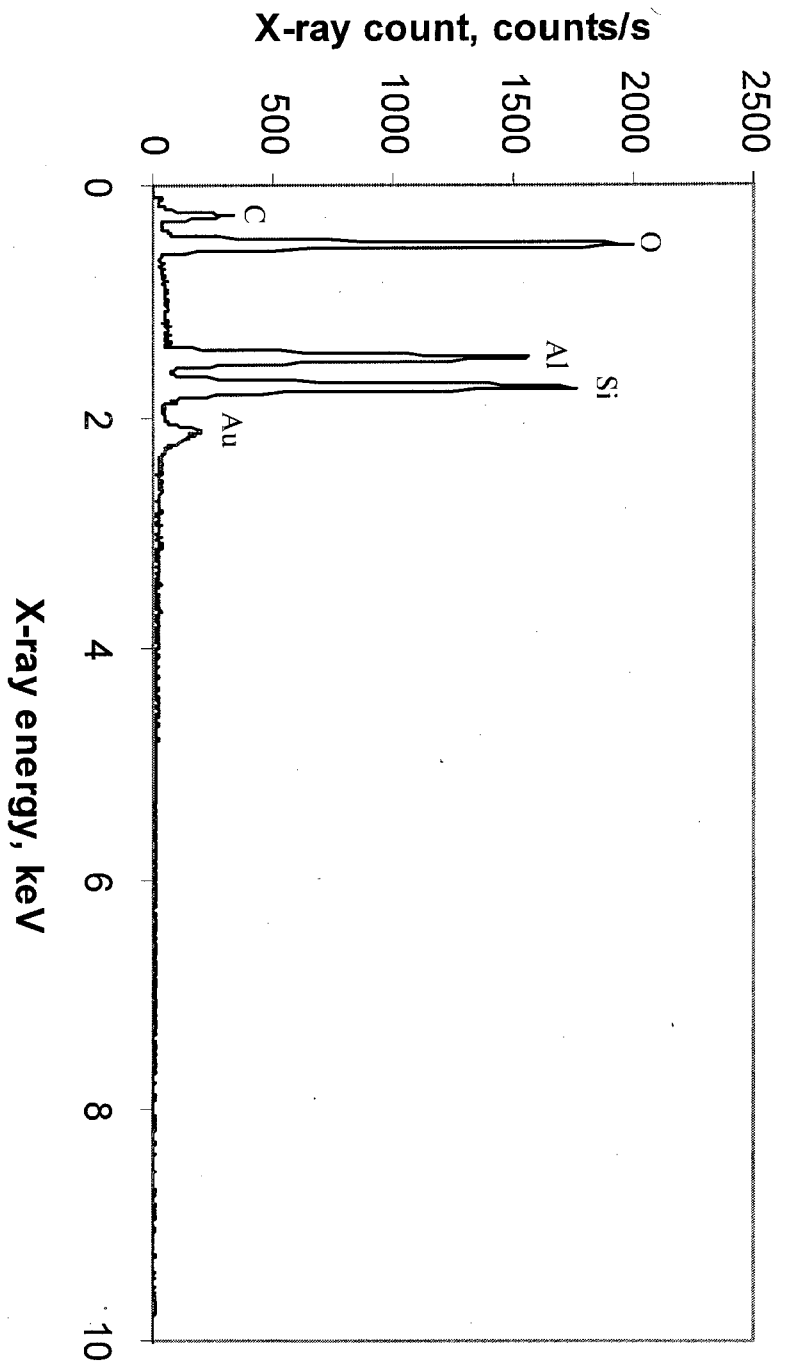


Figure 3.44. Energy dispersive X-ray spectrum of HTV SIR specimen aged in distilled water (0.005 mS/cm) at 75 °C for 576 h and allowed to recover at room temperature for 2700 h prior to spectroscopy.

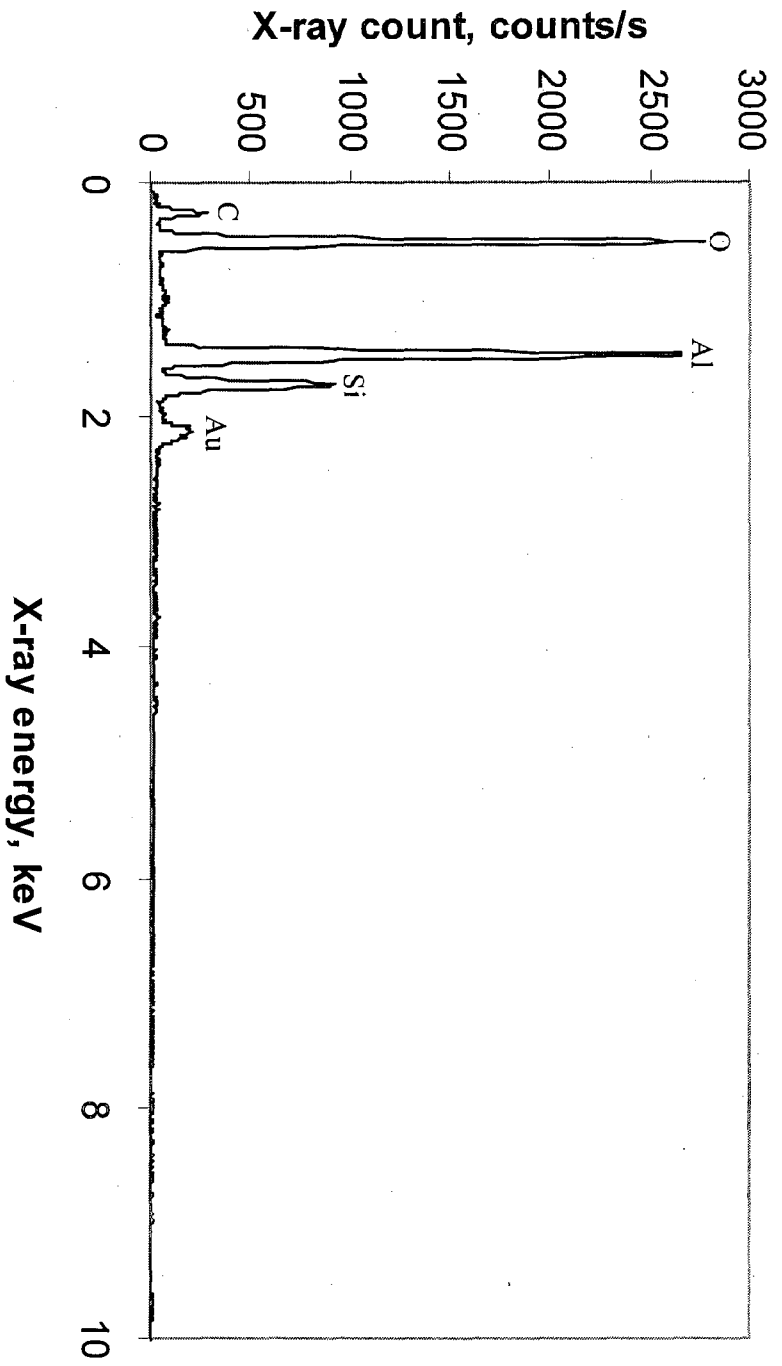


Figure 3.45. Energy dispersive X-ray spectrum of HTV SIR specimen aged in distilled water (0.005 mS/cm) at 98 °C for 576 h and allowed to recover at room temperature for 2700 h prior to spectroscopy.

3.9 ATR-FTIR Spectroscopy Results

3.9.1 Experimental Procedure

Attenuated total reflection Fourier transform infrared (ATR-FTIR) spectroscopy has been used to investigate the effect of various stresses on polymeric insulation surfaces. Utilization of ATR-FTIR to study the hydrophobicity of silicone rubber insulators has been previously reported [26-29].

ATR uses a waveguide crystal in contact with the sample surface to gain an infrared spectrum of the material. The penetration depth of the radiation into the sample is proportional to the wavelength of the radiation. The main proviso regarding the use of ATR is that the surface of the sample has to be sufficiently flat or flexible to permit intimate contact over the area of the crystal [73].

In this study, a Bruker Equinox 55 Fourier Transform Infrared Spectrometer, equipped with ZnSe ATR crystal and a DTGS detector was used to record the spectra. Each spectrum was taken with a resolution of 4 cm^{-1} . Before recording the spectra of the actual HTV SIR specimens, an IR background was obtained without sample. Then, the specimens were tested one by one and the crystal was carefully cleaned after each test by methanol. In order to ensure the reproducibility of the results, each specimen was tested twice.

3.9.2 Results

Some typical characteristic IR absorption bands for pure polydimethylsiloxanes (PDMS) are shown in Table 3.6, where the wave numbers for the corresponding bonds are presented. The selected specimens had been in saline solutions of 1 and 100 mS/cm at 0 and 98 °C for 576 hours. Then, the specimens were allowed to recover in air at room temperature for 2700 hours. Figures 3.45-3.48 show the ATR FTIR spectra of the four selected specimens each compared with the virgin

sample. Wave number in these figures is a wave property inversely related to wavelength and it is a spatial analogue of frequency. The unit Wavenumber is cm^{-1} , called "reciprocal centimeter".

Table 3.6. Characteristic IR Absorption Bands in Silicones [10]

Wave numbers (cm^{-1})	Bond
2962–2960	CH in CH_3
1440–1390	CH_3 in Si-CH_3
1280–1240	Si-CH_3
1100–1000	Si-O-Si
870–850	$\text{Si}(\text{CH}_3)_3$
840–790	$\text{Si}(\text{CH}_3)_2$
750	$\text{Si}(\text{CH}_3)_3$

The peaks of interest which can be seen in the spectra of virgin as well as aged specimens with different absorbance levels are as follows:

- 3400-3600 cm^{-1} shows the presence of OH groups
- 2960 cm^{-1} is due to C-H stretching bond in CH_3 group
- 1255 cm^{-1} is due to the deformation of CH in Si-CH_3 groups
- 1005-1100 cm^{-1} is due to the absorption of Si-O bond in Si-O-Si chain
- 785 cm^{-1} this sharp peak is due to the stretching vibrations of $\text{Si}(\text{CH}_3)_2$ group

It is apparent from the spectra of Figures 3.45-3.46 that there is not any appreciable difference in absorbance of aged samples compared to the virgin one. This is in good agreement with the observed experimental results as well as the previous report [29] in which three cleaned operated weathershed samples

and the same number of cleaned new weather-shed samples were immersed into distilled water for 96 h. Then, the investigation for loss and recovery of hydrophobicity was conducted. The recovery of hydrophobicity was checked after keeping these samples in the standard environment for 48 hours and found to be the same for the aged and the new ones.

As shown in Figures 3.47-3.48, if we regard the absorbance intensity of Si-CH₃, C-H and Si-O-Si in the spectrum of the virgin sample as a reference (100%), then their ratio was found to be decreased after aging of the samples in the solutions of different conductivities at 98 °C. This is consistent with the previous report [43] in which a significant decrease has been described in the intensities of Si-CH₃ and Si-O-Si groups as observed in the ATR FTIR spectra of the HTV SIR samples after aging in water at 80 °C for 500 h.

In this study, a net weight loss of 2.42% and 2.24% has been observed due to the aging of HTV SIR specimens in solutions of 1 and 100 mS/cm respectively at 98 °C for 576 h. Therefore, the decrease in intensity might be due to the loss of LMW fluid at high temperature. In addition, another explanation would be the dissolving of alumina trihydrate from bulk into the water at high temperatures. This caused an increased intensity of Al and decreased intensity of hydrophobic groups on the surface of the aged insulator specimens as explained in section 3.8.3 of chapter 3.

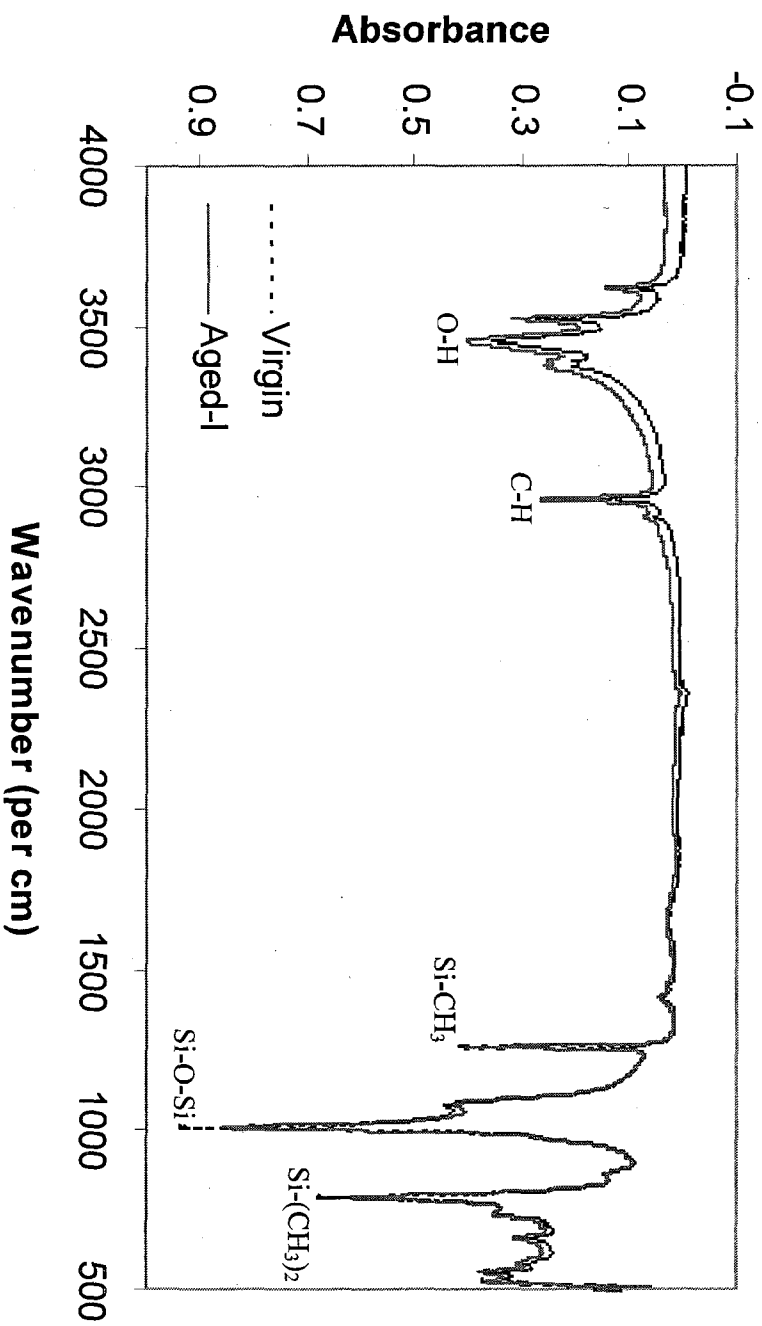


Figure 3.46. Comparison between the ATR-FTIR spectra of a virgin HTV SIR specimen and the aged-I, the specimen aged in saline water of 1 mS/cm conductivity at 0 °C for 576 h. The aged specimen had been allowed to recover in stationary air at room temperature for 2700 h before the spectra.

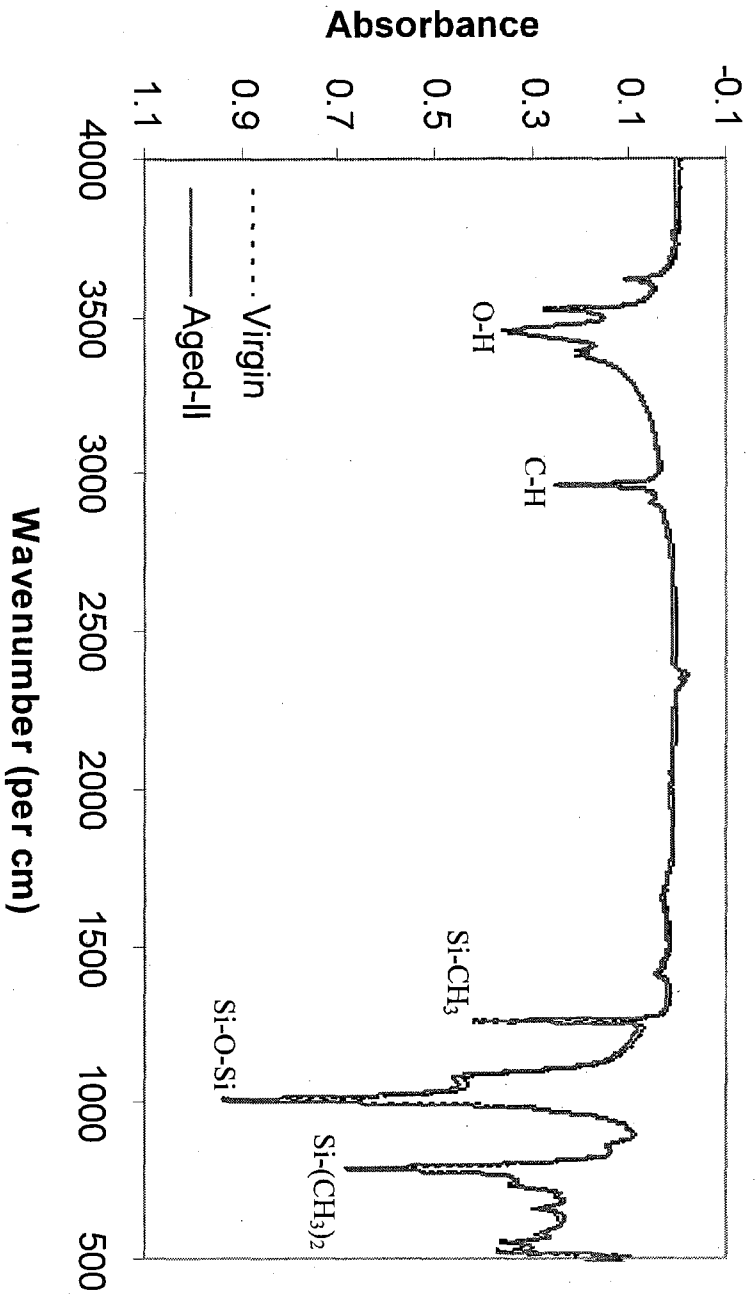


Figure 3.47. Comparison between the ATR FTIR spectra of a virgin HTV SIR specimen and the aged-II, the specimen aged in saline water of 100 mS/cm conductivity at 0 °C for 576 h. The aged specimen had been allowed to recover in stationary air at room temperature for 2700 h before the spectra.

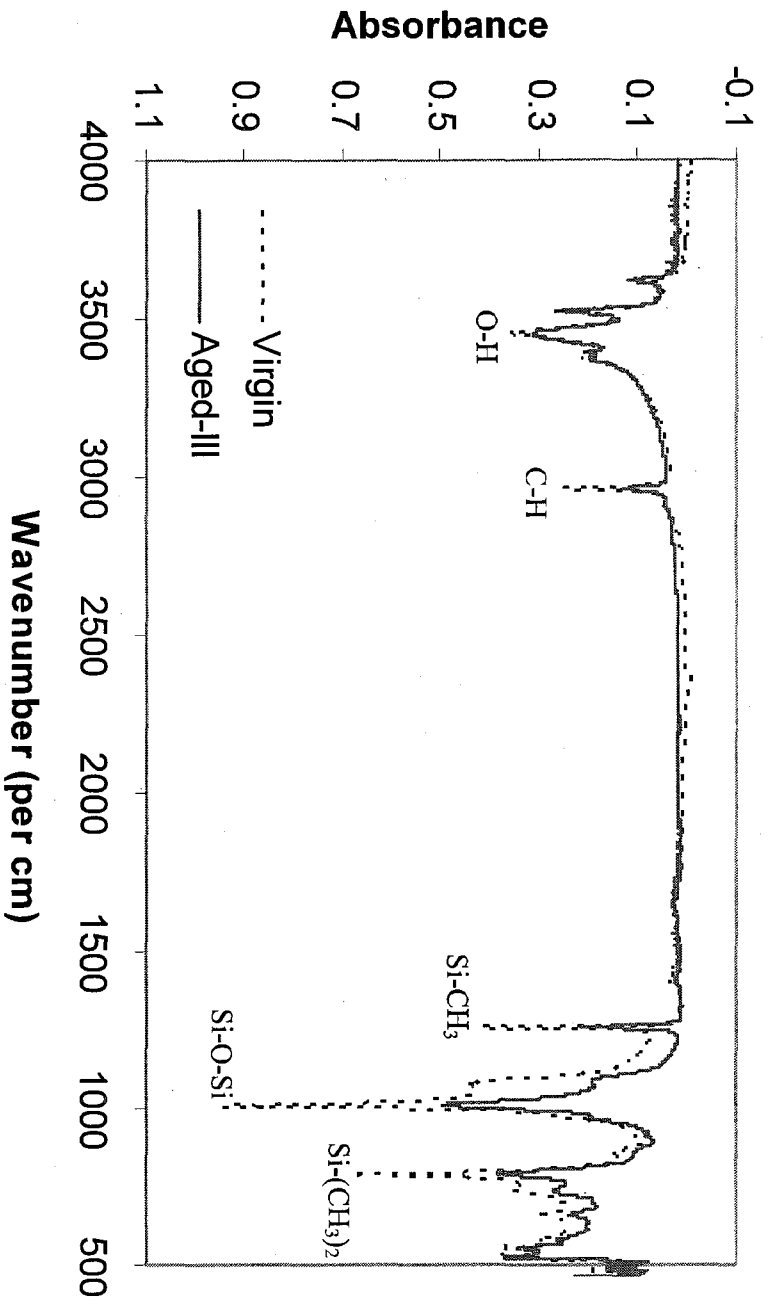


Figure 3.48. Comparison between the ATR FTIR spectra of a virgin HTV SIR specimen and the aged-III, the specimen aged in saline water of 1 mS/cm conductivity at 98 °C for 576 h. The aged specimen had been allowed to recover in stationary air at room temperature for 2700 h before the spectra.

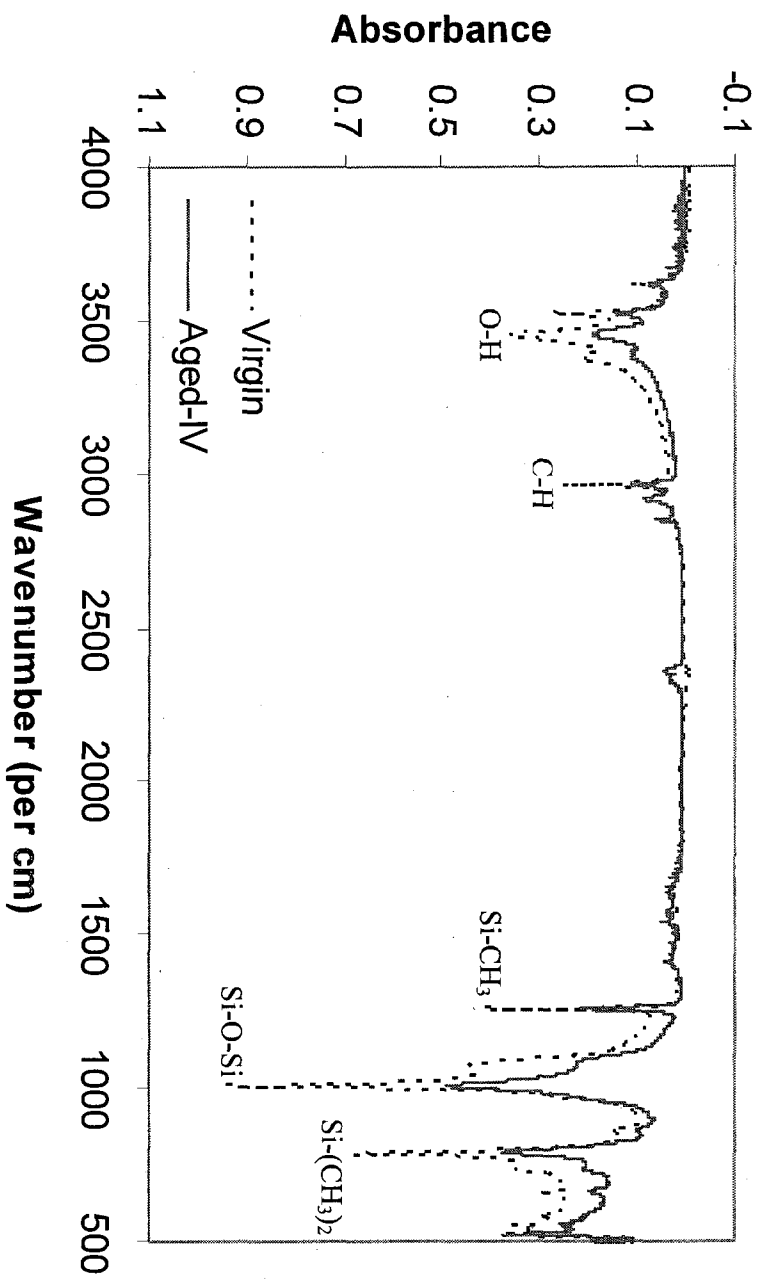


Figure 3.49. Comparison between the ATR FTIR spectra of a virgin HTV SIR specimen and the aged-IV, the specimen aged in saline water of 100 mS/cm conductivity at 98 °C for 576 h. The aged specimen had been allowed to recover in stationary air at room temperature for 2700 h before the spectra.

CHAPTER 4

4 Surface Properties of HTV SIR Insulator during Long Term Aging

4.1 Introduction

In chapter 3, the loss of hydrophobicity of HTV SIR in the presence of water solutions of different conductivities at different temperatures for 576 h and later on their recovery for 2700 h at room temperature has been studied. In order to observe the changes in the surface roughness and hydrophobicity and their correlation with the weight of the specimens during aging over a longer period of time, the samples of HTV SIR were immersed in glass jars containing different saline solutions at different temperatures for 3000 hours. Afterwards, the changes were further monitored for 3000 h during their recovery at room temperature.

For this purpose, the HTV SIR specimens of the same size 1 cmx 1 cmx 0.5 cm as used in chapter 3 were cut from the weather-sheds of the same 46 KV outdoor insulator. Similar studies of aging for a longer period of time have previously been conducted on high voltage organic insulating materials like PTFE for 4000 h [38], Delrin for 2160 h [51], EPDM for 6000 h [73], HDPE for 3000 h [62] and XLPE for 3000 h [63].

4.2 Effect of Temperature and Saline Water on Weight

Figures 4.1 to 4.5 show the percentage change in weight of HTV SIR specimens due to absorption of water having four different conductivity levels of 0.005, 1, 10 and 100 mS/cm as a function of time and kept at five different temperatures 0 ± 1 , 22 ± 3 , 50, 75 and 98 °C. The aging of HTV SIR specimens due to immersion in

saline solutions at different temperatures as a function of immersion time for 576 h has already been reported in chapter 3. In this part of the study, the time of immersion was extended up to 3000 h.

Figure 4.1 shows the increase in weight during 3000 h of immersion at 0 °C which is 0.70, 0.61, 0.48 and 0.11 % for solutions having conductivities of 0.005, 1, 10 and 100 mS/cm respectively. Similarly, Figure 3.2 shows the increase in weight at 25 °C and is 1.41, 1.28, 0.94 and 0.16% for solutions having conductivities of 0.005, 1, 10 and 100 mS/cm respectively. There is a trend of increasing weight even after 3000 hours of immersion in solutions of all conductivities at 0 and 25 °C as shown in Figures 4.1-4.2.

Similarly, Figures 4.3-4.5 show the change in weight during immersion in solutions of conductivities 0.005, 1, 10 and 100 mS/cm at 50, 75 and 98 °C, respectively. In these Figures, it is seen that there is an increase in weight initially during few hours and afterwards there is a decrease. From the figures, it is apparent that the rate of absorption of the saline solutions increased with the increase of temperature. Moreover, after attaining the maximum weight, there is a greater weight loss gradient with the increase of temperature for the solutions of all conductivities.

At 50 °C, the net weight increase of 1.08, 1.03, 0.81 and 0.08 % were observed for solutions having conductivities of 0.005, 1, 10 and 100 mS/cm, respectively at the end of 3000 h. At 75 °C, the net weight increased by 0.45% and 0.06% for solutions having conductivities of 1 and 10 mS/cm, respectively whereas the weight decreased by 0.11% and 0.66 % for the solutions having conductivities of 0.005 and 100 mS/cm at the end of 3000 h. However, at 98 °C, there is a net weight decrease of 10.81, 8.92, 8.33 and 7.43 % for solutions having conductivities of 0.005, 1, 10 and 100 mS/cm, respectively, at the end of 3000 h. Also at high temperature, the increase in weight reached saturation and

afterwards it decreased with a greater weight increase/decrease gradient for all salinity levels.

Figure 4.6 shows the change in weight of the specimens kept in stationary air at the five different temperatures described above. At 0 °C, there was a minor increase in the weight by 0.09% initially and afterwards there was no change whereas at 22 °C (room temperature), almost there was no variation in the weight. At 50 and 75 °C, there was a decrease in the weight by 0.14 and 0.28% respectively and afterwards, it became constant.

This decrease in the weight at a faster rate in the first few hours might be due to the instantaneous evaporation of water contents of the specimens at temperatures higher than room temperature. However, at 98 °C, a continuous decrease in the weight was observed over the entire period of 3000 hours with a total weight loss of 0.97%. Table 4.1 shows a summary of the changes in the weight of the HTV SIR specimens during the aging process.

Table 4.1. Percentage weight gain (+) or loss (-) of the HTV SIR specimens after aging in different stress conditions at the end of 576 hours

Aging Temperature (°C)	Aging in Air	Aging in Saline Water (mS/cm)			
		0.005	1	10	100
0	0.09	0.70	0.61	0.48	0.11
25	0	1.41	1.28	0.94	0.16
50	-0.14	1.08	1.03	0.81	0.08
75	-0.28	-0.11	0.45	0.06	-0.66
98	-0.97	-10.81	-8.92	-8.33	-7.43

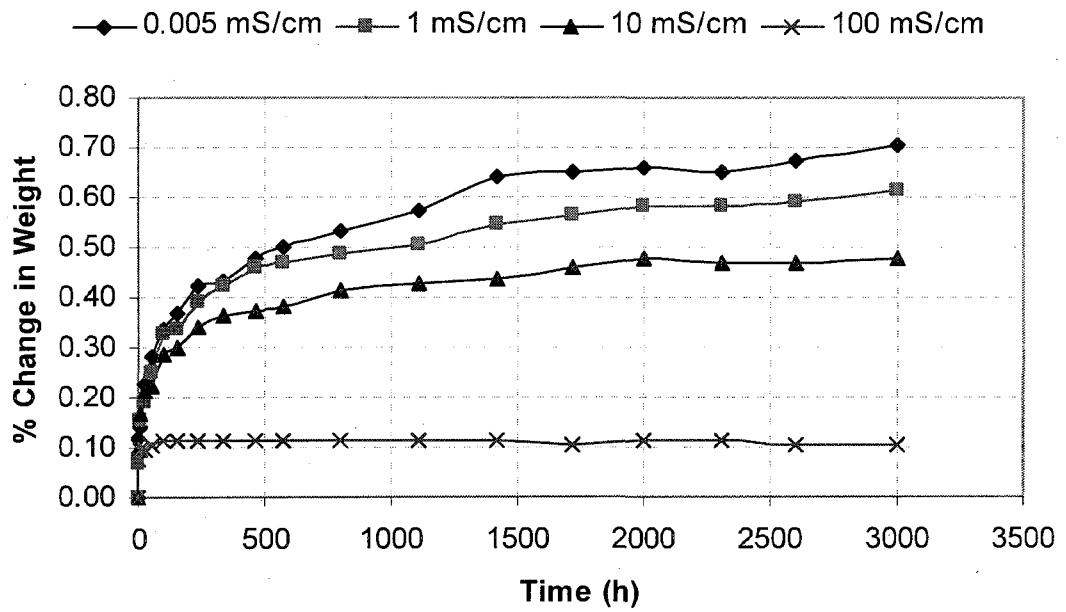


Figure 4.1. Percentage change in weight of HTV SIR specimens as a function of time during immersion in saline solutions of different conductivities at 0 °C for 3000 h.

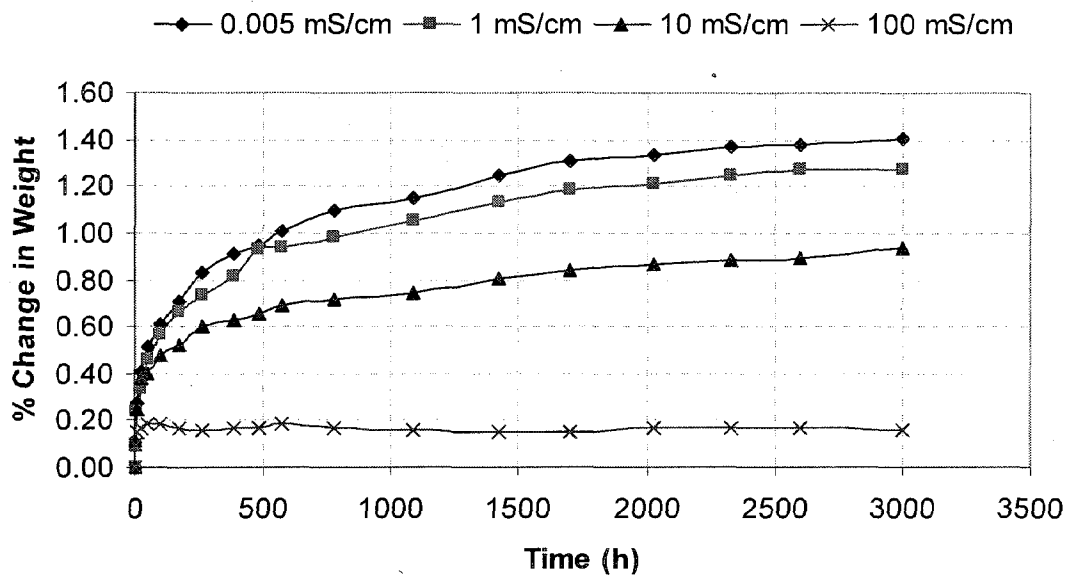


Figure 4.2. Percentage change in weight of HTV SIR specimens as a function of time during immersion in saline solutions of different conductivities at 22 °C for 3000 h.

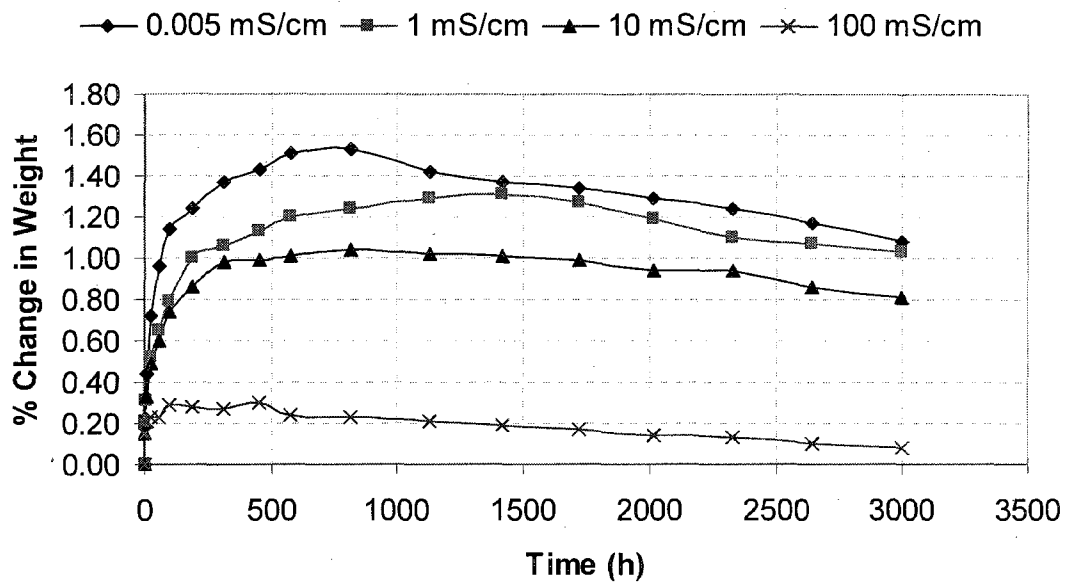


Figure 4.3. Percentage change in weight of HTV SIR specimens as a function of time during immersion in saline solutions of different conductivities at 50 °C for 3000 h.

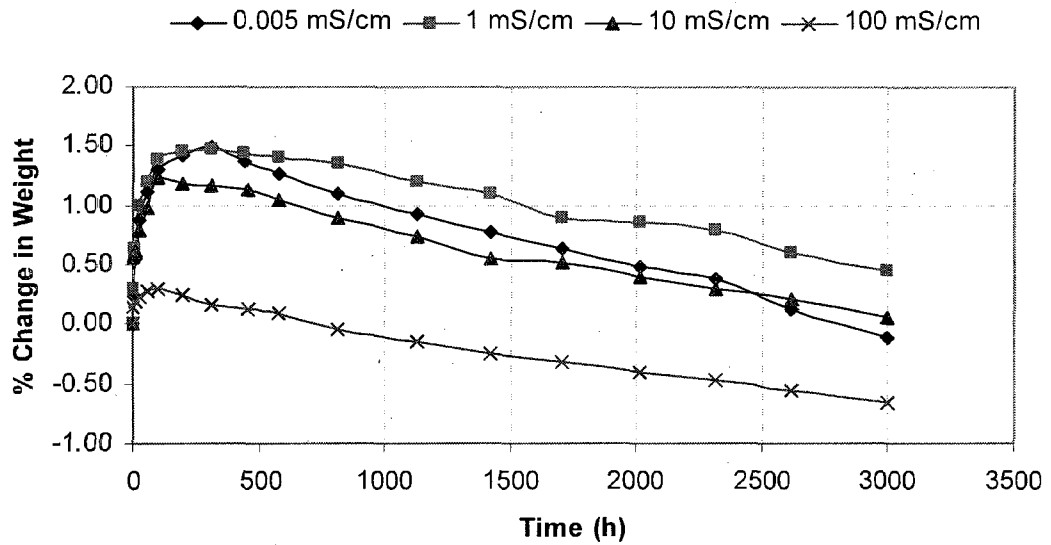


Figure 4.4. Percentage change in weight of HTV SIR specimens as a function of time during immersion in saline solutions of different conductivities at 75 °C for 3000 h.

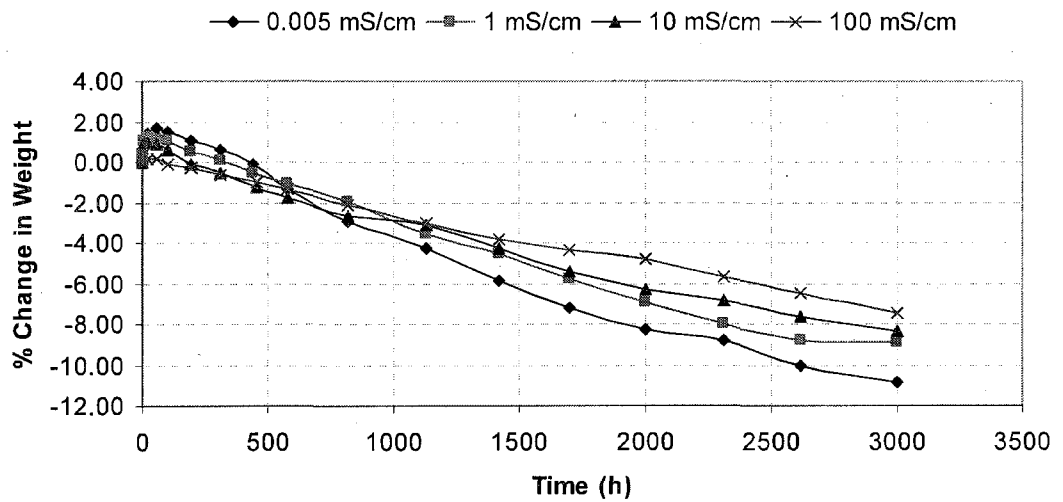


Figure 4.5. Percentage change in weight of HTV SIR specimens as a function of time during immersion in saline solutions of different conductivities at 98 °C for 3000 h.

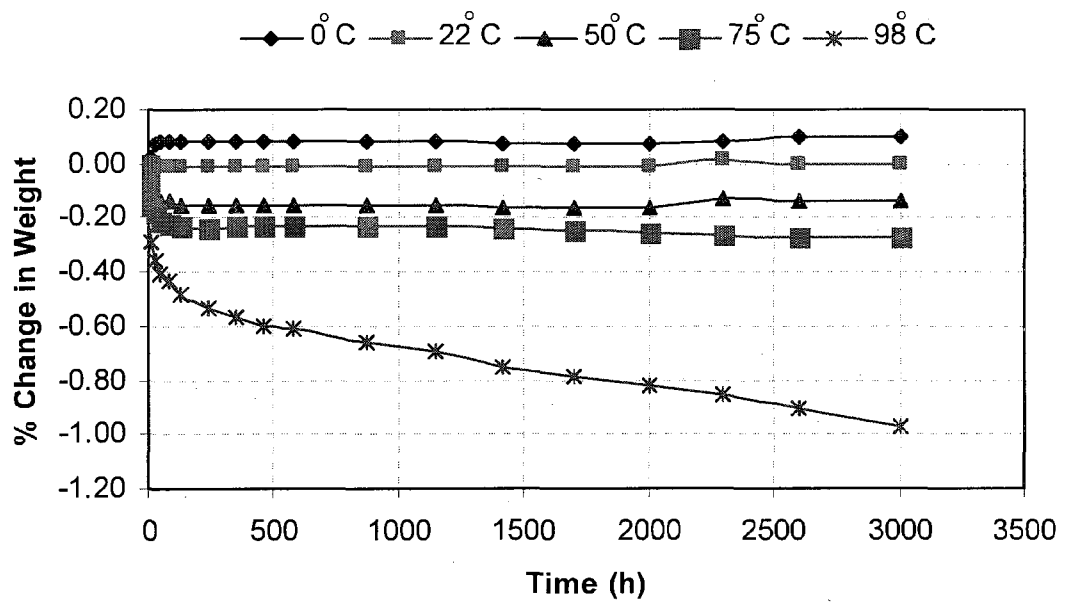


Figure 4.6. Percentage change in weight of HTV SIR specimens as a function of time during aging in stationary air at different temperatures for 3000 h

4.3 Effect of Temperature and Salinity on Contact Angle

Figures 4.7 to 4.11 show the variation of the contact angle on the surface of the HTV SIR specimens as a function of time at temperatures of 0, 22, 50, 75 and 98 °C, respectively. For each temperature, four solutions of different conductivities of 0.005, 1, 10 and 100 mS/cm were used. The contact angle of the virgin specimens was measured to be $100 \pm 5^\circ$. It is apparent from the figures that in the beginning, the contact angle and therefore the hydrophobicity decreased appreciably when the samples were immersed at temperatures between 0 to 98 °C regardless of the conductivity of the solution. Figures 4.7-4.10 show that the contact angle did not decrease below 65° during aging at temperatures 0-75 °C for 3000 h. However, a greater decrease in the contact angle has been observed for the specimens aged in different conductivities at 98° C.

As shown in Figure 4.11, there is not much difference in the contact angle of distilled water on the surface of HTV SIR specimens being aged in solutions of different conductivities at 98 °C for up to 1000 h. However, the value of the contact angle started varying after 1000 h depending on the conductivity of the solution. The final values of the contact angle observed at the end of the aging period of 3000 h are 15, 25, 45 and 55° for the solutions of 0.005, 1, 10 and 100 mS/cm, respectively.

Therefore, a decrease of 86, 73, 55 and 48° in the contact angles of the specimens immersed in 0.005, 1, 10 and 100 mS/cm saline solutions, respectively was observed after 3000 h at 98 °C. This reduction in the contact angle and therefore the loss of hydrophobicity was largely due to the absorption of water by the specimens. The higher decrease of the contact angle at low salinity levels is related to the higher rate of absorption of water into the polymer and a greater change in the weight during aging at high temperature.

The decrease in hydrophobicity discussed above can be explained in terms of weight loss. For example, there was a weight loss of 5.9% in the specimen after

1420 h of immersion in a solution of 0.005 mS/cm at 98 °C and the drop of distilled water completely spread out over the surface. The droplet of methylene iodide also started spreading out over the surface but less than that of distilled water. This shows that the surface became hydrophilic after 1420 h. Similarly after 2618 h, there was a weight loss of 10% and the droplet of distilled water used to measure the contact angle spread out over the surface immediately. Also, the droplet was absorbed by the sample within one minute and similar observation was for the droplet of methylene iodide. However, the surface of the specimens became completely wet at the end of aging period of 3000 h and it took fifteen minutes to dry up.

The decrease in the contact angle of distilled water on the surface of HTV SIR specimens with the decrease of salinity during aging has already been reported in chapter 3 which is consistent with these observations. This decrease in the contact angle at low salinity is related to the higher rate of absorption of water by the specimens in the solutions of low conductivity. It is worth mentioning here that every time before measurement of the contact angle, the salt particles were washed away from the surface by a spray of distilled water.

Figure 4.12 shows the change in the contact angle of HTV SIR specimens kept in air at different temperatures from 0 to 98 °C. There was a slight decrease in the contact angle at 0°C whereas no reasonable change was observed at 22 °C. However, there was an increase in the contact angle with the increase of temperature from 50 to 98°. This increase is consistent with the results of the previous chapter in which the increase in the contact angle of distilled water on the surface of HTV SIR specimens has been observed at higher temperatures (50-98 °C). After about 1000 h, there was a saturation point and no further increase in the contact angle although in some cases, there was a minor decrease after saturation.

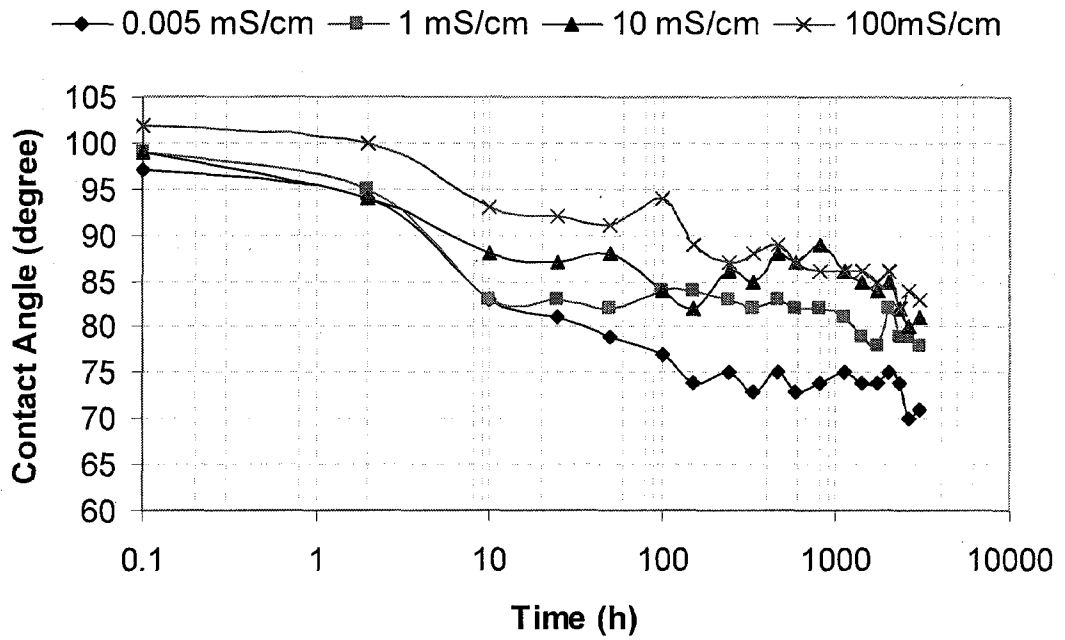


Figure 4.7. Time variation of contact angle of distilled water on the surface of HTV SIR specimens during aging in water solutions of different conductivities at 0 °C for 3000 h.

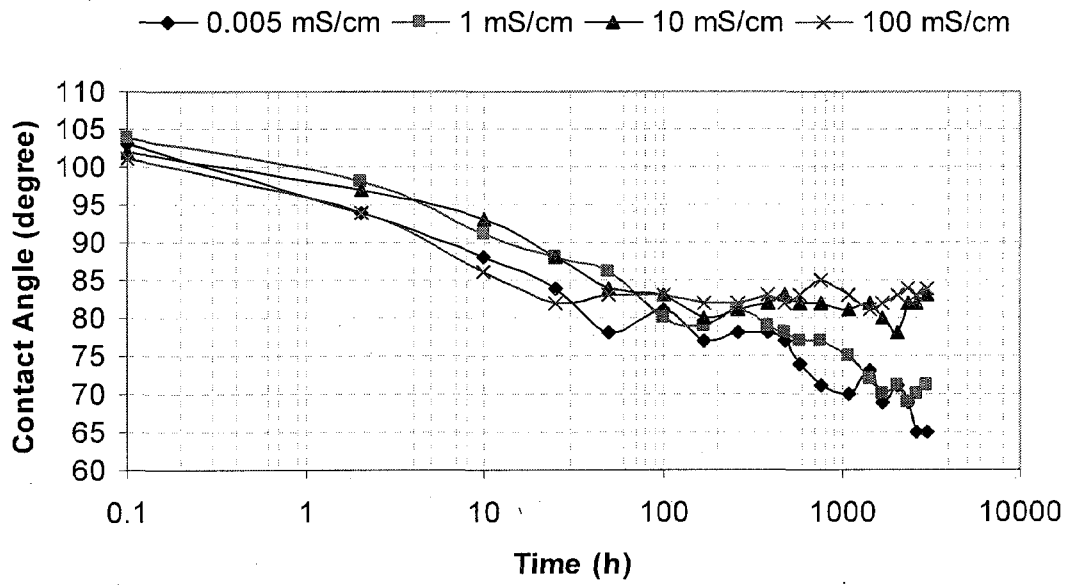


Figure 4.8. Time variation of contact angle of distilled water on the surface of HTV SIR specimens during aging in water solutions of different conductivities at 22 °C for 3000 h.

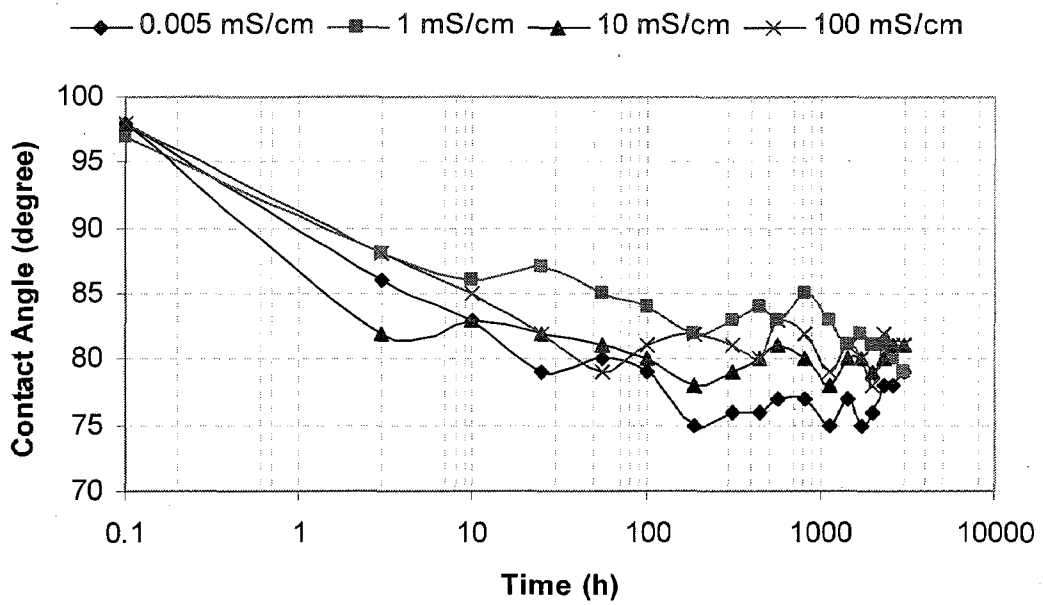


Figure 4.9. Time variation of contact angle of distilled water on the surface of HTV SIR specimens during aging in water solutions of different conductivities at 50 °C for 3000 h.

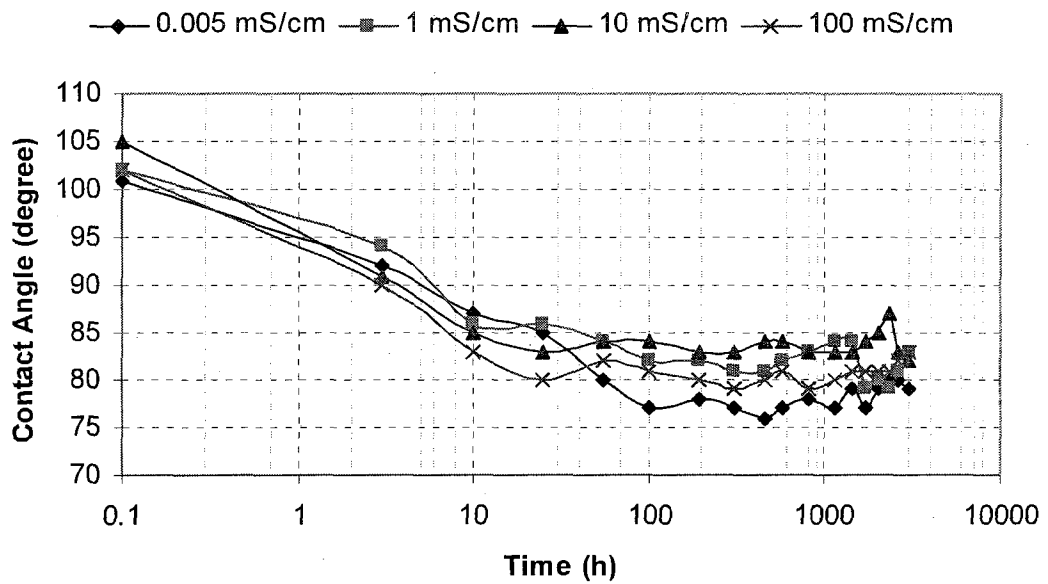


Figure 4.10. Time variation of contact angle of distilled water on the surface of HTV SIR specimens during aging in water solutions of different conductivities at 75 °C for 3000 h.

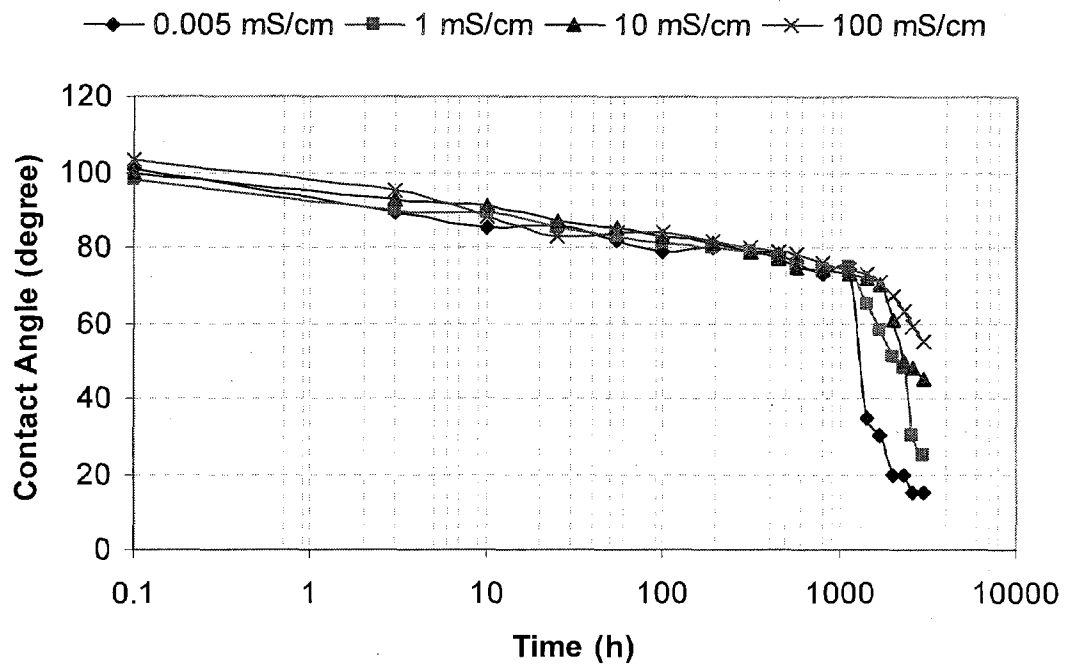


Figure 4.11. Time variation of contact angle of distilled water on the surface of HTV SIR specimens during aging in water solutions of different conductivities at 98 °C for 3000 h.

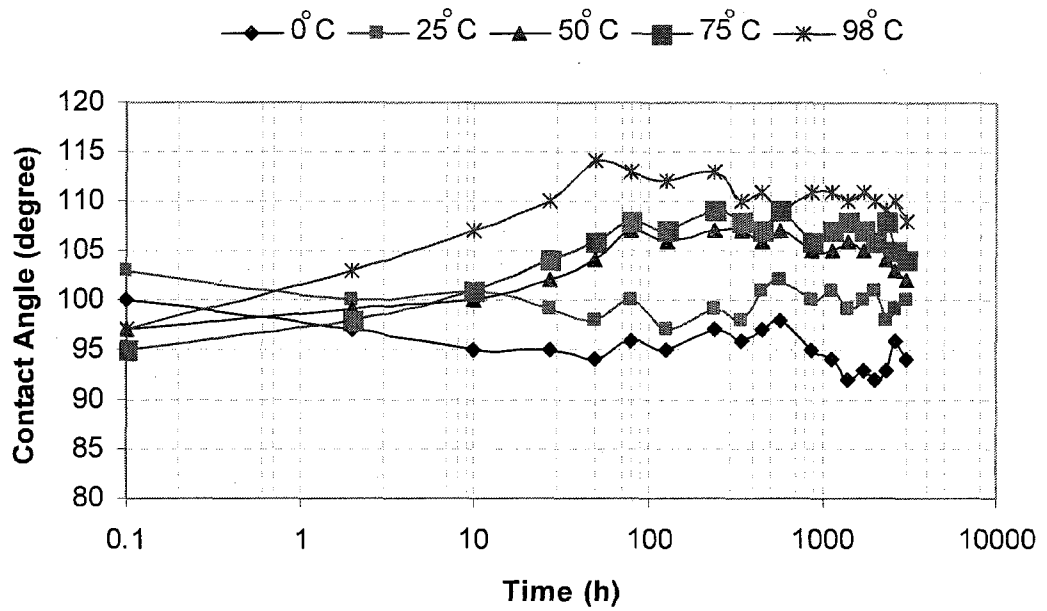


Figure 4.12. Time variation of contact angle of distilled water on the surface of HTV SIR specimens during aging in stationary air at different temperatures for 3000 h.

4.4 Effect of Temperature and Salinity on Surface Roughness

Figures 4.13-4.17 show the variation in the average surface roughness (ASR) of HTV SIR specimens as a function of time during immersion in saline solutions of different conductivities at 0, 25, 50, 75 and 98 °C, respectively. The variation in surface roughness is not significant up to a temperature of 75 °C even when the immersion period was extended to 3000 h as shown in Figures 4.13-4.16.

Figure 4.17 shows an appreciable increase in ASR in most of the samples during aging at 98 °C which can be linked to an excessive weight loss of the samples in low conductivity solutions at high temperature. It is apparent from the figure that there is not much change in ASR of all the four samples up to 1000 h of immersion. However, after about 1000 h of immersion the ASR started increasing in the specimens which were being aged in solutions of 0.005, 1 and 10 mS/cm conductivities. The surface of the specimens aged in 0.005 mS/cm solution became hard and brittle. Also, the surface was so delicate that it started to disintegrate by itself.

Careful examination of the samples aged in solutions of 1 and 10 mS/cm at 98 °C showed cracks on the surface. Ultimately, these cracks caused an appreciable increase in ASR of the samples as shown in Figure 4.17. However, a minor change in ASR was observed in a solution of 100 mS/cm at 98 °C and this invariance in ASR might be due to a smaller decrease in weight as a function of time in a solution of high conductivity. So, it can be concluded that the loss of weight caused a variation in ASR accordingly.

Figure 4.18 shows a change in ASR as a function of time in air at different temperatures which is not appreciable at any temperature. Figure 4.6 shows very minor variation in weight during aging in air at temperatures 0-98 °C, the maximum decrease of 0.97% at 98 °C. Ultimately, there is not any appreciable difference in ASR of HTV SIR specimens during aging in air at all temperatures.

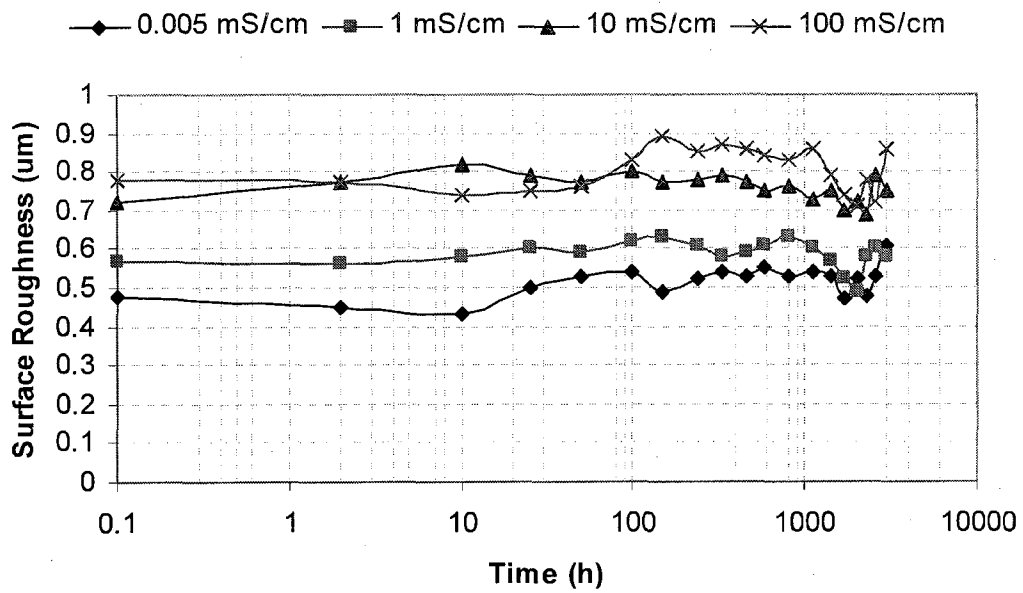


Figure 4.13. Time variation of average surface roughness of HTV SIR specimens during aging in different salinities at 0 °C for 3000 h.

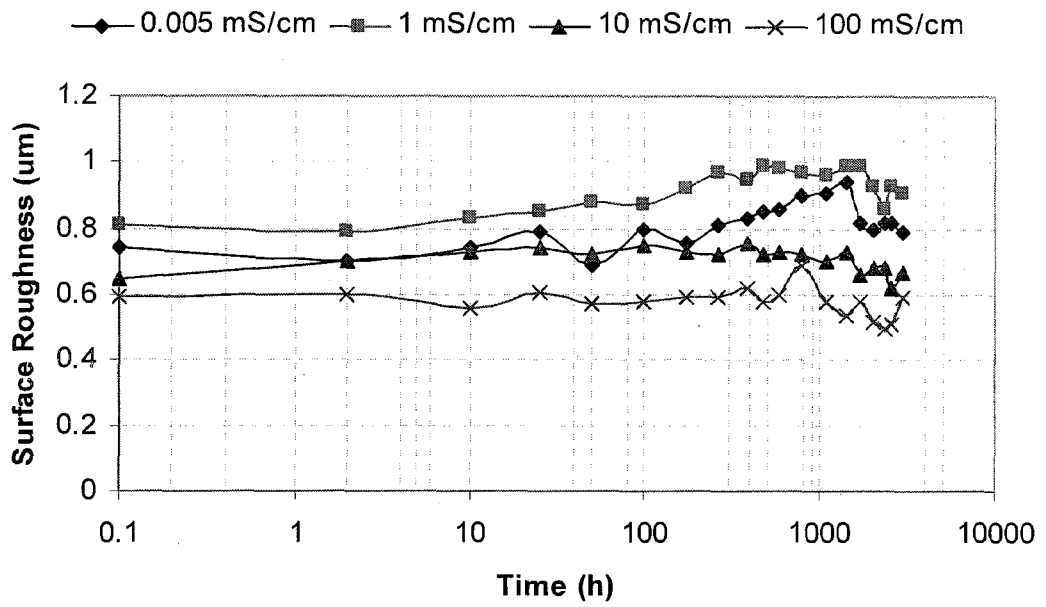


Figure 4.14. Time variation of average surface roughness of HTV SIR specimens during aging in different salinities at 25 °C for 3000 h.

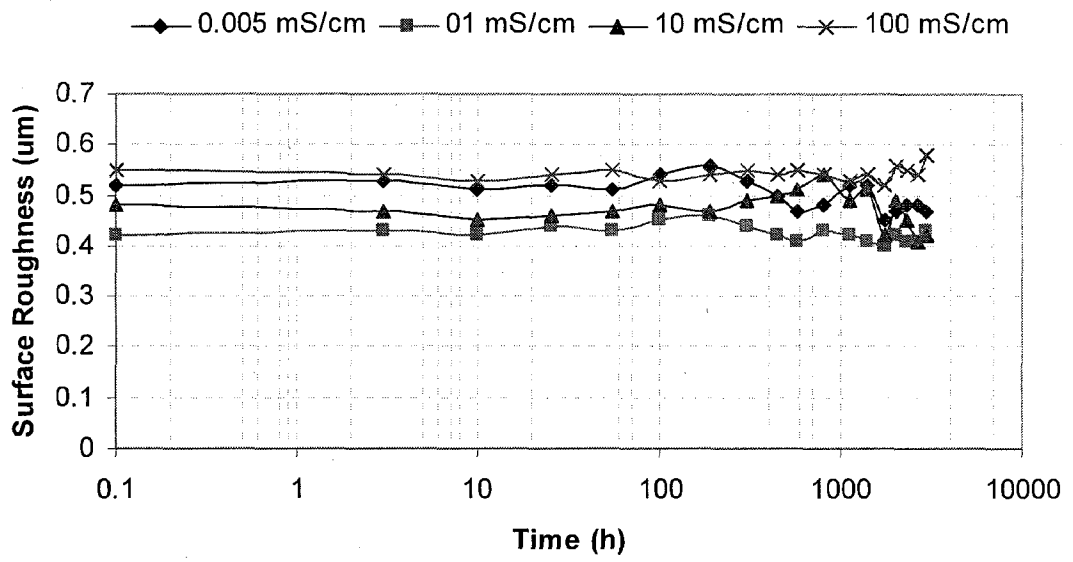


Figure 4.15. Time variation of average surface roughness of HTV SIR specimens during aging in different salinities at 50 °C for 3000 h.

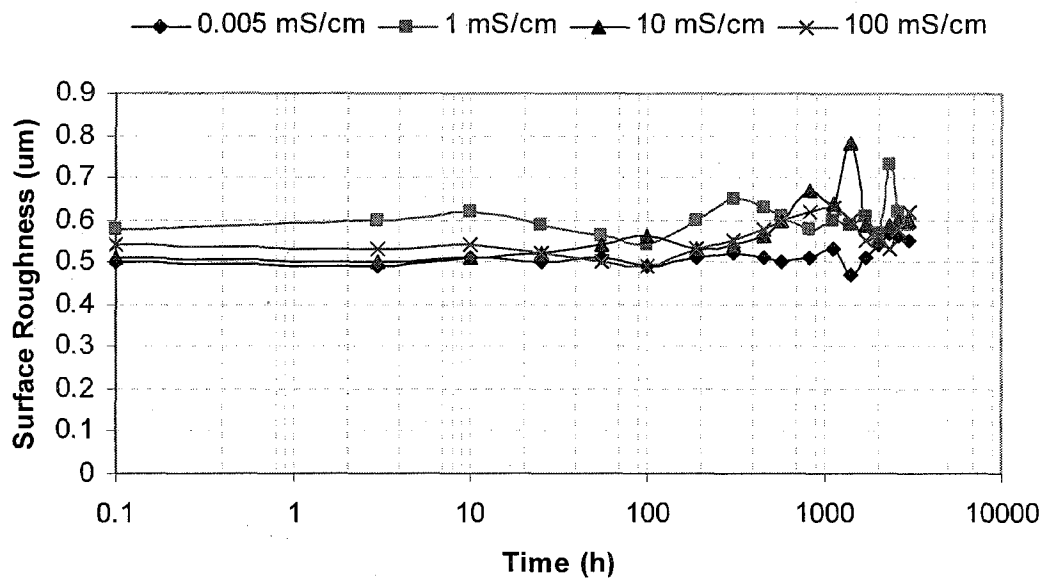


Figure 4.16. Time variation of average surface roughness of HTV SIR specimens during aging in different salinities at 75 °C for 3000 h.

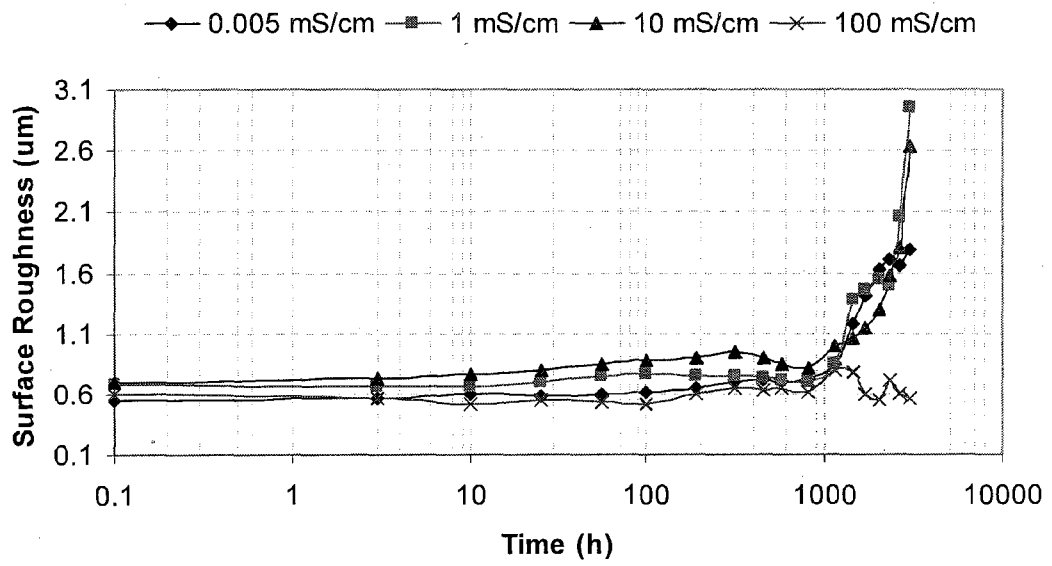


Figure 4.17. Time variation of average surface roughness of HTV SIR specimens during aging in different salinities at 98 °C for 3000 h.

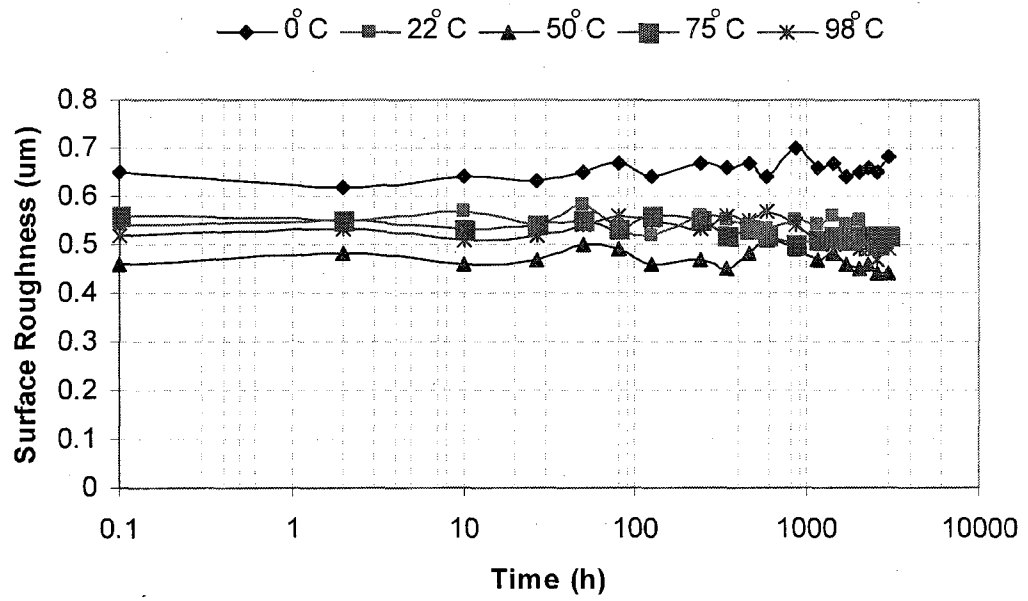


Figure 4.18. Time variation of average surface roughness of HTV SIR specimens during aging in stationary air at different temperatures for 3000 h.

4.5 Change in Weight during Recovery

After removal of the specimens from the saline solutions they were left in air at 22 ± 3 °C and 55 ± 15 % humidity for up to 3000 h. Figures 4.19-4.23 show the variation of weight as a function of time during the recovery process. All the specimens that were aged in saline solutions at different temperatures lost weight during recovery at room temperature. However, the loss of weight was faster in the beginning of the recovery period and then gradually saturated with the passage of time. The percentage reduction in weight due to drying of the specimens during the recovery process caused a change in contact angle as well. The changes in the weight were correlated to the surface roughness and the contact angle of distilled water on the surface of HTV SIR specimens and hence to the recovery of hydrophobicity.

The time period of weight to reach a saturation point during the recovery process, ranged from 24 h to more than 3000 h depending on the aging temperature. As the aging temperature was increased, the weight loss as well as the time period of evaporation also increased. The weight loss due to evaporation at room temperature ranged from 0.67 % for the specimens aged in distilled water at 0 °C to 4.54 % at 98 °C after 3000 h of recovery period. In other words, the higher the aging temperature, the greater was the percentage weight loss of the HTV SIR specimens during recovery in air. Also, the percentage weight loss increased with the increase of aging period.

It has been observed from the figures that at all temperatures, the percentage reduction in weight increased with decreasing salinity. This is because at a fixed temperature of the saline solution, the intake of water was observed to be higher in low salinity water. Therefore, the loss of water during the recovery in air was also expected to be higher. The higher the aging salinity level, the lower was the percentage of weight loss of the specimens during the recovery period which was the result of less absorption of water during aging at high salinity level. Table 4.2

shows a summary of the changes in weight of the HTV SIR specimens during the aging process.

Table 4.2 Percentage of net weight gain (+) or loss (-) of the HTV SIR specimens at the end of recovery period of 3000 h after aging in different stress conditions for 3000 h.

Aging Temperature (°C)	Aging in Air	Aging in Saline Water (mS/cm)			
		0.005	1	10	100
0	0.09	0.03	0.02	0.02	-0.02
22	0.03	-0.10	-0.13	-0.06	-0.06
50	-0.01	-0.64	-0.39	-0.37	-0.25
75	-0.06	-1.84	-1.54	-1.52	-1.03
98	-0.62	-14.86	-12.44	-9.80	-8.39

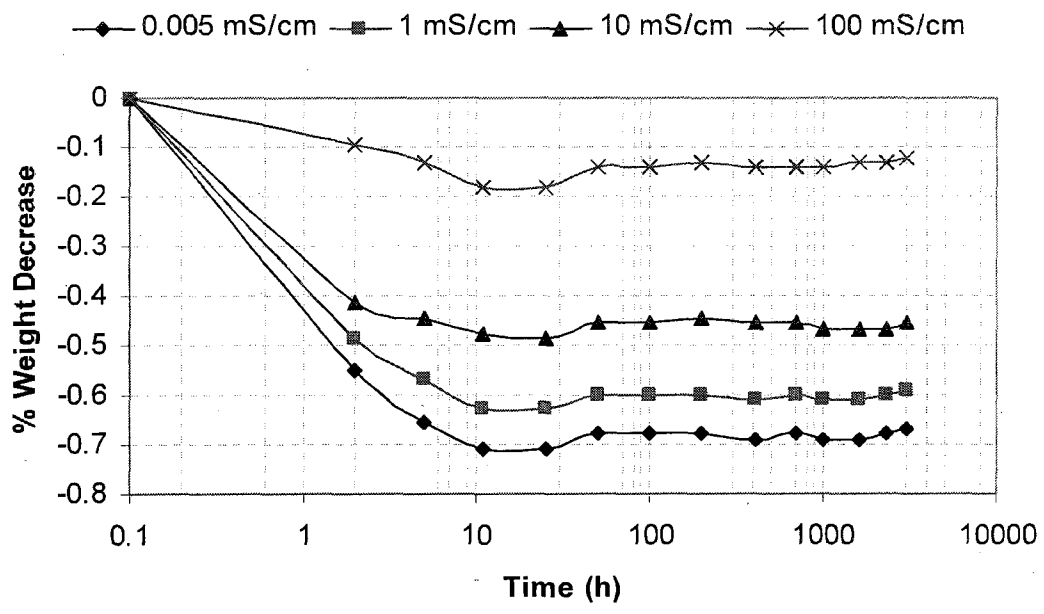


Figure 4.19. Percentage change in weight of HTV SIR specimens as a function of time during recovery in stationary air at room temperature for 3000 h. The specimens had been aged in solutions of different conductivities at 0 °C for 3000 h.

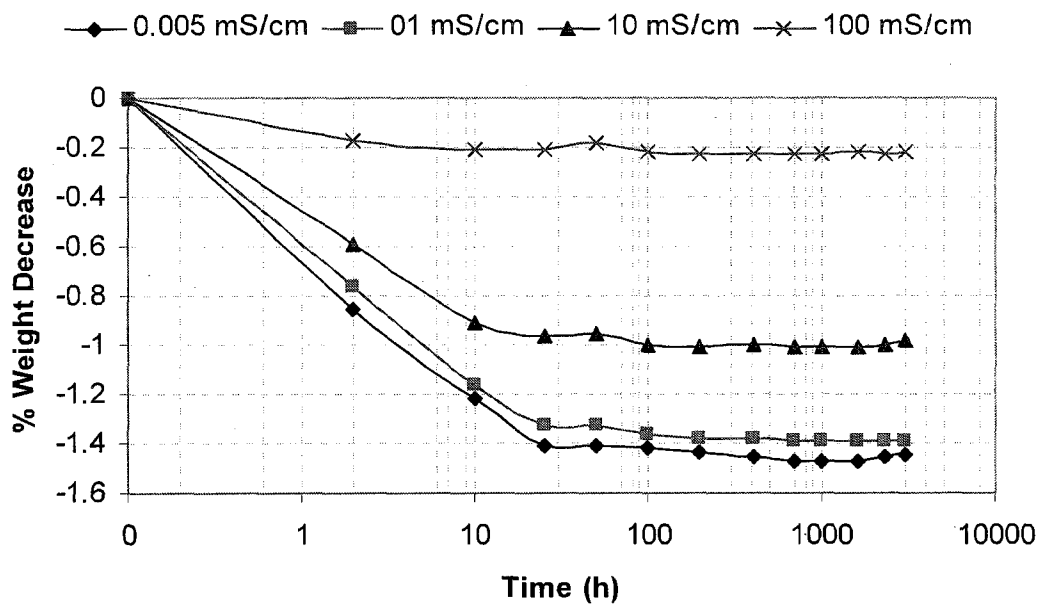


Figure 4.20. Percentage change in weight of HTV SIR specimens as a function of time during recovery in stationary air at room temperature for 3000 h. The specimens had been aged in solutions of different conductivities at 25 °C for 3000 h.

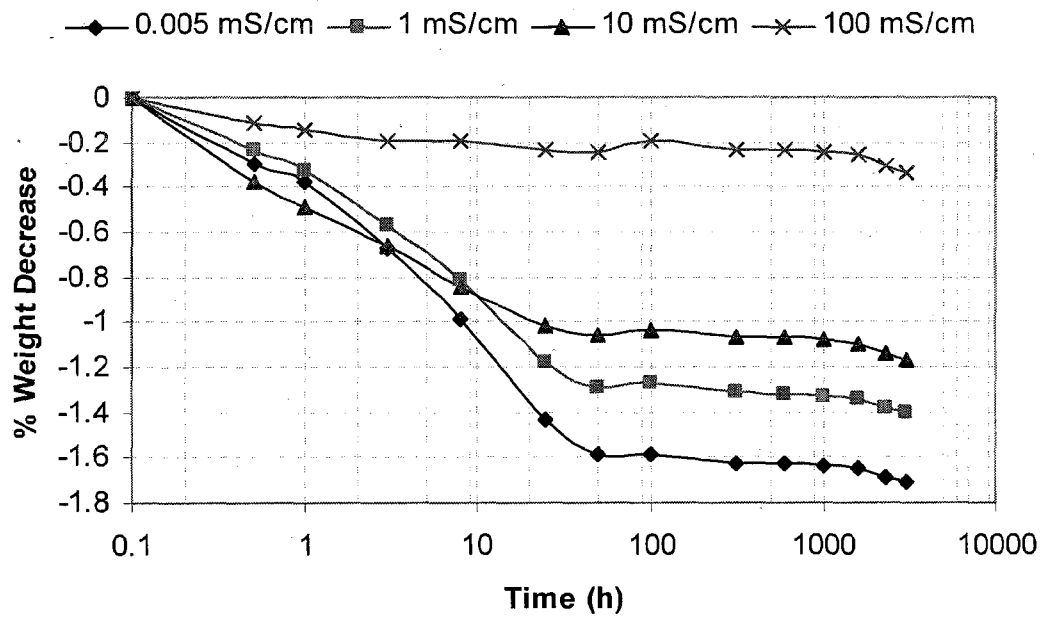


Figure 4.21. Percentage change in weight of HTV SIR specimens as a function of time during recovery in stationary air at room temperature for 3000 h. The specimens had been aged in solutions of different conductivities at 50 °C for 3000 h.

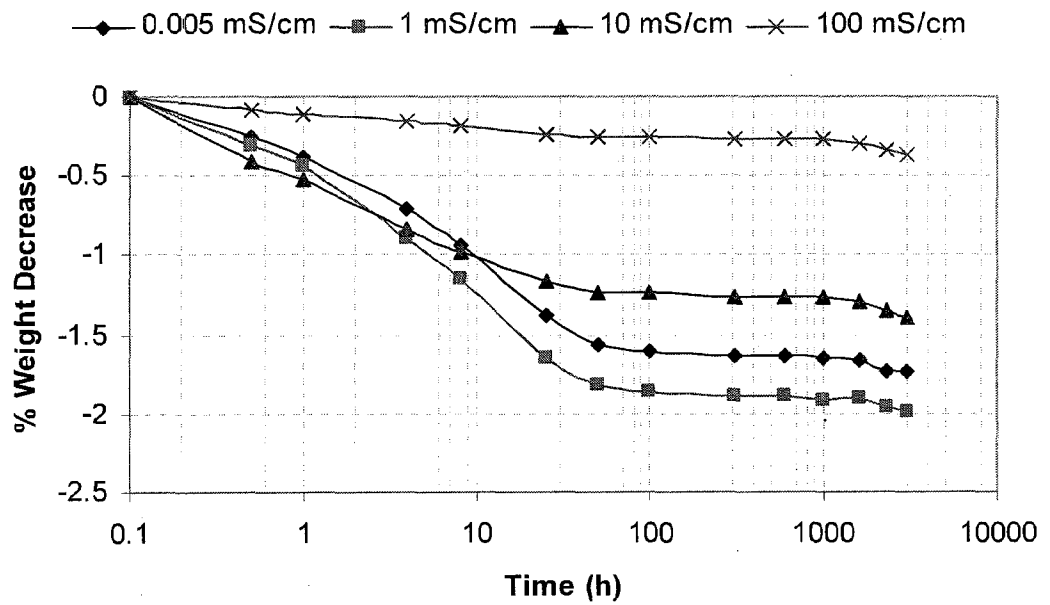


Figure 4.22. Percentage change in weight of HTV SIR specimens as a function of time during recovery in stationary air at room temperature for 3000 h. The specimens had been aged in solutions of different conductivities at 75 °C for 3000 h.

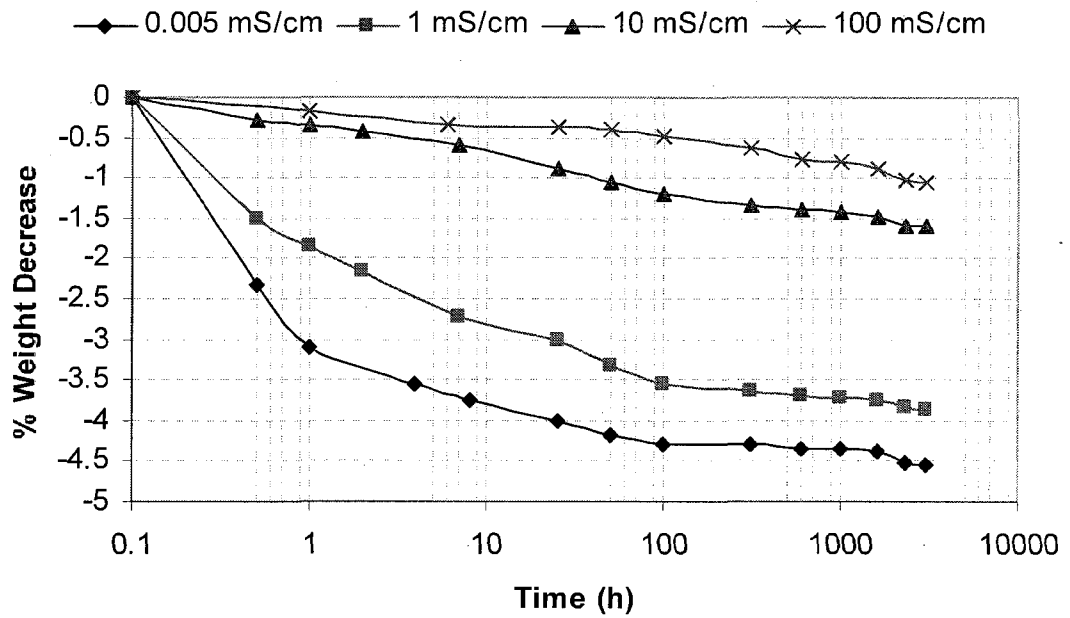


Figure 4.23. Percentage change in weight of HTV SIR specimens as a function of time during recovery in stationary air at room temperature for 3000 h. The specimens had been aged in solutions of different conductivities at 98 °C for 3000 h.

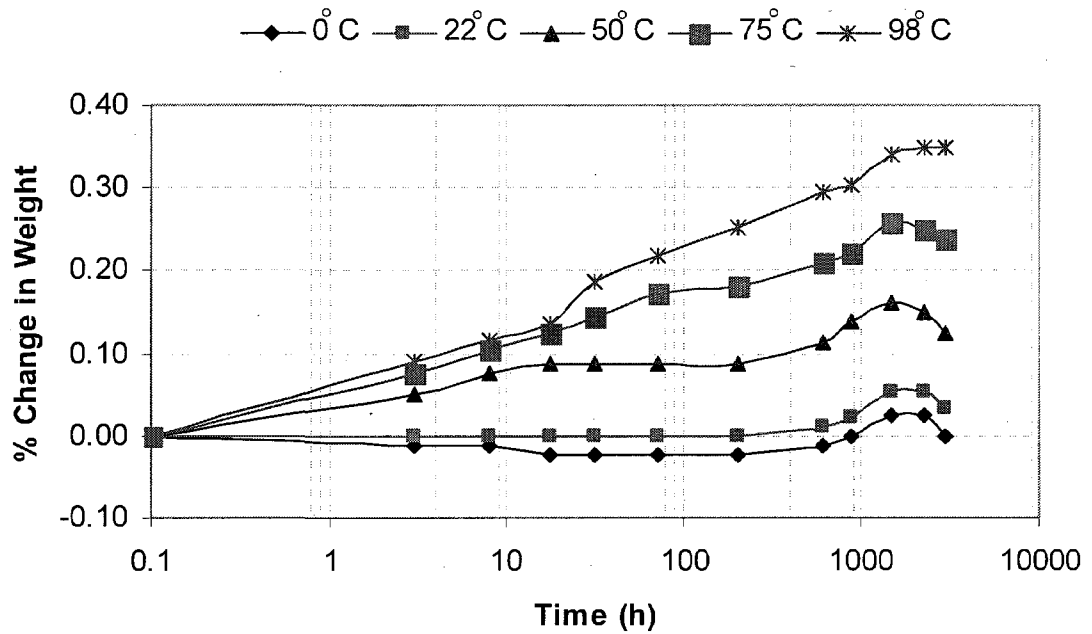


Figure 4.24. Percentage change in weight of HTV SIR specimens as a function of time during recovery in air at room temperature for 3000 h. The specimens had been aged in stationary air at different temperatures for 3000 h.

4.6 Change in Contact Angle during Recovery

Figures 4.24-4.28 show the time variation of the contact angle of distilled water on the surface of HTV SIR specimens during recovery in stationary air at room temperature. These specimens had previously been aged in saline solutions of four different conductivity levels of 0.005, 1, 10 and 100 mS/cm at 0, 23, 50, 75 and 98 °C for 3000 hours. The initial values shown in the recovery graphs are actually the final values of contact angle at the end of 3000 h of immersion period. The recovery as a function of time of all the specimens in this chapter was monitored up to 3000 h.

The contact angle decreased from the original value of 100 ± 5 after immersion depending on the conductivity of saline solution and temperature. It has been observed that higher absorption of water in low conductivity solution caused the HTV silicone rubber surface to be more hydrophilic. The recovery of the contact angle at room temperature after aging the process has two distinct stages. Initially, it recovers quickly during the evaporation of the absorbed water and afterwards the recovery is slow that is due to the diffusion of LMW fluid from bulk as explained in chapter 3.

Moreover, higher values of the contact angle have been observed during recovery for the specimens that had previously been immersed in high salinity solutions in the temperature range (0-75 °C). This may be explained as due to the low absorption of water at high salinity. However, the detail regarding higher hydrophobicity during recovery period with the increase of salinity needs to be investigated further. Table 4.3 shows the comparison of the contact angles of distilled water on the surface of the specimens at three stages of aging and recovery process:

- Contact angle of the virgin specimens prior to aging

- Contact angle at the end of the aging that is also called the beginning of the recovery period
- Contact angle at the end of the recovery period

According to Table 4.3, the aged specimens can be divided into the following categories based on the changes in their contact angles during aging and recovery processes:

- d) The contact angle regained its original value after recovery that is the contact angle of the virgin one $100\pm 5^\circ$. These include the specimens aged in 0.005 mS/cm at 25 and 98 °C; 1 mS/cm at 0 and 75 °C; 10 and 100 mS/cm at 75 °C; and in air at 25, 50, 75 and 98 °C.
- e) The contact angle of the specimens gained a higher than its original value after recovery. These include the specimens aged in 1 mS/cm at 25 and 98 °C; 10 mS/cm at 0, 25 and 98 °C; 100 mS/cm at 0 and 25 °C; and in air at 0 °C.
- f) The contact angle did not regain its original value after recovery that is the contact angle of the virgin one $100\pm 5^\circ$. These include the specimens aged in 0.005 mS/cm at 0, 50 and 75 °C; 1 and 10 mS/cm at 50 °C; and 100 mS/cm at 50 at 98 °C.

From the above part a), it is clear that ten of the specimens aged in different conditions recovered their original contact angle at room temperature. Four of these recovered samples had been aged in air at 22, 50 75 and 98 °C. However, seven specimens mentioned in part c) above did not recover their virgin value when they previously had been aged in solutions of different conductivities.

On the other hand, three out of eight specimens recovered to a higher value of contact angle than the virgin value when they were aged in saline solution of 10

mS/cm conductivity. Two of them each were aged in solutions of 1 mS/cm and 100 mS/cm at 98 °C. The specimen aged in air only at 0 °C recovered to a higher value of contact angle than the virgin during recovery at room temperature.

The recovery of HTV SIR specimens to a higher hydrophobicity level after aging is linked to the diffusion of LMW fluid from the bulk to the surface at high temperatures. Moreover, aging of the specimens in higher salinity solutions at low temperatures also caused the contact angle to recover in stationary air to a higher value than that of the virgin specimens, similar to the results of chapter 3. The specimens aged in 100 mS/cm at 98 °C did not recover to the virgin value due to aging in high salinity as well as high temperature.

Table 4.3. Comparison between the contact angles of HTV SIR specimens at different stages: (a) contact angle of the virgin specimens, (b) contact angle after aging of 3000 h, (c) contact angle after recovery of 3000 h.

Aging stress	Measurement condition	0 °C	25 °C	50 °C	75 °C	98 °C
0.005 (mS/cm)	Virgin	97	103	98	101	101
	After aging	71	65	79	79	15
	After recovery	89	98	87	94	100
1 (mS/cm)	Virgin	99	104	97	102	98
	After aging	78	71	79	83	25
	After recovery	99	106	88	101	111
10 (mS/cm)	Virgin	99	102	98	105	100
	After aging	81	83	81	82	45
	After recovery	106	110	85	101	126
100 (mS/cm)	Virgin	102	101	98	102	103
	After aging	83	84	79	83	55
	After recovery	112	108	89	105	79
Air	Virgin	100	103	97	95	97
	After aging	94	100	102	104	108
	After recovery	108	99	100	99	98

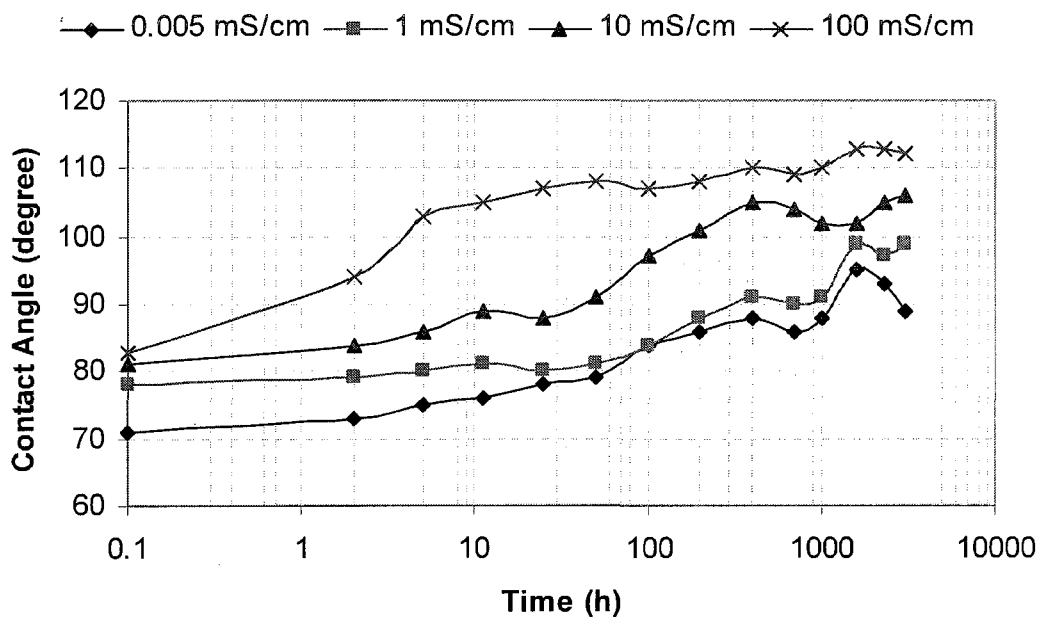


Figure 4.25. Time variation of the contact angle of distilled water on the surface of HTV SIR specimens during recovery in stationary air at room temperature for 3000 h. The specimens had been aged in solutions of different conductivities at 0 °C for 3000 h.

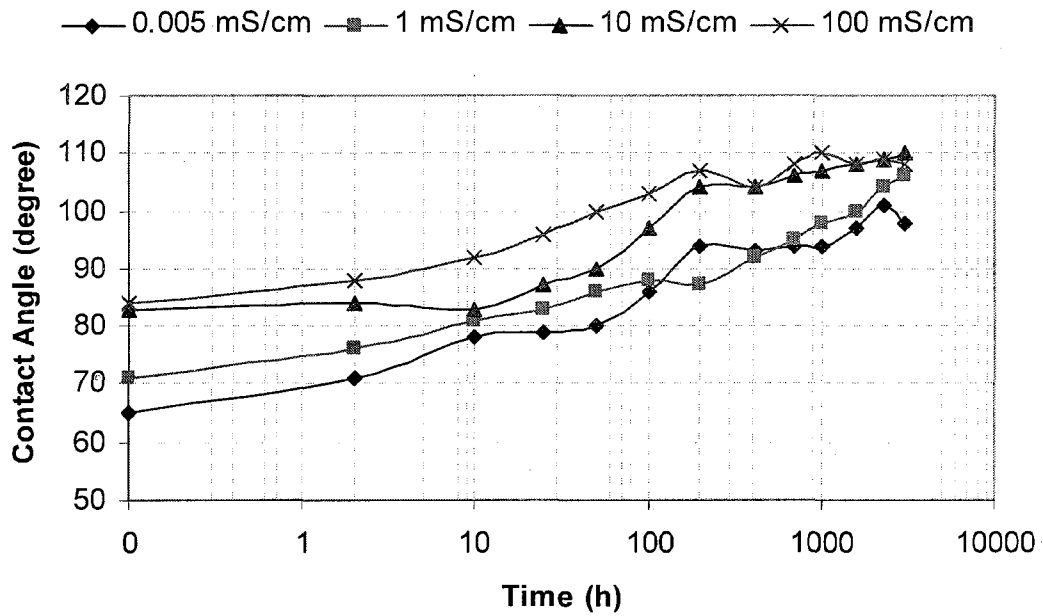


Figure 4.26. Time variation of the contact angle of distilled water on the surface of HTV SIR specimens during recovery in stationary air at room temperature for 3000 h. The specimens had been aged in solutions of different conductivities at 25 °C for 3000 h.

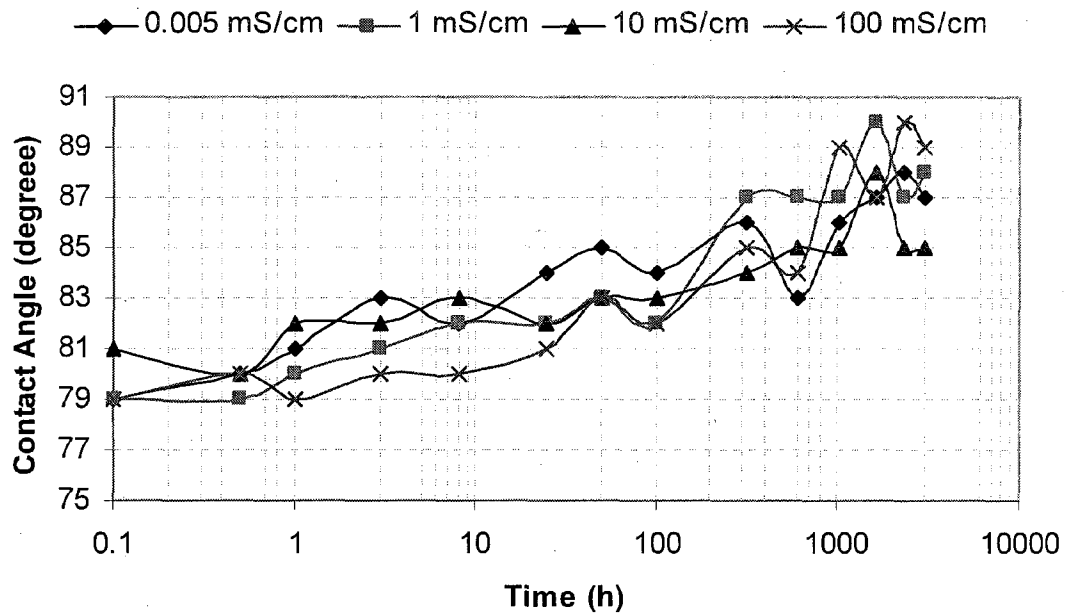


Figure 4.27. Time variation of the contact angle of distilled water on the surface of HTV SIR specimens during recovery in stationary air at room temperature for 3000 h. The specimens had been aged in solutions of different conductivities at 50 °C for 3000 h.

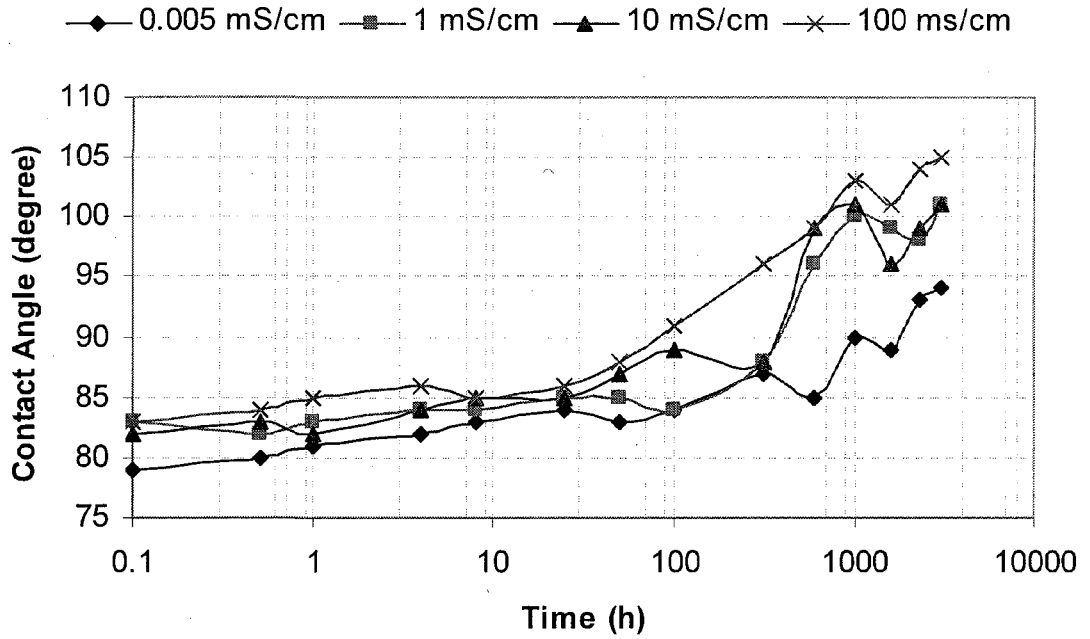


Figure 4.28. Time variation of the contact angle of distilled water on the surface of HTV SIR specimens during recovery in stationary air at room temperature for 3000 h. The specimens had been aged in solutions of different conductivities at 75 °C for 3000 h.

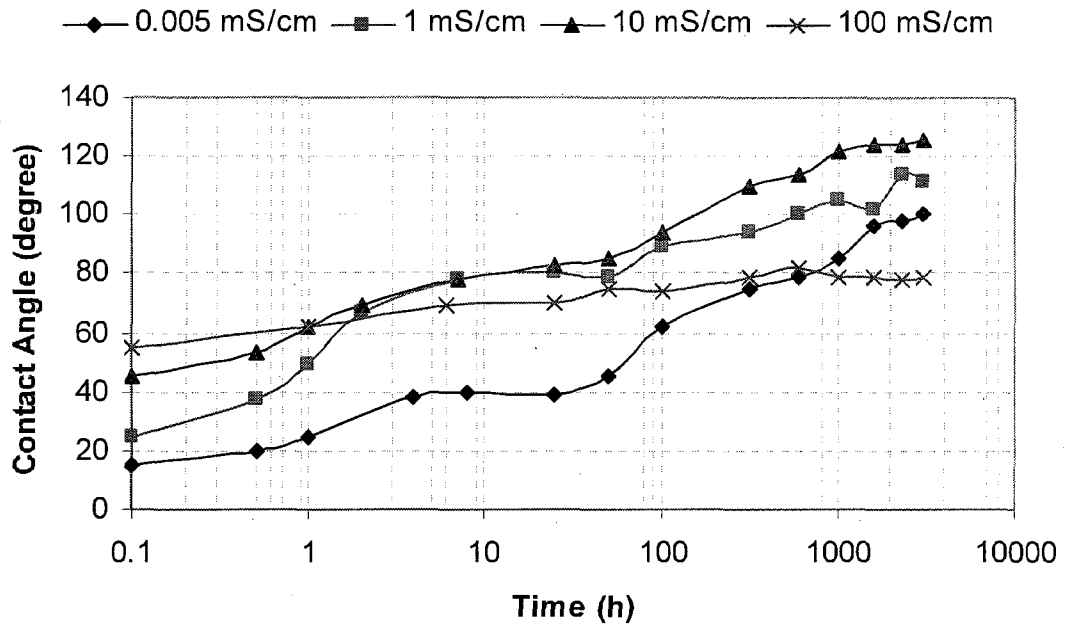


Figure 4.29. Time variation of the contact angle of distilled water on the surface of HTV SIR specimens during recovery in stationary air at room temperature for 3000 h. The specimens had been aged in solutions of different conductivities at 98 °C for 3000 h.

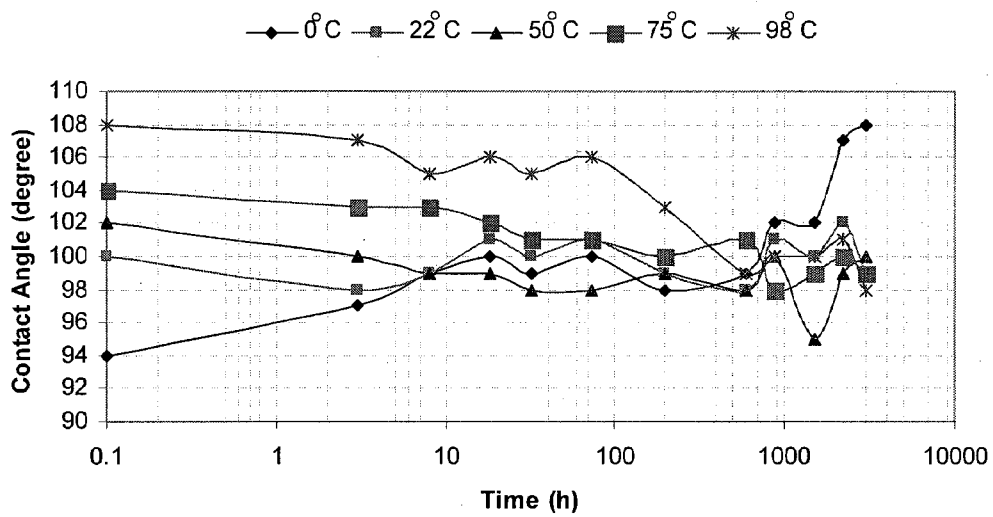


Figure 4.30. Time variation of the contact angle of distilled water on the surface of HTV SIR specimens during recovery in stationary air at room temperature for 3000 h. The specimens had been aged in air at different temperatures for 3000 h.

4.7 ASR during Recovery

The change in ASR of HTV SIR specimens as a function of time at room temperature during 3000 h of recovery period is shown in Figures 4.31-4.36. In most cases, there is a decrease in surface roughness during the recovery process and this decrease may be related to the decrease in weight due to the evaporation of water. Table 4.4 shows the comparison of surface roughness of HTV SIR specimens in μm at three different stages of aging and recovery process:

- Surface roughness of the virgin specimens prior to aging.
- Surface roughness at the end of aging for 3000 h that is also called the beginning of the recovery period.
- Surface roughness at the end of the recovery period for 3000 h.

According to Table 4.4 specimens can be divided into the following two categories based on the changes in their ASR during aging and recovery process:

- a) The HTV SIR specimens retained a higher ASR than its original value after recovery which was aged in solutions of 0.005, 1, and 10 mS/cm conductivity at 98 °C.
- b) The specimens aged in different saline solutions at 0, 25, 50 and 75 °C; 100 mS/cm at 98 °C; and in stationary air at all temperatures 0-98 °C regained their ASR either to the original value or in some cases dropped from their virgin value during the recovery process. However, this variation was within $\pm 0.1 \mu\text{m}$ of the virgin value which is not prominent.

The detail results of part a) show that the HTV SIR specimens aged in solutions of 0.005, 1, and 10 mS/cm conductivity at 98 °C, gained ASR of

1.25, 2.27 and 1.95 μm , respectively and retained almost the same value even during the recovery process. Therefore, the increase in ASR was permanent at 98 °C which might be related to the weight loss of the specimens because a net weight loss of 14.86, 12.44 and 9.80 % was observed for the specimens aged in solutions of 0.005, 1 and 10 mS/cm, respectively at 98 °C. From these results, it can be concluded that the variation in weight caused a variation in surface roughness.

From the above part b), it is clear that in most cases there was an increase in ASR of HTV SIR specimens during immersion in saline solutions of different conductivities at temperatures of 0-75 °C and 100 mS/cm at 98 °C which was temporary and might be related to the absorption of water. Also, this variation did not exceed $\pm 0.1 \mu\text{m}$ and therefore is not appreciable. Moreover, the specimens aged in stationary air at different temperatures have a variation of only $\pm 0.1 \mu\text{m}$ during aging and recovery process. Such a small change in ASR is negligible and does not predict any deterioration of the samples.

Table 4.4 Comparison of the surface roughness of HTV SIR specimens in μm at different stages: (a) virgin specimens, (b) after aging of 3000 h and (c) after recovery of 3000 h.

Aging stress	Measurement condition	0 °C	25 °C	50 °C	75 °C	98 °C
0.005 (mS/cm)	Virgin	0.48	0.74	0.52	0.50	0.54
	After aging	0.61	0.79	0.47	0.55	1.79
	After recovery	0.39	0.67	0.55	0.55	1.48
1 (mS/cm)	Virgin	0.57	0.81	0.42	0.58	0.68
	After aging	0.58	0.91	0.43	0.59	2.95
	After recovery	0.56	0.80	0.44	0.64	3.07
10 (mS/cm)	Virgin	0.72	0.65	0.48	0.51	0.69
	After aging	0.75	0.67	0.42	0.64	2.64
	After recovery	0.73	0.62	0.42	0.51	2.46
100 (mS/cm)	Virgin	0.78	0.59	0.55	0.54	0.60
	After aging	0.86	0.59	0.58	0.62	0.48
	After recovery	0.81	0.54	0.55	0.60	0.64
Air	Virgin	0.65	0.54	0.46	0.56	0.52
	After aging	0.68	0.50	0.44	0.52	0.49
	After recovery	0.59	0.48	0.47	0.55	0.49

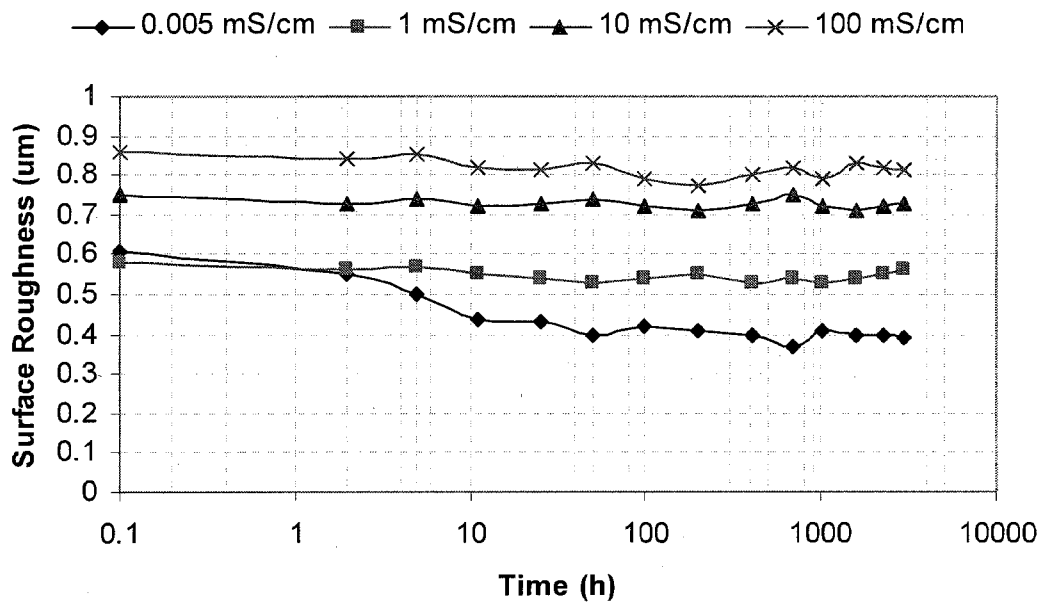


Figure 4.31. Time variation of the surface roughness of HTV SIR specimens during recovery in stationary air at room temperature for 3000 h. The specimens had been aged in solutions of different conductivities at 0 °C for 3000 h.

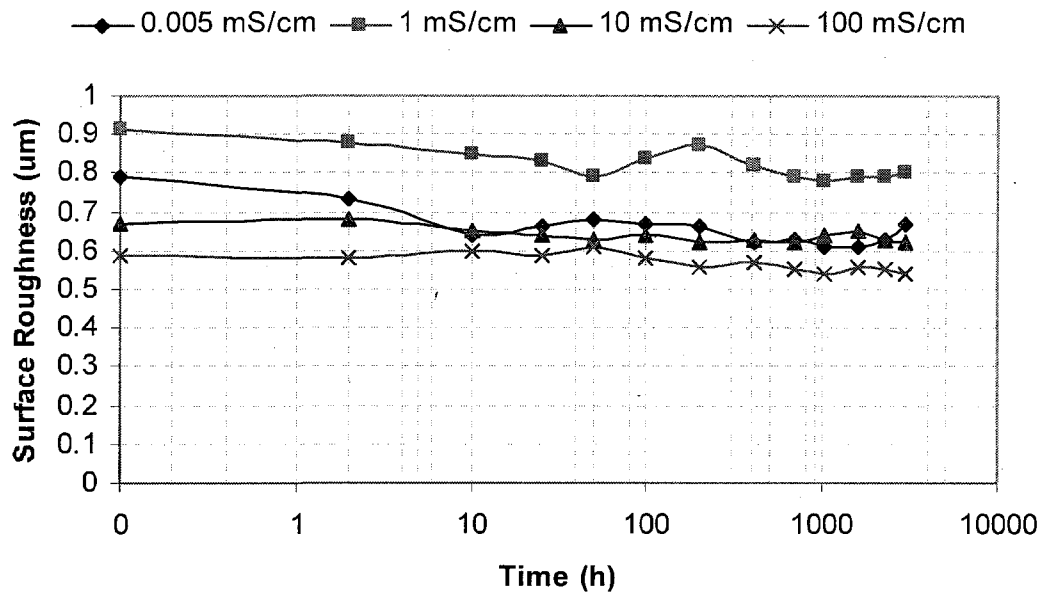


Figure 4.32. Time variation of the surface roughness of HTV SIR specimens during recovery in stationary air at room temperature for 3000 h. The specimens had been aged in solutions of different conductivities at 22 °C for 3000 h.

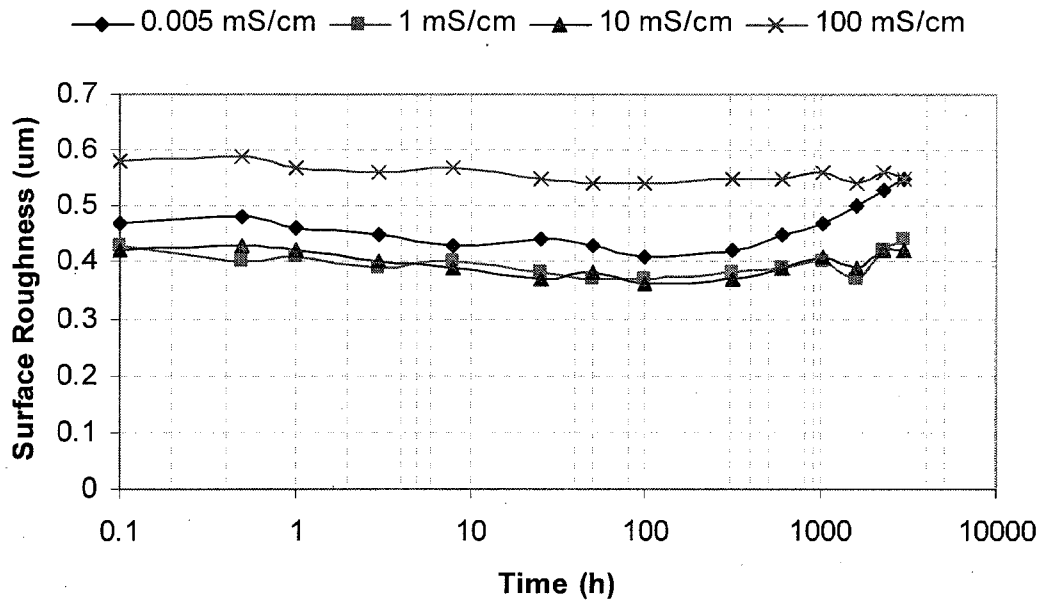


Figure 4.33. Time variation of the surface roughness of HTV SIR specimens during recovery in stationary air at room temperature for 3000 h. The specimens had been aged in solutions of different conductivities at 50 °C for 3000 h.

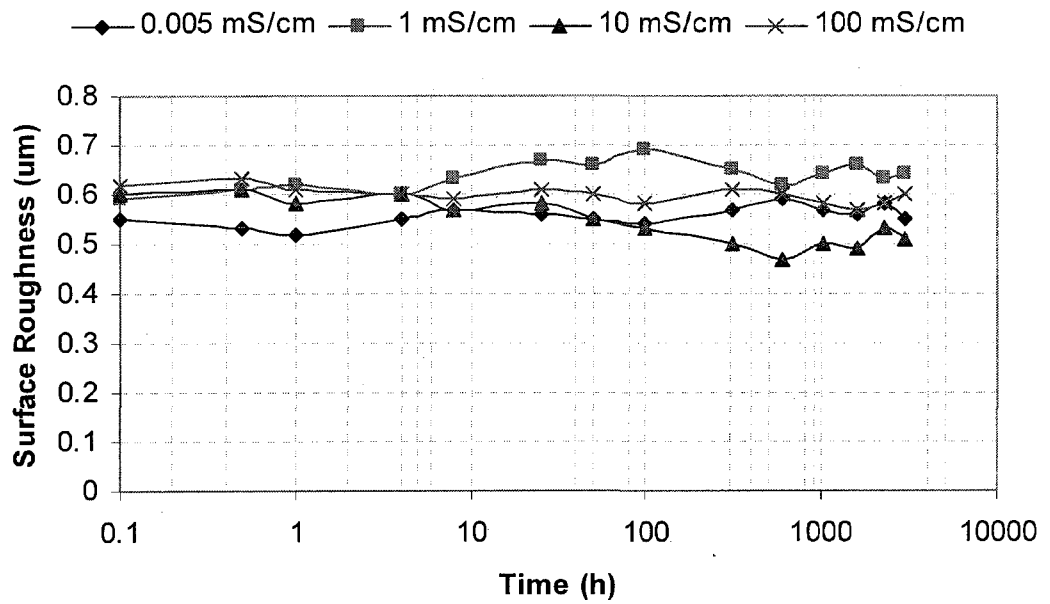


Figure 4.34. Time variation of the surface roughness of HTV SIR specimens during recovery in stationary air at room temperature for 3000 h. The specimens had been aged in solutions of different conductivities at 75 °C for 3000 h.

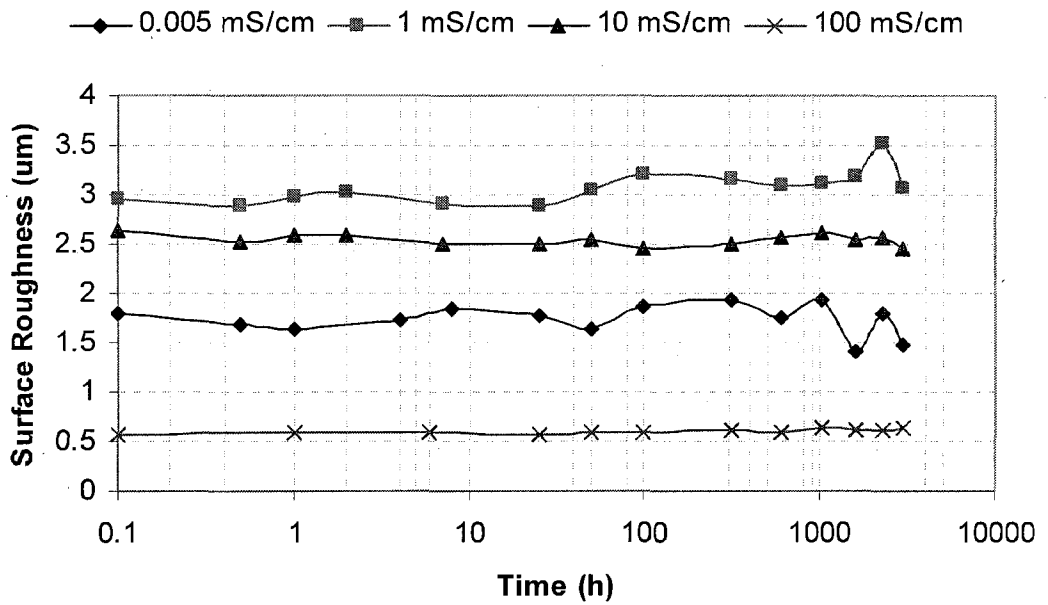


Figure 4.35. Time variation of the surface roughness of HTV SIR specimens during recovery in stationary air at room temperature for 3000 h. The specimens had been aged in solutions of different conductivities at 98 °C for 3000 h.

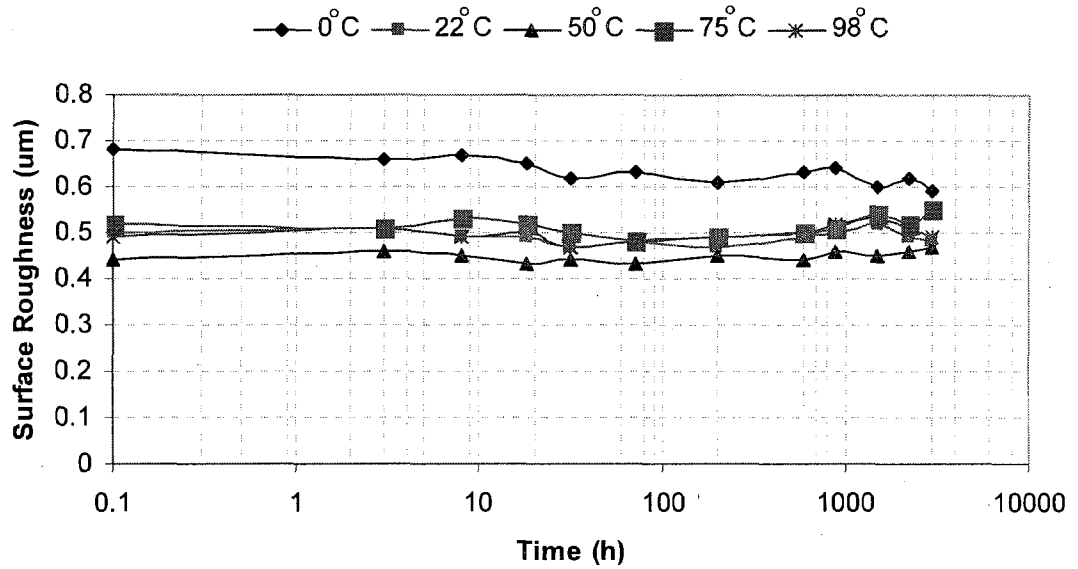


Figure 4.36. Time variation of the surface roughness of HTV SIR specimens during recovery in air at room temperature for 3000 h. The specimens had been aged in stationary air at different temperatures for 3000 h.

4.8 SEM and EDS Results

The loss and recovery of hydrophobicity depends on the physical and chemical changes on the surface of the insulating materials. In order to study these changes, four HTV SIR specimens used for the aging process in this chapter were utilized for SEM/EDS analysis and compared to a virgin specimen. These specimens had previously been aged in 0.005 mS/cm conductivity solution at 25, 50, 75 and 98 °C for 3000 h and were allowed to recover at room temperature for further 3000 h. The experimental procedure for SEM and EDS has already been described in section 3.8.1 of chapter 3.

Figures 4.37-4.44 show the SEM photographs of some aged HTV SIR specimens taken at 100 and 1000 times magnifications. The SEM images of a virgin sample in Figure 3.34-3.35 show that the ATH filled silicone rubber have not much higher packing density; therefore, a greater number of voids are present and this is consistent with the report of [30]. However, the virgin surface is more homogeneous and smooth as compared to the surfaces of the aged specimens.

The aged specimens exhibit rougher surfaces and phase difference due to changes in the filler and rubber on the surface because of aging. The SEM images of Figures 4.37-4.38 show the changes on the surface due to aging in distilled water at room temperature and very slightly differ from the virgin sample. However, the HTV SIR specimens aged in distilled water at 50, 75 and 98 °C for 3000 h had a significant change on the surface due to their deterioration at higher temperature as shown in the SEM micrographs of Figures 4.39-4.44. The surface became hard and brittle with a loss of its original color whereas obvious cracks were also observed at 98 °C as seen by the naked eye.

Figures 4.45-4.48 are the energy dispersive x-ray spectra of the same specimens described above for the SEM images. Al, Si, O, C and Au are the significant elements which have been detected on the surface of all the HTV SIR specimens

as in chapter 3. The Au peaks found in all the spectra, actually come from the gold coating which is used to provide the proper grounding for the samples. As described in section 3.8.2 of chapter 3, the Si and O detected in the x-ray count originate from (Si-O-Si) backbone of the silicone polymer chain. Whereas the Al, was detected due to the presence of alumina trihydrate (ATH) filler which is added to the base polymer during the manufacturing process to improve its mechanical performance and to reduce the flammability.

The EDS spectra of Figures 4.45-4.48 in this chapter are differing in number of counts per second from the spectra of Figures 3.42-3.45 of Chapter 3. This can be explained as that the beam current in each spectra may not be the same which results in different number of counts per second in different spectra. Therefore, the number of counts per second may differ in different spectra and is not important. However, the ratio of the intensity of the peaks in the same spectrum depicts the ratio of concentration of the elements on the surface of the sample.

The spectrum of Figure 4.45 is almost similar to the spectrum of a virgin sample given in Figure 3.42 of chapter 3. However, the spectra of Figures 4.46-4.48 show higher intensity of Al and lower intensity of Si as well as C on the surface of the specimens aged in distilled water at 50, 75 and 98 °C for 3000 h. This increase in Al on the surface aged samples with the increase of temperature is consistent with the results of chapter 3. So, it is clear that ATH dissolved into the water at high temperature and ultimately, increased its intensity on the surface of the aged insulator specimens as well. Two additional small peaks of Ca and Cu appeared only in the spectra of the specimen aged at 98 °C which have negligible counts compared to those mentioned and are not important for the purpose of this study.

Table 4.5 gives the intensity ratios of Al/Si, Al/O, Al/C and O/Si in each spectrum of the specimens aged in distilled water at 22, 50, 75 and 98 °C along with the

virgin one as given in Figures 4.45-4.48. Higher intensity of Al and lower intensity of Si as well as C can be observed from the table with the increase of aging temperature which is consistent with the previous report [70].

Table 4.5. Chemical component changes with temperature in HTV SIR aged in distilled water (0.005 mS/cm) for 3000 h and allowed to recover at room temperature for 3000 h prior to spectroscopy.

Aging Temperature	Al/Si	Al/O	Al/C	O/Si
Virgin	0.84	0.84	5.21	1.00
22 °C	0.75	0.90	2.61	0.84
50 °C	1.03	0.93	6.48	1.11
75 °C	1.81	1.19	9.16	1.52
98 °C	1.52	0.92	8.20	1.65

There is an adequate increase in the ratio of O/Si on the surface of the HTV SIR specimens with the increase of aging temperature as observed from the above table. The increase in oxygen on the surface of the aged specimens results from crosslinking and oxidation during aging in water solutions. This increased level of oxygen on the surface is responsible for developing hydrogen bonding forces between the HTV SIR and water. However, the Table 4.5 does not show any appreciable change in the ratio of Al/O which indicates that intensity of both of these elements increased at the same time on the surface of the aged specimens with the increase of aging temperature.

Another explanation for such high Al/C, Al/Si and O/Si ratios can be that ATH decomposes on heating, thus releasing O on the surface. This O can combine with Al and Si to form alumina (Al_2O_3) and silicone dioxide (SiO_2), respectively on the surface of the specimens as a result of aging.

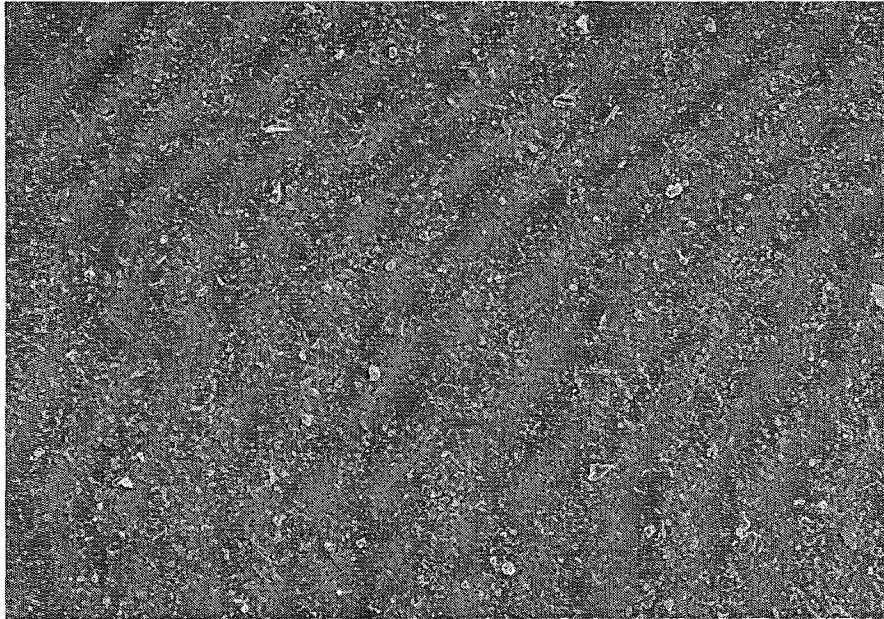


Figure 4.37. SEM image of the surface of the HTV SIR specimen aged in distilled water at 22 °C for 3000 h and dried in stationary air at room temperature for 3000 h prior to the imagery; magnification: x100 and width: 132 μm .

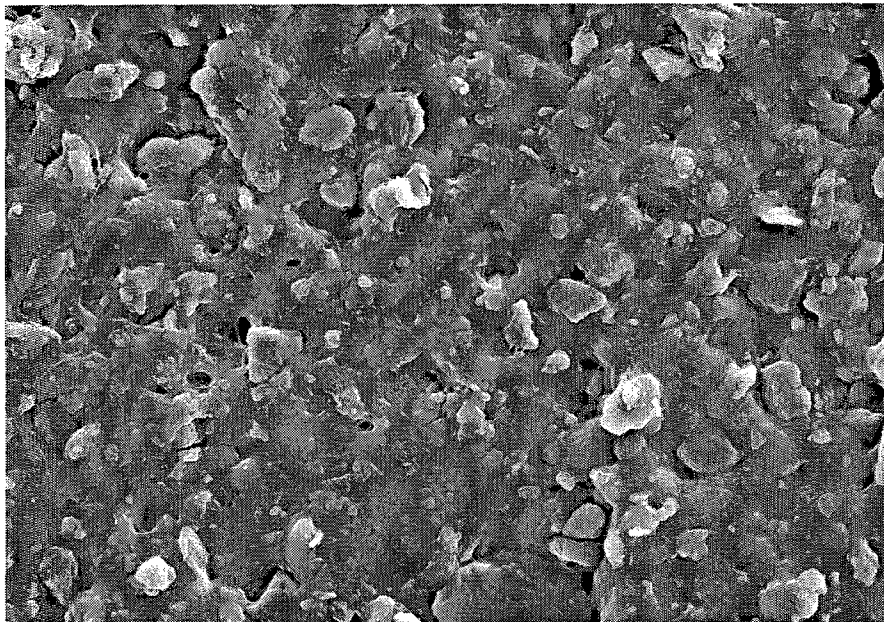


Figure 4.38. Same as top figure, except the magnification: x1000.

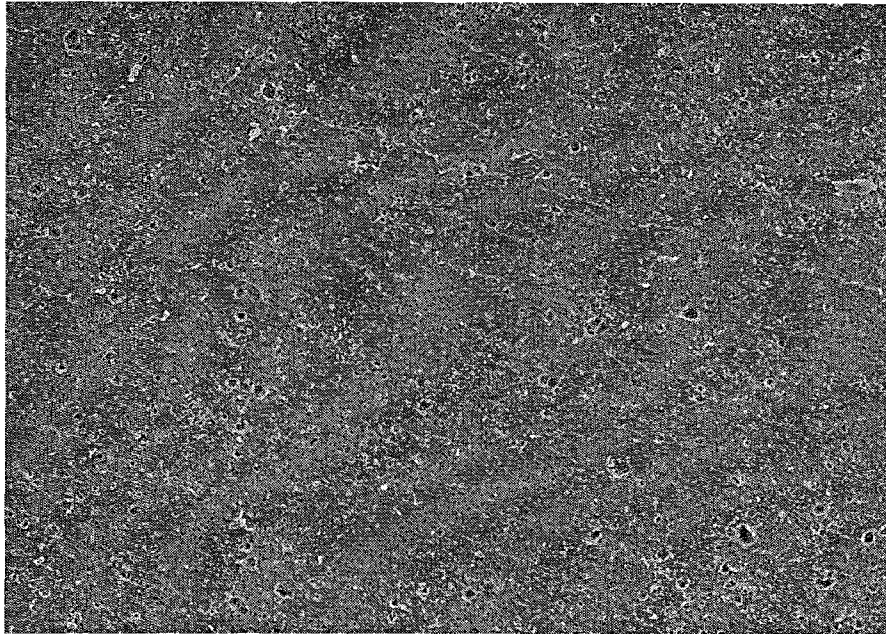


Figure 4.39. SEM image of the surface of the HTV SIR specimen aged in distilled water at 50 °C for 3000 h and dried in stationary air at room temperature for 3000 h prior to the imagery; magnification: x100 and width: 132 μm .

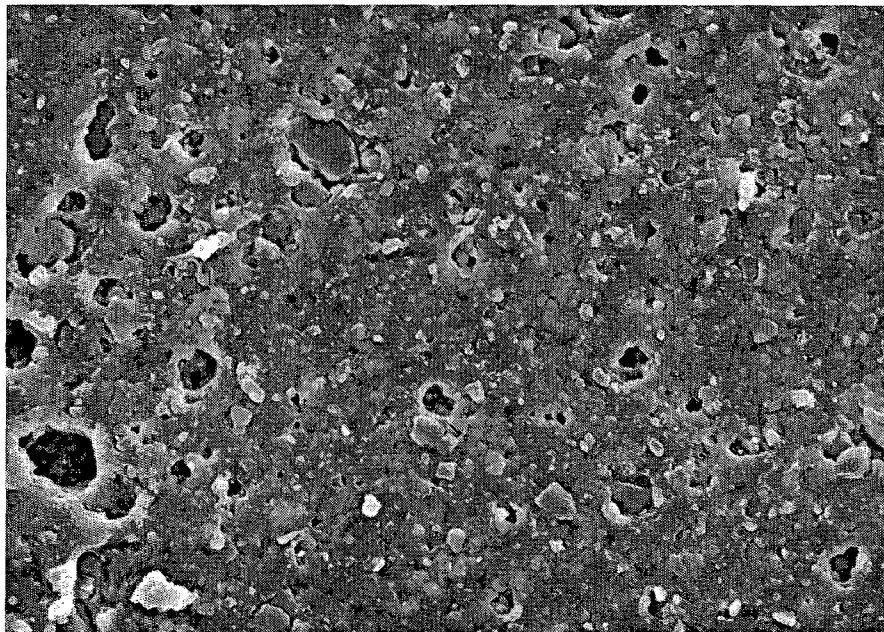


Figure 4.40. Same as the top figure, except the magnification: x1000

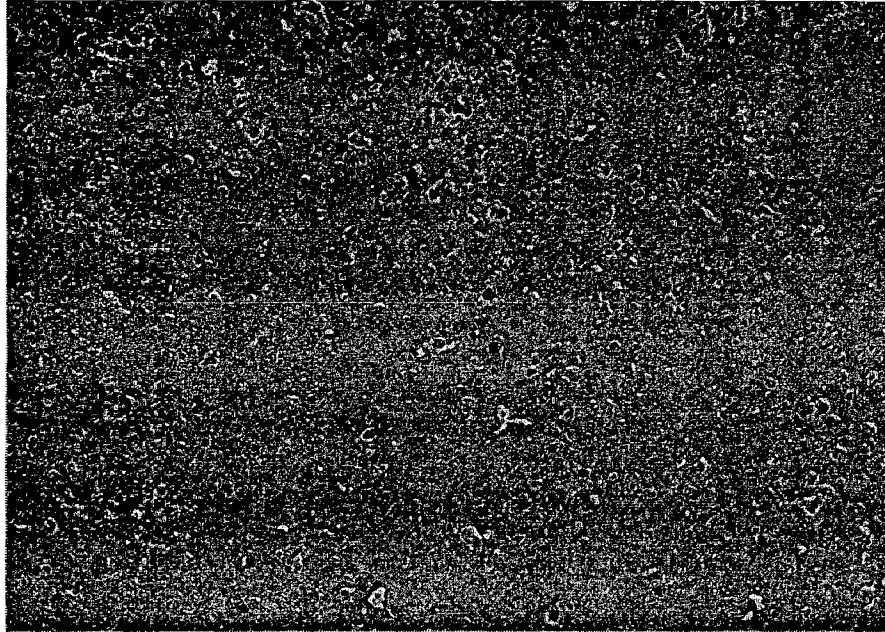


Figure 4.41. SEM image of the surface of the HTV SIR specimen aged in distilled water at 75 °C for 3000 h and dried in stationary air at room temperature for 3000 h prior to the imagery; magnification: x100 and width: 132 μm .

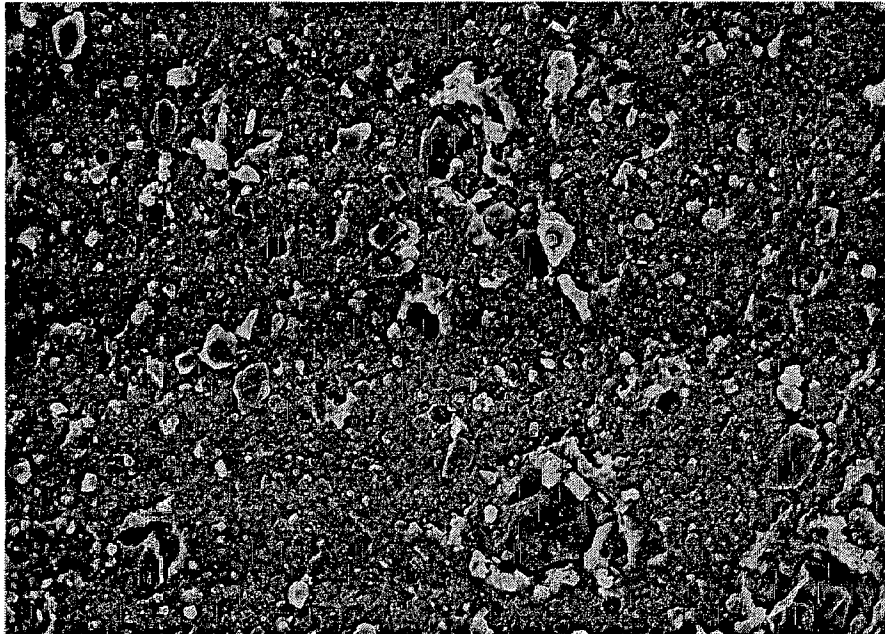


Figure 4.42. Same as the top figure, except the magnification: x1000

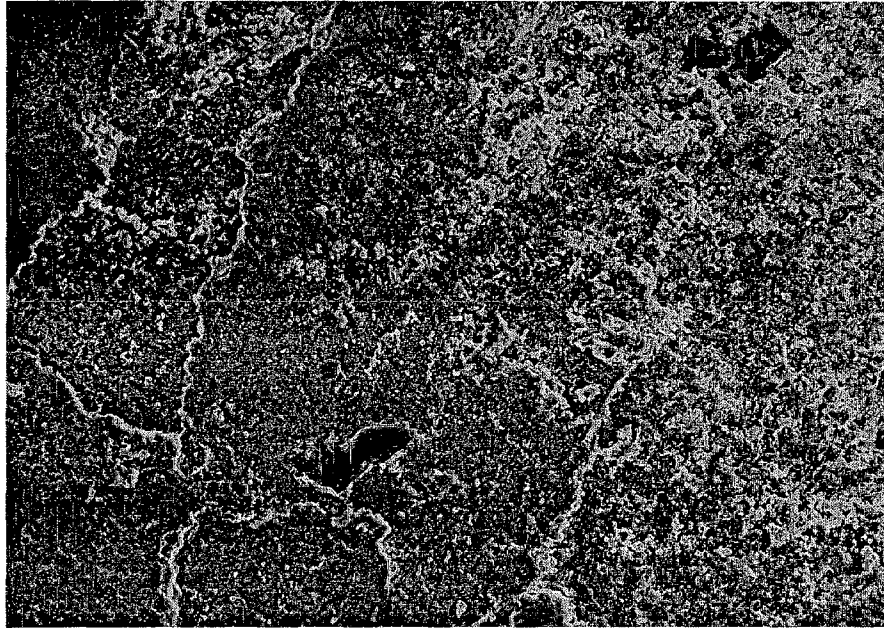


Figure 4.43. SEM image of the surface of the HTV SIR specimen aged in distilled water at 98 °C for 3000 h and dried in stationary air at room temperature for 3000 h prior to the imagery; magnification: x100 and width: 132 μm .

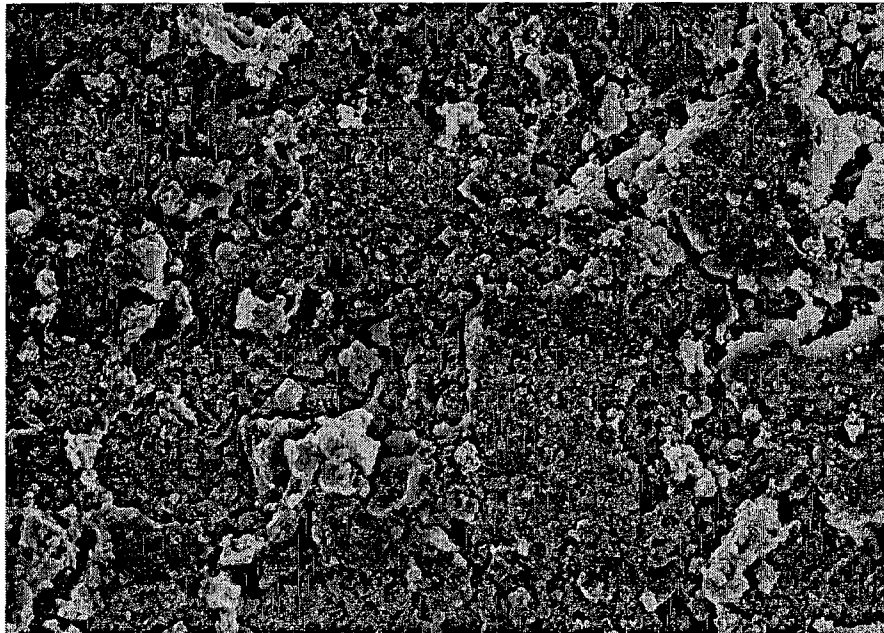


Figure 4.44. Same as the top figure, except the magnification: x1000

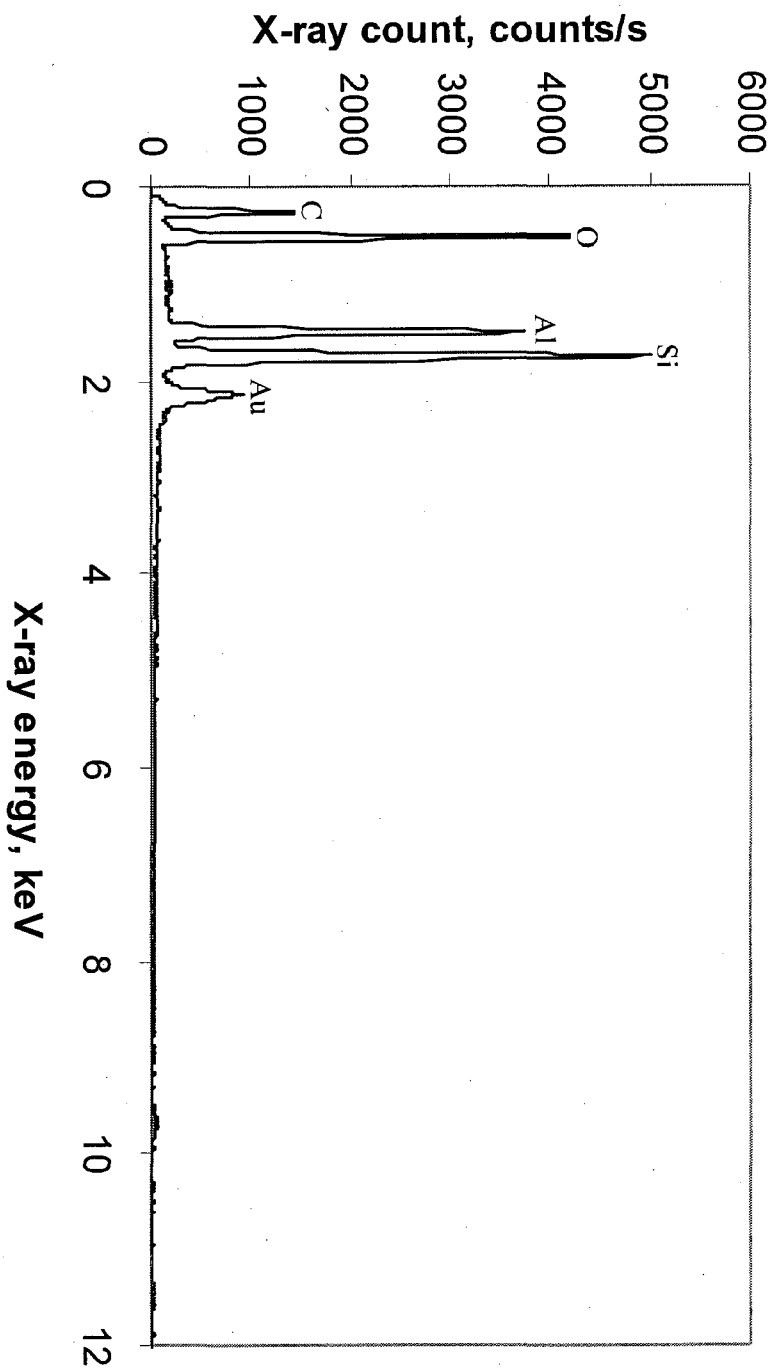


Figure 4.45. Energy dispersive x-ray spectrum of HTV SIR specimen aged in distilled water at 22 °C for 3000 h and allowed to recover at room temperature for 3000 h prior to the spectroscopy.

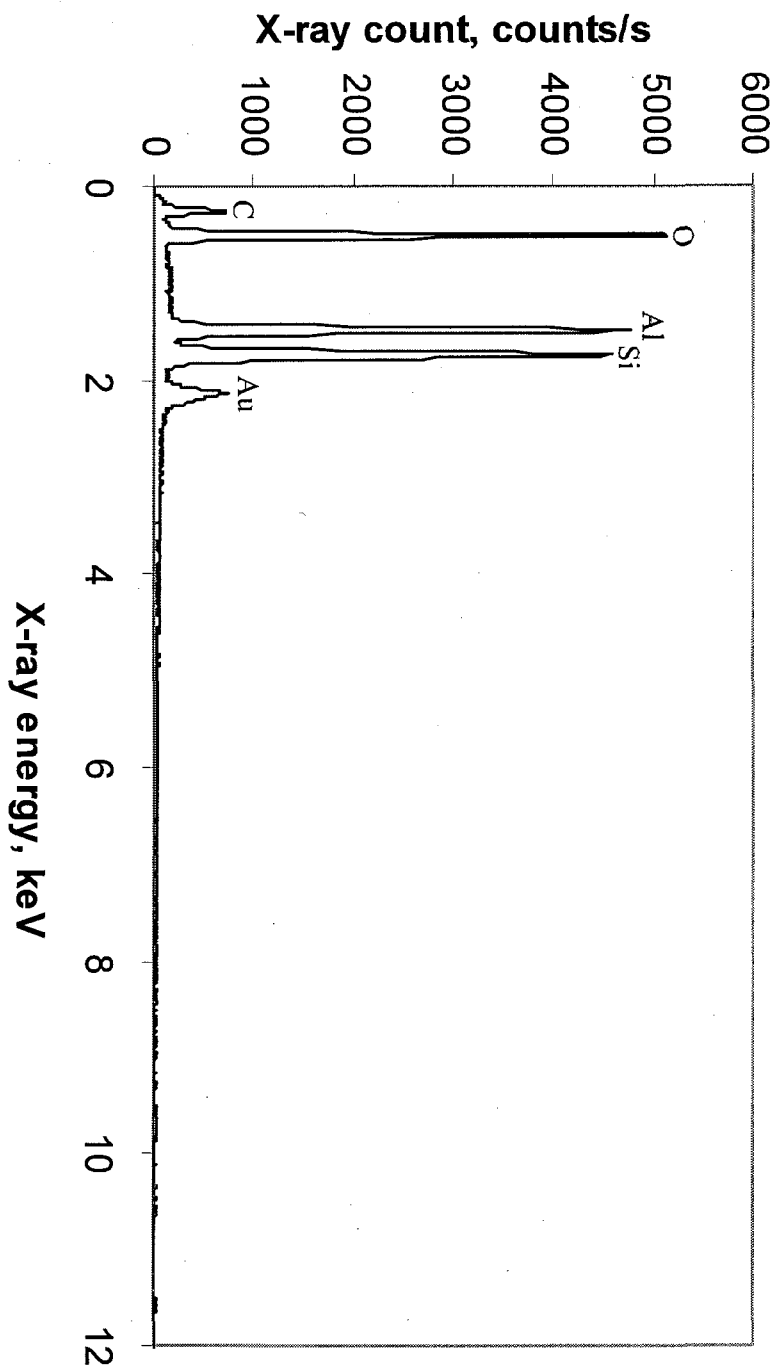


Figure 4.46. Energy dispersive x-ray spectrum of HTV SIR specimen aged in distilled water at 50 °C for 3000 h and allowed to recover at room temperature for 3000 h prior to the spectroscopy.

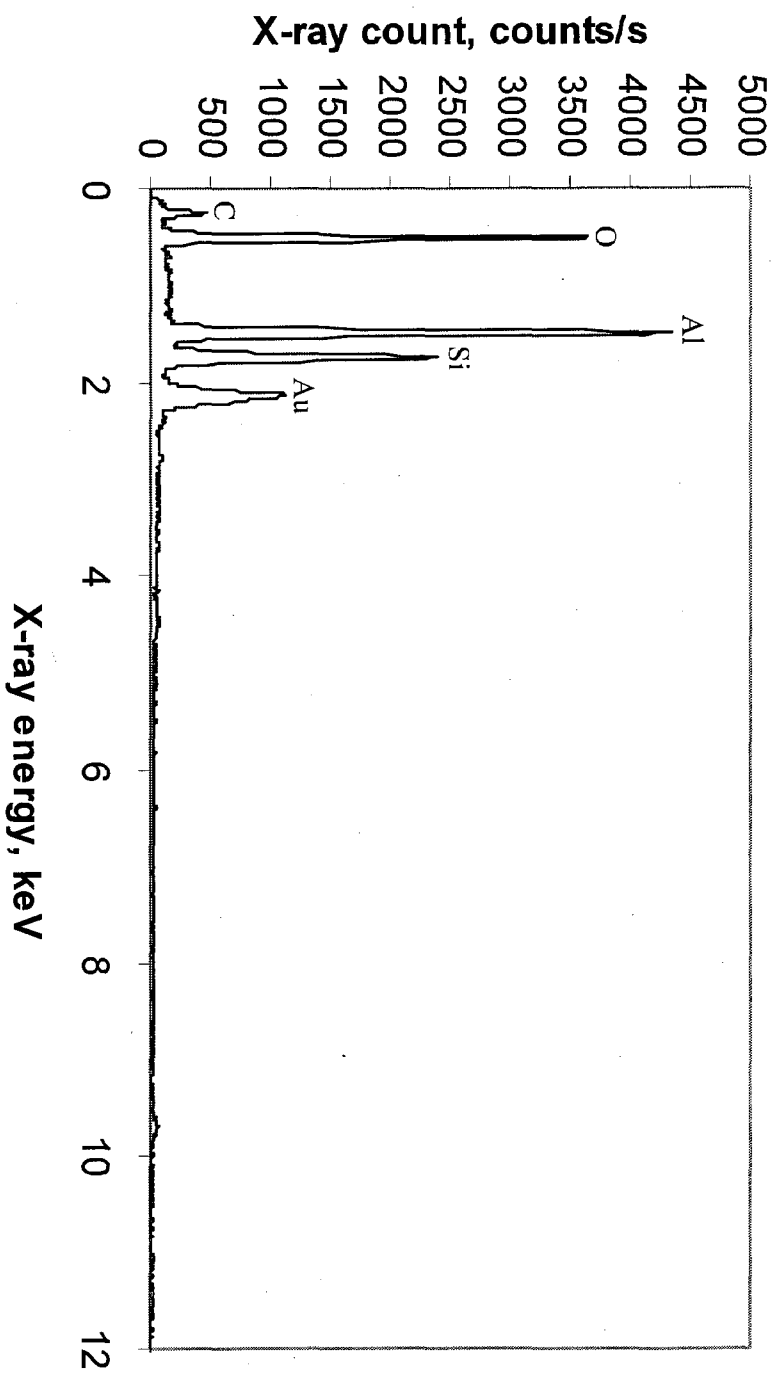


Figure 4.47. Energy dispersive x-ray spectrum of HTV SIR specimen aged in distilled water at 75 °C for 3000 h and allowed to recover at room temperature for 3000 h prior to the spectroscopy.

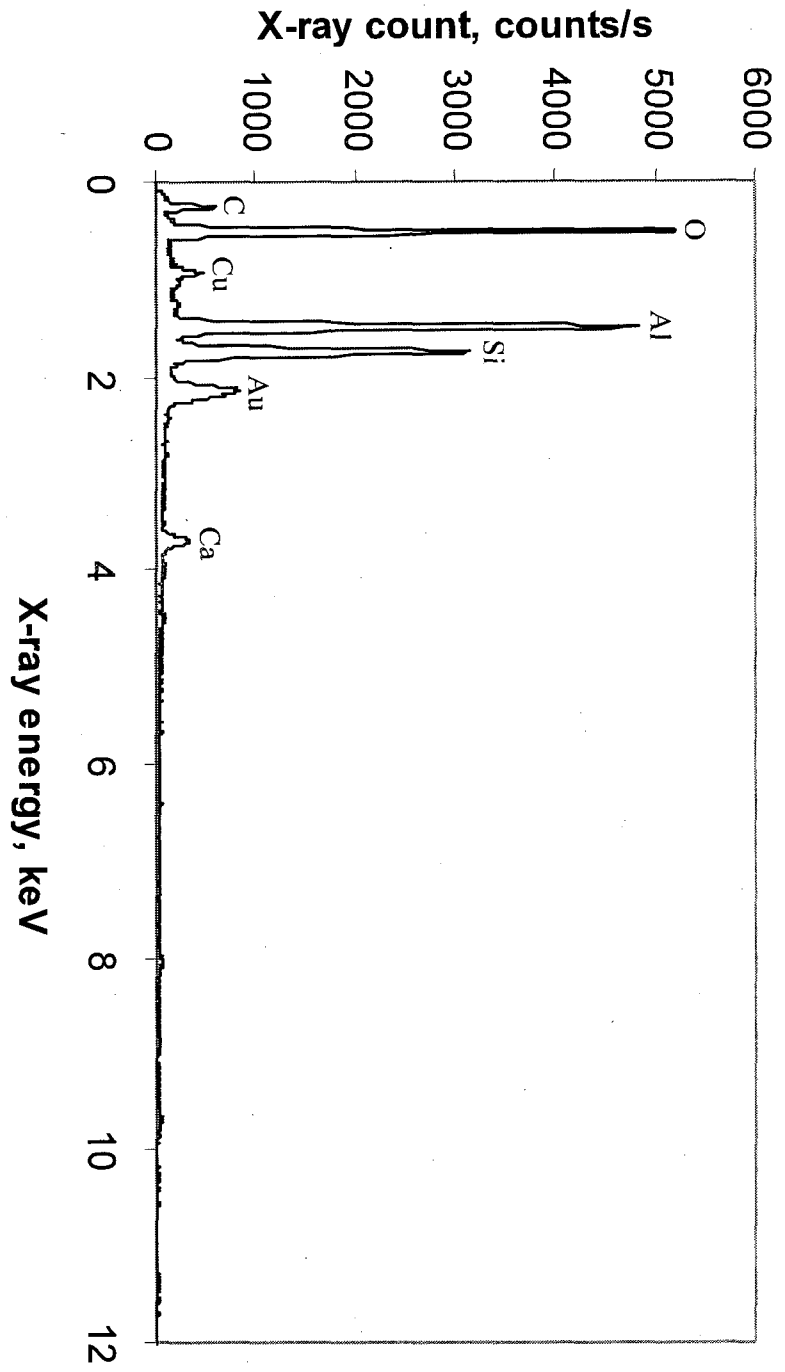


Figure 4.48. Energy dispersive x-ray spectrum of HTV SIR specimen aged in distilled water at 98 °C for 3000 h and allowed to recover at room temperature for 3000 h prior to the spectroscopy.

4.9 ATR-FTIR Spectroscopy Results

The ATR FTIR spectroscopy has been utilized to find out the surface changes that occurred due to the long term aging. For this purpose, five HTV SIR specimens were selected which had previously been aged in different saline solutions at different temperatures. Four of the selected specimens were aged in saline solution of 1 mS/cm at 22, 50, 75 and 98 °C while the fourth one in 100 mS/cm at 98 °C for 3000 hours. Afterwards, the specimens had been allowed to recover in stationary air at room temperature for further 3000 hours. The experimental procedure along with some typical characteristic infrared absorption bands for pure polydimethylsiloxanes (PDMS) is given in section 3.9 of chapter 3.

Figures 4.49-4.53 show the ATR FTIR spectra of the five selected specimens each compared with the virgin sample. Wave number in these figures is a wave property inversely related to wavelength and it is a spatial analogue of frequency. The unit of Wavenumber is cm^{-1} , called "reciprocal centimeter". The peaks of interest which can be seen in the spectra of virgin as well as aged specimens with different absorbance levels are as follows:

- 3400-3600 cm^{-1} shows the presence of OH groups
- 2958 cm^{-1} is due to C-H stretching bond in CH_2 and CH_3 units
- 1730 cm^{-1} is relatively weak absorption of C=O (carbonyl) group
- 1255 cm^{-1} is due to the deformation of CH in Si- CH_3 groups
- 1015-1100 cm^{-1} is due to the absorption of Si-O bond in Si-O-Si chain
- 785 cm^{-1} this sharp peak is due to the stretching vibrations of $\text{Si}(\text{CH}_3)_2$ group

Figure 4.49 shows that the ATR FTIR spectra of the virgin and the aged-V samples are almost completely over lapping. So, it is clear that the aging in saline solution of 1 mS/cm conductivity at room temperature did not bring any

apparent change on the surface of HTV SIR specimen even after 3000 h. However, as the aging temperature was increased beyond the room temperature, an appreciable difference in absorbance of aged samples to the virgin one was observed as shown the Figures 4.50-4.53.

As shown in Figures 4.50-4.52, if we regard the absorbance intensity of Si-CH₃, C-H and Si-O-Si in the spectra of virgin sample as a reference (100%), then their ratio found to be decreased after aging the samples in the saline solution of conductivity, 1 mS/cm at 50, 75 and 98 °C. This difference in absorbance levels has been found to have increased with the increase of aging temperature. These observations are consistent with the results of section 3.9.2 of chapter 3.

Similarly, Figure 4.53 shows the comparison of the specimen aged in 100 mS/cm at 98 °C for 3000 h to the virgin one. An appreciable decrease in intensity levels of different groups in the aged sample can be observed as compared to the virgin one but less than that of the Figure 4.52. It is suggested that aging in saline solutions removed some CH₃ groups from the side chains of PDMS molecules. So, this process caused a significant decrease in CH₃ on the surface and increased oxygen possibly from crosslinking or oxidation of CH₃ to CH₂OH. In addition, loss of these groups increased due to aging at higher temperatures and decreased in higher salinity solutions.

This is consistent with the previous report of [43] in which a significant decrease has been described in the intensities of Si-CH₃ and Si-O-Si as observed in ATR FTIR spectra of HTV SIR samples after aging in water at 80 °C for 500 h. This decrease in intensity might be due to the more weight loss of LMW fluid at high temperature. In this study, a net weight loss of 0.13, 0.39 and 1.54% has been observed due to the aging of HTV SIR specimens in solutions of 1 mS/cm at 22, 50 and 75 °C. Where as, an excessive weight loss of 8.4% was caused due to the aging in a solution of conductivity 100 mS/cm at 98 °C for 3000 h.

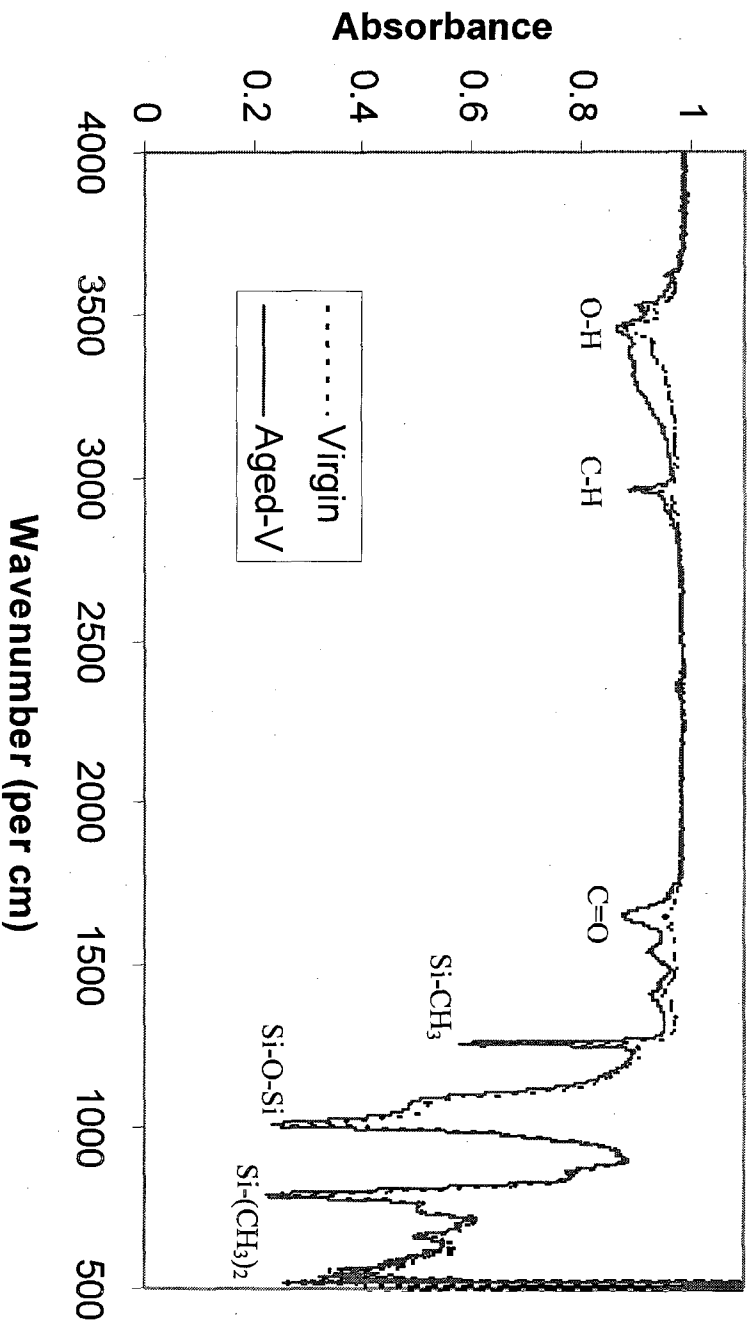


Figure 4.49. Comparison between the ATR FTIR spectra of a virgin HTV SIR specimen and the aged-V, the specimen aged in saline water of 1 mS/cm conductivity at 22 °C for 3000 h. The aged specimen had been allowed to recover in stationary air at room temperature for 3000 h before the spectra.

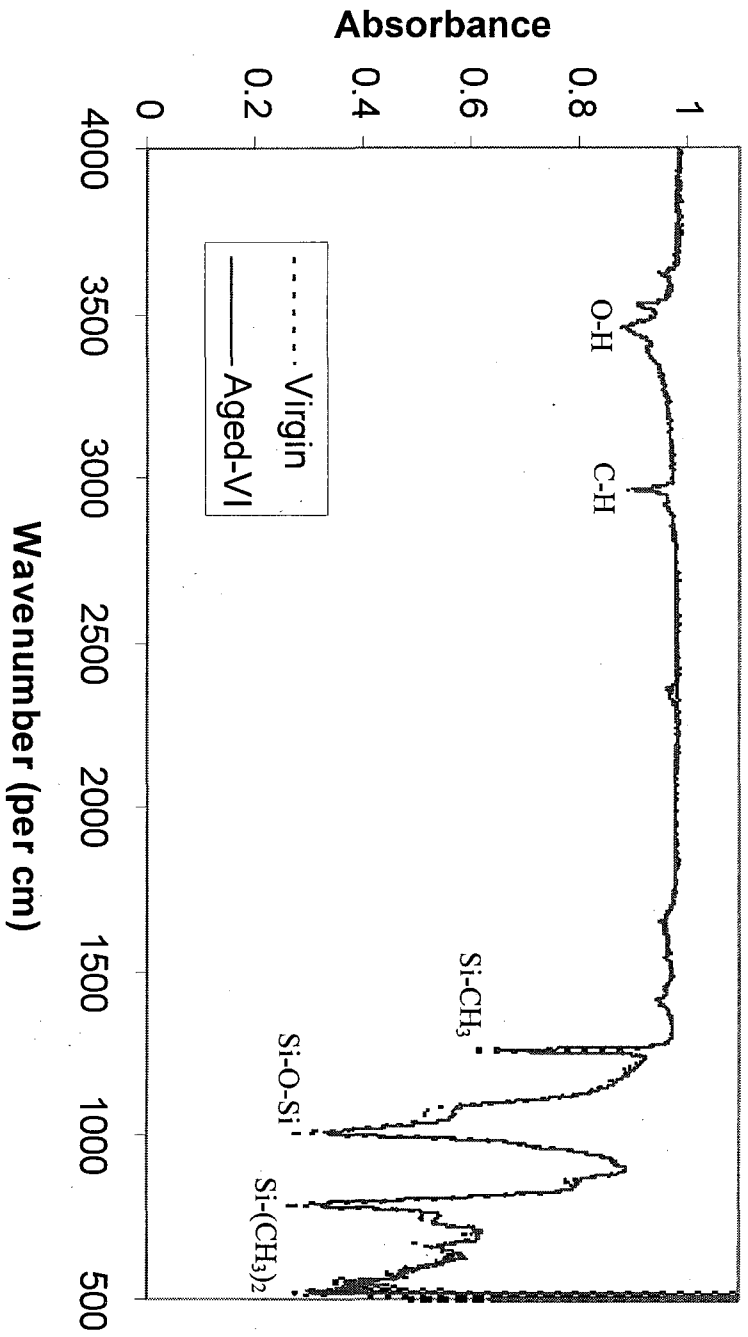


Figure 4.50. Comparison between the ATR FTIR spectra of a virgin HTV SIR specimen and the aged-VI, the specimen aged in saline water of 1 mS/cm conductivity at 50 °C for 3000 h. The aged specimen had been allowed to recover in stationary air at room temperature for 3000 h before the spectra.

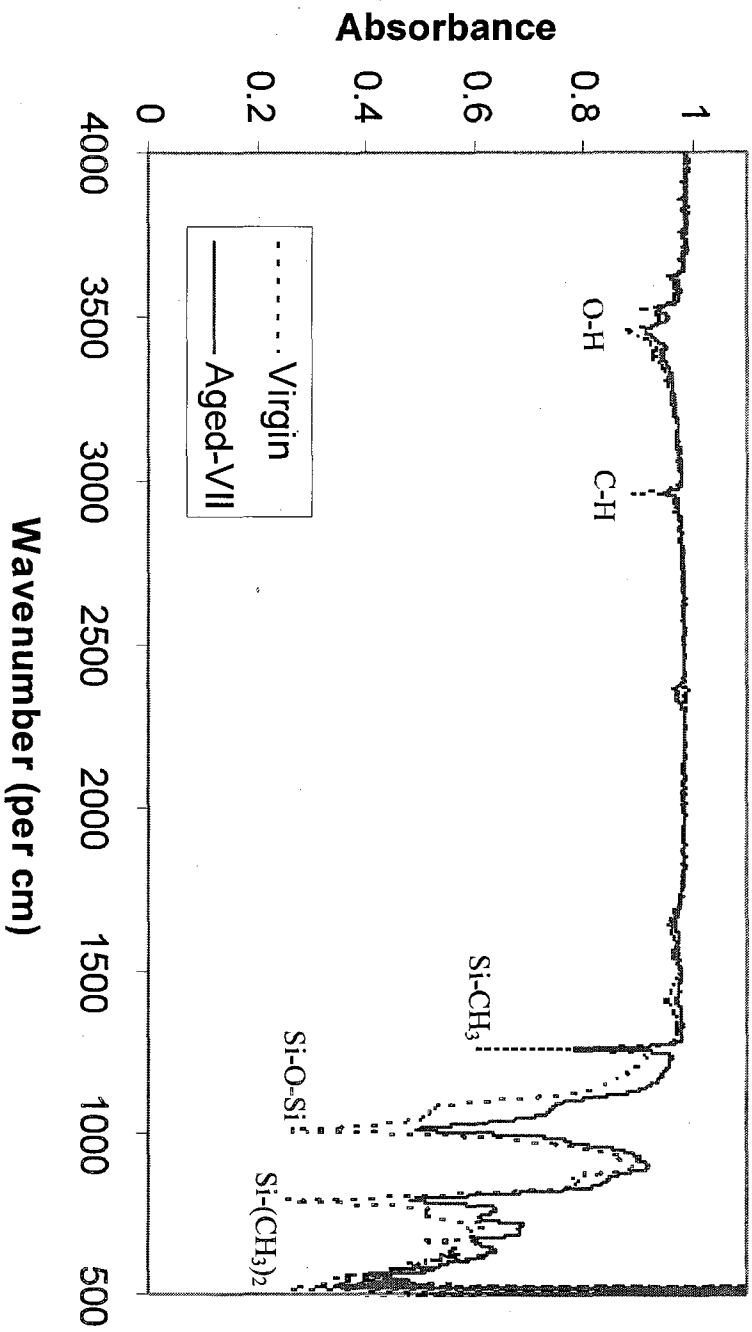


Figure 4.51. Comparison between the ATR FTIR spectra of a virgin HTV SIR specimen and the aged-VII, the specimen aged in saline water of 1 mS/cm conductivity at 75 °C for 3000 h. The aged specimen had been allowed to recover in stationary air at room temperature for 3000 h before the spectra.

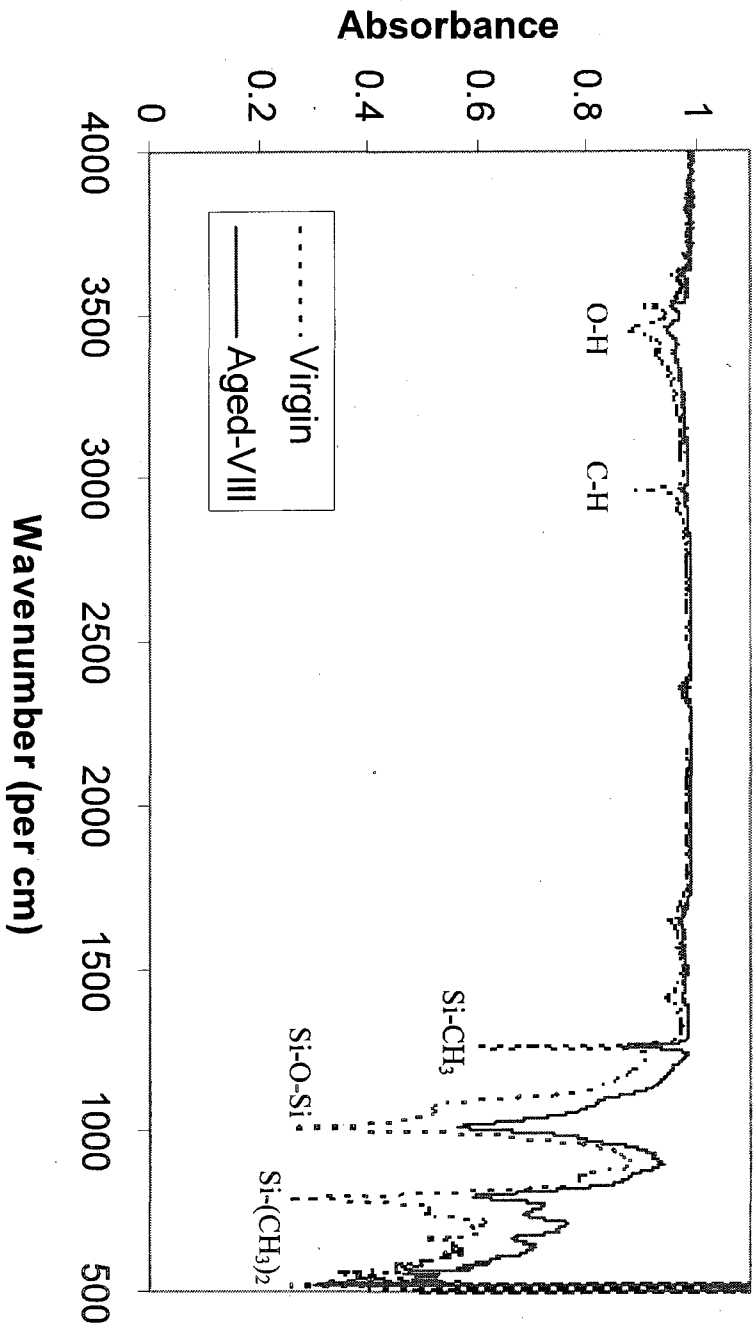


Figure 4.52. Comparison between the ATR FTIR spectra of a virgin HTV SIR specimen and the aged-VIII, the specimen aged in saline water of 1 mS/cm conductivity at 98 °C for 3000 h. The aged specimen had been allowed to recover in stationary air at room temperature for 3000 h before the spectra.

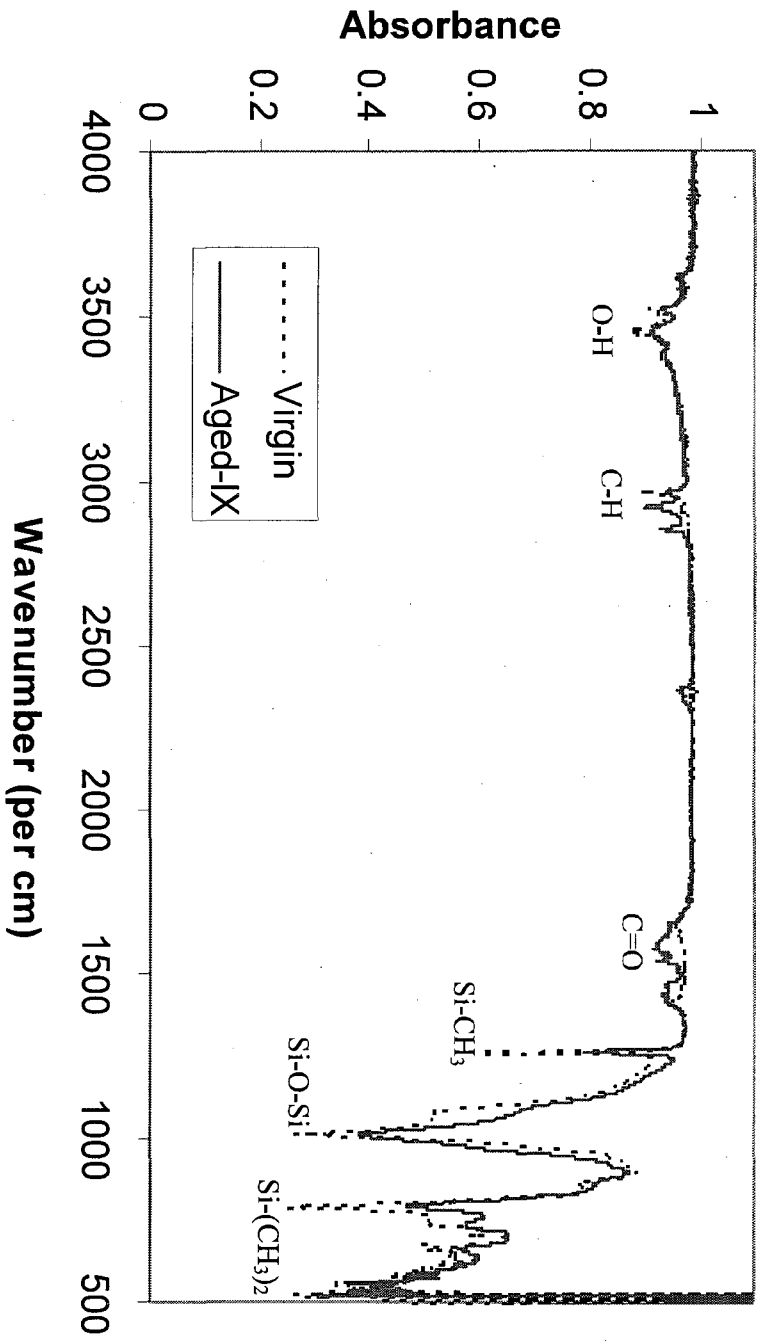


Figure 4.53. Comparison between the ATR FTIR spectra of a virgin HTV SIR specimen and the aged-IX, the specimen aged in saline water of 100 mS/cm conductivity at 98 °C for 3000 h. The aged specimen had been allowed to recover in stationary air at room temperature for 3000 h before the spectra.

case, the specimens were immersed in hexane for 1000 h followed by 1000 h for evaporation in air. Moreover, two different specimens at different temperatures 22 ± 3 °C and 45 ± 1 °C were used in order to precede the experiments. The latter temperature has been used to accelerate the extraction process of LMW fluid.

6.2.2 Results and Comparisons

Figure 6.1 shows the percentage of weight gain of HTV SIR specimens during immersion in hexane for 100 h. The weight of the specimens increased rapidly in first ten hours and after that the absorption slowed down. The specimens reached a steady state value of 55.03 and 52.49% at 22 and 45 °C, respectively. Figure 6.2 shows the percentage of weight loss during evaporation of hexane for 100 h. There was a rapid decrease in the weight during first three hours due to evaporation of hexane and afterwards the rate of evaporation slowed down. The specimens lost a weight of 36.39 and 35.39% at 22 and 45 °C, respectively.

Figure 6.3 shows the percentage of weight gain of the specimens during long term immersion in hexane. The specimens gained a maximum increase in weight of 57.88 and 54.90% at 22 and 45 °C, respectively during immersion for 1000 h. Figure 6.4 shows the percentage of weight loss during evaporation of hexane for 1000 h. The specimens lost a weight of 37.59 and 36.55% at 22 and 45 °C, respectively during long term evaporation of 1000 h. Moreover, lower percentage of saturated weight has been observed in the Figures 6.1-6.4 in the case of higher temperature 45 °C which is consistent with the previous report mentioned in chapter 5 of the thesis [73].

From Figures 6.1-6.4, it can be seen that in all the cases, the weight of specimens reached a saturated point within 24 h of either immersion or evaporation for both temperatures 22 °C and 45 °C. Therefore, for convenience and reliable results during further experiments in this study, a time period of 96 h was chosen to be

sufficient for complete absorption of hexane followed by 48 h of evaporation in air, both at 22 and 45 °C which is consistent with the previous report on HTV SIR [77]. In the literature, 48 h of immersion in hexane followed by 120 h of evaporation in air, both at 50 °C were used for EPDM [73], also 96 h of immersion followed by 24 h of evaporation time at room temperature for EPDM [Cao], and 48 h of evaporation at 44 °C has been used for alloy of EPDM/SIR [80]

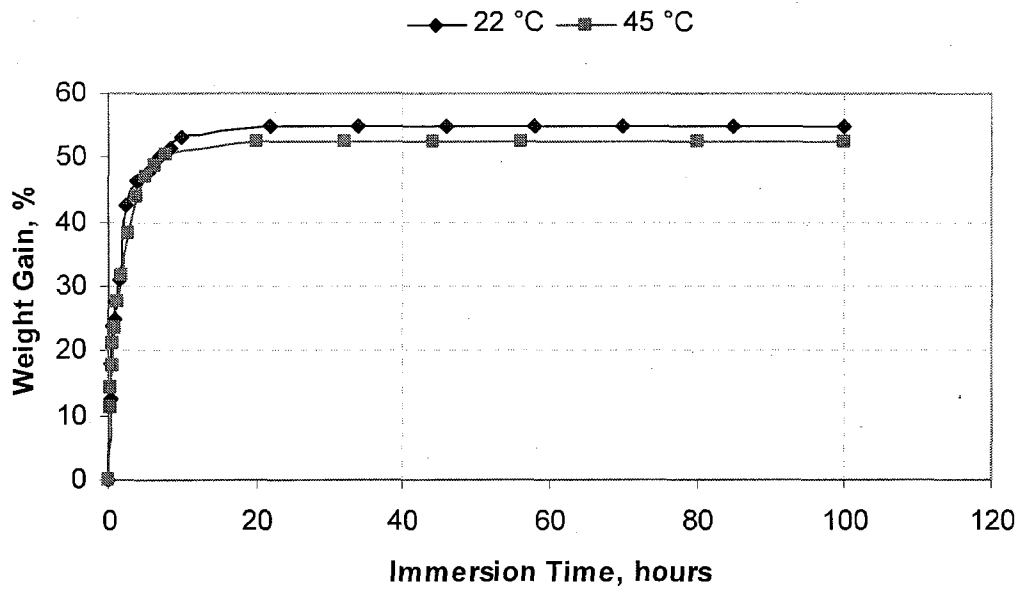


Figure 6.1. Percentage of weight gain of HTV SIR specimens during short-term immersion in hexane at 22 °C.

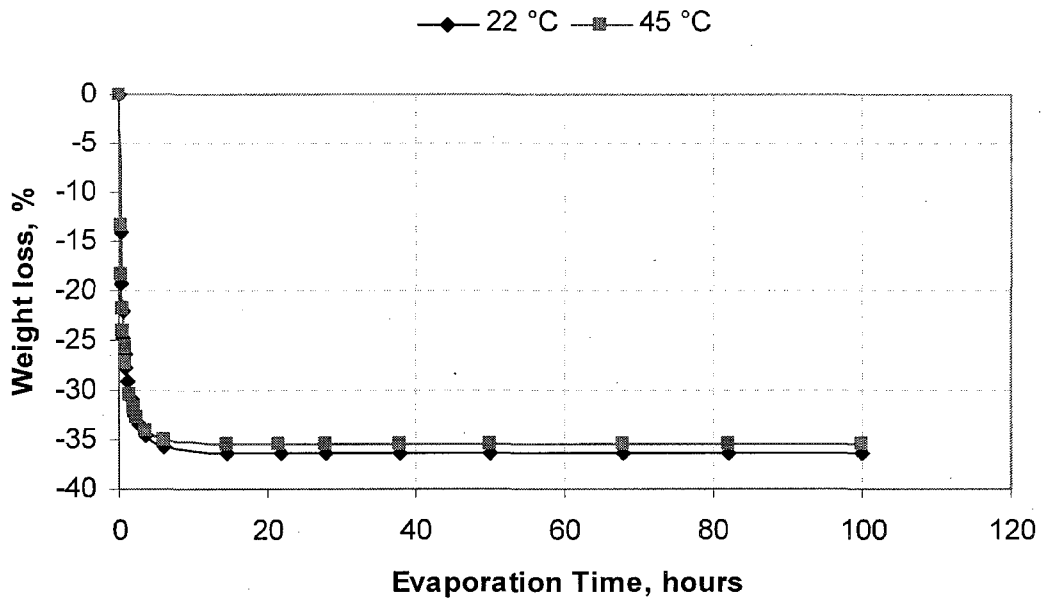


Figure 6.2. Percentage of weight loss of HTV SIR specimens during short-term evaporation in air at 22 °C.

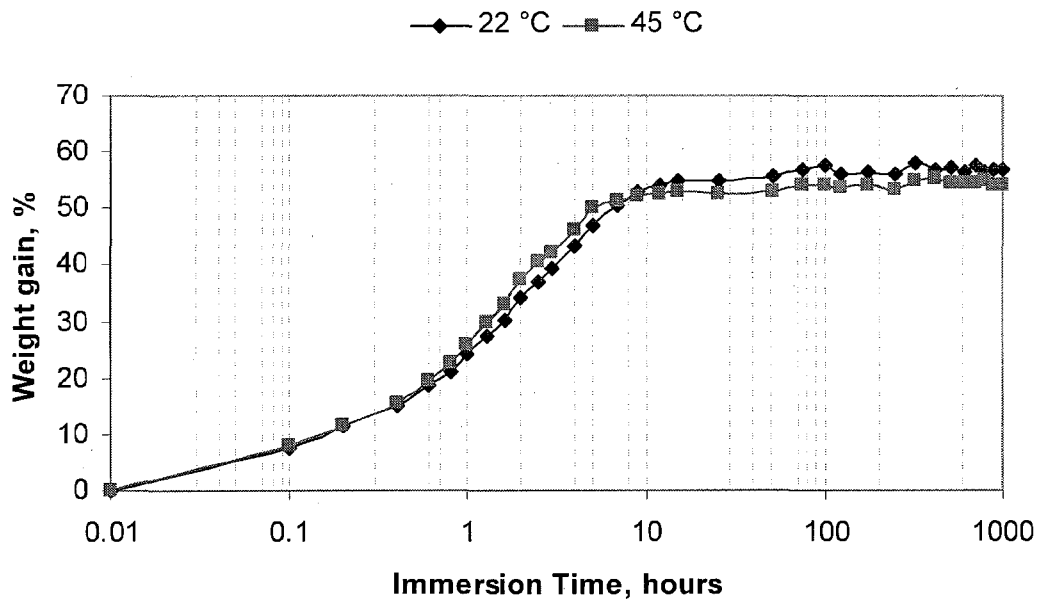


Figure 6.3. Percentage of weight gain of HTV SIR specimens during long-term immersion in hexane at 22 °C.

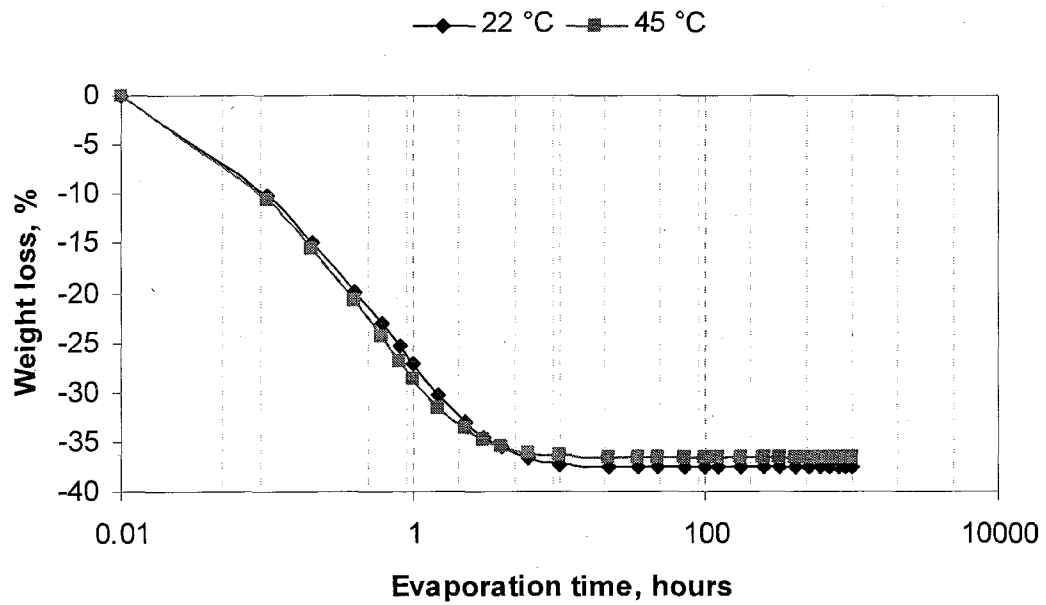


Figure 6.4. Percentage of weight loss of HTV SIR specimens during long-term evaporation in air at 22 °C.

6.3 Characterization of LMW Fluid

Characterization means a group of scientific techniques to identify the chemical composition of an unknown material (sample). These include mass spectrometry (MS) to identify the mass of the sample, nuclear magnetic resonance (NMR) spectroscopy to identify the hydrogen and carbon atoms and IR spectroscopy to identify the functional groups in the sample. Utilization of such techniques for identification of LMW fluid has previously been reported [73, 81-82]

The extracted fluid from the HTV SIR specimens is a solution of LMW fluid and hexane. The LMW fluid was separated from hexane by simple evaporation technique using a rotary evaporator. The boiling point of hexane is 69 °C but the evaporation process only took a few minutes at 30 °C under the reduced pressure. The dried sample was then inserted in the high vacuum pump for one hour to achieve maximum dryness and finally subjected to the characterization.

6.3.1 NMR Spectroscopy

In the first step, the compound was identified by using the NMR which is one of the most reliable techniques to identify the structure of an unknown compound. The NMR was obtained by applying high electromagnetic energy at suitable frequency to the sample. The compound in hexane was dried under vacuum and dissolved in Deuterated Chloroform (CDCl_3) to get ^1H (proton) NMR using a Bruker Avance 500 MHz spectrometer.

Figures 6.5-6.7 show the spectra of analytical hexane, silicone fluid (1000 cp) and the LMW fluid extracted in hexane from HTV SIR specimen, respectively. It can be seen that all the major peaks in the spectrum of Figure 6.7 closely match the spectra of Figures 6.5-6.6. The spectra show some extra peaks of hexane and silicone fluid. These peaks were characterized by comparing the reported NMR spectra of the respective samples. In the NMR spectrum, the height of each peak corresponds to the number of protons contributing.

6.3.2 Infrared Spectroscopy

Infrared (IR) spectroscopy was an inevitable tool for analytical chemists before the advent of nuclear magnetic resonance (NMR) spectroscopy. Although NMR spectroscopy tells us about the structure of an unknown compound, IR is still an important technique for chemists because of its usefulness for identification of functional groups in a compound. IR is a set of radiation which is present in electromagnetic spectrum between microwaves and visible region.

In order to identify the functional group present in the extracted LMW fluid, the IR spectrum was collected. In this technique, just like mass spectroscopy, sample can be used both in solid and solution forms. We used the latter one, the sample was dissolved in acetone, a very polar solvent and a drop of it was transferred onto potassium bromide (K Br) plate. After letting the acetone to evaporate, a thin layer of sample was left behind. The sample was then inserted into the instrument and the spectrum was collected and processed.

Figure 6.8 shows the infrared spectrum of the LMW fluid extracted in hexane from the HTV SIR specimens. The peak at 2960 cm^{-1} is due to C-H stretching bond in CH_3 group and at 1260 cm^{-1} is due to the deformation of CH in Si-CH_3 groups. Whereas, the peaks at $1013\text{-}1082\text{ cm}^{-1}$ are due to the absorption of Si-O bond in Si-O-Si chain and the sharp peak at 796 cm^{-1} is due to the stretching vibrations of $\text{Si}(\text{CH}_3)_2$ group. When this spectrum is compared to Figure 6.9, the IR spectrum of polydimethylsiloxane (PDMS) taken from [83] indicates clearly that the extracted fluid contains PDMS.

6.3.3 Mass Spectrometry

Mass spectrometry is an analytical technique that measures the mass to charge ratio of the charged particles. The instrument used is called as mass spectrometer and consists of three main parts; an ion source used to convert the

sample into ions, the mass analyzer and a detector. On subjecting the sample to mass spectrometer; first the sample is converted into ions, secondly the ions are separated on the basis of different masses, and the third step is the detection of the number of ions of each mass produced. Finally the collected data is transformed into a mass spectrum.

The fluid contents used for identification by MS, were extracted by immersing the HTV SIR specimens in distilled water at 98 °C for 576 h which is one of the aging conditions of chapter 3. The fluid was allowed to evaporate in air to get the extracted contents in solid form. In order to determine the mass of the extracted fluid, Varian 1200 L Quadropole Mass Spectrometer was used. The sample used was in solid state and the direct insertion technique was employed at 20 eV to get the mass chromatogram at 200 °C.

The fluid extracted from HTV SIR specimens was identified as silicone fluid composed of siloxane molecules as shown in mass spectrum of Figure 6.10. The dimethylsiloxane $[\text{Si}(\text{CH}_3)_2\text{O}]$ molecule units of $n^+=2$ to $n^+=6$ were identified as cyclic units in the spectrum whereas n^+ means number of siloxane units in the cyclic structures. The mass peaks at 148, 222, 296, 370 and 444 are considered as normal molecular weights for $n^+=2$, $n^+=3$, $n^+=4$, $n^+=5$ and $n^+=6$ cyclic units respectively.

Similarly, the mass peaks at 133, 207, 281, 355 and 426 are considered as molecular weights with one methyl group ($\text{CH}_3=15$) missing for $n^+=2$, $n^+=3$, $n^+=4$, $n^+=5$ and $n^+=6$ cyclic units respectively. The chemical structures and the corresponding molecular weights for $n^+ = 2, 3, 4, 5$ and 6 units of siloxane identified from the MS of the extracted fluid are given in Table 6.1. The presence of siloxane molecules in the mass spectrum of Figure 6.10 indicates that polydimethylsiloxane units would migrate as a fluid to the surface and maintain the hydrophobicity of the surface.

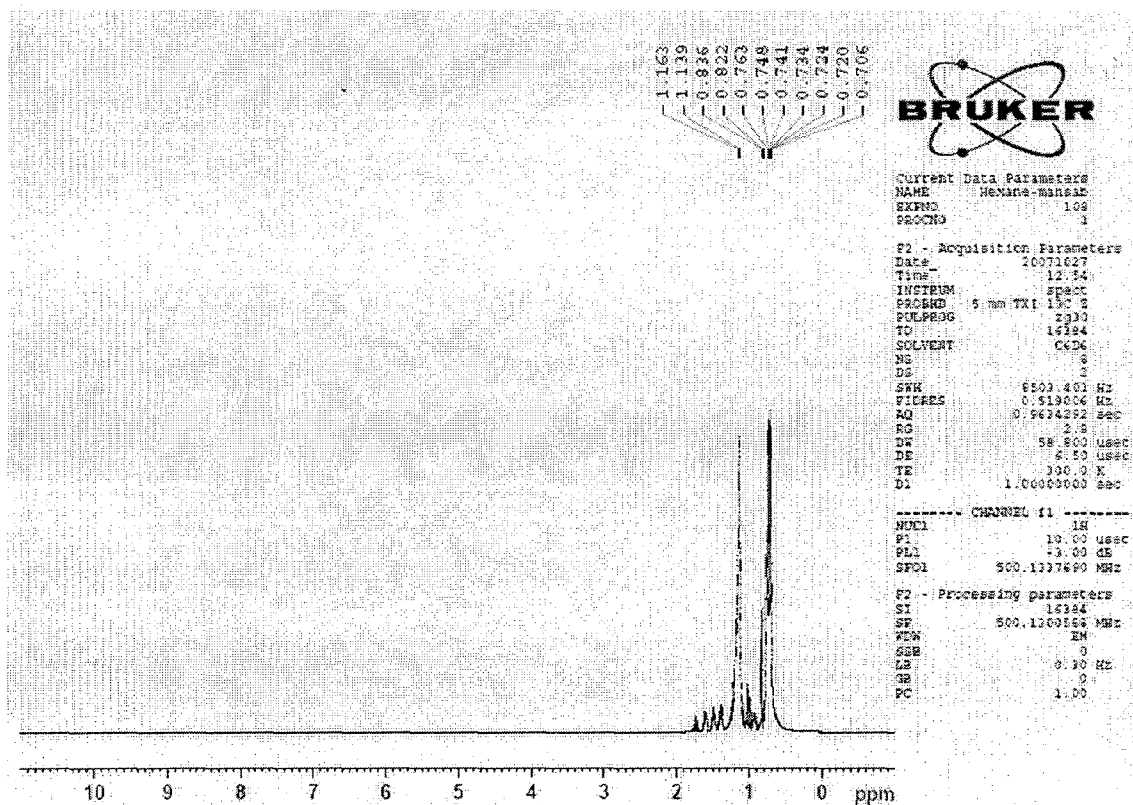


Figure 6.5. NMR spectra for analytical hexane

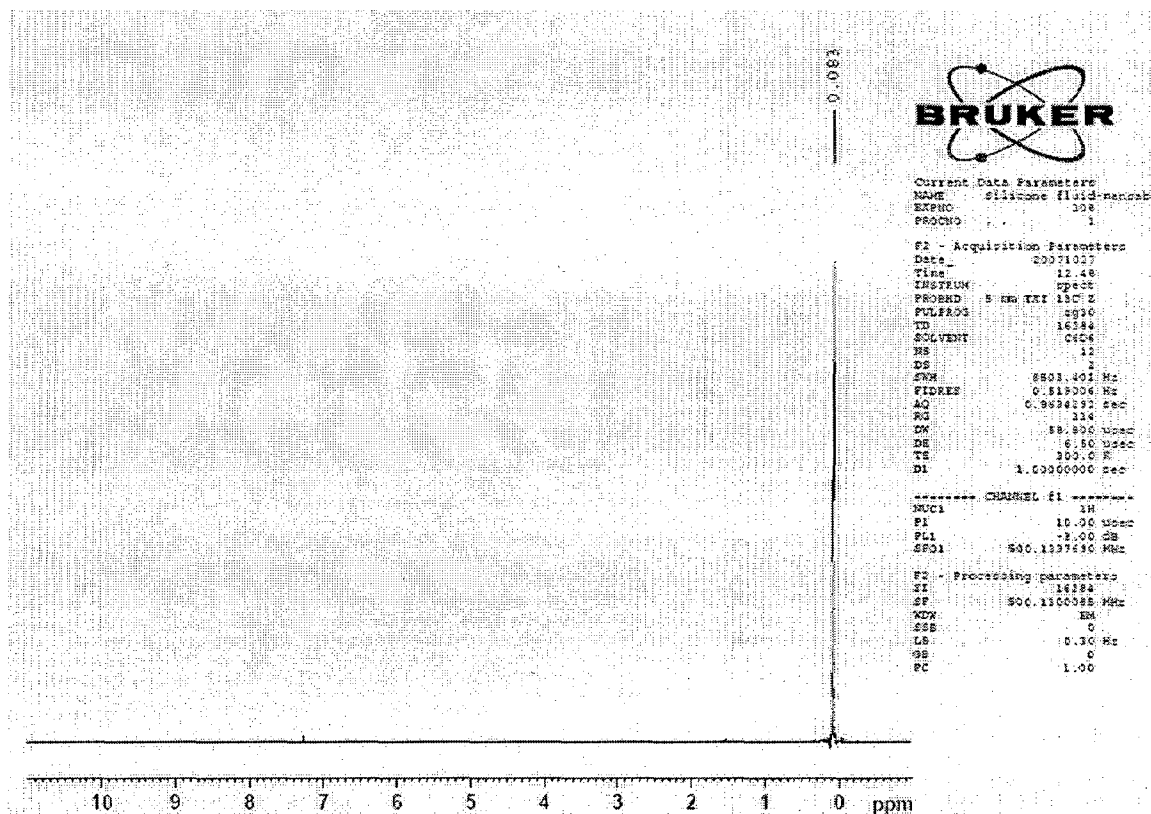


Figure 6.6. NMR spectra for silicone fluid (1000 centipoise viscosity)

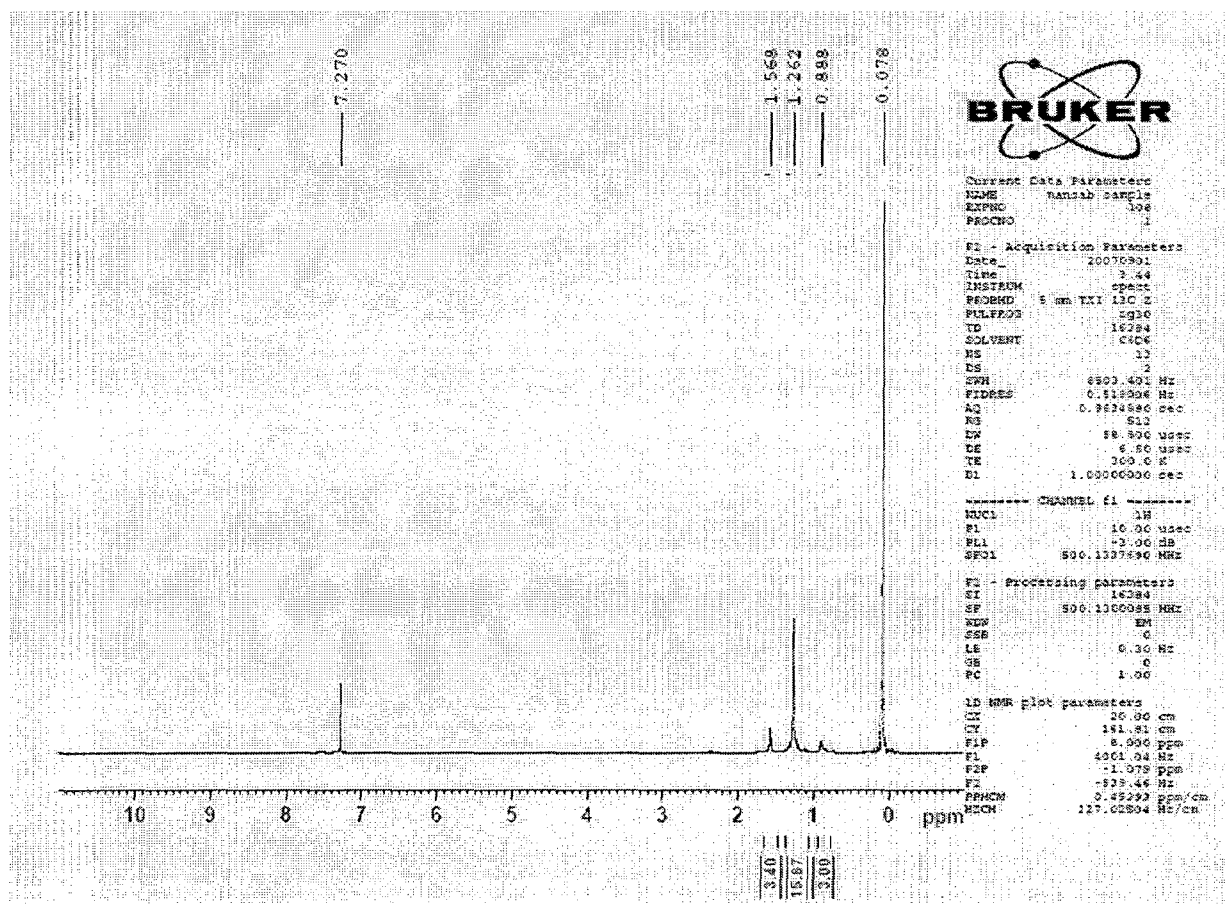


Figure 6.7. NMR spectra of the mixture of hexane and LMW fluid extracted from the HTV SIR specimens

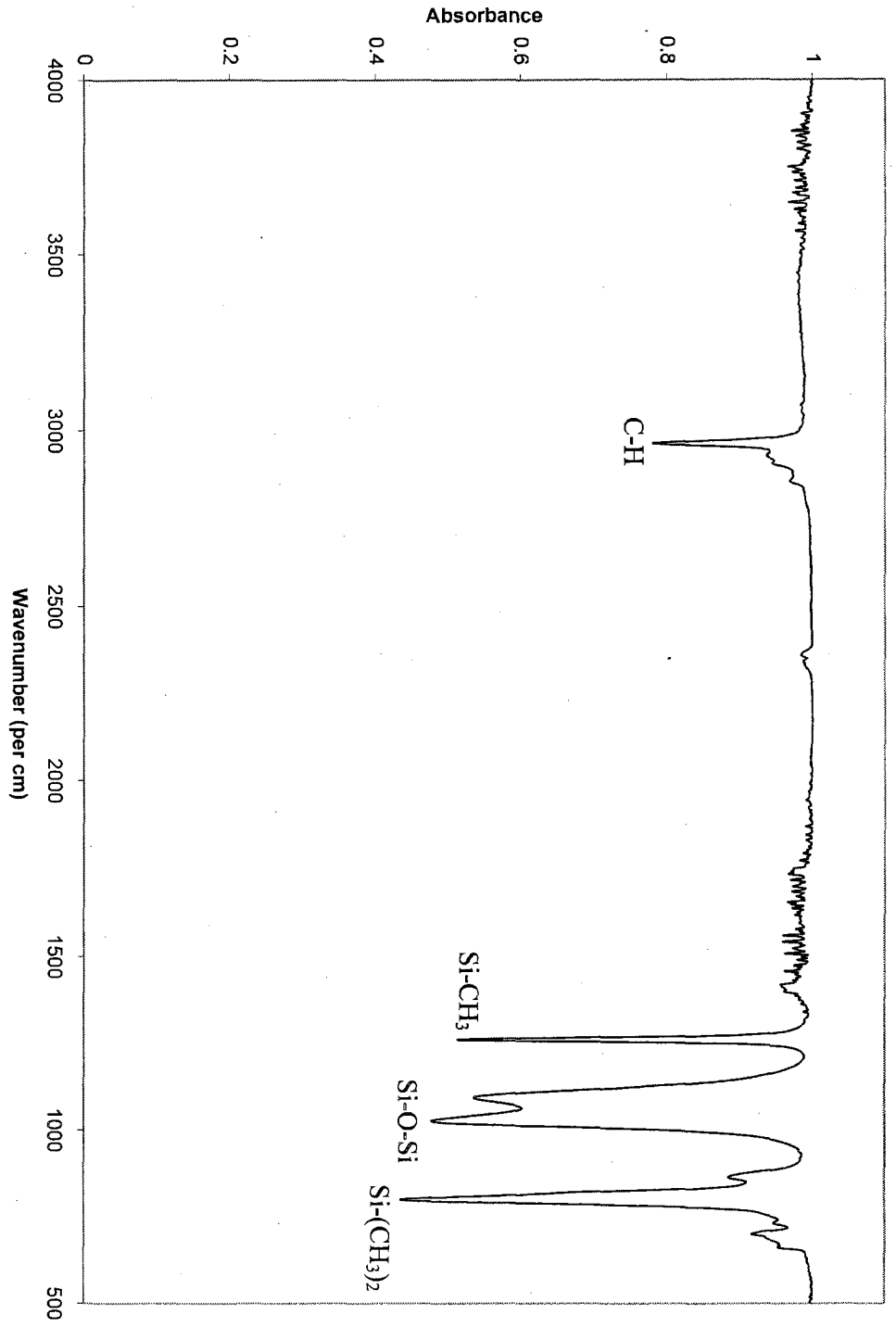


Figure 6.8. IR spectrum of the fluid extracted from HTV SIR specimens in hexane

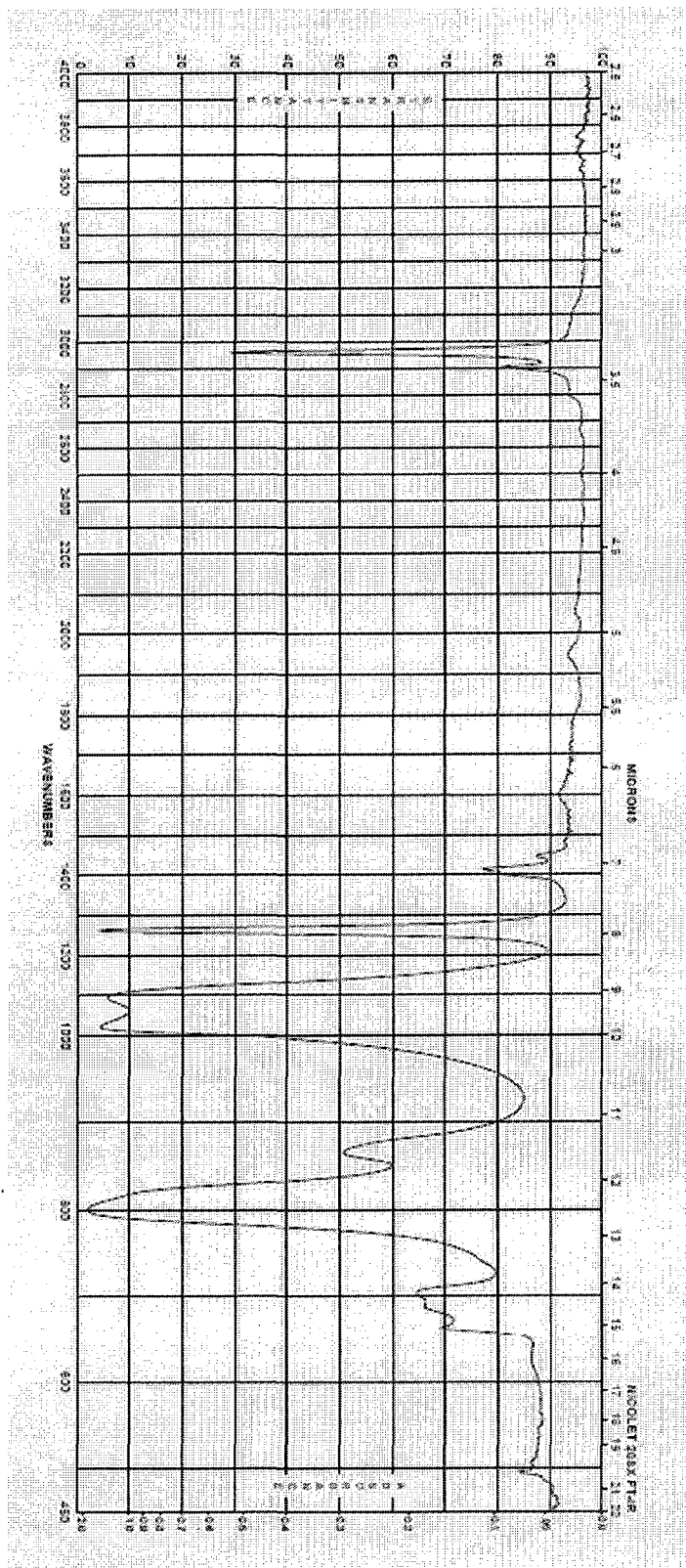


Figure 6.9. IR spectrum of PDMS [83]

MS Data Review Active Spectrum Plot - 5/1/2008 11:05 PM

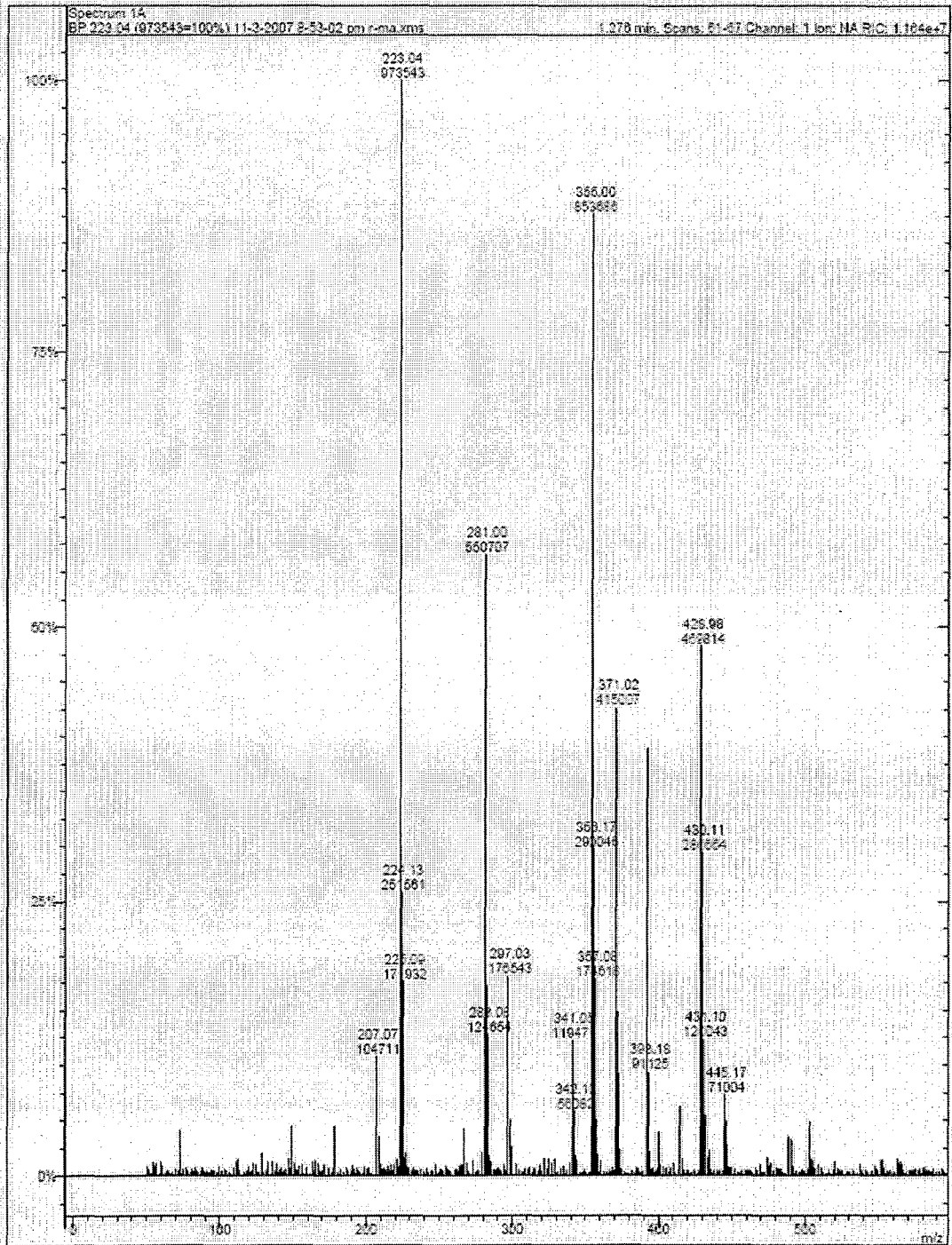
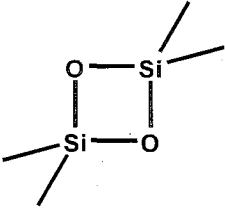
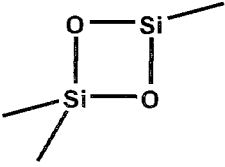
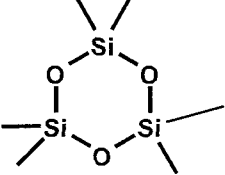
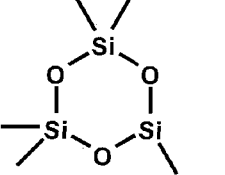
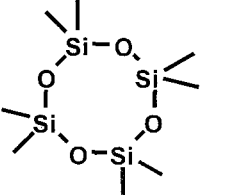
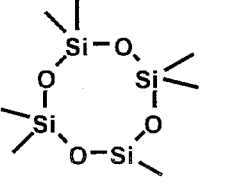
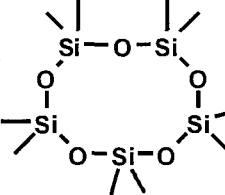
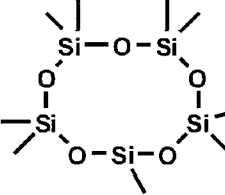
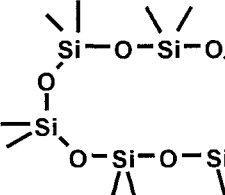
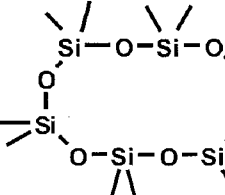


Figure 6.10. Mass spectrometry (MS) of the fluid extracted from the HTV SIR insulator specimens heated in distilled water at 98 °C for 576 h.

Table 6.1. Chemical structures along with the corresponding molecular weights of $n^+=2, 3, 4, 5$ and 6 units of siloxane identified from the mass spectrum of the fluid extracted from the HTV SIR specimens heated in distilled water at 98 °C.

n^+	Normal molecular weight	Structures	Molecular Weight with missing one methyl group	Structures
2	148		133	
3	222		207	
4	296		281	
5	370		355	
6	444		426	

6.4 Effect of Heat on Regeneration of LMW Fluid

The amount of low molecular weight (LMW) fluid on the surface and in the bulk of the material plays an important role in maintaining the hydrophobicity during the life time of HTV SIR used as insulators. Therefore, it is very important to determine the amount of LMW fluid in the virgin as well as the aged specimens in order to assess the hydrophobicity behavior during their life time operation. The following complementary experiments were conducted in order to establish the effect of heat on the regeneration and diffusion of LMW fluid from the bulk of the polymeric insulating material to the surface. The loss and regeneration of LMW fluid after being subjected to repeated heat treatment has previously been reported in EPDM and an alloy of EPDM/SIR [73, 79-80, 84]

6.4.1 Hexane-Heat-Hexane Test Sequence for Virgin Samples

The HTV SIR specimens were subjected to two kinds of sequential treatments: hexane-heat-hexane test sequence. In this test sequence, first the specimens were immersed in analytical hexane for 96 h at room temperature followed by evaporation in air for 48 h to extract the LMW fluid contents. In order to find out the impact of heating time on the regeneration of LMW fluid, the specimens were then heated at 200 °C for 2, 4, 8, 16 and 32 h. Then, the specimens were again immersed in hexane followed by evaporation in air to extract the LMW fluid second time. The specimens were heated second time at 200 °C to generate the LMW fluid. Finally, there was a third immersion in hexane for 96 h followed by the evaporation in air for 48 h.

Table 6.2 shows the summary of the percentage of weight loss of the HTV SIR specimens after each step of the sequential treatment. The percentage of the extracted LMW fluid contents from the virgin specimens is given in the first row; by 1st immersion in hexane for 96 h followed by evaporation in air for 48 h. This amount of extracted LMW fluid is much higher than the amount extracted during

the second and third immersions. Moreover, the percentage weight loss during first heating at 200 °C is almost more than three times as compared to the weight loss during the second heat treatment. This higher decrease in weight during the first heat treatment might be due to the instant evaporation of water contents of the specimens at temperatures higher than the room temperature.

The amount of weight loss during the heating process in air increased with the increase of heating time duration e.g., weight loss by 1.09, 1.30, 1.69, 2.20 and 2.49% for time durations of 2, 4, 8, 16 and 32 h, respectively. However, the increase in the extracted LMW fluid contents during the second and third immersion in hexane due to the increase in heating time duration is small. The reason behind this might be that a portion of the regenerated fluid was evaporated during the heating process. The results are also given in the shape of a graph of Figure 6.11.

Table 6.2. Percentage of weight loss of HTV SIR specimens at different steps of hexane-heat-hexane sequential treatment.

Hexane-Heat-Hexane test sequence	Amount of extracted LMW fluid and weight loss for different heating durations (%)				
	2 h	4 h	8 h	16 h	32 h
1 st Immersion in Hexane for 96 h	1.40	1.40	1.39	1.39	1.35
1 st Heating at 200 °C	1.09	1.30	1.69	2.20	2.49
2 nd Immersion in Hexane for 96 h	0.11	0.12	0.18	0.24	0.23
2 nd Heating at 200 °C	0.24	0.45	0.62	0.86	0.76
3 rd Immersion in Hexane for 96 h	0.09	0.10	0.14	0.18	0.20
Total Weight Loss (%)	2.91	3.34	4.02	4.87	5.03

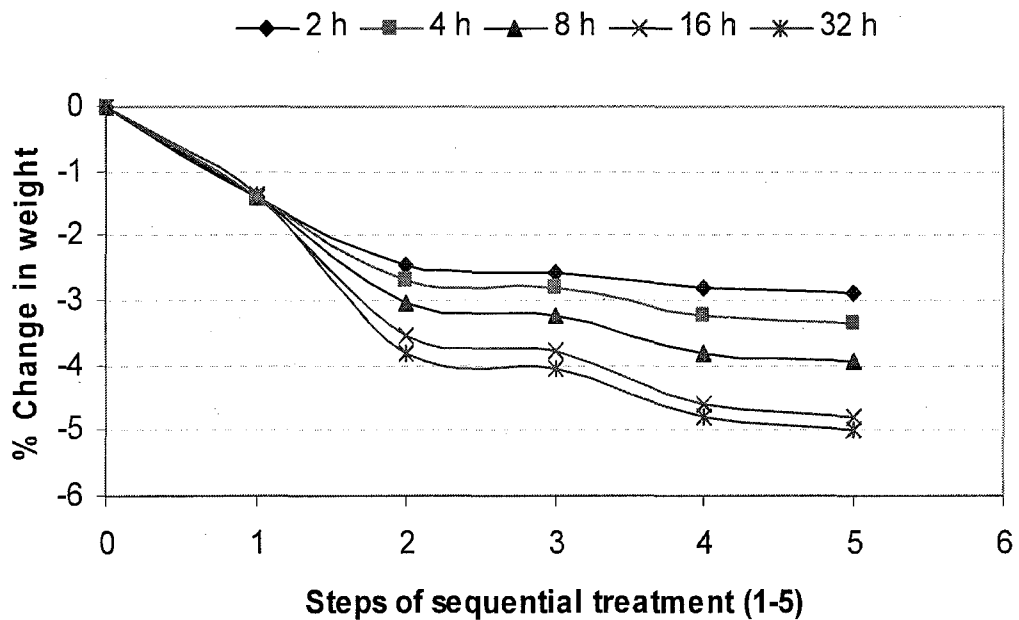


Figure 6.11. Percentage of total weight loss of the HTV SIR specimens at different steps of the hexane-heat-hexane sequential treatment for five different heating durations: 2, 4, 8, 16 and 32 h.

Description of the steps of the sequential treatment:

- 1-First Immersion in hexane for 96 h followed by the evaporation in air for 48 h
- 2-First heating in air at 200 °C for 2, 4, 8, 16 and 32 h
- 3-Second Immersion in hexane for 96 h followed by the evaporation in air for 48 h
- 4-Second heating in air at 200 °C for 2, 4, 8, 16 and 32 h
- 5-Third Immersion in hexane for 96 h followed by the evaporation in

6.4.2 Hexane-Heat-Hexane Test Sequence for Aged Samples

Four HTV SIR specimens were chosen from different aging conditions of chapter 4 for hexane-heat-hexane test sequence and were compared to a virgin specimen. The list of the specimens selected from different conductivity levels and temperatures with aging time of 3000 h is given in Table 6.2. All aged specimens had been allowed to recover in stationary air at room temperature for further 3000 h prior to the test sequence.

Table 6.3. The HTV SIR specimens selected from different aging conditions for Hexane-Heat-Hexane test sequence. The specimens had been allowed to recover for 3000 h prior to the test sequence.

Specimen No.	Temperature (°C)	Water Conductivity (mS/cm)	Aging Time (h)
Virgin	22	air	virgin
Aged-I	0	100	3000
Aged-II	50	0.005	3000
Aged-III	75	0.005	3000
Aged-IV	98	100	3000

In order to find out the impact of aging on the regeneration of LMW fluid, the specimens were subjected to two kinds of sequential treatments: hexane-heat-hexane test sequence similar to section 6.4.1 except, the heating time was kept constant for sixteen hours. First, the specimens were immersed in analytical hexane for 96 h at room temperature followed by evaporation in air for 48 h to extract the LMW fluid contents. Then, the specimens were heated at 200 °C for 16 h to generate the LMW fluid. This heating in air generated the fluid as well as lost it via evaporation. The loss was calculated from the difference in weights before and after the heating in air.

Again, the specimens were immersed in analytical hexane for 96 h at room temperature followed by evaporation in air for 48 h to extract the LMW fluid contents second time. Also, there was a second heating at 200 °C for 16 h which caused a loss of 0.86%. Finally, the specimens were immersed in analytical hexane for 96 h at room temperature followed by evaporation in air for 48 h to extract the LMW fluid contents third time. The percentage reduction in weight due to each individual treatment as well as the total reduction at the end of the all five individual treatments is given in Table 6.3.

Table 6.4. Percentage weight loss of different aged HTV SIR specimens of Table 6.3 compared with the virgin one through sequential hexane-heat-hexane treatment.

Hexane-Heat-Hexane test sequence	Amount of extracted LMW fluid and weight loss of different selected samples of Table 1.2 during Hexane-Heat-Hexane test sequence (%)				
	Virgin	Aged-I	Aged-II	Aged-III	Aged-IV
1 st Immersion in Hexane for 96 h	1.39	1.35	1.33	1.37	2.55
1 st Heating at 200 °C (16 h)	2.20	3.21	3.40	3.47	3.16
2 nd Immersion in Hexane for 96 h	0.24	0.49	0.54	0.53	0.56
2 nd Heating at 200 °C (16 h)	0.86	1.13	0.94	0.91	1.22
3 rd Immersion in Hexane for 96 h	0.18	0.34	0.25	0.24	0.36
Total Weight Loss (%)	4.87	6.37	6.32	6.38	7.63

The amount of extracted LMW fluid from the specimen previously been aged at 98 °C is 2.55% which is much higher than the other chosen specimens. This might be caused due to the scission of longer PDMS molecular chains during aging at higher temperature. Moreover, the loss of weight due to heating at 200 °C during the hexane-heat-hexane test sequence was appreciably less in the

virgin HTV silicone rubber specimens as compared to the specimens aged in saline solutions at different temperatures. This heating of aged specimens in air generated the higher amount of LMW fluid as well as lost it via evaporation.

The Table 6.3 also shows that the amount of LMW fluid extracted through first, second and third immersion from the virgin samples was lower as compared to the aged specimens and this amount of extracted LMW fluid found to be increased with the increase of aging temperature. In addition, the total percentage weight loss at the end of the hexane-heat-hexane test sequence is higher for the aged specimens as compared to the virgin one as shown in Figure 6.12. The specimens aged at 0, 50 and 75 °C have almost the same weight loss, whereas, the weight loss in the specimen aged at 98 °C is much higher.

Therefore, this hexane-heat-hexane test sequence for the virgin as well as aged HTV SIR specimens proved that aging in saline solutions at different temperatures caused the scission of longer PDMS molecular chains and this process was accelerated with the increase of aging temperature. The common observation for all the specimens is that the amount of LMW fluid extracted by the second and third immersion is appreciably less than the first immersion. Also, the percentage weight loss during first heating was more than twice, the weight loss during second heat treatment.

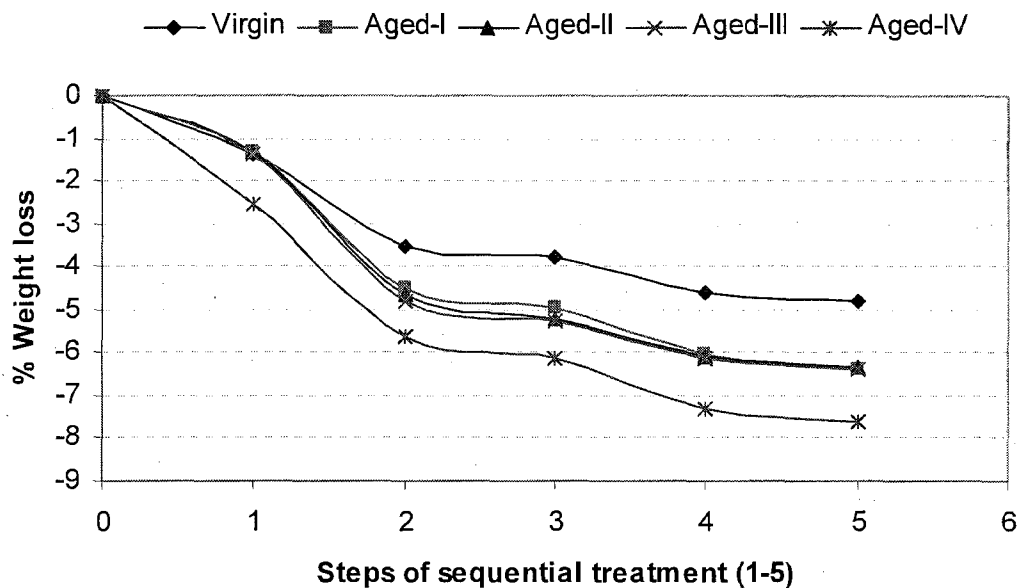


Figure 6.12. Percentage of total weight loss of the virgin as well as the aged HTV SIR specimens at different steps of the hexane-heat-hexane sequential treatment

Description of the steps of the sequential treatment:

1-First Immersion in hexane for 96 h followed by the evaporation in air for 48 h

2-First heating in air at 200 °C for 16 h

3-Second Immersion in hexane for 96 h followed by the evaporation in air for 48 h

4-Second heating in air at 200 °C for 16 h

5-Third Immersion in hexane for 96 h followed by the evaporation in air for 48 h

CHAPTER 7

7 Conclusions and Suggestions for Future Work

7.1 Conclusions

In this study, the characteristics of high voltage polymeric insulator with HTV SIR as weather-shed material have been investigated. The actual environmental simulations were made by submerging samples in saline water having four different conductivity levels of 0.005 (distilled water), 1, 10 and 100 mS/cm. These salinities were chosen to simulate conditions near seashore. These saline solutions were kept at different temperatures 0, 22 (room temperature), 50, 75 and 98 °C for 576 as well as 3000 hours. The samples were also kept in *stationary air at different temperatures for different time durations.*

This is an extended laboratory study of the mechanisms responsible for the loss and recovery of hydrophobicity of HTV SIR specimens during aging by the measurement of weight, contact angle and surface roughness. In addition, the results were analyzed using IR, NMR, GC-MS, SEM, EDS and ATR FTIR spectroscopy. Two different sets of experiments were conducted for different time durations during aging and recovery processes: short term aging and long term aging.

7.1.1 Short Term Aging Results

In short term aging, the HTV SIR specimens were aged in different saline solutions at different temperatures for 576 h and afterwards were allowed to recover at room temperature for 2700 h.

- i. The net weight loss of HTV SIR specimens was maximum for aging at 98 °C. The weight losses were 3.59, 2.42, 2.62 and 2.24% which occurred in the solutions of 0.005, 1, 10 and 100 mS/cm, respectively.
- ii. The contact angle of the HTV SIR specimens decreased by 10-15° from the virgin value of 100±5° rapidly within the first ten hours of immersion in different saline solutions at different temperatures which is almost 75% of the maximum drop of the contact angle over a period of 576 h. The contact angle continued to decrease during prolonged immersion in different saline solutions at all temperatures but at a very low rate after ten hours.
- iii. The hydrophobicity of the HTV SIR specimens recovered in stationary air at room temperature for up to 2700 h. The specimens had been divided into the following three categories based on the changes in their contact angles during the recovery process:
 - a. The contact angle reached its original value after recovery that is the contact angle of the virgin specimen 100±5°; these included the specimens aged in 0.005 mS/cm at 0 °C and 98 °C; 1 mS/cm at 0 °C; 10 mS/cm at 25, 50 and 75 °C; 100 mS/cm at 25, 75 and 98 °C; and in air at 0 and 25 °C.
 - b. The contact angle of the specimens reached a higher than its virgin value after recovery; these included the specimens aged in saline solutions of 1 mS/cm at 98 °C; 10 mS/cm at 0 and 98 °C; 100 mS/cm at 0 and 50 °C; and in air at 50, 75 and 98 °C.
 - c. The contact angle did not reach its virgin value 100±5°, after recovery; these included the specimens aged in 0.005 mS/cm and 1 mS/cm at 25, 50 and 75 °C.

- iv. For the specimens kept in air at 0, 22 and 50 °C for 576 h and later on allowed to recover at room temperature for 2700 h, the changes in weight are 0%. However, at 75 and 98 °C, the net weight decrease is considerable and is as high as 0.62%. Moreover, the specimens kept in stationary air at 50, 75 and 98 °C, lost their weight at a faster rate in the first few hours. This might be due to the instant evaporation of water contents of the specimens at temperatures higher than room temperature.
- v. For specimens kept in air for 576 h at temperatures higher than room temperature, e.g., 50, 75 and 98 °C, there was an increase in the contact angle with the increase of temperature. For example, at 98 °C, the contact angle increased from 97° to 114° after 50 h. However, the contact angle decreased from 100° to 92° at 0 °C after 1400 h, whereas, no appreciable change was observed at 22 °C.
- vi. The HTV SIR specimens subjected to different aging conditions up to a period of 576 h, had variation in their ASR in the range of $\pm 0.16 \mu\text{m}$ during aging and recovery process which is not appreciable.
- vii. The SEM images demonstrated that the specimen aged at 50 °C did not appear to be significantly different from the virgin specimen in surface morphology owing to a lower aging temperature. However, the specimens aged at 75 °C and 98 °C in distilled water for 576 h had a significant change in surface morphology and roughness due to adequate filler dispersion as compared to the virgin sample. The surface of these specimens also became hard along with an apparent change in their color as seen by the naked eye.
- viii. The concentration ratios of Al/Si, Al/O, Al/C and O/Si on the surface of the HTV SIR specimens aged in distilled water at 50, 75 and 98 °C along with the virgin one was higher with the increase of temperature. Therefore, it is

apparent that the ATH dissolved into water as well as diffused to the surface at high temperature and ultimately, increased its intensity on the surface of the aged insulator specimens.

- ix. It is evident from the ATR FTIR spectra of aged HTV SIR specimens that the surface changes are mainly due to the changes in Si-O and Si-CH₃ bondings. The aging of the specimens in saline solutions at 75-98 °C for 576 h caused the loss of hydrophobic groups CH₃, from Si-CH₃ and increased the Si-O bonding from crosslinking. Another cause of decrease of hydrophobic groups might be the dispersion of ATH filler on the surface due to its dissolution in water at higher temperature.

7.1.2 Long Term Aging Results

In long term aging, the HTV SIR specimens were aged in different saline solutions at different temperatures for 3000 h and afterwards were allowed to recover at room temperature for further 3000 h.

- i. The net weight loss of HTV SIR specimens was maximum for aging at 98 °C. The weight losses by 14.86, 12.44, 9.80 and 8.39% which occurred in the solutions of 0.005, 1, 10 and 100 mS/cm, respectively.
- ii. There was a decrease of 10-15° in the contact angle of the HTV SIR specimens within the first ten hours of immersion in different saline solutions at different temperatures similar to the results of the experiments of short term aging (576 h). The contact angle continued to decrease with prolonged immersion in saline solutions but at a very low rate after 10 to 3000 h at 0-75°C. However, this decrease became rapid again after 1200, 1300 and 1700 h for the solutions of 0.005, 1 and 10 mS/cm, respectively at 98° C, whereas, for the solution of 100 mS/cm, the contact angle

decreased continuously and almost at a steady rate over the period of 10 to 3000 h.

- iii. The hydrophobicity of the HTV SIR specimens recovered in stationary air at room temperature for up to 3000 h. The specimens had been divided into the following three categories based on the changes in their contact angles during the recovery process:
 - a. The contact angle regained its virgin value $100\pm 5^\circ$, after recovery; these included the specimens aged in 0.005 mS/cm at 25 and 98 °C; 1 mS/cm at 0 and 75 °C; 10 and 100 mS/cm at 75 °C; and in air at 25, 50, 75 and 98 °C.
 - b. The contact angle of the specimens reached a higher than its original value after recovery; these included the specimens aged in 1 mS/cm at 25 and 98 °C; 10 mS/cm at 0, 25 and 98 °C; 100 mS/cm at 0 and 25 °C; and in air at 0 °C.
 - c. The contact angle could not regain its original value $100\pm 5^\circ$, after recovery; these included the specimens aged in 0.005 mS/cm at 0, 50 and 75 °C; 1 and 10 mS/cm at 50 °C; and 100 mS/cm at 50 at 98 °C.
- iv. The changes in weight of the HTV SIR specimens kept in air at 0, 22, 50 and 75 °C for 3000 h and later on had been allowed to recover at room temperature for 3000 h are $\pm 0.06\%$ which is negligible. However, at 98 °C, the net weight decrease is considerable and is as high as 0.62%. Moreover, the specimens kept in stationary air at 50, 75 and 98 °C lost their weight at a faster rate in the first few hours which might be due to the instant evaporation of water contents of the specimens at temperatures higher than room temperature.

- v. There was an increase in contact angle of the specimens kept in air for 3000 h at temperatures higher than the room temperature, e.g., 50, 75 and 98 °C. For example, the contact angle increased from 97° to 114° after 50 h at 98 °C. However, the contact angle decreased from 100° to 92° after 1400 h at 0 °C, where as, no appreciable change was observed in the contact angle of the specimens kept at 22 °C.
- vi. The ASR of the HTV SIR specimens increased from 0.54 to 1.79, 0.68 to 2.95 and 0.69 to 2.64 μm during aging at 98 °C in the solutions of 0.005, 1 and 10 mS/cm, respectively for 3000 h. For all other aging conditions, the variation in ASR was in the range of $\pm 0.16 \mu\text{m}$ from the virgin value and therefore, was not considerable.
- vii. The aged specimens exhibited rougher surfaces and phase difference due to changes in the filler and rubber on the surface because of aging. The SEM images showed that the surface of the specimens aged in distilled water at room temperature slightly differed from the virgin sample. However, the HTV SIR specimens aged in distilled water at 50, 75 and 98 °C for 3000 h had a significant change on the surface due to their deterioration at higher temperature as demonstrated by the SEM micrographs. Moreover, the surface became hard and brittle with the loss of its original color. Also, obvious cracks were observed as seen by the naked eye, on the surface of the specimens aged in solutions of 0.005, 1 and 10 mS/cm at 98 °C.
- viii. It is evident from the ATR FTIR spectra of aged HTV SIR specimens that the surface changes are mainly due to the changes in Si-O and Si-CH₃ bonding. The aging of the specimens in saline solutions at 50-98 °C for 3000 h caused the loss of hydrophobic groups CH₃, from Si-CH₃ and increased the Si-O bonding from crosslinking. Another cause of the

decrease of hydrophobic groups might be the dispersion of ATH filler on the surface due to its dissolution in water at higher temperatures.

7.1.3 Summary of the Results

- The change in weight of the specimens during aging in different saline solutions was more rapid in solutions of low conductivity.
- The change in the weight of the specimens during aging in different saline solutions was more rapid at higher temperatures.
- The lower rate of absorption of saline water was observed during aging of the specimens in higher conductivity solutions.
- The hydrophobicity of HTV SIR specimens decreased during aging in the saline solutions with the increase of immersion time. This loss of hydrophobicity is associated with the physical and chemical changes on the surface under wet conditions at different temperatures.
- The hydrophobicity increased when the specimens were subjected to heat (50-98 °C) in air. This is associated with the diffusion of LMW fluid from the bulk to the surface.
- There was a little decrease in contact angle due to aging in stationary air at 0 °C and almost no change at room temperature (22 °C).
- The weight and ASR decreased while the contact angle increased during the recovery process of the HTV SIR specimens after aging in different saline solutions.
- The higher values of contact angles have been observed during recovery in air for samples which were immersed in solutions of high conductivity.

- The surface of the HTV SIR specimens became completely hydrophilic due to aging in distilled water at 98 °C after 3000 h.
- The ASR increased appreciably (0.94 – 2.39 μm) due to aging in saline solutions of conductivities, 0.005, 1 and 10 mS/cm at 98 °C for 3000 h. For all other aging conditions, the change in ASR was within $\pm 0.16 \mu\text{m}$ from the virgin value.

7.2 Suggestions for Future Research

1. The LMW fluid extracted from the aged HTV SIR specimens need to be analyzed and identified by different techniques. The aged specimens should be chosen after aging in saline solutions of different conductivities at different temperatures for different time durations.
2. The study of the effect of R.F. discharge on the hydrophobicity of HTV silicone rubber insulator.
3. The extensive laboratory study by applying DC/AC electrical stresses on HTV SIR insulator to find out their effects by the measurement of weight, contact angle of distilled water and the average surface roughness. The SEM, EDS and ATR FTIR techniques can be used to demonstrate the surface degradation and other surface compositional changes.
4. The results of laboratory study and the actual field service conditions need to be correlated. In this way, it can be assessed that the artificial accelerated aging stresses as well as the theoretical approaches how closely reflect the actual field service conditions.
5. The HTV silicone rubber can be manufactured by using different vulcanizing catalysts and curing temperatures. The properties of these new materials should be studied by the application of accelerated laboratory aging stresses. In this way, materials with excellent properties can be obtained for high voltage insulation.

References

- [1] R. G. Neimi and T. Orbeck, "High Surface Protective Coatings for High Voltage Insulators", IEEE PES Summer Meeting, paper C72 557-7, 1972
- [2] B. F. Hampton, "Flashover Mechanism of Polluted Insulation", Proc. IEEE, Vol. 111, pp. 985-990, 1964
- [3] R. Hackam, "Outdoor HV Composite Polymeric Insulators", IEEE Transaction on Dielectrics and Electrical Insulation, Vol. 6, No. 5 pp.557-585, 1999.
- [4] S. Wu, "Polymer Interface and Adhesion", Marcel Dekker Inc., New York and Basel, pp. 30, 139 and 215-219, 1982.
- [5] J. N. Israelachvili, "Intermolecular and Surface Forces", Academic Press, UK and USA, pp. 201-206 and 312-322, 1992.
- [6] R. S. Bernstorff and T. Zhao, "Aging Tests of Polymeric Housing Materials for Non-Ceramic Insulators", IEEE Electrical Insulation Magazine, Vol. 14, No. 2, pp. 26-33, 1998.
- [7] T. Tokoro, R. Hackam, "Loss and Recovery of Hydrophobicity and Surface Energy of HTV Silicone Rubber", IEEE Trans. on Dielectrics and Electrical Insulation, Vol. 8, pp. 1088-1097, 2001.
- [8] S. M. Gubanski, "Modern Outdoor Insulation—Concern and Challenges", 14th International Symposium on High Voltage Engineering, Delft, Netherlands, August, 2003.
- [9] A. A. Al-Arainy, M. I. Qureshi and N. H. Malik, "Electrical Insulation in Power Systems" by Marcel Dekker Inc., New York, 1988.

- [10] W. Noll, "Chemistry and Technology of Silicones", Academic Press, 1968.
- [11] R. S. Gorur, E. A. Chemey and R. Hackam, "Factors Influencing the Performance of Polymeric Insulating Materials in Contaminated Environments", Conference on Electrical Insulation and Dielectric Phenomena, pp. 339-344, 1986.
- [12] J. Kindersberger, M. Kuhl, "Effect of Hydrophobicity on Insulator Performance", Proceedings of 6th International Symposium on High Voltage Engineering (ISH), New Orleans, USA, paper 12-01, pp.1-4, 1989.
- [13] R. S. Gorur, J. W. Chang and O. G. Amburgey, "Surface Hydrophobicity of Polymers Used for Outdoor Insulator", IEEE Trans. PD, Vol. 5, pp. 1923-1928, 1990.
- [14] J. K. KIM, I. KIM, "Characteristics of Surface Wettability and Hydrophobicity and Recovery Ability of EPDM Rubber and Silicone Rubber for Polymer Insulators", Journal of Applied Poly Science, Vol. 79, pp. 2251-2257, 2001.
- [15] S. H. Kim and R. Hackam, "Formation of Silicone Fluid at the Surface of Silicone Rubber Coating due to Heat", Annual Report of 1993 CEIDP, pp.605-611, 1993.
- [16] J. W. Chang and R. S. Gorur, "Surface Recovery of Silicone Rubber Used for HV Outdoor Insulation", IEEE Trans. On Dielectrics and Electrical Insulation, Vol. 1, No. 6, pp. 1039-1046, 1994,
- [17] G. G. Karady, M. Shah and R. L. Brown, "Flashover Mechanism of Silicone Rubber Insulators Used for Outdoor Insulation", IEEE Transaction on Power Delivery, Vol. 10, No.4, pp. 1965-1971, 1995.

- [18] H. Homma, T. Kuroyagi, C. L. Mirky, J. Ronzello and S. A. Boggs, "Diffusion of Low Molecular Weight Siloxane from Bulk to Surface", Conference Record of ISEI, pp. 279-282, 1996.
- [19] D. H. Han, H. Y. Park, M. S. Ahn and D. P. Kang, "The Effect of Silicone Fluid on the Properties of Silicone Rubber for Composite Insulators", Proceedings of 5th ICFADM, pp. 730-733, 1997.
- [20] N. Yoshimura, S. Kumagai and S. Nishimura, "Electrical and Environmental Aging of Silicone Rubber Used in Outdoor Insulation", IEEE Transactions on Dielectrics and Electrical Insulation, Vol.6, No.5, pp.632-650, October, 1999.
- [21] S. H. Kim, E. A. Cherney and R. Hackam, "The Loss and Recovery of Hydrophobicity RTV Silicone Rubber Insulator Coatings", IEEE Trans. PD, Vol. 5, pp. 1491-1499, 1990.
- [22] R. S. Gorur, A. de la O, H. El-Kishky, M. Chowdhary, H. Mukherjee, R. Sundaram and J. T. Burnham, "Sudden Flashover of Nonceramic Insulators in Artificial Contamination Tests", IEEE Trans. on Dielectrics and Electrical Insulation, Vol. 4, No. 1, pp. 79-87, 1997.
- [23] A. de la O, R. S. Gorur and J. T. Bumhum, "Electrical Performance of Non-ceramic Insulators in Artificial Contamination Tests -Role of Resting Time", IEEE Transactions on Dielectrics and Electrical Insulation, Vol. 3, No. 6, pp. 827-835, 1996.
- [24] C. S. Huh and T. H. Lee, "A Study on the Determining Surface Erosion of Silicone Rubber in Salt Fog Condition", Proceedings of 5th ICPADM, pp. 336-340, 1997.

- [25] H. Hillborg and U.W. Gedde, "Hydrophobicity Changes in Silicone Rubbers", IEEE Transactions on Dielectrics and Electrical Insulation, Vol. 6, No. 5, pp. 703-717, 1999.
- [26] J. S. T.Looms, "Insulators for High Voltages" Peter Peregrinus Ltd., London, UK, pp. 42-50, 1988.
- [27] Suwarno, Salama, K. T. Sirait and H. C. Kaerner, "Dielectric Properties and Surface Hydrophobicity of Silicone Rubber under the Influence of the Artificial Tropical Climate", Proceedings of 1998 International Symposium on Electrical Insulating materials, Toyohashi, Japan, 1998.
- [28] R. Omranipour, L Meyer, S. Jayaram and E. Cherney., "Inclined plane tracking and erosion evaluation of filled and unfilled silicone rubber", Conference on Electrical Insulation and Dielectric Phenomena, pp. 625-628, 2001.
- [29] S. H. Kim, E.A. Cherney and R. Hackam, "Effects of Filler Level in RTV Silicone Rubber Coatings Used in HV Insulators", IEEE Transactions on Electrical Insulation, Vol. 27, No., 6, pp. 1065-1072, 1992.
- [30] L. Meyer, R. Omranipour, S. Jayaram and E. A. Chernney, "The Effect of ATH and Silica on Tracking and Erosion Resistance of Silicone Rubber Compound for Outdoor Insulation", IEEE International Symposium on Electrical Insulation, Boston, MA, USA, pp. 271-274, 2002.
- [31] V. Rajini, K. Kanchana, V. Gowrishree and K. Udayakumar, "Comparison of Surface Tracking in Polymeric Insulating Materials", IEEE Inter. Conference on Power System Technology, Singapore, pp. 1513-1517, 2004.

- [32] M. A. Pradeep, N. Vasudev, P. V. Reddy and D. Khastgir, "Effect of ATH Content and Aging Properties of EVA and Silicone Rubber Blends for High Voltage Insulator Compound", *Journal of Applied Polymer Science*, Vol.104, pp. 3505-3516, 2007.
- [33] R. S. Gorur, E. A. Cherney and R. Hackam, "A Comparative Study of Polymeric Insulating Materials under Salt-Fog Conditions", *IEEE Trans. on Electrical Insulation*, Vol. EI-21, No. 2, pp. 175-182, 1986.
- [34] L. Meyer, "Tracking and Erosion Resistance of RTV Silicone Rubber: Effect of Filler Particle Size and Loading", *IEEE/PES Transmission and Distribution Conference & Exposition*, pp. 453-456, 2004.
- [35] A. H. El-Hag, L. C. Simon, S.H. Jayaram and E. A. Cherney, "Erosion Resistance of Nano-Filled Silicone Rubber", *IEEE Trans. on Dielectrics and Electrical Insulation*, Vol. 13, No. 1; pp. 122-128, 2006.
- [36] J. Mackevich and S. Simmons, "Polymer Outdoor Insulating Materials Part II: Material Considerations", *IEEE Electrical Insulation Magazine*, Vol. 13, No. 4, pp. 10-16, 1997.
- [37] B. Marungsri, H. Shinokubo, R. Matsuoka and S. Kumagai, "Effect of Specimen Configuration on Deterioration of Silicone Rubber for Polymer Insulators in Salt Fog Ageing Test", *IEEE Transactions on Dielectrics and Electrical Insulation*, Vol. 13, No. 1; pp. 129-138, 2006.
- [38] H. Z. Syed, "Aging Characteristics of Polytetrafluoroethylene (PTFE)", M.A.Sc. Thesis, University of Windsor, 2002.
- [39] Bok-Hee Youn and Chang-Su Huh, "Surface Degradation of HTV Silicone Rubber and EPDM Used for Outdoor Insulators under Accelerated

Ultraviolet Weathering Condition", IEEE Trans. on Dielectrics and Electrical Insulation, Vol. 12, No. 5; pp. 1015-1024, 2005.

- [40] T. Berger, S. Sundhararajan and T. Nagaosa, "Influence of Temperature on the Hydrophobicity of Polymers", Conference on Electrical Insulation and Dielectric Phenomena, Minneapolis, pp. 394-397, 1997.
- [41] S. Kumagai, X. Wang and N. Yoshimura, "Surface Hydrophobicity of Water-absorbed Outdoor Polymer Insulating Materials", Proceedings of the 5th International Conference on Properties and Applications of Dielectric Materials, pp. 750-753, 1997.
- [42] Y. Zhu, M. Otsubo and C. Honda, "Degradation of Polymeric Materials Exposed to Corona Discharges", Polymer Testing, vol. 25, Issue 3, pp. 313-317, 2006.
- [43] T. Hashiguchi, N. Arise, M. Otsubo, C. Honda and O. Takenouchi, "Water Absorption, Hydrophobicity Characteristics and Surface Change of Polymer", IEEE Conference on Electrical Insulation and Dielectric Phenomena, pp. 195-198, 2000.
- [44] K. Haji, Y. Zhu, M. Otsubo and C. Honda, "Surface Modification of Silicone Rubber after Corona Exposure", Plasma Processes and Polymers, 4, S1075-S1080, 2007.
- [45] S. H. Kim, E. A. Cherney and R. Hackam, "Hydrophobic Behavior of Insulators Coated With RTV Silicone Rubber", IEEE Trans. EI, Vol. 27, pp. 610-622, 1992.
- [46] S. H. Kim, E. A. Cherney and R. Hackam, "Artificial Testing and Evaluation of RTV Coatings in a Salt-Fog Chamber", IEEE Trans. EI, Vol. 26, pp. 797-805, 1991.

- [47] H. Deng, R. Hackam and E. A. Cherney "Influence of Thickness, Substrate Type, Amount of Silicone Fluid and Solvent Type on the Electrical Performance of RTV Silicone Rubber Coatings", *IEEE Trans. PD*, Vol. 11, pp. 431-443, 1996.
- [48] J. Kim, M. K. Chaudhary, and M. J. Owen, "Hydrophobicity Loss and Recovery of Silicone HV Insulation", *IEEE Trans. DEI* Vol. 6, pp. 695-702, 1999.
- [49] A. K. Bhowmick, J. Konar, S. Kole and S. Narayanan, "Surface Properties of EPDM, Silicone Rubber and Their Blend during Aging", *I. Applied Polymer Science*, Vol. 57, pp. 631-637, 1995.
- [50] S. Wu, "Polymer Interface and Adhesion", Marcel Dekker Inc., New York and Basel, pp. 12 and 257-260, 1982.
- [51] H. Tajalli, "Electric Surface Properties of Delrin Used for High Voltage Insulation", M.A.Sc. Thesis, University of Windsor, pp. 16-24, 2005.
- [52] S. M. Chaudhry and S. Kamal, "Introduction to Statistical Theory Part-I and Part-II" Ilmi Kitab Khana, Urdu Bazar, Lahore, pp. 1, 67 and 94-98, 2002
- [53] L. P. van Reeuwijk, "Guidelines for Quality Management in Soil and Plant Laboratories (FAO Soils Bulletin-74)", International Soil Reference and Information Centre, FAO-UN, Rome, 1998.
- [54] M. R. Chaudhary, "Polymer's Modern Statistics" Polymer publication, Urdu Bazar, Lahore, pp. 39, 40, 77 and 93, 2001.
- [55] T. Tokoro, R. Hackam, "Effect of Water Salinity and Temperature on the Hydrophobicity of Ethylene Propylene Diene Monomer Insulator", *IEEE*

Conference on Electrical Insulation and Dielectric Phenomena, pp. 424-427, 1996.

- [56] T. Tokoro, R. Hackam, "Effect of Water Salinity and Temperature on the Hydrophobicity of Ethylene Propylene Diene Monomer Insulator", IEEE Proceedings of the 5th International Conference on Properties and Applications of Dielectric Materials, pp. 82-85, 1997.
- [57] T. Tokoro, R. Hackam, "Effect of Water Salinity, Electric Stress and Temperature on the Hydrophobicity of Nylon", IEEE Conference on Electrical Insulation and Dielectric Phenomena, pp. 290-293, 1995.
- [58] T. Tokoro, R. Hackam, "Recovery of Hydrophobicity of Nylon Aged by Heat and Saline Water", IEEE International Symposium on Electrical Insulation, pp. 283-286, 1996.
- [59] T. Tokoro, R. Hackam, "Loss and Recovery of Hydrophobicity, Surface Energies, Diffusion Coefficients and Activation Energy of Nylon", IEEE Transactions on Dielectrics and Electrical Insulation, Vol. 6, No. 5, pp. 754-762, 1999.
- [60] C. M. Berger and C. L. Henderson, "The Effect of Humidity on Water Sorption in Photoresist Polymer Thin Films" Polymer, 44, pp. 2101-2108, 2003.
- [61] L. A. McDonough, "Microscopy and Spectroscopy of Water Uptake in Polymer Photoresists", PhD Thesis, University of Colorado, USA, 1998.
- [62] M. A. Khan and R. Hackam, "Loss of Hydrophobicity of High Density Polyethylene" IEEE Conference on Electrical Insulation and Dielectric Phenomena, pp. 378-381, 1997.

- [63] M. A. Khan and R. Hackam, "Surface Properties of Cross-linked Polyethylene", IEEE Conference on Electrical Insulation and Dielectric Phenomena, pp. 673-677, 1998.
- [64] T. Tokoro, M. Nagao and M. Kosaki, "Effect of Water Absorption on the High-Field Dielectric Property of Silicone Rubber", Proceedings of International Symposium on Electrical Insulating Materials, pp. 461-464, 1998.
- [65] Z. Li, X. Liang, Y. Zhou, J. Tang, J. Cui and Y. Liu, "Influence of temperature on the hydrophobicity of silicone rubber surfaces", IEEE Conference on Electrical Insulation and Dielectric Phenomena, pp. 679-682, 2004.
- [66] H. Homma, C. R. Lee, T. Kuroyagi and K. Izumi, "Evaluation of Time Variation of Hydrophobicity of Silicone Rubber using Dynamic Contact Angle Measurement", Proceedings of the 6th International Conference on Properties and Applications of Dielectric Materials, pp. 637-640, 2000.
- [67] F. Exl, Kindersberger, "Contact Angle Measurement on Insulator Surfaces with Artificial Pollution Layers and Various Surface Roughnesses", Tsinghua University, Beijing, China, August 25-29, 2005
- [68] Y. Zhu, M. Otsubo, C. Honda and S. Tanaka, "Loss and Recovery in Hydrophobicity of Silicone Rubber Exposed to Corona Discharge", Science Direct-Polymer Degradation and stability, Vol. 91, Issue 7, pp. 1448-1454, 2007.
- [69] S. Kumagai and S. Yoshimura, "Hydrophobicity Transfer of RTV Silicone Rubber aged in Single and Multiple Environmental Stresses and the

Behavior of LMW Silicone Fluid", IEEE Trans. on Power delivery, Vol. 18, No. 2, pp. 506-516, 2003.

- [70] S. Han, J. Y. Yoon, K. S. Park and S. O. Han, "Surface Degradation of Silicone Rubber Exposed under Accelerated Aging condition", Conference on Electrical Insulation and Dielectric Phenomena, Minneapolis, pp. 439-443, 1997.
- [71] R. Sundararajan, J. Graves, A. Mohammed and A. Baker, "Performance Evaluation of Polymeric Insulators Aged in Lab and Field", IEEE, pp. 219-224, 2003.
- [72] D. H. Han, H. G. Cho and S. W. Han, "Effects of Alumina Trihydrate on the Electrical Properties of HTV Silicone Rubber", Proceedings of 7th international Conference on Properties and Applications of Dielectric Materials, Nagoya, pp. 381-384, 2003.
- [73] B. Elahipanah, "Effect of Heat and Saline Water on the Hydrophobic Behavior of EPDM Insulator", M.A.Sc., Thesis, University of Windsor, 2006.
- [74] J. N. Israelachvili, "Intermolecular and Surface Forces", Academic Press, UK and USA, pp. 83-87, 1992.
- [75] R. F. Gould, "Contact Angle, Wettability and Adhesion", Advances in Chemistry Series, Vol. 43, 1964.
- [76] S. Wu, "Polymer Interface and Adhesion", Marcel Dekker Inc., New York and Basel, pp. 178-181, 1982.
- [77] H. Zhang, "Aging Characteristics of Solid Polymeric materials used for Electrical Insulation", M.A.Sc., Thesis, University of Windsor, 2000.

- [78] J. W. Chang, "Study of Surface Hydrophobicity Recovery Characteristics and Aging of Silicone Rubber used for High Voltage Outdoor Insulation", PhD Thesis Report, Arizona State University, 1994.
- [79] L. Cao and R. Hackam "Low Molecular Weight Fluid in EPDM" IEEE Conference on Electrical Insulation and Dielectric Phenomena Proc., Vol. 2, pp. 423-426, 1997.
- [80] K. Iida and R. Hackam "Effects of Heating on the Generation of Fluid in an Alloy of EPDM/SIR", 7th International Conference on Properties and Applications of Dielectric Materials, pp. 603-606, 2003.
- [81] L. Cao and R. Hackam "Diffusion of Low Molecular Weight Fluid in EPDM" IEEE Conference on Electrical Insulation and Dielectric Phenomena, pp. 84-87, 1998.
- [82] L. Cao and R. Hackam "Effects of Heating on the Presence of Fluid in EPDM" IEEE International Symposium on Electrical Insulation Proc., Vol. 2, pp. 360-364, 1998.
- [83] Aldrich Library of FT-IR spectra, 2nd edition, 3-volume set, 1997.
- [84] K. Iida and R. Hackam "Effect of Low Molecular Weight Fluid on the Surface Free Energy of an Alloy of EPDM/SIR", International Symposium on Electrical Insulating Materials Proc., pp. 352-355, 2005.

Appendix A: Some Statistical Concepts [52-54]:

A.1 Population and Sample

A population is an aggregate of all individual members or objects of some characteristics of interest where as sample is a subset or part of population.

A.2 Parameter and statistic

Any numerical value obtained from population is called a parameter where as any numerical information obtained from sample is known as a statistic

A.3 Measures of Central Tendency

Measures of central tendency are measures of the location of the middle or the center of a distribution. The definition of "middle" or "center" is purposely left somewhat vague so that the term "central tendency" can refer to a wide variety of measures. The mean is the most commonly used measure of central tendency. The following are the measures of central tendency:

A.4 Arithmetic Mean, Mode and Median

If $x_1, x_2, x_3, \dots, x_n$ are n observations of a variable X, then their arithmetic mean denoted by \bar{X} is defined as a value obtained by dividing the sum of all the observations by their number and is given as

$$\bar{X} = \frac{\sum x_i}{n} \quad \text{Where } i=1, 2, 3 \dots n$$

The Mode is defined as the most repeated value in the given set of n data and Median is the $(\frac{n+1}{2})^{\text{th}}$ value in a set of given data arranged in ascending or descending order of magnitude.

A.5 Measures of dispersion

Measures of dispersion are important for describing the spread of the data, or its variation around a central value. One of the measures of dispersion is a variance (standard deviation)

A.6 Variance and Standard Deviation

The variance is defined as the sum of the squared deviations from the mean, divided by n. If $x_1, x_2, x_3, \dots, x_n$ are n observations of a variable X and \bar{X} is their arithmetic mean, then their variance denoted by S^2 is given as following

$$S^2 = \frac{\sum(x_i - \bar{x})^2}{n}, \quad \text{Where } i = 1, 2, 3, \dots, n$$

The standard deviation is the most commonly used measure of the spread or dispersion of data around the mean and is defined as the square root of the variance (S^2). Operationally, there are several ways of calculations of standard deviation denoted by s and are given as

$$S = \sqrt{\frac{\sum(x_i - \bar{x})^2}{n}} \quad \text{Or} \quad S = \sqrt{\frac{1}{n}[\sum x_i^2 - \frac{\sum x_i^2}{n}]}$$

A.7 Interval Estimation

The process of making judgment about the unknown parameter by using the sample information is known as estimation. Where as an interval estimation is a process of estimating an unknown population parameter is an interval computed from a random sample of size n of the variable X having values $x_1, x_2, x_3, \dots, x_n$ with a statement of how confident (e.g., 90%, 95% or 99%) we are that the interval contains the unknown parameter. A confidence interval estimate is of the form $L < \theta < U$ where L and U are the lower and upper limits computed from sample information and θ be the unknown parameter. The interval (L, U) is called a $100(1-\alpha) \%$ confidence interval for the unknown parameter θ . The probability $(1-\alpha)$ associated with interval estimate is called confidence coefficient or level of confidence and α is the probability that the parameter θ will lie outside the interval (L, U) . For example, if $\alpha = 0.05$ then the probability that the interval (L, U) contains θ is 0.95.

A.8 Confidence Interval Estimation of a Population Mean

Let us consider a random sample $x_1, x_2, x_3, \dots, x_n$ of size n from normal distribution with mean μ and known (or unknown) standard deviation σ , then $100(1-\alpha) \%$ confidence interval for μ is:

$$\bar{X} \pm z_{\alpha/2} \frac{\sigma}{\sqrt{n}}$$

where,

\bar{X} = sample mean

σ = population standard deviation

n = sample size

$z_{\alpha/2}$ = table value

When sample size $n > 30$ and σ is unknown, we estimate σ by the sample standard deviation S which can be replaced by σ . Thus $100(1-\alpha)$ % confidence interval for μ is

$$\bar{X} \pm z_{\alpha/2} \frac{S}{\sqrt{n}}$$

$1-\alpha = 95\%$ Level of confidence

$$\alpha = 1 - 0.95$$

$$= 0.05$$

$$\alpha/2 = 0.025$$

$$z_{\alpha/2} = z_{0.025} = 1.96 \text{ (Table value)}$$

$$\bar{x} \pm z_{\alpha/2} \frac{s}{\sqrt{n}} = 101 \pm 1.96 \left(\frac{7.28}{\sqrt{33}} \right)$$

$$= 101 \pm 2.5$$

Also, when sample size $n \leq 30$, then $100(1-\alpha)$ % confidence interval for μ is

$$\bar{X} \pm t_{\alpha/2(n-1)} \sqrt{\frac{s^2}{n}} \quad \text{And} \quad s^2 = \frac{\sum(x_i - \bar{x})^2}{n-1}$$

where,

s^2 = unbiased variance

$t_{\alpha/2(n-1)}$ = table value at $(n-1)$ degrees of freedom

Appendix B. MATLAB Code for Calculations of Surface Energies

```
clc

%Distilled Water Parameters

Theta_deg_DW=35; %Contact angle with distilled water

Theta_DW=Theta_deg_DW*pi/180;

%Literature values

Gamma_L1=72.8e-3; %Surface energy for distilled water

Gamma_LD1=22.1e-3; %Dispersive component for distilled water

Gamma_LH1=50.7e-3; %Polar component for distilled water

%Methylene Iodide Parameters

Theta_deg_MI=31; %Contact angle with methylene iodide

Theta_MI=Theta_deg_MI*pi/180;

%Literature values

Gamma_L2=50.8e-3; %Surface energy for methylene iodide

Gamma_LD2=44.1e-3; %Dispersive component for methylene iodide

Gamma_LH2=6.7e-3; %Polar component for methylene iodide

%Calculation of parameters for equations

c1=Gamma_L1*(1+cos(Theta_DW));

c2=Gamma_L2*(1+cos(Theta_MI));

W1=4*(Gamma_LD1+Gamma_LH1)-c1;

X1=4*Gamma_LD1*Gamma_LH1-(c1*Gamma_LH1);

Y1=4*Gamma_LD1*Gamma_LH1-(c1*Gamma_LD1);
```

```

Z1=c1*Gamma_LD1*Gamma_LH1;
W2=4*(Gamma_LD2+Gamma_LH2)-c2;
X2=4*Gamma_LD2*Gamma_LH2-(c2*Gamma_LH2);
Y2=4*Gamma_LD2*Gamma_LH2-(c2*Gamma_LD2);
Z2=c2*Gamma_LD2*Gamma_LH2;

%In order to calculate Gamma_sd and Gamma_sh and then Gama_s equal to
%Gamma_sd+Gamma_sh,the polynomial coefficients need to be defined
p1=(W1*X2-W2*X1);
p2=(W2*Z1+X2*Y1)-(Y2*X1+Z2*W1);
p3=Y2*Z1-Z2*Y1;
P1=[p1 p2 p3];
Gamma_sd=roots(P1) %Dispersive component
hx=Z1-X1*Gamma_sd;
hx1=Y1+W1*Gamma_sd;
Gamma_sh=hx./hx1 %Polar component
Gamma_s=Gamma_sd+Gamma_sh %Total surface energy
Gamma_sl=Gamma_s-Gamma_L1*(cos(Theta_DW)) %Interfacial energy
%W_sl=Gamma_s+Gamma_L1-Gamma_sl
W_sl=Gamma_L1*(1+cos(Theta_DW)) %Energy of adhesion for water

```

Vita Auctoris

Name	Mansab Ali
Place of Birth	Nankana Sahib, Pakistan
Year of Birth	1963
Education	University of Engineering and Tech., Lahore, Pakistan 1984-1989, B.Sc. in Electrical Engineering University of Windsor, Windsor, Ontario, Canada 2005-2008, M.A.Sc. in Electrical Engineering